FUNCTIONAL ANALYSIS OF THE ROLE OF INTERFERON GAMMA THROUGH THE CHARACTERISATION OF CONDITIONAL INTERFERON GAMMA RECEPTOR TWO MOUSE MUTANTS.

A thesis submitted to The University of Manchester for the degree of Doctor of Philosophy (Ph.D) in the Faculty of Life Sciences

2011

RUTH AMY FORMAN

CONTENTS

LIST OF FIGURES AND TABLES

Chapter One

Chapter Two

Chapter Three

Chapter Four

Chapter Five

Chapter Six

ABSTRACT

The data presented within this thesis shows the generation and characterisation of a complete-, macrophage/granulocyte- and T cell-specific IFNγR2 deficient mouse mutant. This mutant mouse is a valuable tool in dissecting the mechanism of action of the pleiotrophic cytokine IFNγ.

The global mutant mouse was tested in three models *in vivo* – DSS induced colitis, *Trichuris muris* infection and EAE. The aim of the DSS-induced colitis model was to test the role of IFNγ in the innate immune system and, despite previous reports demonstrating IFNγ deficient mice are protected from DSS-colitis, our IFNγR2 deficient mice displayed equal or more severe colitis than control mice. We hypothesise that this discrepancy is due to differences in the gut microbiota.

The *Trichuris muris* model was utilised as a method of examining the role of IFNγ in the adaptive immune system. The complete IFNγR2 mutant was resistant to a low dose *T. muris* infection; however, neither the T cell specific nor the macrophage/granulocyte specific mutant duplicated the resistant phenotype observed in the global knock-out mice. Analysis of a double conditional T cell and macrophage/granulocyte specific IFNγR2 mutant produced inconsistent results. Initial experiments suggested that, in combination, these deficiencies are sufficient to duplicate the resistant phenotype observed in the global mutant mice, but this was not reproducible.

The final *in vivo* model that we used to analyse IFNγR2 mutant mice was EAE. This model was chosen as, for a long time, the mechanism of action and the involvement of IFNγ in EAE has been a matter of uncertainty. These results demonstrated that global IFNγR2 mutant mice demonstrate an atypical phenotype, with no signs of recovery. In contrast, control mice develop classical EAE symptoms with almost complete recovery prior to the termination of the experiment.

The IFNγ receptor mutant mouse generated will be of great value to the scientific community as IFNγ has been demonstrated to play a role in multiple diseases and this tool allows the mechanism of action of this cytokine to be unravelled.

DECLARATION OF ORIGINALITY

Data contained within chapter six of this thesis was performed in collaboration with Vinko Tosevski under the supervision of Professor Burkhard Becher at the University of Zurich and may be submitted as part of his thesis at the University of Zurich.

No other part of this thesis has been submitted in support of an application for any degree or qualification of The University of Manchester or any other University or Institute of learning.

COPYRIGHT STATEMENT

ACKNOWLEDGEMENTS

This thesis would not have been possible with the help and guidance of my supervisor Werner Muller. I am always amazed at how you seem to know everything and am grateful for the opportunities you have given me to work independently, travel to different places to present my work and meet new people during my thesis. I am also grateful to members of Werner's previous lab at the Helmholtz Institute for Infection Research, Braunschweig especially Anne Fleige and Angela Schippers who initiated this project with their work on the IFNγR2 mouse generation. Fabio Pisano, Nicolas Fasnacht and Marina Pils who were always welcoming on my trips to the lab in Braunschweig and provided useful advice, especially in the first year of my PhD. Finally I'd like to thank the new members of Werner's group, at the University of Manchester, especially Catherine Walker, Brooke Cooper and Bill Moser who have made my last year in the lab more entertaining!

I'd also like to thank the other members of the immunology department at the University of Manchester for their help and support. Especially my co-supervisor Richard Grencis and my advisor Kathryn Else who has always had her door open and been generous with her time. Members of Kathryn's group have been particularly helpful in the lab including Maff Little, Matthew deSchoolmeester and Louise Bell.

I would like to show my gratitude to Prof Burkhard Becher who opened up his lab, at the University of Zurich, to me. In particular, I'd like to thank Vinko Toveski, from his lab, who helped me with all of the experimental autoimmune encephalomyelisis experiments I performed.

Finally I'd like to thank Simon, my husband, for all of his support and encouragement, especially in the last few months as I've been writing this thesis. I couldn't have done it without you to keep me sane!

ABBREVIATIONS

AAM	Alternatively activated macrophage
ADCC	Antibody dependent mediacted cytotoxicity
ANOVA	Analysis of varience
APC	Antigen presenting cell
ATG16L1	Autophagy-related 16-like 1
BBB	Blood brain barrier
BSA	Bovine serum albumin
CD	Crohn's Disease
CMV	cytomegalovirus
CNS	Central nervous system
Cre	Causes recombination
Cre-ER^{T}	Cre-modified estrogen receptor
DAB	3,3'-diaminobenzidine
DALYs	Disability-adjucted life-years
DC	Dendritic cell
DMEM	Dulbecco's Modification of Eagle's Medium
dNTP	Deoxyribonucleotide triphosphate
DSS	Dextran sodium sulphate
EAE	Experimental autoimmune encephalomyelitis
EC	Epithelial Cell
ECL	Enhanced chemiluminescence
EDTA	Ethylenediaminetetraacetic acid
ELISA	Enzyme-Linked ImmunoSorbent Assay
ES	Embryonic stem
E/S	Excretory/secretory
FITC	Fluorescein isothiocyanate
FoxP3	Forkhead box P3
FRT	Flp recognition target
GAS	Interferon gamma - activated sequence
GM-CSF	Granulocyte-macrophage colony-stimulating factor

HAT	Histone acetyltransferases
HBSS	Hank's Buffered Salt Solution
HDAC	Histone deacetylase
HE	Heterozygous
H&E	Hematoxylin-eosin
HLA	human leukocyte antigen
HO	Homozygous
IBD	Inflammatory Bowel Disease
ICAM	Intercellular cell adhesion molecule
IFN	Interferon
IFNγR	Interferon gamma receptor
IKK	IκB kinase
IL	Interleukin
ISG	Interferon gamma stimulated gene
KO	Knock-out
LFA	lymphocyte function-associated antigen
loxP	Locus of crossover (x) in P1
LBD	Ligand binding domain
L. major	*Leishmania major*
LPS	Lipopolysaccharide
MAdCAM	Mucosal addressin cell adhesion molecule
MAPK	Mitogen activated protein kinase
MDR-1	Multidrug resistance 1
MHC	Major histocompatibility complex
MIIG	Macrophages insensitive to interferon gamma
MLN	Mesenteric lymph node
MOG	Myelin oligodendrocyte glycoprotein
MOM	Mouse on Mouse
mRNA	messenger ribonucleic acid
MS	Multiple Sclerosis
Neo	Neomycin cassette

NK	Natural Killer
NO	Nitric oxide
NOD2	Nucleotide-binding oligomerisation protein 2
OD	Optical density
PBS	Phosphate buffered saline
PCR	Polymerase chain reaction
PE	Phycoerythrin
PGRP	Peptidoglycan recognition protein
p.i.	Post infection / post immunisation
PKC	Protein kinase C
PLP	Proteolipid protein
PPMS	Primary progressive multiple sclerosis
PRMS	Progressive relapsing multiple sclerosis
RAG	Recombination activating gene
RRMS	Relapsing remitting multiple sclerosis
SCID	Severe combined immunodeficient
SPF	Specified pathogen free
SPMS	Secondary progressive multiple sclerosis
STAT	Signal Transducers and Activators of Transcription
STH	Soil-transmitted helminth
TDS	Trichuris dysentery syndrome
tet	Tetracycline
tetO	Tet operon
TBS	Tris buffered saline
TGFβ	Transforming growth factor beta
TLR	Toll-like receptor
TMB	3,3',5,5'-Tetramethylbenzidine
T. muris	*Trichuris muris*
TNBS	2,4,6-trinitrobenzene sulphonic acid
TNF	Tumour Necrosis Factor
tTA	Tet transactivator gene

T. trichiura	*Trichuris trichiura*
UC	Ulcerative Colitis
VCAM	Vascular cell adhesion molecule
VLA	Very late antigen-4
WT	Wild type

CHAPTER ONE

Introduction

This introduction will begin with a review on the generation of conditional knock-out mice, followed by an overview of IFNγ and the IFNγ signalling pathways. The introduction will culminate with an overview of the three *in vivo* models employed within this thesis to test the conditional knock-out mice: inflammatory bowel disease and the model of dextran sodium sulphate-induced colitis; intestinal nematode infection and the model *Trichuris muris* and finally multiple sclerosis and the murine model of experimental autoimmune encephalomyelitis.

1.1 GENERATION OF CONDITIONAL KNOCK-OUT MICE

The use of laboratory mice has had a prominent role in studying human diseases, initially through naturally occurring mouse mutants and more recently through the generation of genetically modified animals (for review see (Austin *et al.*, 2004)). Mice are good model organisms for studying human biology and disease as a high level of homology has been demonstrated between the mouse and human genomes, at the sequence level (Gregory *et al.*, 2002).

The introduction of foreign DNA into the mouse germ-line was first described in 1980 (Gordon *et al.*, 1980). This was followed by a successful gene transfer experiment, inserting the rat growth hormone fused to the mouse metallothionein-I promoter into mice. Animals containing this gene grew faster and larger than littermate controls, reaching up to twice their normal size demonstrating successful expression of the gene (Brinster & Palmiter, 1984). Advances in techniques then led to the first mouse gene targeting experiment in 1987. This method allows the inactivation of a specific locus within the mouse genome (Thomas & Capecchi, 1987). In this experiment gene inactivation was achieved by replacing the chosen gene segment with a mutant version, through homologous recombination in embryonic stem (ES) cells. As homologous recombination is an infrequent event in mammalian cells, isolation of mutant ES cells was selected for through the addition of the neomycin resistance gene in the targeted locus. This neomycin expression allows recombined ES cells to be easily selected at the same time as inactivating the target gene (Thomas & Capecchi, 1987). Microinjection of mutant ES cells into

mouse blastocysts was then performed to generate germ-line chimaeras (Bradley *et al.*, 1984), and interbreeding of heterozygous siblings then produces mice homozygous for the desired mutation.

This conventional gene targeting method, creating a global knock-out, can create an embryonic lethal phenotype if the gene is involved in development. Moreover, a gene may exert its function in different cell types resulting in complex phenotypes where it is difficult to determine cell-autonomous effects from more complex interactions (Rajewsky *et al.*, 1996). Recent advances in the genetic manipulation of mice and the development of site-specific recombinase systems have allowed the conditional inactivation of a gene and have proved a powerful tool in the elucidation of gene function (Gu *et al.*, 1994).

The two main recombinase systems that have been use for mouse gene targeting experiments are the Cre-loxP system (Gu *et al.*, 1994; Lakso *et al.*, 1992) and the Flp-FRT system (Dymecki, 1996). The Cre-loxP system was introduced over 15 years ago and has become a favoured approach in biomedical and immunological research (for review see (Schmidt-Supprian & Rajewsky, 2007)).

1.1.1 The Cre-loxP system

The site-specific Cre-loxP recombination system was originally isolated from bacteriophage P1 where it is important in the viral life cycle (Abremski & Hoess, 1984). The system consists of two components: the loxP recognition site and the Cre protein. The loxP (locus of crossover (x) in P1) recognition site is a 34-bp consensus sequence. This sequence consists of two 13-bp inverted repeats flanked by an 8-bp nonpalindromic core, which defines the orientation of the recognition site (Kwan, 2002) (Fig 1.1A). The size of the loxP sites mean it is large enough to be unlikely to occur at random within the mouse genome, but it is small enough to not interfere with gene expression. The second component is the Cre (causes recombination) protein, which carries out the recombination between two loxP sites (Abremski & Hoess, 1984) (Fig 1.1B). The relative orientation of the loxP sites is important. A DNA fragment between two loxP sites in the same orientation is excised in a circular form, whereas, a fragment between two loxP sites in opposing orientations will be

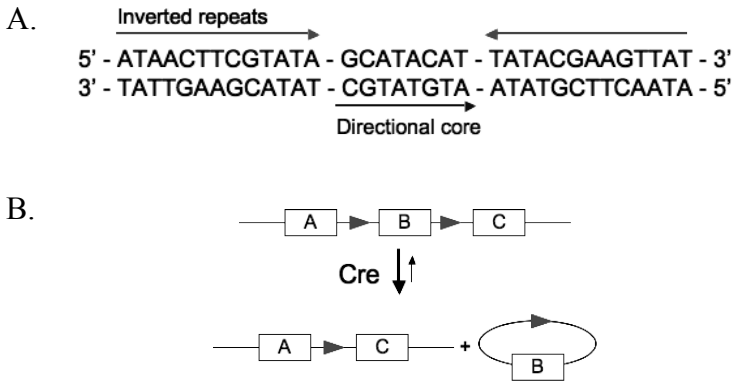

Fig 1.1 The Cre-loxP system A. The loxP recognition site – two 13bp inverted repeats flanking an 8-bp nonpalindromic core **B.** The Cre protein carries out recombination between 2 loxP sites (represented by ▶) excising the exon(s) contained within the loxP sites. Adapted from (Hoess & Abremski, 1985) and (Kwan, 2002).

inverted with respect to the rest of the DNA. An important characteristic of this reaction is it's autonomy. Cre recombinase has high fidelity, without the need for accessory proteins, (Abremski *et al.*, 1983), and this allows the system to be manipulated for use in mammalian cells.

The targeting vector used to create the loxP flanked ("floxed") gene needs to incorporate several essential components. This includes two arms of DNA sequence homologous to that of the ES cells to be targeted, and a positive selection gene cassette (e.g. neomycin), within the two homology arms, allowing for selection of integration. The vector can also include a negative selection gene (e.g. thymidine kinase or diptheria toxin) outside of the two homology arms, to allow selection against random integration (see review of gene targeting strategies by (Cheah & Behringer, 2000)).

The addition of a selectable marker e.g. neo^r into the targeted gene has been demonstrated to potentially complicate results. Chen *et al.* observed that the presence of a neo^r cassette blocked the normal splicing of the target gene. Other experiments have shown the insertion of a neo^r cassette can disrupt the amino acid sequence and introduce stop codes in the gene of interest (Hirotsune *et al.*, 1998). This interference in the transcription or splicing of the target or neighbouring genes can make the

interpretation of a specific phenotype potentially very difficult (Chen *et al.*, 1999; Pham *et al.*, 1996). To circumvent this complication, new gene targeting techniques have aimed to delete the selectable marker after confirmation of homologous recombination.

One of the most popular strategies currently used, in the generation of a conditional knock out mouse, to delete the selectable marker, is the 3-loxP approach. The targeting vector in this method uses three loxP sites in the same orientation – two flanking the selectable marker and the third one positioned to cause the desired excision after Cre recombination (Gu *et al.*, 1994) (see Fig 1.2A). In this method, once it has been established that the 3-loxP gene construct has successfully targeted the gene locus, the selectable marker can be removed by transiently expressing Cre. Transient Cre expression produces three possible recombination products and the desired clone, containing the floxed gene, can be isolated.

Recently, the 2-loxP 2-Flp recognition target (FRT) method has become increasingly popular. This more elegant method eliminates the need to screen for the desired clone, by flanking the positive selection marker with FRT sites instead of loxP sites (Jung *et al.*, 1993) (see Fig 1.2B). The positive selection marker can be deleted, following confirmation of homologous recombination, through the transient expression of Flp. Flp is a recombinase enzyme derived from Saccharomyces cerevisiae (Dymecki, 1996) and acts in a similar manner to Cre, causing recombination between FRT sites (Meyers *et al.*, 1998). This Flp-mediated deletion can be performed *in vitro* or *in vivo* by breeding mice containing the target gene with Flp deleter mice (Meyers *et al.*, 1998) (see Fig 1.2). If the deletion is performed *in vivo* the need to manipulate the ES cells is minimised and therefore the preservation of germline competency is enhanced. However, this needs to be weighed up against the increased potential for genetic contamination.

Once mice, containing the floxed target gene with deleted selectable marker, have been generated, mice with a cell-specific gene deletion can then be created by inter-crossing with mice expressing Cre in the selected cell lineage (Gu *et al.*, 1994). In

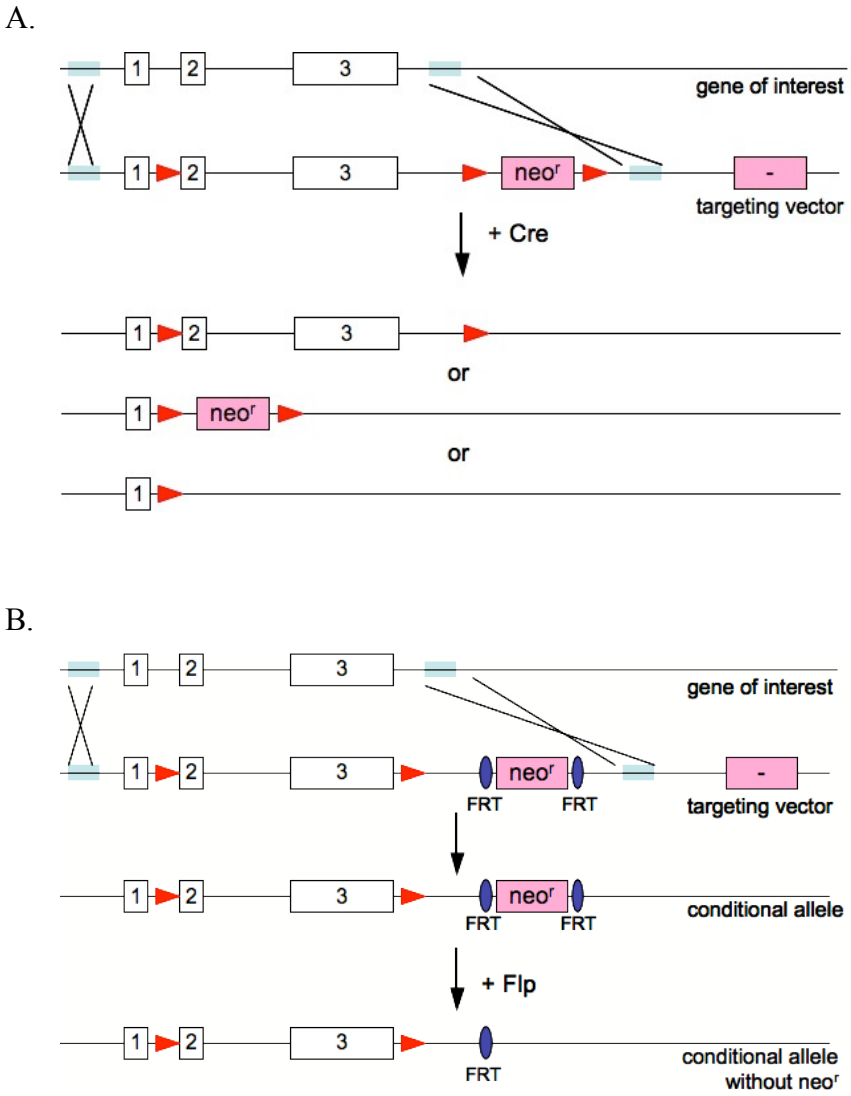

Fig 1.2 Gene targeting approaches allowing the deletion of the positive selection cassette A. 3-loxP approach. The targeting vector has three loxP sites in the same orientation – two flanking the selectable marker and the third one flanking the exon(s) to be deleted. Following, transient Cre expression the desired clone, containing the floxed gene, can be isolated. **B** 2-loxP 2- FRT method. The targeting vector has two loxP sites flanking the exon(s) to be deleted and 2 FRT sites flanking the positive selection marker. The positive selection cassette can be deleted using the transient expression of Flp, which causes recombination between FRT sites. sites of homologous recombination ► loxP sites ⬮ FRT sites neor positive selection cassette 1 exons. Adapted from (Kwan, 2002)

these offspring, carrying both the loxP flanked gene and Cre transgene, the target gene will be excised in only the tissues expressing Cre recombinase. This a powerful system and there is now a large collection of Cre mice which express the Cre recombinase under different promoters (Nagy *et al.*, 2009). Therefore, once mice containing the floxed target gene have been generated, multiple conditional knock-out mice can be created through breeding with the appropriate Cre lines.

Despite the wealth of data generated through the use of conditional gene targeted mice there are still come drawbacks with this system. For example, some promoters are tissue-specific in adults, but can be active in multiple tissues during development, resulting in a complicated gene deletion pattern (Castrop *et al.*, 2006). These drawbacks have led to the generation of methods allowing the temporal control of gene deletions. There are currently two approaches established: the Cre-Estrogen receptor system (Metzger *et al.*, 1995) and the tetracycline (tet) – dependent system (Gossen & Bujard, 1992).

The Cre-Estrogen receptor system involves the fusing of the ligand-binding domain (LBD) of the hormone receptor to the Cre protein. This takes advantage of the nature of hormone receptors, which are located in the cytoplasm, and only upon binding to their ligands are they translocated to the nucleus. Therefore, the autonomous nuclear translocatory ability of Cre is blocked, and the fusion protein is held in the cytoplasm. Upon exposure to the ligand, and after binding to the LBD, nuclear localisation occurs and subsequent recombination at loxP sites results in the deletion of the gene of interest (Fig 1.3A). Initial fusion proteins were generated using the LBD of the estrogen receptor, however, using this system endogenous estrogen could cause background levels of Cre-mediated excision. Furthermore, treatment with estrogen, to induce the deletion, could have biological consequences independent of deletion due to the presence of high levels of the hormone (Metzger *et al.*, 1995). This problem has been circumvented through the generation of a mutated estrogen receptor LBD fused to the Cre protein (Cre-ER^T). This LBD doesn't bind the naturally occurring 17β-estradiol but binds the synthetic ligands tamoxifen and 4-hydroxytamoxifen (4-OH-tamoxifen) (Feil *et al.*, 1996).

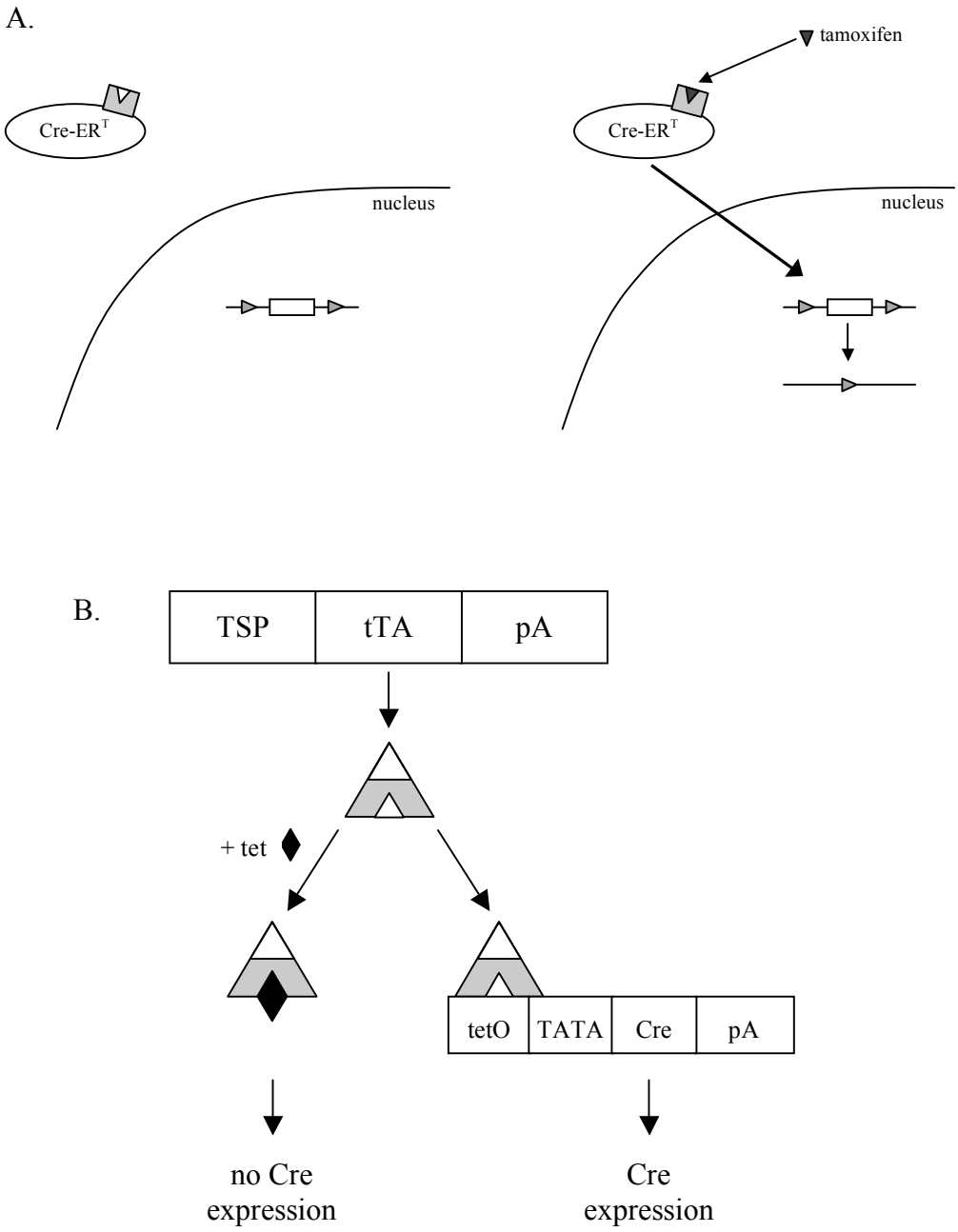

Fig 1.3 Systems for temporal control of gene expression A. The Cre-ER^T system. Under basal conditions in the absence of tamoxifen the Cre-ER^T protein remains in the cytoplasm and no recombination occurs between the two loxP sites When tamoxifen is given to the mice / introduced into the system it binds the mutated estrogen receptor ligand binding domain resulting in the movement of the Cre-ER^T protein to the nucleus. The Cre protein then induces recombination between the two loxP sites. **B.** The tTA system. Under basal conditions the tTA (tetR-VP16) fusion protein can bind to the *tetO* sequences, resulting in transcriptional activation of Cre and therefore recombination at target sites. When tetracycline (or doxycyclin) tTA undergoes a conformational change, is unable to bind the *tetO* sequence and therefore no transcription of Cre occurs. TSP, tissue-specific promoter; TATA, representing a minimal promoter required for transcription; pA, polyA signal sequence (adapted from (Branda & Dymecki, 2004)).

The second system, allowing the temporal control of gene deletion, is the tet responsive system. This system involves two components (1) a transactivator gene which encodes a fusion protein that specifically binds tet (or the tet analogue doxycycline) and operator sequences of the tet operon (*tetO*) and (2) a *tetO::recombinase* transgene, where a minimal promoter e.g. CMV drives expression of the Cre recombinase protein (see Fig 1.3B) (Gossen & Bujard, 1992). The fusion protein encoded by the transactivator gene is termed tTA and contains a tetracycline repressor (from *E. Coli*) fused to the herpes simplex viral protein 16 (VP16) transactivation domain. This fusion protein can be driven either by a cell-specific or a globally active promoter. Therefore, in the absence of tet the transactivator gene tTA is able to bind to *tetO* DNA, activating transcription of Cre. After tet administration, tet prevents tTA binding to *tetO* and therefore results in suppression of transcription (Gossen & Bujard, 1992) (see Fig 1.3B). A similar system has been generated with a 'reverse' tTA (rtTA) which only binds *tetO* in the presence of tet, therefore the administration of tet activates transcription. The disadvantage of this system is that it involves three genetic manipulations: the floxed allele, the tTA or rTA system under the control of a specific promoter and the tet operator driving the expression of Cre. This can result in the need for multiple time-consuming breedings and therefore, in practice, the Cre-ER^T system is more commonly used.

In summary, the Cre-LoxP system is an extremely powerful method for dissecting the cytokine network during homeostasis and disease. The value of this method is exemplified in the generation of the gp130 conditional mutant mice. Gpl30 is the signal-transducing subunit shared by the receptors for the IL-6 family of cytokines. Global inactivation of gp130 in mice results in lethality between day 12.5 post coitum and term, due to altered myocardial development and hematopoiesis (Yoshida *et al.*, 1996). To circumvent this, a floxed gp130 mouse was created and this has allowed several conditional knock-out mice to be generated though breeding with various Cre expressing lines (Betz *et al.*, 1998). The first conditional gp130 mouse generated was the result of a cross to the Mx-Cre line. MxCre mice contain an interferon responsive promoter so floxed genes are deleted in all haematopoietic stem cells, endothelial cells and liver cells after infection with IFN-α, IFN-β or

synthetic double-stranded RNA (Kuhn *et al.*, 1995). These gp130$^{fl/fl}$MxCre conditional mutant mice exhibit neurological, cardiac, haematopoietic, immunological, hepatic and pulmonary defects. This clearly demonstrated the importance of gp130 dependent cytokines, not only during development, but also after birth, in the main regulatory functions of the body (Betz *et al.*, 1998). Subsequently crosses have been made to various other Cre lines, including lines which are specific for the liver e.g. Alfp-Cre (hepatocyte-specific), the heart e.g. MLC2vCreKI (Cardiac myocyte-specific), the brain e.g. GFAP-Cre (Astrocyte-specific) and immune cells e.g. CD4-Cre (T cell-specific) (Drogemuller *et al.*, 2008; Fasnacht & Muller, 2008; Hirota *et al.*, 1999; Streetz *et al.*, 2003). These mice have revealed the important role of gp130 in counterbalancing apoptotic signals and demonstrate that gp130 dependant cytokines have the potential to act over a long range (for a review of the gp130 conditional mouse mutants see (Fasnacht & Muller, 2008)).

1.2 INTERFERON-γ

Interferons were originally described, in 1957, by Issacs and Lindenmann as a soluble factor produced by virus-infected cells, that can transfer virus resistance to uninfected cultures (Isaacs & Lindenmann, 1957). Since then, the family has grown and interferons (IFNs) are now divided into three major groups: IFN type I, II and III

The IFN-I family includes IFNα, IFNβ, IFNδ, IFNε, IFNχ, IFNτ and IFNω. The different family members can promote different biological responses but are all structurally related and signal through the same receptor subunits. Interferon-γ (IFNγ), was originally identified as 'macrophage-activation factor' (Schroder *et al.*, 2004), and is the sole type II interferon. The IFN-III family is a relatively recent addition and includes three proteins, namely IFN-λ1 (IL-29), IFN-λ2 (IL-28A), and IFN-λ3 (IL-28B), that all signal through the IFN-λ receptor. The biological role of these proteins is not fully understood but appears to be similar to that of the IFN-I family (for an overview of the IFN-III family see (Kotenko *et al.*, 2003)).

1.2.1 IFNγ structure and signalling

The IFNγ receptor complex is composed of four transmembrane polypeptide chains: two ligand-binding chains (IFNγR1) and two accessory chains (IFNγR2) which do not bind IFNγ but are required for signal transduction (Hemmi *et al.*, 1994; Krause *et al.*, 2006; Platanias, 2005; Regis *et al.*, 2006). It has been demonstrated that in its resting state, the receptor chains of the IFNγ complex are a preassembled tetramer on the cell membrane held together by an interaction involving Jak1 (Regis *et al.*, 2006). Within this complex, IFNγR1 and IFNγR2 are constitutively associated with the inactive forms of the tyrosine kinases Jak1 and Jak2, respectively.

IFNγ binding, and subsequent rearrangement and dimerisation of the receptor subunits, results in the transactivation of Jak1 and Jak2. This then allows for the phosphorylation of Tyr440 on IFNγR1, generating a docking site for STAT1 (Platanias, 2005). After its recruitment, STAT1 is activated by phosphorylation at Tyr701, resulting in its homodimerisation and nuclear translocation. The STAT1

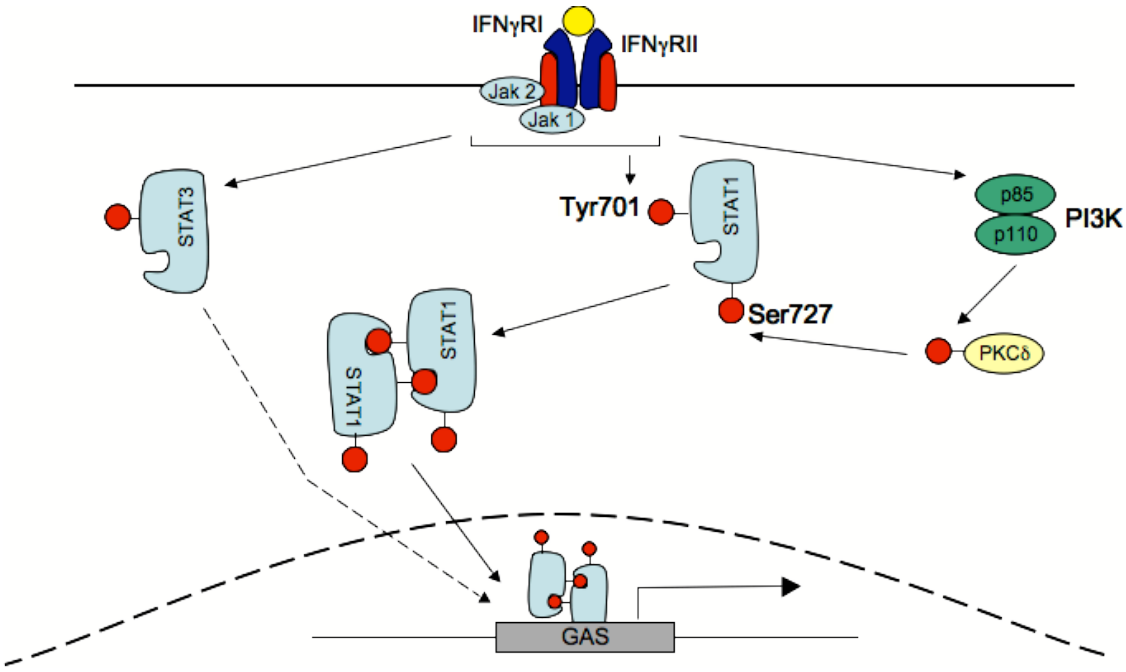

Fig 1.4. **IFNγ signalling pathway.** IFNγ binds to the receptor resulting in Jak 1 and 2 transactivation, phosphorylation of IFNγR1 and STAT1 recruitment. STAT1 homodimerises and translocates to the nucleus to regulate transcription. Supplementary pathways activate PI3K and its effector kinases AKT, MAPK, and PKCδ, which phosphorylate STAT1, potentiating its actions. Independent pathways also play a role including an IκB Kinase (IKK)-dependent, NFκB-independent pathway and STAT3 pathway. Adapted from Platanias et al 2005

dimers interact in the nucleus with specific DNA sequences called IFNγ-activated sequences (GAS). GAS are located in the promoter regions of IFNγ-stimulated genes (ISGs), and in this way regulate transcription (Fig 1.4) (Regis *et al.*, 2006; Sizemore *et al.*, 2004). Active STAT1 in the nucleus is acetylated by histone acetyltranserases (HATs), which flags STAT1 for dephosphorylation and therefore deactivation by the STAT1 phosphatase TCP45 (Kramer *et al.*, 2009). Dephosphorylated STAT1 shuttles back to the cytoplasm where histone deacetylases (HDACs) deacetylate STAT1, completing the phosphorylation – acetylation cycle (Kramer *et al.*, 2009).

Although STAT1 is essential for cells to respond fully to IFNγ there is accumulating evidence that several supplementary pathways function in parallel with JAK-STAT1 (Gough *et al.*, 2007; Platanias, 2005; Sizemore *et al.*, 2004). Moreover, the JAK-STAT pathway alone is not sufficient for the generation of all the biological

activities of IFNγ (for review see (Platanias, 2005)). Many of these supplementary pathways activate kinases, such as PI3K and its effector kinases Akt, MAPK, and PKCδ. These kinases are involved in the phosphorylation of serine 727 on STAT1 (Fig 1.4) (Gough *et al.*, 2007; Platanias, 2005) and potentiates the ability of STAT1 to activate gene transcription (Leon *et al.*, 2006).

However, ISGs can also be activated independently of STAT1 through various pathways, including the activation of an IκB Kinase (IKK)-dependent, NFκB-independent pathway. This pathway appears to be essential for the induction of a subset of ISGs, including inflammatory and antiviral responses, expression of MHC class I and growth control (Sizemore *et al.*, 2004). Furthermore, in the absence of STAT1, IFNγ can activate STAT3 which is able to drive the expression of some genes that normally respond to STAT1 (Qing & Stark, 2004). Nevertheless, the analysis of STAT1 deficient mice and cells over-expressing a constitutively active STAT1 mutant protein, demonstrate that STAT1 is required for most of the responses induced by IFNγ (Lu *et al.*, 1998; Qing & Stark, 2004).

1.2.2. Expression of IFNγ receptors

It has been demonstrated that the IFNγR1 chain is highly and uniformly expressed on T, B and myeloid cells, where as IFNγR2 chain is highly expressed on B cells and myeloid cells but has a limited expression on T cells (Bernabei *et al.*, 2001; Regis *et al.*, 2006). IFNγR2 levels appear to govern the ability of cells to respond to IFNγ, with an increase in IFNγR2 expression resulting in the switch from a proliferative to an apoptotic outcome following IFNγ stimulation. This is evident in $CD4^+$ Th1 cells where the low IFNγR2 chain expression elicits a response to IFNγ, with enhanced MHC class I expression and cell proliferation, but is unable to trigger the apoptotic pathway (Bernabei *et al.*, 2001; Lu *et al.*, 1998; Regis *et al.*, 2006).

1.2.3. Effects of IFNγ signalling

It is now recognised that IFNγ has pleiotropic immunomodulatory, antiviral, anti-neoplastic and pro-inflammatory activities (Bernabei *et al.*, 2001; Leon *et al.*, 2006; Regis *et al.*, 2006; Schroder *et al.*, 2004).

Initially thought to be produced exclusively by Th1 $CD4^+$ T cells, $CD8^+$ T cells and natural killer (NK) cells, there is now evidence that other cells including B cells, NKT cells and professional antigen presenting cells (APCs) may also secrete IFNγ. This production is controlled primarily through IL-12 and IL-18 secretion (for a review see (Frucht *et al.*, 2001)).

IFNγ has several important effects including up-regulation of cell surface MHC class I and class II, skewing of the immune response to a Th1 phenotype, up-regulation of adhesion molecules and chemokine expression, induction of key antiviral enzymes e.g. PKR, activation of microbicidal effector functions, apoptosis, cell growth inhibition and reduction of epithelial barrier function (Adams *et al.*, 1993; Bernabei *et al.*, 2001; Gough *et al.*, 2007; Schroder *et al.*, 2004; Steimle *et al.*, 1994). This is achieved through the activation of a variety of different ISGs with specificity achieved, in part, through the variation in availability of key signalling effectors (Rose *et al.*, 2007). IFNγ is also able to promote inflammatory processes through the inhibition of the anti-inflammatory cytokines IL-10 and TGFβ e.g. IFNγ induces the inhibitory Smad7 which binds to the TGFβ receptor complex, preventing its interaction and phosphorylation of Smad3, resulting in the loss of TGFβ signalling in the nucleas (Ulloa *et al.*, 1999). The inhibition of these molecules is thought to be an important mechanism to ensure effective pathogen clearance (Herrero *et al.*, 2003).

1.2.3.1 Role of IFNγ in Macrophages

IFNγ is thought to be one of the most important mediators for activating macrophages (Hu *et al.*, 2005). Indeed, exposure to IFNγ results in the altered expression of 25% of the genome (Ehrt *et al.*, 2001). This has downstream actions, which include the promotion of microbial killing, production of inflammatory mediators and antigen presentation (see review by (Schroder *et al.*, 2004)). Furthermore, IFN*γ* has the ability to "prime" macrophages for faster and heightened responses to LPS, other Toll-like receptor (TLR) ligands and other cytokines such as tumour necrosis factor (TNF) (Bundschuh *et al.*, 1997; Pace *et al.*, 1983; Sweet *et al.*, 1998). While some genes e.g. CpG -induced iNOS, require IFN*γ* priming for induction (Sweet *et al.*, 1998) in other cases IFNγ priming shifts the dose response

curve, so a lower concentration of TLR agonist can have an effect (Costelloe *et al.*, 1999). It is thought that IFNγ not only achieves this priming effect through the enhancement of positive TLR signalling (reviewed by (Schroder *et al.*, 2006)), but also by inhibiting TLR-induced negative feedback (Hu *et al.*, 2006).

1.2.3.2 Role of IFNγ in T cells

IFNγ is the major effector cytokine of Th1 immunity and is able to reinforce Th1 development as well as inhibiting Th2 and Th17 differentiation (Gajewski & Fitch, 1988; Harrington *et al.*, 2005). Initially evidence using the intracellular protozoan *Leishmania major* suggested that IFNγ played an important role in Th1 differentiation (Scott, 1991; Wang *et al.*, 1994). However, further work demonstrated that whilst IFNγ is crucial for the elimination of *L. major*, IFNγ mediated signals were not necessary for the differentiation of cells towards a Th1 phenotype (Swihart *et al.*, 1995). It has since been demonstrated that IFNγ enhances responsiveness to IL-12 in naïve T cells, thus increasing Th1 development, but is not vital for the development of a Th1 response (Wenner *et al.*, 1996).

Moreover, recently a more complex picture of IFNγ-mediated regulation of Th17 cells has emerged. Despite the ability of IFNγ to inhibit Th17 differentiation (Harrington *et al.*, 2005), it is now apparent that at many inflammatory sites T cells can co-express IFNγ and IL-17. This is thought to occur due to plasticity in the Th17 cell lineage, resulting in Th17 cells evolving to become IFNγ-expressing cells (Lee *et al.*, 2009). As well as IFNγ IL-17 double positive cells, it has also been demonstrated that IFNγ IL-10 double positive T cells can also be detected and it is proposed than these cells are important in governing the extent of APC activation (Anderson *et al.*, 2007; Jankovic *et al.*, 2007).

1.2.3.3. IFNγ homeostatic functions

As well as its pro-inflammatory effects, IFNγ also possess a number of important homeostatic functions, which limit inflammation-associated tissue damage. This is achieved, in part, through the attenuation of tissue destructive molecules e.g. matrix metalloproteinases (Ho *et al.*, 2008). Another important homeostatic mechanism is the attenuation of granulopoiesis and myelopoiesis (Matthys *et al.*, 1999). This has

been clearly demonstrated in IFNγ deficient mice which display a large expansion of macrophages and granulocytes upon exposure to mycobacteria (Murray *et al.*, 1998). This synergises with the IFNγ induced inhibition of chemokine production e.g. CXCL6 and suppression of adhesion molecule expression to alter the monocytes chemotactic response. These effects of IFNγ result in a decreased infiltration of neutrophils and monocytes into tissues (Hu *et al.*, 2008; Kelchtermans *et al.*, 2007).

1.2.4. IFNγ deficiency

Mice deficient in IFNγ, IFNγR1 or IFNγR2 develop normally and are fertile but demonstrate an increased susceptibly to microbial pathogens and parasites (Huang *et al.*, 1993; Lu *et al.*, 1998; Scharton-Kersten *et al.*, 1996). Moreover, IFNγR2 deficient mice display altered immunoglobulin class switching with B cells unable to class switch to IgG2a in response to IFNγ.

Dighe and colleagues created transgenic mice over-expressing a dominant negative IFNγR1 chain on either T cells or macrophages. This data suggests that Th1 cell development *in vivo* requires a functional IFNγ receptor on macrophages, but not on T cells (Dighe *et al.*, 1995). A similar method was subsequently adopted by Lykens and colleagues to create mice with "macrophages insensitive to IFNγ" (MIIG mice). These mice express a dominant negative IFNγR1 chain under the CD86 promoter and therefore have monocytes, macrophages, dendritic cells and mast cells unresponsive to IFNγ. Using this mouse model they were able to demonstrate impaired parasitic control and heightened mortality after *Trypanosoma cruzi*, *Leishmania major* and *Toxoplasma gondii* infection (Lykens *et al.*, 2010).

Additionally, humans with mutations in components of the IFNγ receptor-signalling pathway have been identified. Such individuals have profound immunodeficiency's, especially to intracellular bacterial infections, with some individuals dying in early childhood as a result of uncontrolled mycobacterial infections (for review see (Filipe-Santos *et al.*, 2006)).

1.3 INFLAMMATORY BOWEL DISEASE

Inflammatory Bowel Disease (IBD) is a chronic, relapsing, idiopathic inflammation of the gastrointestinal tract that causes significant morbidity. Clinical symptoms include weight loss, diarrhoea accompanied by blood, abdominal pain and malnutrition (Cho, 2008; Neuman, 2007) all of which can substantially affect a patient's quality of life, largely as a result of the psychosocial implications (Ghosh & Mitchell, 2007). An increased incidence of colorectal cancer is the most lethal, long-term complication of IBD (Jess *et al.*, 2006). This can be attributed to alterations in the intestinal epithelium that are initiated and, at least partially, sustained by chronic inflammation (Harpaz & Polydorides, 2010). However, recent data suggests that with current therapies the risk for developing IBD-related colorectal cancer is limited (Baars *et al.*, 2010).

There are estimated to be as many as 2.2 million people in Europe (Loftus, 2004) and 1 in 400 people in the UK affected by IBD (Butcher, 2007). As the peak onset age is early, between 15 and 30 years, IBD commonly requires a lifetime of care (Loftus *et al.*, 1998). Patients need to take regular medication, even when well, and make considerable lifestyle adaptations to reduce relapses and prevent complications (Nightingale, 2007). Current treatment strategies for IBD include corticosteroids, immunomodulators e.g. azathioprine and methotrexate and more recently some biological therapeutics (Strauch & Scholmerich, 2010). Treatment strategies aim to promote mucosal healing and maximise quality of life. However, even anti-TNF antibodies, the best biological treatment for IBD, are not effective in all patients, with remission only achieved in approximately 50% (Trinder & Lawrance, 2009).

The two main forms of IBD are Crohn's disease (CD) and ulcerative colitis (UC). They share many characteristics and end-stage effector pathways of tissue damage, but have distinct morphological, immunological and clinical features (Bouma & Strober, 2003; Peluso *et al.*, 2006). CD is characterised by non-caseating granulomas, lymphoid aggregates and extension of inflammation through all layers of the bowel wall. CD most commonly affects the ileum and colon but can involve

any region of the gut. By contrast, UC is characterised by mucosal inflammation and extensive ulcers, usually confined to the submucosa. UC always involves the rectum and, in some cases, the inflammation extends up to the caecum in a continuous pattern (Arihiro *et al.*, 2002; Cho, 2008; Podolsky, 2002). Currently, the pathogenesis of inflammatory bowel disease is poorly understood, but it is recognised to be complex and multi-factorial. Nevertheless, significant progress and insights have been made through the analysis of genetic, environmental and immunological factors - the main components thought to be involved in the establishment and development of IBD. The current hypothesis is that, both CD and UC, are due to an exaggerated or inappropriate response to normal gut bacterial flora that is, in part, genetically determined (see review by (Bouma & Strober, 2003; Monteleone *et al.*, 2006)).

1.3.1 The role of genetic susceptibility in inflammatory bowel disease

Epidemiological studies have made it clear that genetic factors play an important role in the pathogenesis of IBD, with multiplex IBD families and 5-10% of patients reporting a positive family history (Binder, 1998). Indeed, a positive family history is still the largest independent risk factor for IBD, with genetic factors playing a more

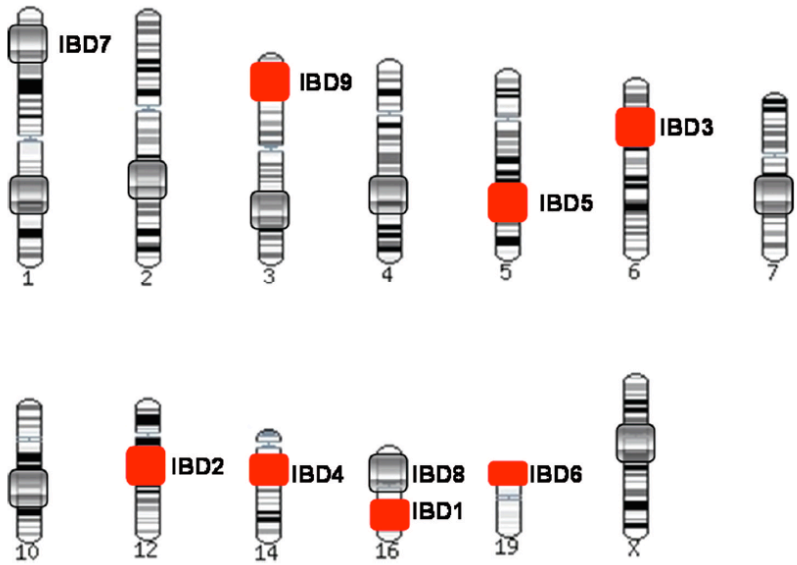

Fig 1.5 Inflammatory bowel disease susceptibility loci Susceptibility loci which have been identified in genome wide scans. Linkage Significance ■ Confirmed and replicated ▭ Other. Adapted from (Limbergen *et al.*, 2007)

prominent role in CD than UC (Hibi & Ogata, 2006). This has been demonstrated through epidemiological studies among affected twins, with a pooled concordance of 58% for CD and 18% for UC in monozygotic twins compared to 0% and 4% for CD and UC respectively in dizygotic twins (Orholm *et al.*, 2000). However, other studies have reported slightly different levels of concordance (Thompson *et al.*, 1996). Despite this variation UC and CD are both polygenic diseases and genomic wide scans have revealed susceptibility regions on several chromosomes (see Fig 1.5). In a few cases the gene or genes underlying the different chromosome loci, linked to IBD, have been identified. The first such gene to be identified was nucleotide-binding oligomerisation protein 2 (NOD2), a region on chromosome 16 associated with CD (Hugot *et al.*, 1996). Currently, the key candidate genes with which susceptibility to IBD is associated are NOD2, the human leukocyte antigen (HLA) region, multidrug resistance 1 (MDR-1), IL-23 receptor and autophagy-related 16-like 1 (ATG16L1), although there are many more putative IBD genes (Limbergen *et al.*, 2007). However, these genes still play a minor role in the pathogenesis of the disease. Based on the known epidemiology of IBD for every affected patient, carrying a single identified polymorphism, approximately 500 individuals with the same polymorphism are completely healthy (Marks & Segal, 2008). This clearly demonstrates other factors must play a role in the development of IBD.

1.3.2 The role of environmental triggers in inflammatory bowel disease

The commensal bacterial flora of the gut is the environmental factor most frequently implicated in the development of IBD. One hypothesis on the aetiology of IBD is that these diseases represent an aberrant, exaggerated immune response by the mucosal immune system to the normal constituents of the mucosal microflora (Bouma & Strober, 2003; Nieuwenhuis & Blumberg, 2006). In this situation the normal symbiotic relationship between commensal gut bacteria and the host is disrupted and exposure to luminal microflora triggers an inflammatory response. Research in animal models suggests that genetic alterations can result in varied responses to the same bacteria e.g. exposure to *Bacteriodes vulgatus* in IL-10 deficient mice results in minimal inflammation, whereas, the same bacteria causes severe inflammation in another model of IBD (HLA-B27 transgenic rats) (Rath *et*

al., 1996; Sellon *et al.*, 1998). Moreover, some bacteria are more capable of inducing gastrointestinal inflammation than others (Rath *et al.*, 2001). Similarly, in humans, it is thought that different bacteria may be responsible for the inflammatory effects seen in different patients, and it is believed unlikely that colitis development is attributable to a single member of the flora.

Despite the inability to identify (a) specific micro-organism(s) there is substantial evidence for their role in IBD. A lot of this evidence comes from mouse models where experimental colitis is less severe or does not develop when the animals are raised in a specific pathogen free (SPF) or a germ free environment respectively (Kuhn *et al.*, 1993; Rath *et al.*, 1996; Sellon *et al.*, 1998). Other studies in humans have demonstrated that the elimination of gut bacteria, using antibiotics or by diverting the fecal stream, is capable of controlling colonic inflammation in specific subgroups of patients with active IBD (Winslet *et al.*, 1994) and antibiotics attenuates colitis in IL-10 deficient mice (Winslet *et al.*, 1994; Zhang *et al.*, 2005). Therefore, when taken together, these experiments clearly highlight the importance of the gut microflora in IBD.

There are several other putative environmental risk factors for IBD including sugar rich foods and excessive sanitation (Baumgart & Carding, 2007; Hanauer, 2006). These risk factors are, in part, supported by epidemiological studies that demonstrate a higher incidence of IBD in industrialised countries and a dramatic increase during the last century (Hanauer, 2006; Loftus, 2004; Lopez-Serrano *et al.*, 2010). However, no clear conclusions have been made as to the role of nutrition, diet and sanitation in IBD. Another risk factor is smoking, which has been demonstrated to have deleterious effects in CD development but a protective effect in UC, although the mechanism for this is unclear (Nightingale, 2007).

1.3.3. The role of immune dysregulation in inflammatory bowel disease

Despite differences in the underlying genetic and environmental aetiology of IBD, an excessive immune response is seen in the gut wall. The traditional view is that IBD is

mediated by the adaptive immune system, however, there is increasing evidence suggesting that the innate immune system may play an important role.

1.3.3.1 Alterations in the intestinal epithelial barrier in inflammatory bowel disease

The first line of defence in the intestine is the epithelial barrier. Made up of gut epithelial cells, mucus producing goblet cells and defensin producing paneth cells, the epithelial barrier serves a vital function in the defensive system of gastrointestinal mucosal system. This cell layer acts as an immunologically inert barrier to the large amount of commensal bacteria found in the external environment, but is also required to mount innate and adaptive responses to invading pathogens (Sansonetti, 2004). In IBD, particularly CD, the epithelial barrier has been demonstrated to be leaky with increased permeability of the intestinal epithelium to specific molecular probes (Irvine & Marshall, 2000). Permeability fluctuates with disease severity (Miki *et al.*, 1998) and an increase in intestinal permeability is able to predict a relapse (Hilsden *et al.*, 1999), indicating the importance of epithelial integrity. Nevertheless, it remains unclear whether this process is a consequence of mucosal inflammation or is an early step in the pathogenesis of CD. Observations of elevated gut permeability among unaffected first degree relatives of patients with CD and increased epithelial permeability preceding diagnosis of CD suggests that a permeability defect may initiate the damage in IBD (Irvine & Marshall, 2000). It has been postulated this is mediated through alterations in epithelial tight junctions (Soderholm *et al.*, 2002). However, the increased permeability may also be, in part, a result of mucin abnormalities evident in both CD and UC patients (Buisine *et al.*, 2001; Smithson *et al.*, 1997). These patients appear to have enhanced mucin degradation and therefore increased exposure of the epithelium to microorganisms and their products.

As well as acting as a physical barrier, gut epithelial cells are able to recognise intestinal bacteria through toll like receptors (TLR) and alterations in TLR expression has been associated with IBD (Cario & Podolsky, 2000). TLRs in healthy patients play an important role in the innate immune system defence and homeostasis, and are involved in the protection of barrier integrity and elimination of

invading micro-organisms. However in IBD, TLRs may induce inappropriate signalling pathways resulting in an aggressive immune response with subsequent tissue injury and inflammation (Cario, 2007). Indeed, a strong up-regulation of TLR4 and TLR2 (Veres *et al.*, 2007) and a down-regulation of TLR3 expression has been demonstrated amongst CD patients. It is unclear whether these alterations are a cause or a consequence of the inflammation seen in the IBD gut (Cario & Podolsky, 2000). However, the recent observation by Veres and colleagues, that a similar TLR expression is seen in the non-inflamed mucosa of children with IBD suggests TLRs do not play a primary role in the development of IBD (Veres *et al.*, 2007).

1.3.3.2. Alterations in the cytokine milieu in inflammatory bowel disease

Activated gut epithelial cells are capable of producing pro-inflammatory cytokines which provide chemotactic signals and are able to induce cell adhesion molecule expression, aiding the accumulation of leukocytes into the inflamed tissue (Gulubova *et al.*, 2007). In IBD, increased levels of endothelial E-selectin (Bhatti *et al.*, 1998), P-selectin (Schurmann *et al.*, 1995), mucosal addressin cell adhesion molecule-1 (MAdCAM-1) (Arihiro *et al.*, 2002), intercellular cell adhesion molecule-1 (ICAM-1) and vascular cell adhesion molecule-1 (V-CAM1) (Gulubova *et al.*, 2007) have been reported together with increased numbers of lymphocyte function-associated antigen-1 (LFA-1), Mac-1 and very late antigen-4 (VLA-4) positive leukocytes in the inflamed tissue (Gulubova *et al.*, 2007). These changes play an important role in the pathogenesis of the disease with a significant correlation between the number of LFA-1, Mac-1, VLA-4 and ICAM-1 positive inflammatory cells and the disease activity of UC patients (Gulubova *et al.*, 2007). Moreover, neutralisation of MAdCAM-1 or its ligand $\alpha_4\beta_7$ integrin has been demonstrated to significantly reduce the severity of colonic inflammation in a $CD45RB^{hi}$ transfer model of colitis (Picarella *et al.*, 1997; Sydora *et al.*, 2002). However, β7 integrin deficiency in IL-2 deficient mice (Sydora *et al.*, 2002) and IL-10 deficient mice (W. Müller, personal communication) does not alter the development and course of the spontaneous colitis seen in these mice. These discrepancies may be a result of the initial differences in the number of pathogenic T cells in the colon (Sydora *et al.*, 2002). In the IL-2/ β7-integrin double deficient mice the local expansion of T cells appears to play a more

important role in the development of colitis than influx of T cells, whereas the converse is true for the $CD45RB^{hi}$ transfer model of colitis.

Nevertheless, the influx of leukocytes, mostly $CD4^+$ T lymphocytes, into the inflamed tissue (Peluso *et al.*, 2006) is believed to be an important step in the pathogenesis of IBD, despite the presence of some models of colitis which can occur in the absence of T cells e.g. in RAG knock-out mice. In both murine models of colitis and in human IBD the blockade of $CD4^+$ T cell activation or activity is able to limit inflammation (Fantini *et al.*, 2007). However, the nature of the infiltrating leukocytes is different in CD and UC. CD is characterised by a prototypic Th1 response, associated with an increase in secretion of IL-12 and IFNγ by isolated mucosal T cells (Parronchi *et al.*, 1997). Conversely, UC is often viewed as a Th2 condition with IL-5 playing a prominent role (Fuss *et al.*, 1996). However, a clear association with IL-4, the prototypic Th2 cytokine, has not been established (Fuss *et al.*, 1996).

1.3.3.3. The role of IL-23 in driving inflammatory bowel disease

IL-23 has been shown to play a key role in intestinal inflammation see in both innate and T cell mediated chronic colitis in mouse models (Hue *et al.*, 2006; Kullberg *et al.*, 2006; Uhlig *et al.*, 2006; Yen *et al.*, 2006) and in human diesease (Duerr *et al.*, 2006).

Mouse models have revealed that IL-23 plays a key role in driving intestinal inflammation mediated by both innate immune cells and T cells (Izcue *et al.*, 2008). Studies have demonstrated IL-23 depletion, using monoclonal antibodies specific for the p19 subunit of the IL-23 receptor, or by genetic deletion attenuates colitis in T cell transfer models (Hue *et al.*, 2006; Kullberg *et al.*, 2006). Depletion also inhibits the spontaneous colitis development normally seen in IL-10 deficient mice (Yen *et al.*, 2006). As well as its role in the adaptive immune system, IL-23 appears to be important in innate mechanisms of intestinal inflammation. This was demonstrated with recombination activating gene (RAG) knock-out mice where IL-23 is required for development of colitis following infection with *Helicobactuer hepaticus* (Hue *et*

al., 2006). In various IBD models it has been established that high levels of IL-23 expression are seen in the inflamed intestine but not in systemic sites and accordingly, systemic immune pathology is not altered by IL-23 depletion (Hue *et al.*, 2006; Uhlig *et al.*, 2006). The importance of IL-23 in mouse models of IBD is reflected in human IBD patients. This has been demonstrated through genome-wide association studies of CD patients and healthy controls (Maloy, 2008). These studies have uncovered several polymorphisms in the IL-23R gene locus, which are associated with either susceptibility or resistance to CD (Consortium, 2007; Duerr *et al.*, 2006).

Recently it has been demonstrated that IL-23 orchestrates intestinal inflammation through a direct effect on T cells. Using IL-23R-deficient $CD4^+$ T cells it has been demonstrated that IL-23 signalling in T cells is crucial for T cell proliferation and accumulation in the colon (Ahern *et al.*, 2010). IL-23 is also known to be important in the expansion and maintenance a novel subset of $CD4^+$ inflammatory T cells known as Th17 cells (Elson *et al.*, 2007; Hue *et al.*, 2006; Maloy, 2008). It is becoming clear that this recently identified T cell subset is responsible for many of the inflammatory responses once attributed to Th1 cells (Kikly *et al.*, 2006). IL-23 also promotes the development IL-$17A^+$IFN-γ^+ double-producing $CD4^+$ T cells and inhibits the induction of $Foxp3^+$ Treg cells (iTregs) in the gut (Ahern *et al.*, 2010; Izcue *et al.*, 2008). These IL-$17A^+$IFN-γ^+ $CD4^+$ T cells are seen in T cell-dependent colitis models (Hue *et al.*, 2006; Kullberg *et al.*, 2006), have been recovered from lesions of human CD patients and are thought to be highly pathogenic (Annunziato *et al.*, 2007). This, in combination with the inhibition of iTreg induction, results in chronic inflammation as the iTreg cells normally help to balance the effects of pathogenic effector T cells during inflammation (Izcue *et al.*, 2009).

1.3.4 Mouse models of inflammatory bowel disease

Mouse models of IBD have contributed to the recent progress in the understanding of mechanisms underlying CD and UC. The key characteristics desired for an optimal model include similar morphological alterations, inflammation, pathophysiology, course and response to treatment as human IBD. It is also preferential for the model

to be on a well-defined genetic background and to have a well-characterised immune response (see review by (Jurjus *et al.*, 2004)). Currently there are well over 50 mouse models used to study intestinal inflammation (Uhlig & Powrie, 2009) and the available models can be broadly divided into four categories: immune cell transfer, gene targeting, spontaneously occurring or chemically induced models (as defined by (Jurjus *et al.*, 2004; Wirtz & Neurath, 2007)).

The primary immune cell transfer model used to create an IBD-like pathology is the CD45RB transfer model. This model transfers $CD4^{+}CD45RB^{Hi}$ T cells isolated from the spleens of donor mice into severe combined immunodeficient (SCID) or RAG1/2 knock-out mice. These immunodeficient mice subsequently develop a wasting syndrome associated with transmural intestinal inflammation (Morrissey *et al.*, 1993).

The second category is gene targeted mice and an increasing number of these transgenic mice are being developed as IBD models, reflecting the heterogeneous nature of human IBD. These mice can be divided into three further categories according to the primary cause of disease onset: defect in epithelial integrity e.g. keratin 8 deficient mice and IKKγ mice; defects in innate immune cells e.g. STAT3 deficient mice, A20 deficient mice; or a defect in the adaptive immune response e.g. IL-10 deficient mice, TCRα deficient mice (Wirtz & Neurath, 2007). The IL-10 deficient mice have been extensively studied since initially described by Kuhn and colleagues (Kuhn *et al.*, 1993). As the colitis phenotype in the IL-10 deficient mice varies with the genetic background of the mice, quantitative trait loci studies of F2 generations have been performed. This has allowed the identification of colitis-modifying genes and has aiding in elucidating the complex genetics underlying susceptibility to IBD (Farmer *et al.*, 2001).

The third category is mice species which spontaneously develop an IBD-like disease without any exogenous manipulation e.g. C3H/HejBir mice (Sundberg *et al.*, 1994).

The final catergory are the inducible colitis models. These are some of the most commonly used animal models for IBD as the procedures are straightforward and onset of inflammation is uniform and immediate. These models include acetic acid-induced, iodoacetamide-induced, indomethacin-induced, 2,4,6-trinitrobenzene sulphonic acid (TNBS)-induced, oxazolone-induced and dextran sodium sulphate (DSS)-induced colitis.

1.3.4.1 Dextran sodium sulphate-induced colitis

Colitis induced by the oral administration of DSS in mice was first described in 1990 by Okayasu and colleagues (Okayasu *et al.*, 1990). It is now established as a reproducible model of acute and chronic colitis with morphological changes corresponding well to the clinical signs of human ulcerative colitis (Okayasu *et al.*, 1990). The acute colitis is characterised by bloody diarrhoea, colonic mucosal inflammation with ulcerations, body weight loss, shortening of the intestine and infiltration of neutrophils (Jurjus *et al.*, 2004; Melgar *et al.*, 2005). Chronic colitis develops several weeks after the cessation of 3-5 cycles of DSS administration and is characterised by the infiltration of chronic inflammatory cells into the mucosa and regenerative changes in the epithelium (Dieleman *et al.*, 1998; Melgar *et al.*, 2005).

Interestingly, Dieleman and colleagues (Dieleman *et al.*, 1994) demonstrated that SCID mice, without T and B cells, were able to develop acute DSS-induced colitis. This suggests that adaptive immunity is not essential in the acute phase of this model (Melgar *et al.*, 2005) and the colitis is thought to be mediated by neutrophils and macrophages.

The mechanism by which DSS induces colitis is unclear, however, several mechanisms have been proposed. These include a direct toxic effect on the epithelium, increased exposure to luminal antigens by destruction of mucin content or altered macrophage function due to ingestion of DSS (Kitajima *et al.*, 1999; Ni *et al.*, 1996; Okayasu *et al.*, 1990). A toxic effect on the epithelium was first observed by Ni and colleagues, who demonstrated a concentration dependent toxicity of DSS on intestinal epithelial cells (Ni *et al.*, 1996). This was supported by experiments

demonstrating that the earliest histological feature observed in DSS-induced colitis is the loss of crypt followed by a separation of the crypt base from the muscularis mucosa (Kitajima *et al.*, 1999). This injury to the colonic epithelium would increase permeability of the intestine therefore, allowing the uptake of bacterial products into the submucosal tissue (Ito *et al.*, 2006; Okayasu *et al.*, 1990). It has also been shown that the DSS is phagocytosed by macrophages in the inflamed mucosa, mesenteric lymph node (MLN) and spleen during the chronic phase of DSS-induced colitis (Okayasu *et al.*, 1990). This may increase susceptibility to luminal bacterial invasion during colitis by preventing the macrophages from ingesting the microbes (Ito *et al.*, 2006; Kitajima *et al.*, 1999).

Acute DSS induced colitis model is a useful model to study the contribution of the innate immune system to colitis development, whereas T cells may play an important role in the chronic and regenerative phases (Dieleman *et al.*, 1998). DSS induced colitis has also been shown to be a relevant model for the translation of data from mice to humans. The therapeutic agents cyclosporine A (CsA), anti-IL-12p40 and anti-CD3 ameliorated the inflammatory response seen in DSS colitis in a similar manner to effects seen in human IBD patients (Melgar *et al.*, 2008). In light of this data it has been suggested the DSS induced colitis model is a useful model for the validation of new therapies for the treatment of IBD.

1.3.5 IFNγ and murine models of colitis

IFNγ receptor deficient mice have been tested in two models of colitis with differing results. In TNBS-induced colitis IFNγR deficient mice appeared pathologically similar to wild type mice (Camoglio *et al.*, 2000; Tozawa *et al.*, 2003). However, in a DSS-induced model of colitis IFNγR deficient mice and treatment of wild-type with anti-IFNγ antibodies attenuated colitis (Ito *et al.*, 2006; Obermeier *et al.*, 1999). This suggests IFNγ may play an important role in, at least, the DSS-induced model of colitis.

1.4 INTESTINAL NEMATODE INFECTION

Gastrointestinal nematodes (also know as round worms) cause some of the most prevalent and chronic human diseases worldwide. Soil-transmitted helminth (STH) and shistosome infections account for more than 40% of the global burden of all tropical diseases excluding malaria (WHO, 1999). STH infections are caused by infection with intestinal nematodes, in particular, *Ascaris lumbricoides,* the whipworm *Trichuris trichiura* and the hookworms *Ancylostoma duodenale* and *Necator americanus*. It is estimated that 4.5 billion people are a risk of STH infection and that the global burden due to STH infection is between 4.5 and 39 million disability-adjusted life years (DALYs) (Keiser & Utzinger, 2008).

There are currently four anthelminthics recommended by the World Health Organisation for the treatment of STH infections. However, efficacies against the different nematodes vary and there is concern that large-scale administration of anthelminthics might result in the development and spread of drug-resistant nematodes (Keiser & Utzinger, 2008). Moreover, even when anthelminthic drugs effectively clear the parasite patients are often re-infected from the environment. Therefore, the development of long-term immunological intervention strategies e.g. vaccines are being extensively researched, however, despite progress there is still no vaccine available against STH infections (for review see (Loukas *et al.*, 2006)).

1.4.1 Trichuris trichiura

Trichuris trichiura (*T. trichiura*) is most common in warm, moist, tropical and subtropical countries, where over 90% of children can be infected in some areas (Stephenson *et al.*, 2000). It is estimated 1050 million people are infected with *T. trichiura* and it causes morbidity in 220 million (Crompton, 1999). Heavy *T. trichiura* infection can cause Trichuris dysentery syndrome (TDS) resulting in chronic dysentery, rectal prolapse, anaemia, poor growth and clubbing of the fingers (Stephenson *et al.*, 2000). *T. trichuria* infection has also been reported to have a detrimental impact on a child's cognitive function (Nokes & Bundy, 1992) and can impair locomotor development (Callender *et al.*, 1992). The consequences of these symptoms are decreased school attendance and ultimately life long reduced

productivity. Indeed, the world bank estimates that intestinal helminth infections account for 16.7 million DALYs lost and is the main cause of disease burden in children 5-14 years of age in developing economies (Montresor A, 2002; World Bank, 1993).

The currently available anthelminthics have a particularly low efficacy when used for *T. trichiura* treatment. After treatment with a single dose of albendazole the risk of still being infected is only reduced 28% compared with approximately 90% for *A. lumbricoides* (Keiser & Utzinger, 2008).

1.4.2 Trichuris muris

The naturally occurring mouse counterpart, *Trichuris muris* (*T. muris*), is a powerful model for *T. trichiura,* and research in this area has provided a lot of information on the immune response to this parasite (Cliffe *et al.*, 2005; Else *et al.*, 1994; Helmby & Grencis, 2003; Liu *et al.*, 2006).

T. muris is transmitted by a faeco-oral route through the ingestion of infective eggs. These infective eggs are larvae in the L1 stage where they can remain infective for many months or years (deSchoolmeester & Else, 2002; Wakelin, 1969). Once ingested, the eggs hatch in the distal ileum, where the bacterial load and temperature provides the optimum conditions to trigger egg hatching (Hayes *et al.*, 2010). After hatching, the larvae penetrate into the epithelium (Helmby & Grencis, 2003) forming syncytical tunnels within which the parasites resides throughout infection (Cliffe *et al.*, 2005). The larvae moult through several stages at approximately days 9-11, 20-21 and 28 post infection (p.i.), before becoming adult by day 35 p.i. (see Fig 1.6) (Panesar, 1989; Wakelin, 1969). Adult worms have their anterior end embedded within the epithelium and their posterior end free in the intestinal lumen, allowing copulation and release of eggs. The eggs are then released into the environment within the faeces and take approximately 2 months to embryonate, become infective and able to restart the sequence.

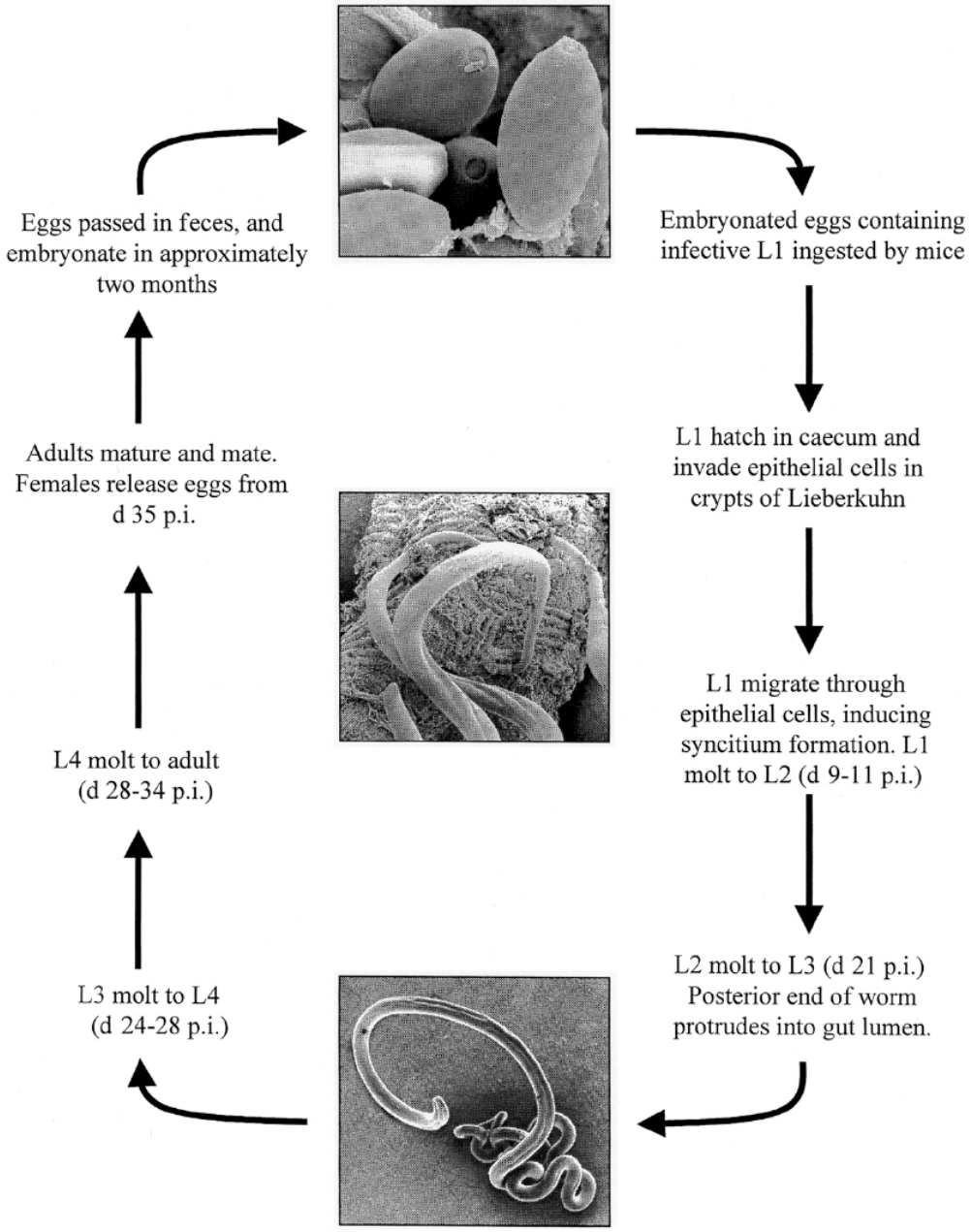

Fig 1.6 *T. muris* life cycle. L1 larvae remain infective for months and once ingested hatch in the large intestine. The larvae then moult through several sages at approximately day 10, 20 and 28 post infection (p.i.) before becoming adult at day 35 p.i. Adapted from (deSchoolmeester & Else, 2002)

T. muris, as observed in humans with variability in susceptibility to *T. trichiura*, causes chronic infections in some mouse strains and is expelled in others (Schopf *et al.*, 2002).

1.4.2.1 The role of T cells in *T. muris* infection

The importance of T cells in resistance to *T. muris* infection was initially demonstrated in experiments where the transfer of a T cell enriched population from infected mice was able to transfer protection to recipient mice (Lee *et al.*, 1983). This was then verified in experiments using nude mice where resistance to the parasite could be restored through lymphoid cell transfer (Ito, 1991). Further work identified the $CD4^+$ T cell compartment as vital for the expulsion of *T. muris* (Else & Grencis, 1996). Moreover, the $CD4^+$ cells are important in the larval stages of the infection, as transferring cells into an established adult infection in SCID mice was unable to restore resistance.

1.4.2.1.1 T helper cell subsets in *T. muris* infection

The type of $CD4^+$ T helper cell response, developed to *T. muris*, is critical to infection outcome (Else & deSchoolmeester, 2003; Else *et al.*, 1994; Helmby & Grencis, 2003). A Th2 response, with high levels of IL-4, IL-5, IL-9, IL-13 and other Th2 cytokines is associated with host protection. In contrast, a Th1 response with the induction of IFNγ, IL-18 and IL-12 is associated with susceptibility to infection (Cliffe *et al.*, 2005; Else & deSchoolmeester, 2003; Else *et al.*, 1994; Liu *et al.*, 2006). Hence, resistant strains such as BALB/K, BALB/c and 129, which expel *T. muris* in larval stages between 14 and 21 days post infection, mount a Th2 response (Schopf *et al.*, 2002). Conversely, susceptible strains such as AKR mice that are unable to expel the parasite and harbour chronic infections, mount an inappropriate Th1 response (Artis *et al.*, 1999; Cliffe *et al.*, 2005; Helmby & Grencis, 2003).

T helper 1 subset

Susceptibility to *T. muris* is not due to the inability to mount an immune response but rather the generation of an inappropriate immune response, with high levels of Th1 cytokines. The role of type 1 cytokines in susceptibility has been clearly

demonstrated, as normally susceptible mice can clear an infection following depletion of IFNγ (Else *et al.*, 1994) or IL-12 (Grencis, 2001), with an expansion of type 2 responses. Furthermore, the administration of recombinant IL-12 to normally resistant mice results in the generation of a type 1 response to *T. muris* and the development of a chronic infection (Bancroft *et al.*, 1997).

Another important cytokine involved in the promotion of a type 1 immune response is IL-18 (Okamura *et al.*, 1995). IL-18 has been demonstrated to be important in *T. muris* infection with the appearance of IL-18 mRNA in the intestines of infected susceptible mice even before the appearance of IL-12 (Helmby *et al.*, 2001). Moreover, IL-18 knock-out mice rapidly expelled their worm burdens (faster than IL-12 knock-out mice). However, surprisingly, the IFNγ response in IL-18 KO mice corresponds to the IFNγ response seen in wild type mice. Indeed, IL-18, instead of functioning as an IFNγ-inducer during *T. muris* infection, acts as a direct regulator of Th2 cytokines such as IL-13 and IL-4 (Helmby *et al.*, 2001).

Recently it has been demonstrated that IL-27, a cytokine with close structural and functional activity to IL-12, can also promote a Th1 response. During *T. muris* infection IL-27/WSX-1 interactions are increased in susceptible mice compared to resistant mice and WSX-1 deficient mice are resistant to *T. muris.* This resistance to infection is associated with a down-regulation of the type 1 immune response and an increased type 2 response (Bancroft *et al.*, 2004). Furthermore, it has been demonstrated that IL-27 signalling involves the common IL-6 receptor subunit gp130. In IL-10 deficient mice, that are normally highly susceptible to *T. muris*, the conditional inactivation of gp130 on T cells results in rapid worm expulsion. This is associated with the up-regulation of regulatory T cells and the development of a strong Th2 polarised response, thought be dependent on IL-27 (Fasnacht *et al.*, 2009).

During *T. muris* infection, in susceptible animals, IFNγ production is increased and this is essential for progression to chronic infection (Cliffe *et al.*, 2005). Indeed, attenuated pathology is seen in SCID mice following anti- IFNγ treatment (Artis *et*

al., 1999). IFNγ is known to drive epithelial cell proliferation and induces CXCL10 production, which, in turn, slows cell movement up the crypt. This promotes crypt cell hyperplasia and increases the epithelial niche that the parasite occupies (Artis *et al.*, 1999; Cliffe *et al.*, 2005; deSchoolmeester *et al.*, 2006).

The importance of IFNγ in driving susceptibility to *T. muris* is demonstrated by the kinetics of worm expulsion in IFN-γ KO and IFN-γ receptor KO mice. These mice display a very early production of type 2 cytokines following infection and more rapid worm expulsion than wild type control animals (unpublished observations in review by (Grencis, 2001)).

T helper 2 subset

The type 2 cytokines have been demonstrated to play an important role in the expulsion of *T. muris*. Studies have demonstrated that blockade of the IL-4 receptor, in normally resistant mice, results in the production of a type 1 immune response and development of a chronic infection. Conversely, the administration of IL-4 to a susceptible mouse, early in infection, expands the type 2 response and results in clearance of the infection (Else *et al.*, 1994). This phenotype has been confirmed using IL-4 knock-out mice, which, dependant on the background strain and sex of mouse, don't generate a type 2 response and are susceptible to infection (Bancroft *et al.*, 2000).

However, there is also an important, IL-4 independent, role of IL-13. This was identified in female IL-4 KO mice on a BALB/c background, which are still able to expel the parasite. However, neutralisation of IL-13 in these mice leads to the establishment of a chronic infection (Bancroft *et al.*, 2000). It has since been demonstrated that IL-13 is important in enhancing the rate of epithelial cell turnover. This can mediate worm expulsion as elevating the rate of epithelial cell turnover is sufficient to displace parasites from the intestine (Cliffe *et al.*, 2005).

The precise mechanism through which the Th2 immune response is able to mediate the expulsion of *T. muris* is not fully understood, although the increase in the

epithelial escalator by IL-13 is thought to play a key role. It has been demonstrated that worm expulsion can occur even in the absence of classical Th2 effector mechanisms such as eosinophilia and mastocytosis (Betts & Else, 1999). Recently RELMβ, a highly specific Th2 cytokine, has been suggested to have an important role in worm expulsion with maximum expression correlating with host protective immunity. It is thought that this is mediated through RELMβ disrupting the ability of *T. muris* to sense their environment (Artis *et al.*, 2004). However, RELMβ null mice are still able to expel *T. muris*, which again demonstrates the redundancy of the responses mounted against the parasites (Artis & Grencis, 2008).

Regulatory T cells

It has become clear over recent years that parasites also stimulate suppressive T-cell populations, termed regulatory T cells (Tregs). Tregs can produce IL-10 and TGFβ, switching off inflammatory immune responses and down regulating effector T cell activation. In *T. muris* it has been demonstrated that there is an association between the presence of Foxp3+ Tregs and the survival of the parasite (D'Elia *et al.*, 2009). These Foxp3+ cells appear to be involved in the control of pathological immune responses as, deletion of these cells results in increased gut pathology following *T. muris* infection (D'Elia *et al.*, 2009).

The importance of IL-10 production during *T. muris* infection has been demonstrated with global IL-10 and IL-10R1 deficient mice. Both of these mutant mice have elevated worm burdens, generate a strong Th1 and Th17 response and display increased intestinal inflammation following *T. muris* infection (Pils *et al.*, 2010b). This increased inflammatory response eventually results in death of the animals due to the breakdown of epithelial barrier function. It has been shown that it is T-cell derived IL-10 that has a vital role in infection outcome through the inhibition Th1 immune responses following infection and the promotion Th2 development (Fasnacht, 2008). The important cells responding to IL-10 is not fully known as the T cell specific deletion of IL-10R1 displays similar expulsion kinetics to wild type mice. Moreover, although deletion of IL-10R1 in monocytes, macrophages and neutrophils leads to higher worm burdens at day 21 p.i., the mice are still resistant to

the parasite and expel before day 35 p.i.. Thus, IL-10 plays an important role in regulation of the Th1 immune response but neither T-cells nor monocytes/macrophages and neutrophils alone are the crucial targets of IL-10 (Pils *et al.*, 2010b).

1.4.2.2 The role of B cells in *T. muris* infection

The role of B cells and antibodies in the expulsion of *T. muris* has been thoroughly investigated, however the data is somewhat contradictory. Initial experiments demonstrated that serum from previously infected mice can transfer some degree of immunity to recipient animals (Selby & Wakelin, 1973). Moreover, parasite specific IgA is capable of transferring immunity (Roach *et al.*, 1991). Further experiments utilising μMT mice, which are deficient in functional B cells, have reinforced the role of B cells in protection against *T. muris* infection. These mice are highly susceptible to infection and the administration of *T. muris* specific IgG1 antibodies from resistant mice is sufficient to prevent worm establishment (Blackwell & Else, 2001). However, there is a wealth contradictory data, which suggests that antibody production isn't important in worm expulsion. Indeed, the transfer of a B cell enriched population from infected mice is insufficient to alter worm expulsion (Lee *et al.*, 1983). Moreover, FcγR deficient mice, which are incapable of binding IgE or IgG and therefore can't generate antibody dependent mediated cytotoxicity (ADCC), are resistant to infection and display similar expulsion kinetics to wild type mice (Betts & Else, 1999). Currently, the general consensus is, that while B cells and antibody responses aren't vital for *T. muris* resistance they play an important role in the protection again secondary infections. It is worth noting that whilst laboratory infections look predominantly at primary infections naturally infected animals are like to be infected multiple times and therefore protection against secondary infections is extremely important.

1.4.2.3 The role of macrophages in *T. muris* infection

The vital role of macrophages in nematode infections has been demonstrated in other models of helminth infection. Experiments using clodronate-loaded liposomes to deplete macrophages *in vivo* has demonstrated a central role for macrophages during

N. brasiliensis (Zhao *et al.*, 2008) and secondary *H. polygyrus* infections (Anthony *et al.*, 2006). Parasite clearance in these models, like in *T. muris*, is dependent on the generation of a Th2 response and the depletion of macrophages prevents worm expulsion.

In *T. muris* infection it has been demonstrated that large numbers of macrophages are found in the intestines of mice infected with *T. muris* (Little *et al.*, 2005) and there is a larger accumulation of macrophages in the lamina propria of resistant mice than susceptible mice (deSchoolmeester *et al.*, 2003). It has been proposed that macrophages may play an important role in the phagocytosis of dead or dying cells and foreign material during infection and the decreased numbers of macrophages in the intestine of susceptible mice may lead to a more chronic inflammatory response due to the decreased phagocytosis. A second role proposed for macrophages during *T. muris* infection is the stimulation of antigen specific T cells in the draining lymph nodes of infected mice (deSchoolmeester *et al.*, 2003). Recent data has demonstrated that macrophage depletion doesn't alter parasite survival but has a profound influence of inflammation in the intestine with no inflammation observed in macrophage-depleted mice (M. Little, personal communication).

1.4.2.4. The role of goblet cells in *T. muris* infection

Goblet cells secrete mucus into the intestinal environment protecting the intestinal epithelium. A marked goblet cell hyperplasia is seen during *T. muris* infection regardless of susceptibility to the parasite but an increase in Muc2 expression in the caecum correlates with worm expulsion. Indeed, Muc2-deficient mice demonstrate a significant delay in worm expulsion despite unaltered adaptive immune responses (Hasnain *et al.*, 2010). This demonstrates that the mucus barrier is an important component of the immune response in the gut to *T. muris* and appears to act independently of the adaptive immune system.

1.4.2.5 The importance of parasite burden and parasite-derived factors in *T. muris* infection

An important factor in determining the susceptibility to *T. muris* is the level of infection. Mice which are normally resistant, and able to expel a high level infection, if subjected instead to a low level infection become susceptible and chronic infections are established (Wakelin, 1973). Furthermore, once a mouse has expelled the parasite it is resistant to subsequent challenges whether they are high or low level infection. Conversely, if you are susceptible to a primary infection, either through the administration of a high or low dose infection, you are primed for susceptibility on further challenges (Bancroft *et al.*, 2001).

As well as the level of infection the parasite genetics have an important role in the outcome of infection. There are currently 3 isolates of *T. muris*, which are used in the laboratory. The E isolate obtained from house mice in Edinburgh in 1954 (Wakelin, 1967), the E-J or J isolate (a subculture of the E isolate maintained in Japan since 1969, (Ito, 1991)) and the S isolate obtained from house mice in Sobreda, Portugal in 1992 (Bellaby *et al.*, 1995). These 3 isolates show different expulsion kinetics in mice with B10.BR mice harbouring chronic infections with the S strain and expelling the E-J isolate before the E isolate (Koyama & Ito, 1996). These differences in expulsion kinetics are thought to be due to the different immune responses provoked by the different isolates. The S isolate excretory/secretory (E/S) proteins have been demonstrated to induce higher levels of IL-12, IL-10 and IL-6 by antigen presenting cells than the E-J or E isolate E/S proteins (D'Elia & Else, 2009; Johnston *et al.*, 2005). Indeed, the E/S proteins of *T. muris* are being investigated and it has been demonstrated that these secreted proteins can interact with the host immune response. One protein that has been isolated from the *T. muris* E/S proteins is a 43kDa *T. muris*-derived protein that shares epitopes with IFNγ. This protein has been demonstrated to be capable of binding IFNγ receptors on host cells and inducing cellular changes similar to those induced by IFNγ. This has been proposed to enable the parasite to drive the host immune response to mount an inappropriate Th1 response and promote it's own survival (Grencis & Entwistle, 1997).

Given the clear association between expulsion of the parasite and the generation of a Th2-skewed immune response, the *T. muris* model is a powerful model for investigation alterations in the host's adaptive immune response. It has previously be demonstrated that IFNγ or IFNγR1 deficient mice demonstrate accelerated expulsion kinetics following the administration of a high dose *T. muris* infection (unpublished observations in review by (Grencis, 2001)). However, it remains to be determined if they are capable of expelling a low dose infection and which cells are the key in responding to IFNγ and altering susceptibility to *T. muris* infection.

1.5 MULTIPLE SCLEROSIS

Multiple sclerosis (MS) is a devastating chronic neurological disease which affects approximately 2 million people worldwide (Zivadinov *et al.*, 2003) including approximately 85,000 in the United Kingdom (Leary *et al.*, 2005) and is the leading cause of disability in young adults. The disease also has a considerable social and economic impact, despite its relatively limited prevalence, due to its long duration and high incidence among young adults. It is estimated that the annual cost in the United Kingdom of MS is £1.34 billion, with costs per person increasing in proportion to the disability they suffer (Kobelt *et al.*, 2000). Globally and in the United Kingdom there is a north-south discrepancy in prevalence rates, with prevalence in south-east Scotland over twice the rates seen in England and Wales, and female:male ratio of between 2.2 and 2.8 (Pugliatti *et al.*, 2006)

MS has been identified as an autoimmune inflammatory disorder in which T cells play a pivotal role. MS results in characteristic areas of demyelination within the central nervous system (Kerstetter *et al.*; Tyas *et al.*, 2007). The accumulation of these MS lesions over time results in progressive neurological deficits such as pain, cognitive impairment, visual and sensory disturbances, limb weakness, gait problems, bladder and bowel symptoms and ultimately failure of axonal conduction and permanent disability in patients (Bjartmar & Trapp, 2003; Kerstetter *et al.*).

The aetiology of the disease is unknown, but the key event in the development of MS is thought to be the breakdown of immune tolerance to central nervous system (CNS) self-antigens in genetically susceptible individuals (David *et al.*, 2005; Frohman *et al.*, 2006; Hafler *et al.*, 2005; Zozulya & Wiendl, 2008). The importance of genetics has been demonstrated through the concordance of the occurrence of disease of 30% in monozygotic twins and 3% in siblings of patients with MS (Sadovnick *et al.*, 1996). These genetic studies have demonstrated the human leukocyte antigen (HLA) region as the only major gene locus associated with MS. *HLA-DR1501* and *HLA-DQ0601* are both associated with 2-4 fold increased risk of developing MS (Olerup & Hillert, 1991).

1.5.1 Types of MS

MS presents with a wide variety of symptoms, which can be broadly classified into 4 groups according to their disease course (see Fig 1.7)

(i) relapsing remitting MS (RRMS): the most common type of MS affecting 85% of MS patients (Leary *et al.*, 2005). RRMS presents with the acute onset of symptoms from which people recover partially or fully and then relapses occur at irregular intervals. When recovery from relapses is incomplete people can accumulate a neurological deficit and disability.

(ii) Secondary progressive MS (SPMS): over time (normally approximately 15 years) a large proportion of people with RRMS enter a secondary progressive stage with the gradual accumulation of irreversible neurological deficit and disability. During this phase they can continue to have relapses.

(iii) Primary progressive MS (PPMS): characterised by a progressive disease from the onset with no relapses and accounts for 10-15% of MS patients (Leary *et al.*, 2005). The average age of onset appears to be later than RRMS – approximately 40 years old with an more equal male:female ratio (Thompson *et al.*, 1997)

(iv) Progressive relapsing MS (PRMS): a progressive disease from the onset with superimposed relapses, although the progressive disease is predominant. Largely similar to PPMS with 10-15% of PPMS patients showing superimposed relapses

1.5.2 MS therapy

Although a lot of progress has been made in MS research, there are still no optimal therapies available to slow or halt disease progression (Hemmer *et al.*, 2006). NICE guidelines recommend that acute relapses are treated with corticosteroids as there is evidence that it accelerates the recovery from a relapse, although the mechanism of action is unknown (Leary *et al.*, 2005). Several immunoprophylactic therapies are available, however, their efficacy at modifying disease course is limited and they are

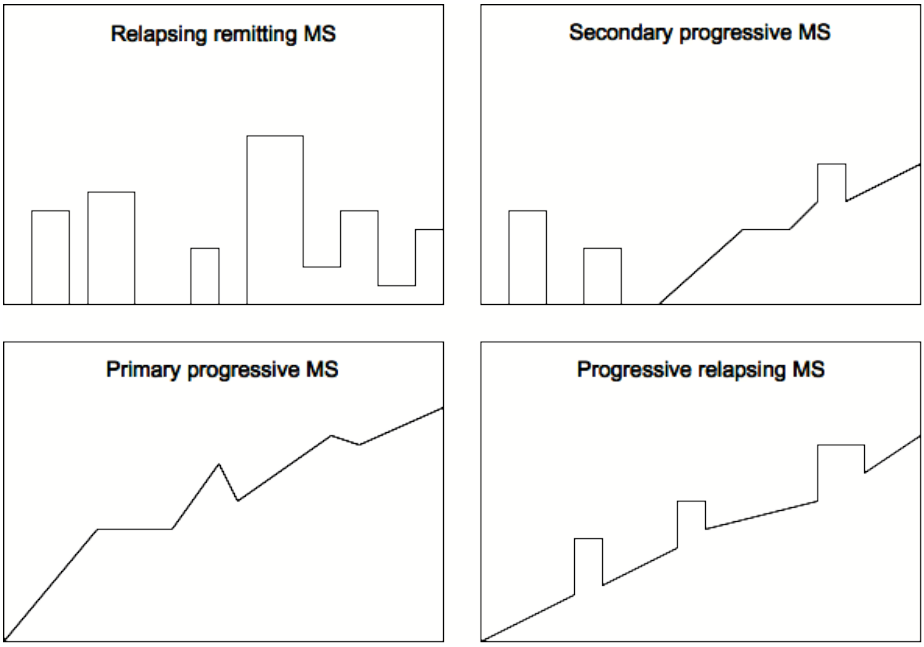

Fig 1.7 Types of multiple sclerosis. A. Relapsing remitting MS with acute onset of symptoms and recovery at irregular intervals **B.** Secondary progressive MS with a gradual accumulation of disability **C.** Primary progressive MS a progressive disease with no relapses **D.** Progressive relapsing MS a progressive disease with superimposed relapses. Adapted from (Lublin & Reingold, 1996)

often accompanied by severe side effects (Pugliatti *et al.*, 2006)

1.5.3 Experiment autoimmune encephalomyelitis

Experimental autoimmune encephalomyelitis (EAE) is an inflammatory disease of the CNS and is currently the most commonly used animal model for the study of MS (Peiris *et al.*, 2007). This model causes clinical symptoms (spontaneous relapses and remissions) and histological manifestations, which closely parallel the human disease (Espejo *et al.*, 2001; Kerstetter *et al.*; Swanborg, 1995).

Active EAE is induced in susceptible animals through immunisation by the subcutaneous injection of an encephalitogenic peptide, normally myelin oligodendrocyte glycoprotein $(MOG)_{35-55}$ or proteolipid protein $(PLP)_{139-151}$ emulsified in complete Freund's adjuvant (CFA), followed by the intraperitoneal injection of pertussis toxin. The other widely used model of EAE is adoptive transfer EAE. Adoptive transfer EAE is induced through the adoptive transfer of activated myelin specific T cells into naïve animals (Goverman, 2009; Steinman & Zamvil,

2006). Different mouse strains and methods of immunisation can result in different disease courses, mimicking some of the different disease progressions seen in MS. For example, immunisation of SJL mice with MOG (with or without the pertussis adjuvant) induces a relapsing remitting EAE whereas MOG immunisation of A.SW mice induces a primary progressive disease course, if immunised without pertussis, or a secondary progressive disease course if pertussis is used (Tsunoda *et al.*, 2000).

1.5.3.1 Pathogenic CD4+ T cells in EAE

The widespread demyelination seen in EAE is the result of a $CD4^+$ T-cell-mediated immune response directed at the myelin sheath within the CNS. Upon activation, $CD4^+$ T cells can differentiate into different effector cells, dependent on the priming immune synapse and cytokines present (Gutcher & Becher, 2007). For many years, IFNγ-secreting Th1 cells were believed to be the pathogenic population central to the autoimmune pathogenesis of EAE and MS (Steinman *et al.*, 2002). Indeed, several observations supported these proposals including experiments demonstrating that cells invading the central nervous system (CNS) during EAE produced IFNγ and other Th1 cytokines (Renno *et al.*, 1995). Moreover, EAE can be induced by the adoptive transfer of encephalitogenic Th1 cells (Gutcher & Becher, 2007; Pettinelli & McFarlin, 1981). Furthermore, the administration of IFNγ to MS patients exacerbates symptoms (Panitch *et al.*, 1987) and levels of IFNγ produced in MS patients in response to PLP and MBP (putative MS autoantigens) correlates with worsening of disease symptoms (Moldovan *et al.*, 2003).

However, the role of IFNγ and other Th1 cytokines has been challenged by the observation that, contrary to expectations, the loss of the major Th1 cytokines, IFNγ, IL-12, and IL-18 does not protect against disease development (Becher *et al.*, 2002; Gutcher *et al.*, 2006; Willenborg *et al.*, 1996). In fact, IFNγ and IL-12 deficiency leads to more severe inflammation in EAE (Becher *et al.*, 2002; Ferber *et al.*, 1996; Willenborg *et al.*, 1996). Therefore, the notion that Th1 cells and Th1 associated cytokines are the instigators of autoimmunity has been re-examined (Haak *et al.*, 2009).

More recently, Th17 cells have been highlighted to have an increased encephalitogenic potential compared to Th1 cells (Langrish *et al.*, 2005). This was demonstrated through IL-23 deficient mice that are completely resistant to EAE, and IL-23 is crucial for Th17 cell development (Cua *et al.*, 2003). However, despite increased levels of IL-17 transcripts in chronic MS lesions (Lock *et al.*, 2002) and the ability of transferred Th17 cells to induce EAE, IL-17a and IL-17f deficient mice remain susceptible to EAE (Haak *et al.*, 2009). Indeed, even anti–IL-17A–treated *Il-17f*$^{-/-}$ mice appear to be fully susceptible to EAE. This suggests that while Th17 cells are associated with an encephalitogenic state, neither IL-17A nor IL-17F appear to have a substantial pathogenic function *in vivo* (Haak *et al.*, 2009).

It is now apparent that both Th1 and Th17 cells can play a pathogenic role in EAE. Indeed, in has been demonstrated that Th1 cells can promote inflammation in the CNS, modifying the conditions to make it more attractive and accessible for Th17 cells to infiltrate the EAE lesions (O'Connor *et al.*, 2008). Adoptive transfer of Th1 or Th17 polarised MOG-specific T cells are both capable of mediating similar clinical symptoms. However, they display a different composition and positioning of infiltrating leukocytes, as Th17 cells home preferentially to the brain resulting in atypical EAE and Th1 cells home preferentially to the spinal cord resulting in classical EAE symptoms (Kroenke *et al.*, 2008; Stromnes *et al.*, 2008). Moreover, Th1-mediated disease is characterised by an infiltration composed primarily of macrophages, whereas in Th17-mediated disease the infiltrate is primarily neutrophils (Kroenke *et al.*, 2008).

To add another layer of complexity to the role of these populations it has now been demonstrated that IFNγ^+ IL-17$^+$ dual producing cells are significantly increased in MS patients in acute relapse, but not during remission. Moreover, these double producers can preferentially cross the blood brain barrier (BBB) due to the synergistic effect of IFNγ up-regulating the expression of ICAM-1 on BBB-endothelial cells and IL-17 disrupting the BBB (Kebir *et al.*, 2009).

1.5.3.2. The role of IFNγ in EAE

The role of IFNγ in the pathogenesis of CNS inflammation has been extremely controversial. It's function as a pro-inflammatory cytokine is clear in some cases, as treatment of MS with IFNγ leads to significant disease worsening (Panitch *et al.*, 1987). Furthermore, the direct injection of IFNγ into normal rat CNS produces inflammation (Sethna & Lampson, 1991; Simmons & Willenborg, 1990). However, i.v. injection of IFNγ can inhibits EAE in rats (Voorthuis *et al.*, 1990) and administration of anti-IFNγ antibodies exacerbates EAE in mice (Billiau *et al.*, 1988; Duong *et al.*, 1994).

These experiments have led to the hypothesis that IFNγ may have different CNS and peripheral actions. In particular it was proposed that peripheral circulating IFNγ may act to inhibit antigen triggered T cell proliferation but induces inflammation in tissues (Krakowski & Owens, 1996). This is supported by experiments which have demonstrated elevated T cell proliferation in IFNγ knock-out mice suggesting a reduced ability to down regulate T cell responses (Dalton *et al.*, 1993). Furthermore, IFNγ has been shown to have several pro-inflammatory actions in the CNS including activation of resident microglia and infiltrating macrophage cells. As well as, the ability to induce MHC class II and co-stimulatory molecule expression in astrocytes (Nikcevich *et al.*, 1997), which all culminate in increased tissue injury (Goverman, 2009; Krakowski & Owens, 1996). Moreover, IFNγ expression in the mature CNS under the control of an oligodendrocyte-specific promoter resulted in the development of demyeliniation, gliosis and inflammation (Horwitz *et al.*, 1997).

However, more recent studies using the adoptive transfer EAE model have provided slightly contradictory results as, the transfer of encephalitogenic cells into WT mice results in spinal cord inflammation but the transfer of the same cells into IFNγR deficient mice led to inflammation specifically in the brain (Lees *et al.*, 2008). The conclusion drawn from this data was that IFNγ activation in the spinal cord results in inflammation but IFNγR signalling in brain resident cells leads to an inhibition of inflammation (Lees *et al.*, 2008).

Therefore, there are still a lot of discrepancies in the literature about the role of IFNγ and Th17 cells in EAE and MS that need further investigation.

1.6 THE AIMS AND STRUCTURE OF THIS THESIS: FUNCTIONAL ANALYSIS OF THE ROLE OF IFNγ IN DSS-INDUCED COLITIS, *T. MURIS* AND EAE

The importance of IFNγ in many mouse models is well established, primarily through the use of IFNγ or IFNγR mutant mice. However, little is known about the specific cells, which are responsible for the pleiotropic effects of this cytokine. The generation of a conditional knockout IFNγR2 mouse will allow the dissection of the IFNγ network and clarification of the role of IFNγ in these *in vivo* models.

The DSS-induced colitis system is a well-defined acute colitis model that has been shown to be IFNγ-dependent and driven by innate immunity. This will provide a good model to investigate the role of IFNγ in innate-cell driven intestinal inflammatory responses. In contrast, the *T. muris* model is known to rely on the adaptive immune system with the generation of a Th2-biased immune response vital for resistance to the parasite. This model will allow the investigation of IFNγ responding cells in adaptive intestinal immunity. Finally, the role of IFNγ in EAE has been widely investigated but with somewhat contradictory results, therefore this system is a good mechanism to finally dissect the role of IFNγ in EAE.

My hypotheses are stated in the introduction of each chapter and the overall aims of my thesis are:

1. To generate a global-, T cell- and macrophage-specific knockout of IFNγR2. The results of chapter 3 describe the breeding and genotyping performed to generate these mice and the *in vitro* functional confirmation of abrogation of IFNγ signalling. Finally, the phenotype of unchallenged complete IFNγR2 deficient mice is assessed

2. To examine the role of IFNγ in the innate-driven model of DSS-induced colitis. The results of chapter 4 describe *in vivo* studies using the IFNγR2 deficient mice subject to DSS-induced colitis.
3. To investigate the role of IFNγ in *T. muris* infection and to dissect the cells responsible for the effects of IFNγ during infection. The results of chapter 5 describe *in vivo* studies using the IFNγR2$^{\Delta/\Delta}$, IFNγR2$^{fl/fl}$, IFNγR2$^{fl/fl}$CD4Cre^{+}, IFNγR2$^{fl/fl}$LysMCre^{+} and IFNγR2$^{fl/fl}$CD4Cre^{+}LysMCre^{+} mice during low dose *T. muris* infection.
4. To investigate the role of IFNγ during EAE and to try and elucidate the mechanisms behind the different EAE phenotypes seen in the IFNγR2-deficient animals. The results in chapter 6 describe studies performed during time at a collaborators laboratory in Zurich examining the IFNγR2 knock-out mice in EAE.

The results of this thesis demonstrate the successful characterisation of an IFNγR2 global and conditional knock-out mouse mutant and the phenotype of these animals in several *in vivo* models. Some of the data obtained during this work contradicts existing published data. The novel discoveries and their implications will be analysed in the following chapters.

CHAPTER TWO

Materials and Methods

2.1 ANIMALS

An overview of the mice strains and abbreviations used in this thesis is given in Table 2.1. All mice were imported from the Helmholtz Centre for Infection Research, Braunschweig, Germany. Imported mice were colonised with the Charles River altered Schaedler flora (CRASF®) which has been demonstrated to remain stable for years when mice are housed in individually ventilated cages (Stehr *et al.*, 2009). At the University of Manchester mice were kept in the Biological Services Unit in individually ventilated cages. The mice were sacrificed by schedule 1 methods in accordance with the animals (scientific procedures) act 1986. All experiments were performed under Project Licence (4032/17) and all breeding under Project Licence (4031/67) granted by the Home Office (U.K.) and conducted in accordance with University of Manchester guidelines.

For all EAE experiments mice were exported to the University of Zurich where mice were maintained in individually ventilated cages and treated according to institutional guidelines for animal care and use. Animal experiments undertaken at the University of Zurich were approved by the Swiss Veterinary Office.

Sex-matched mice 6-9 weeks old were used for all experiments.

Complete Designation	**Abbreviation**	**Functional abberation**	**Reference**
C57BL/6J	B6	wildtype	-
C57BL/6J;129-Ifngr2^{tm1HZI}	IFNγR2$^{fl/fl}$	IFNγR2 flox	unpublished
C57BL/6J;129-Ifngr2^{tm2HZI}	IFNγR2$^{\Delta/\Delta}$	IFNγR2 knock-out	unpublished
C57BL/6J-*Tg(CD4-cre)1Cwi*/J	CD4-Cre	T cell Cre expression	(Lee *et al.*, 2001)
C57BL/6JP2-*Lzm-s2*$^{tm1(cre)Cgn}$	LysM-Cre	Macrophage/neutrophils Cre expression	(Clausen *et al.*, 1999)
C57BL/6J-*Tg(KRT14-cre)1Cgn*	K14-Cre	Oocytes, keratinocytes Cre expression	(Hafner *et al.*, 2004)

Table 2.1 Mouse strains used for breeding and experiments. All mice were imported from the Helmholtz Centre for Infection Research, Braunschweig, Germany and maintained at the University of Manchester in accordance with the animals (scientific procedures) act of 1986.

2.1.1 Genotyping

2.1.1.1. Isolation of genomic DNA

A portion of a mouse tail or mouse ear punches were digested at 54°C overnight in 200µl tail-lysis buffer (appendix A) and 2µl proteinase K (Promega, 10mg/ml). Cell debris and fur were separated by centrifugation at 12,000g for 10min. The supernatant was transferred into a new tube and stored at 4°C.

2.1.1.2. Genotyping using PCR

To genotype IFNγR2 mice and the different *Cre* mouse strains the following PCR protocols were applied. The genotype was confirmed by a duplicate PCR from a second genomic DNA isolate, performed post-autopsy, for all mice that were used experimentally. Primers were ordered from Eurofins-MWG Operon (0.01µmol scale HPSF purification) and made up to a concentration of 10pmol/µl. All primers are represented in the 5' to 3' orientation. Subsequent to PCR, the products were subjected to gel electrophoresis on ethidium bromide (Sigma-Aldrich) or SafeView (NBS Biologicals) stained 2% agarose gels (Lonza).

Mastermix A: Bio-X-Act short acting DNA polymerase:

2.5µl	10xPCR Buffer, 15mM MgCl2 (Bioline)
0.5µl	10mM dNTPs (Bioline)
1.0µl	50mM MgCl2 (Bioline)
1.0µl	Primer **A**, 10pmol/µl
1.0µl	Primer **B**, 10pmol/µl
0.25µl	Bio-X-Act Polymerase (Bioline)
17.75µl	Nuclease free water (Ambion)
1µl	template DNA

PCR-Programme A:

1. 95°C	5min
2. 95°C	60sec
3. annealing temperature	60sec
4. 68°C	40sec
5. go to 2:	34x
6. 68°C	5min
7. 4°C	for ever

Mastermix B: AmpliTaq Gold polymerase

2.5µl	10xPCR Buffer, 15mM MgCl2 (Applied Biosystems)
0.5µl	10mM dNTPs (Bioline)
0.5µl	50mM MgCl2 (Applied Biosystems)
0.5µl	Primer **A**, 10pmol/µl
0.5µl	Primer **B**, 10pmol/µl
0.5µl	AmpliTaq Gold Polymerase (Applied Biosystems)
19µl	Nuclease free water (Ambion)
1µl	template DNA

PCR-Programme B:

1. 94°C	1min
2. 94°C	30sec
3. annealing temperature	30sec
4. 72°C	30sec
5. go to 2:	34x
6. 72°C	5min
7. 4°C	for ever

Detection of the IFNγR2 flox allele

To differentiate between IFNγR2fl/fl, IFNγR2fl/wt and IFNγR2wt/wt mice a PCR was performed using the Bio-X-Act polymerase (mastermix A) and the following 3-primer approach

Primers:	**LoxP1**	5' – TGA GTT CCA AGC AAG ACA GA – 3'
	LoxPsite	5' – AAG TTA TGG TCT GAG CTC GC – 3'
	LoxP2	5' – CAG GGT AGA AAA GAT GTG CA – 3'

Product: IFNγR2 flox allele: 392bp and 191 bp

IFNγR2 WT allele: 358 bp

All other PCRs were performed using a standard 2-primer approach as detailed below:

Gene	**Primers**	Polymerase	Product size	Annealing temperature
Neomycin resistance cassette	**neo-1** 5`- CTG TCC GGT GCC CTG AAT GA-3` **neo-2** 5`- TGG TCG AAT GGG CAG GTA GC -3`	Amplitaq gold	248bp	61.8°C
IFNγR2 Delta allele	**delta-1** 5`- TGA GTT CCA AGC AAG ACA GAG CC -3` **delta-2** 5`- GTA GAA TGC GGC CGC GTT TA -3`	Amplitaq gold	278bp	55°C
IFNγR2 wild-type allele	**wt-1** 5'- CCC ATC TGT CCC TCT GCT TGT -3' **wt-2** 5'- AGA GCC CAT GTG GTC GGA TT -3'	Amplitaq gold	198bp	52°C
Non specific *Cre*	**cretot-1** 5`- CTG TCC GGT GCC CTG AAT GA -3` **cretot-2** 5`- CTC GAC CAG TTT AGT TAC CC-3`	Amplitaq gold	350bp	60°C
CD4 specific *Cre*	**cd4cre-1** 5`-ACC AAC AAG AGC TCA AGG AGA CCA-3` **cd4ccre-2** 5`-GAT GAG TTG CTT CAA AAA TCC CTT CCA-3`	Bio-X-Act	900bp	60°C
LysM specific *Cre*	**lysM-1** 5`-GTA TGC TTA TTC TTG GGC TGC CAG A-3` **lysM-2** 5`-CCC AGA AAT GCC AGA TTA CG-3`	Bio-X-Act	800bp	60°C

Table 2.2 Paired primers used in genotyping PCRs. Product lengths given in base pairs. All primers were purchased from MWG. IFNγR and neo PCRs were designed using Vector NTi software. *Cre* primer sequences were provided by previous members of W. Müller's lab (Braunschweig, Germany) or by A. Roers (Dresden, Germany).

2.2 EXPERIMENTAL MODELS

2.2.1. Infection with *Trichuris muris*

Infections with *T. muris* were carried out at the University of Manchester. 20-25 viable E isolate *T. muris* eggs (provided by Prof. Else, University of Manchester) were counted into a volume of 200µl and give to mice by oral gavage using a metal 20 gauge needle. At specified days post infection (p.i.) the mice were sacrificed by carbon dioxide (CO_2) asphyxiation. At autopsy serum was harvested, mesenteric lymph nodes excised, a snip of the proximal colon removed and fixed in paraffin, and the remaining caecum and colon frozen for worm counts.

2.2.2. Induction of colitis using DSS

Induction of DSS-colitis was carried out at the University of Manchester. A solution

containing DSS (MP Biomedicals, MW: 36,000-50,000) in sterilized water was used to induce colitis in mice. Drinking water containing the specified percentage of DSS was given for 7 days (unless specified) *ad libitum*. The DSS treatment period was followed by 3 days of normal drinking water. During the entire period, bodyweight and clinical symptoms for each mouse were assessed daily. If any mouse lost more than 20% body weight, compared to untreated mice, they were euthanised. At day 10, mice were sacrificed by CO2 asphyxiation. Serum was harvested, the entire colon was excised, measured and rolled up in a "Swiss roll" for histology. The 'swiss roll' was an adaptation of the method described by Moolenbeek and Ruitenberg. In contrast to the small intestine they describe, we did not divide the colon into sections and rolled up the entire length of the colon without opening it longitudinally and cleaning (Moolenbeek & Ruitenberg, 1981).

2.2.2.1. Clinical scoring for colitis

Clinical scoring was used to monitor the health of DSS-treated mice for animal welfare reasons. The following symptoms were assessed: diarrhoea, occult blood in the faeces and behaviour. Diarrhoea was graded from 1 to 3 for mild, moderate and severe. Low amounts of blood visible in faeces resulted in a grade of 1, moderate amounts were graded as 2 and if blood was visible around the anus the resulting score was 3. The behaviour of the animal was graded as 1 if piloerection was visible. Mild apathy and a hunchback position resulted in a behaviour score of 2. Moderate to severe apathy was graded as 3. Macroscopically visible inflammation of the intestine was graded upon autopsy. A grade of 1 was assigned if faeces were not well formed, 2 if swelling was present or 3 if swelling and hyperaemia were present.

2.2.3. Induction of EAE

The induction of EAE was performed at the University of Zurich. Mice were immunised subcutaneously with 200 g of MOG (35–55) (MEVGWYRSPFSRVVHLYRNGK, GenScript) emulsified in complete Freund's adjuvant (CFA, Difco). Mice received 200ng pertussis toxin (Sigma-Aldrich) intra-peritoneally at the time of immunisation and 48 hours later. During the entire period clinical symptoms for each mouse were assessed daily (see Table 2.3). Any mouse

scoring 3 or more for 7 days, 3.5 or more for 3 days or a score of 4 was euthanised. Additionally, once a score of 1.5 was achieved food and drink was provided inside the cage. At day 21-25 post immunisation, mice were sacrificed by CO_2 asphyxiation. Mice were perfused with PBS through the heart before the brain and spinal cord were excised.

2.2.3.1. Clinical scoring for EAE

Classical EAE scoring system

Score	Clinical symptoms	Assessment
0	No detectable signs of EAE	
0.5	Distal limp tail	
1.0	Complete limp tail	
1.5	Limp tail and hind limb weakness	One leg occasionally falls through the grid
2.0	Unilateral partial hind limb paralysis	One leg consistently falls through the grid
2.5	Bilateral partial hind limb paralysis	Cage grid test bilaterally positive
3.0	Complete bilateral hind limb paralysis	
3.5	Complete bilateral hind limb paralysis and partial forelimb paralysis	
4.0	Moribund (mouse completely paralyzed)	
5.0	Dead	

Table 2.3 Clinical Scoring system used to assess the severity of EAE. Mice were assessed daily for the development of clinical symptoms of EAE.

Mice displaying atypical EAE were scored according to the following system. A score of 0.5 was assigned when, upon suspension by the tail, an asymmetrical rotation of the body was observed. A score of 1.0 was given when a clear tilting of the head was observed when mice were placed onto a flat surface, this increased to a score of 2.0 when the head and body were both tilted. Finally, a score of 3.0 was assigned when the mice displayed evidence of vertigo and were incapable of walking in a straight line.

2.2.4. Serum analysis

Blood samples were harvested directly from the heart upon necropsy. The blood was left for a minimum of 1 hour at 37°C to clot and serum isolated by centrifugation at 5,000x*g* for 8min twice. The serum was then isolated and stored at -80°C.

2.3 HISTOLOGY

Caecum sections and/or colon sections, whole colon or brain and spinal cord were removed and fixed with 4% formalin or, if specified, adapted neutral buffered formalin (NBF) fixative (see Appendix A) for 24-48 hrs. Fixed tissues were dehydrated through a graded series of ethanol, cleared in xylol and infiltrated with paraffin in a dehydration automat (Citadel 2000, Shandon) using a standard protocol. Specimens were embedded in paraffin (Histocentre2, Shandon), sectioned on a microtome (5µm sections) and allowed to dry for a minimum of 4 hours at 37°C. Prior to staining slides were deparaffinised with citroclear and rehydrated through alcohol (100% to 50%) to PBS or water.

2.3.1. Hematoxylin-eosin (H&E) staining

H&E staining was performed by placing slides in harris hematoxylin (Sigma-Aldrich) for 3min. After washing in tap water and differentiation in acidified alcohol (1% HCl (Sigma-Aldrich) in 70% ethanol) for 10 secs, sections were counterstained with eosin (Merck) for 4min. The sections were washed in tap water and dehydrated in ethanol, followed by citroclear and mounted using Depex mountant (BDH Laboratory Supplies).

2.3.1.1. Histological score – longitudinal colon

Histological scoring was used to evaluate the severity of colitis in DSS-treated mice microscopically using H&E stained sections. The method was adapted in the lab of Werner Muller (HZI, Braunschweig) from the TJL-score, developed for scoring colitis in mice by The Jackson Laboratory (Bleich *et al.*, 2004). The colon was divided into a proximal (oral), middle and distal (aboral) section, each of approximately the same size. The three sections were scored for the general criteria: severity, degree of ulceration, degree of oedema and percentage of area involved.

The grading was performed blinded to the genetic status of the animals. Grades applied for severity were 0 = no alterations, 1 = mild, 2 = moderate, 3 = severe alterations. Focally small or widely separated multi-focal areas of inflammation limited to the lamina propria were graded as mild lesions (1). Multi-focal or locally extensive areas of inflammation extending to the submucosa were graded as moderate lesions (2). If the inflammation extended to all layers of the intestinal wall or the entire intestinal epithelium was destroyed, lesions were graded as severe (3). Ulceration was graded as: 0 = no ulcer, 1 = 1-2 ulcers (involving up to a total of 20 crypts), 2 = 1-4 ulcers (involving a total of 20-40 crypts) and 3 = any ulcers that exceed the previous. Oedema was graded as 1 if only mild epithelial or submucosal oedema (less than the muscular layer in thickness) was present. Mild epithelial oedema associated with mild submucosal oedema or more moderate submucosal oedema (1 to 2 times as thick as the muscular layer) was graded as 2. Every oedema more extensive than the previous was graded as 3.

A 10% scale was used to estimate the area involved into the inflammatory process. 0 = 0%, 1 = 30%, 2 = 40% -70%, 3 = > 70%. The scores were added up to a total of up to 12 per section and the scores of the three sections to a total of up to 36 per colon sample.

2.3.1.2. Histological score – transverse colon

Sections were scored from 0-3 for each of the following parameters – severity of inflammation, degree of ulceration, degree of oedema and percentage of area involved. Each parameter was defined as above (Section 2.3.1.1)

2.3.1.3. Colon measurements

The measurement of crypt depth was performed on digital photomicrographs of H&E stained sections taken at 100 × magnification. A minimum of 20 measurements of crypt depth were taken, from 3 sections evenly distributed across the specimen, using ImageJ software (http://rsb.info.nih.gov/ij).

2.3.2. Goblet cell staining

Mucins in goblet cells were stained with 1% alcian blue (Sigma-Aldrich) in 3%

acetic acid (Sigma-Aldrich, pH 2.5) for 5 mins. Sections were washed in distilled water and treated with 1% periodic acid, 5mins (Sigma-Aldrich). Following washes in distilled water, tap water (5mins) and a rinse in distilled water sections were treated with Schiff's reagent (Vicker's Laboratories) for 15mins. Slides were again washed in distilled water, tap water (5 mins) and rinsed in distilled water before counterstaining in Mayer's haematoxylin (Sigma-Aldrich). Slides were blued in tap water, dehydrated and mounted in depex mounting medium (BDH Laboratory Supplies). Goblet cells were stained blue (acid mucins), magenta (neutral mucins) or purple (acid / neutral mixed mucins) with grey/blue nuclei**.** For enumeration of goblet cell staining, the average number of cells from 20 crypts was taken from three different sections per mouse.

2.3.3. Arginase 1 immunohistochemistry

Endogenous peroxidase activity was blocked for 20 min with methanol containing 0.005% hydrogen peroxide (Sigma-Aldrich) at 4°C. Sections were then washed in PBS, incubated in pepsin digest-all^{TM} 3 (Zymed Laboratories) at 37°C for 10mins to unmask antigens, washed in PBS and endogenous avidin and biotin biding sites blocked using a commercial kit according to the manufacturer's instructions (Vector Laboratories). The sections were incubated at room temperature for 1 h with mouse Ig blocking reagent from Vector mouse-on-mouse (M.O.M.) Basic Immunodetection kit according to the manufacturer's instructions (Vector Laboratories). Sections were washed in PBS and incubated for 10 mins in M.O.M. diluent before incubation for 30mins with anti mouse Arginase-1 (BD biosciences, 1:500). Sections were washed in PBS and incubated for 10mins in M.O.M. biotinylated anti-mouse IgG reagent. A Vectastain Elite avidin-biotin-peroxidase complex kit, followed by a 3,3'-diaminobenzidine (DAB) chromagen kit, were then used according to the manufacturer's instructions (Vector Laboratories). The sections were counterstained in Hematoxylin QS (Vector Laboratires), dehydrated and mounted. Slides were blinded and positive cells counted in a minimum of 20 crypts from 3 sections evenly distributed across the specimen.

2.3.4. CD3, F4/80, CD45 and IBA-1 immunohistochemistry

Endogenous peroxidase activity was blocked for 20 min with methanol containing

0.005% hydrogen peroxide at 4°C. Sections were then washed in PBS, incubated in pepsin digest-all™ 3 (Zymed Laboratories) at 37°C for 10mins to unmask antigens for CD3 and F4/80 staining or were boiled in citrate buffer (see Appendix A) for 2 mins and left to cool for 10 mins in the case of CD45 and IBA-1 staining. Slides were then washed in PBS and endogenous avidin and biotin binding sites blocked using a commercial kit according to the manufacturer's instructions (Vector Laboratories). The sections were incubated at room temperature for 1 h in 7% goat serum (Vecor Laboratories; for CD3 and IBA-1) or 7% rat serum (Sigma-Aldrich; for F4/80 and CD45), washed and incubated overnight at 4°C with primary antibody (CD45 (1:1400, AbD serotec), IBA-1 (1:1000, Wako), CD3 (1:100, DAKO), biotin-F4/80 (1:25, AbD serotec)). Sections were washed and incubated with goat anti-rat (for CD45) or goat anti-rabbit (for CD3, IBA-1) secondary antibodies (Jackson ImmunoResearch) for 1 hour at room temperature (no secondary antibody was applied to the biotin-F4/80 antibody). A Vectastain Elite avidin-biotin-peroxidase complex kit, followed by a DAB chromagen kit, were then used according to the manufacturer's instructions (Vector Laboratories). The sections were counterstained in Hematoxylin QS (Vector Laboratires), dehydrated and mounted. Slides were blinded and positive cells counted in a minimum of 20 crypts from 3 sections evenly distributed across the specimen.

2.3.5. Scoring of microglial activation

Microglial activation was scored on IBA-1 stained sections in ten x1000 fields of view based on a morphological criteria adapted from (Sanchez-Guajardo *et al.*, 2010). Four cellular profiles were defined as: Score 1: cells with no visible cytoplasm, a round dense nucleus and long thin processes with little branching – deemed 'resting' microglia. Score 2: cells with a visible thin cytoplasm surrounding a dense nucleus and long, mainly thin processes with many branches. Score 3: enlarged and irregular body with less defined nucleus and shorter processes of increased thickness with little branching. Score 4: large cell body, predominately occupied by the cell nucleus with only a few thick and short processes.

2.4 ISOLATION OF CELLS

2.4.1 Isolation of cells from the spleen

The spleen was excised from mice and placed in complete RPMI (see Appendix A). The spleen was then homogenized by passing through a 100µm cell strainer (BD Biosciences). After centrifugation at 250x*g* for 5mins, the cell pellet was incubated for 10min at room temperature with 3ml lysing buffer (BD Pharm Lyse™, BD Biosciences) for erythrolysis. The suspension was then washed and resuspended in complete RPMI.

2.4.2 Isolation of cells from lymph nodes

The lymph nodes were excised from mice and placed in complete RPMI. The lymph nodes were homogenized by passing through a 100µm cell strainer. After centrifugation at 250x*g* for 5 mins, the cell pellet was washed twice and resuspended in complete RPMI.

2.4.3 Isolation of T cells

To isolate T cells the pan T cell isolation kit (Miltenyi Biotec) was used. Cells were isolated from spleen and/or lymph nodes (see sections 2.4.1 and 2.4.2) and resuspended in 40µl MACS buffer (Appendix A) per 10^7 cells. 10µl of Biotin-Antibody cocktail was added per 10^7 cells and incubated for 10 minutes at 4°C. 30µl MACS buffer and 20 µl of anti-biotin microbeads were added per 10^7 total cells and incubated for a further 15 minutes at 4°C. Cells were washed with MACS buffer and resuspended in 500 µl of MACS buffer per 10^8 cells. LS columns were prepared by rinsing with 3ml MACS buffer before adding the cells. The unlabelled T cell enriched effluent was collected and the column washed three times with 3ml of MACS buffer. The labelled non T-cells were then eluted by removing the column from the magnetic field and flushing out the cells using 5ml of MACS buffer. The T cell purity was assessed before and after isolation by FACS analysis.

2.4.4 Isolation of Peritoneal Lavage Cells

Peritoneal lavage cells were isolated by injecting 5ml of complete RPMI into the

mouse peritoneal cavity, gently agitating the fluid and aspirating. This was performed twice. Cells were then centrifuged, at 250x*g* for 5mins, resuspended in red blood cell lysis buffer (BD Pharm Lyse™, BD Biosciences) for 5mins before washing, counting and plating out at 2 x10^6cells/ml. Cells were left for a minimum of 2 hours to adhere before removing the supernatant (and non-adherent contaminating cells). Cells were and stimulated with IFNγ (eBioscience, 0 or 100ng/ml, 20mins) to analyse STAT1 phosphorylation or ± LPS (Sigma-Aldrich; 100ng/ml) ± IFNγ (eBioscience, 50ng/ml) ± IL-4 (Peprotech, 50ng/ml), for 24 hours at 37°C, 5% CO2 to analyse macrophage activation.

2.5 RE-STIMULATION OF MESENTERIC LYMPH NODE CELLS

Mesenteric lymph nodes were isolated (see section 2.4.2), plated at 5x10^6 cells/ml and re-stimulated with 50 μg/ml parasite E/S antigen (provided by Prof. Else, University of Manchester) at 37°C, 5% CO2 for 48 hrs. Supernatants were harvested and stored at –20°C until use.

2.6 RNA EXTRACTION AND RT-PCR

Upon sacrifice mice colon sections were place in tubes containing 1ml of Trizol (Invitrogen) and immersed in liquid nitrogen before storing at -80°C. Tissue samples homogenised using a FastPrep homogeniser (MP biologicals) and cell debris pelleted by centrifuging at 8500xg for 10min at 4°C. The resulting tissue homogenate supernatant was added to 0.2ml chloroform (Sigma-Aldrich) and vigorously shaken for 15 seconds. Samples were left for 3mins at room temperature before centrifuging at 8500xg for 15mins at 4°C. The RNA containing aqueous phase was the precipitated using 0.5ml isopropanol (Sigma-Aldrich) and incubated at room temperature for 10mins. RNA was pelleted by centrifuging at 8500xg for 10mins at 4°C. RNA pellets were washed in 75% ethanol (Sigma-Aldrich), air-dried, resuspended in 40μl RNAse/DNAse free water (Ambion) and stored at -80°C. The concentration of total RNA was measured by absorbance at 260 nm on a Nanodrop ND-1000 spectrophotometer (Labtech International). 1μg of total RNA was reverse transcribed using SuperScript 2 (Invitrogen) in a final volume of 40 μl according to the manufacturer's instructions and stored at −20° until used.

2.7 QUANTITATIVE PCR

Quantitative PCR was performed using SYBR green (Quantace) on an OPTICON DNA engine with OPTICON monitor software version 2·03 (Real-Time systems; MJ Research). Amplification of mRNA encoding Hprt1, 18S or β-actin was performed to control for the starting amount of cDNA. Expression levels of genes of interest are shown as fold change over that seen in naïve animals after normalization to housekeeping gene levels using the ΔΔCt method.

Primers used:

Gene	Sense Primer	Anti sense primer	T_m (°C)
Hprt1	GTAATGATCAGTCAACGGGGGAC	CCAGCAAGCTTGCAACCTTAACCA	60
18S	AGTCCCTGCCTTTGTACACA	GATCCGAGGGCCTCACTAAC	60
β-actin	GTGGGCCGCTCTAGGCACCAA	CTCTTTGATGTCACGCACGATTTC	60
SOCS1	TCCGTTCGCACGCCGATTAC	TCAAATCTGGAAGGGGAAGG	60
Ifi205	ATATCCCAGGTCTCATCTTCGG	TGTGATTTTTGGTTCTTAGCCG	60
IP-10	GCTTGAAATCATCCCTGCGA	GGCAATGATCTCAACACGTGG	60
IFNγ	AAGACTGTGATTGCGGGGTTG	GAGCGAGTTATTTGTCATTCGGG	60
iNOS	CCCTTCCGAAGTTTCTGGCAGC	GGCTGTCAGAGCCTCGTGGCTTTGG	60

Table 2.4 Paired primers used in quantitative PCRs. All sequences are shown in the 5'–3' direction. All primers were purchased from Eurofins-MWG.

2.8 FLOW CYTOMETRY

2.8.1 Nine Fluorescence Parameter Flow Cytometry

As described by (Frischmann & Müller, 2006). Antibodies were titrated to determine the optimum concentration of use; importantly CD4 and CD8 (PE-Cy5) antibodies were titrated to ensure non-overlapping antibody intensity. After washing in FACS buffer (Appendix A) nucleated cells were incubated on ice for 30 min with the following directly coupled fluorochrome-labeled antibodies in FACS staining buffer (Appendix A):

Antibody	Clone	Supplier	Concentration
CD4 PE-Cy5	GK1.5	eBioscience	2.5µg/ml
CD8 PE-Cy5	53-6.7	BD Biosciences	0.64µg/ml
CD19 APC	1B3	BD Biosciences	0.1µg/ml
IgM PE	eB121-15F9	eBioscience	0.1µg/ml
IgD FITC	11-26c	eBioscience	0.1µg/ml
F4/80 PE	CI:A3-1	Serotec	0.3µg/ml
CD49b FITC	DX5	BD Bioscience	0.5µg/ml
Gr-1 PE	RB6-8C5	eBioscience	0.1µg/ml
Gr-1 FITC	RB6-8C5	eBioscience	0.1µg/ml
PI	-	Sigma-Aldrich	0.5µg/ml

Table 2.5 Anitbodies used for nine-parameter FACS analysis All antibodies were titrated to determine optimum concentration of use.

After washing with FACS buffer, cells were re-suspended in FACS buffer and measured on a FacsCalibur (BD Biosciences) using Cell Quest software (BD Biosciences). Samples were acquired through a live gate without compensation until at least 10,000 events were recorded. PI positive cells were excluded from the analysis by gating. Using FlowJo software (Tree star), the data was compensated and

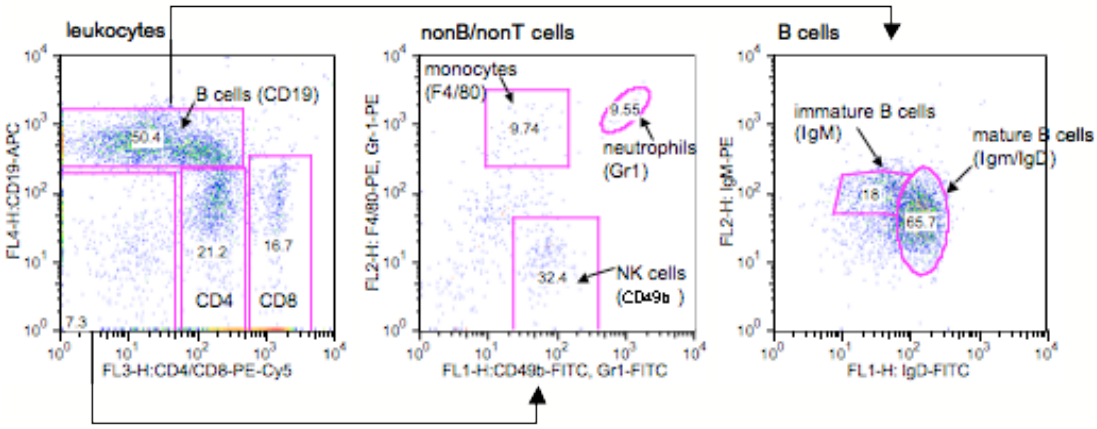

Figure 2.1 Gating strategy used to separate the different leukocyte populations. Leukocytes were separated and differentiated into T cells ($CD4^+$ and $CD8^+$), B cells, and non-B/non-T cells using CD19-APC (FL4) to select B cells and PE-Cy5-CD4/8 (FL3) to select T cells and all $FL4^-FL3^-$ cells were designated non-B/non-T cells. Non-B/non-T cells were differentiated in NK cells (FITC-$CD49b^+$), macrophages/ monocytes (PE-$F4/80^+$), and neutrophils (FITC-$Gr1^+$ PE-$Gr\text{-}1^+$). B cells were then differentiated into immature (PE-IgM^+) and mature B cells (PE-IgM^+ FITC-IgD^+).

analyzed (Fig 2.1). First, leukocytes were separated and differentiated into T cells ($CD4^+$ and $CD8^+$), B cells, and non-B/non-T cells using APC for B cells and PE-Cy5 for T cells. B cells were then differentiated into immature (PE-IgM^+) and mature B cells (PE-IgM^+, FITC-IgD^+). Non-B/non-T cells were differentiated in NK cells (FITC-$CD49b^+$), macrophages/ monocytes (PE-$F4/80^+$), and neutrophils (FITC-$Gr1^+$ PE-$Gr\text{-}1^+$). The percentage of every cell type was calculated by FlowJo software.

2.8.2 Brain FACS analysis

Brain and spinal cord were cut into small pieces and incubated in complete RPMI containing collagenase (Gibco, 0.2mg/ml) and DNase (Gibco). Cells were homogenised and strained through a 100μm nylon filter. After centrifugation at 400x*g* for 10mins at 4°C, the cell suspension was resuspended in 30% Percoll (Pharmacia) and centrifuged at 8500x*g* for 30 minutes at 4°C. The inter-phase cells were collected and washed in PBS prior to staining. The cells were stained with primary antibodies for 30 minutes at 4°C, washed, and incubated with streptavidin-conjugated APC or PerCP antibodies (BD Biosciences) for 15 minutes. The cells were washed and analyzed with a FACSCanto II flow cytometer using BD FACSDiva software (BD Biosciences).

2.8.3 Phosphorylated STAT1 FACS analysis

Cells were re-suspended in PBS and 4% formaldehyde added to a final concentration of 3% formaldehye. Cells were fixed for 10mins at 37°C and then chilled on ice for 1 min. Extra-cellular staining (APC-F4/80 (AbD Serotec), PE-CD11b (BD Biosciences)) was performed at 4°C for 30mins. Cells were washed, re-suspended in PBS and permeabilised through the addition of ice-cold methanol whilst gently vortexing to a final concentration of 90% methanol, then incubated at 4°C for 30mins. Cells were washed twice in FACS buffer, resuspended in 50μl of staining buffer for 10mins at room temperature before the pSTAT1 antibody (Cell Signaling Technologies) was added to the samples for 1 hour at room temperature. Cells were washed in FACS buffer before re-suspending in PBS and analysed using an LSR II flow cytometer with FACSDiva software (Becton Dickenson).

2.9 WESTERN BLOTTING

Spleen cells (5 x 10^6 cells/ml) were cultured for 20 mins in media alone or in the presence of 10 ng/ml IFNγ or IL-6 (eBioscience, UK) or 10^4-10^6 U/ml IFNα (W. Müller, HZI, Braunschweig). Cells were lysed in Western blot lying buffer (see Appendix A) and stored at -20°C until use. Laemelli buffer (Appendix A) was added to protein samples and heated at 100°C for 3 min. Samples were subjected to sodium dodecyl sulfate polyacrylamide gel electrophoresis on 10% acrylamide gels (Appendix A) at 100V through the stacking gel and 150V through the resolving gel until the tracking dye reached the bottom of the gel. Gels were positioned on PVDF membranes (BioRad) activated in methanol (BDH) for 1min and placed in a BioRad semi-dry blot cell above three sheets of Whatman paper (Whatman) soaked in buffer API (Appendix A) and two sheets of Whatman paper soaked in buffer APII (Appendix A) and below 4 sheets of Whatman paper soaked in CP buffer (Appendix A). Blotting was performed for 30mins at 200mA. Blots were stained with Ponceau S (Appendix A) and divided into two sections at approximately 75kDa ensuring all major bands were avoided. Blots were incubated with blocking solution (5% w/v milk in Tween TBS (TwTBS, see Appendix A)) for 90mins at room temperature before incubation with rat anti-mouse phosphorylated STAT1 or Jak1 (Cell Signalling Technologies; 1:1000 in 4% w/v BSA (Sigma-Aldrich) in TwTBS) and mouse anti-mouse β-actin (Sigma-Aldrich; 1:1000 in 4% w/v BSA (Sigma-Aldrich) in TwTBS) overnight at 4°C with rocking. The blots were washed 3 times with TwTBS for 15mins before incubation with secondary antibody (Stratech Scientific; horseradish-peroxidase-conjugated goat anti-mouse or anti-rabbit; 1:10,000 in 0.5% milk TwTBS) for 90 min. The blots were washed 3 times with TwTBS for 30mins, 10mins, 10mins and signals were visualised by using an enhanced chemiluminescence (ECL) system (Amersham). After visualising, the section of the membrane containing the larger fragments was washed in TwTBS for 15mins prior to being placed in strip buffer (see Appendix A) at 80°C for 30-40mins. The membrane was then rinsed with dH_2O and washed for at least 15mins in TwTBS. The membrane was incubated with rat anti-mouse STAT1 overnight (Santa Cruz; 1:1000 in 4% w/v BSA (Sigma Aldrich) in TwTBS), secondary antibody applied as before and ECL used to develop.

2.9 *TRICHURIS MURIS* SPECIFIC IgG1 AND IgG2A/C ELISA.

To analyse *T. muris* specific antibody responses in the serum of infected mice ELISAs were performed. ELISA plates were coated overnight at 4°C with 5μg/ml *T. muris* overnight E/S (provided by Prof. Else, University of Manchester) in 0.05M carbonate bicarbonate buffer (see Appendix A). Following coating, plates were washed (5 times) in PBS-Tw and non-specific binding blocked using 3% BSA (Sigma-Aldrich) in PBS for 1hr at 37°C. Plates were washed (5 x in PBS-Tw) and diluted serum (1:20 – 1:2560) added to the plate and incubated for 1hr at 37°C. After washing (5x in PBS-Tw), biotinylated rat anti-mouse IgG1 (BD Biosciences, 1:500) or IgG2a/c (BD Biosciences, 1:1000) was added to the plate for 1hr at room temperature. The plates were washed (5 x with PBS-Tw) and incubated with streptavidin - β - peroxidase (SA-POD, Roche, 1:1000) for 1hr at room temperature. Finally plates were washed (5x with PBS-Tw) and developed with 3,3', 5,5' tetramethylbenzidine (TMB substrate reagent kit, BD), colour development was stopped using sulphuric acid (Sigma-Aldrich). Plates were then read using a Dynex MRX11 plate reader (Dynex Technologies) at 405nm with a reference of 490nm.

2.10 DETERMINATION OF NITRITE CONCENTRATION

To determine classical macrophage activation nitrite production was determined by mixing 50μl of culture medium with 50μl of Griess reagent (1 part 0.1% N-(1-napthyl)ethyldiamine dihydrochloride / 60% ethanoic acid plus 1 part 1% sulfanilamide / 30% ethanoic acid (all Sigma-Aldrich)) in a 96 well plate. The absorbance was measured using a Dynex MRX11 plate reader (Dynex Technologies) at 570nm with background absorbance at 630nm subtracted.

2.11 DETERMINATION OF ARGNIASE ACTIVITY

To determine alternative macrophage activation argniase activity was evaluated. 50μl of 0.1% Triton X-100 (Sigma-Aldrich) containing 5μg pepstatin, 5μg aprotinin and 5μg antipain as protease inhibitors (all Sigma-Aldrich) were added to cells. The mixture was then incubated for 30mins at room temperature with agitation. After the cells were lysed 50μl of 10mM $MnCl_2$, 50mM Tris-HCl, pH7.5 (Sigma-Aldrich) was added, to activate the enzyme, for 10mins at 55°C. Arginine hydrolysis was initiated

by the addition of 25µl of 0.5M arginine (Sigma-Aldrich), pH9.7 to a 25µl aliquot of the activated lysate. Incubation was performed at 37°C for 60min and the reaction stopped by the addition of 400µl stop solution containing H_2SO_4, H_3PO_4, H_2O (1:3:7 v/v; Sigma-Aldrich). The urea formed was colourimetrically quantified at 540nm after the addition of 25µl 9% iso-nitrosopropiophenone (ISPF; dissolved in 100% ethanol, Sigma-Aldrich) and heating at 95°C for 45min. After 10min in the dark the OD at 540nm was determined with a Dynex MRX11 plate reader (Dynex Technologies) using 200µl aliquots. A calibration curved was prepared with increasing amounts of urea (Sigma-Aldrich) between 1.5mg and 30µg. In this case 100µl of urea solution at the appropriate concentrations, 400µl stop solution and 25µl ISPF were added and the procedure followed as described above.

2.12 CYTOKINE BEAD ARRAY (CBA)

To analyse cytokine levels in the serum and re-stimulated lymph node supernatant of mice IL-4, IL-6, IL-10, IL-13, IL-17, IFNγ, TNFα and MCP-1 were measured using a BD CBA mouse soluble protein flex set (BD Biosciences) using the manufacturers instructions. Briefly, supernatants are incubated with capture beads of a distinct fluorescence intensity and coated with capture antibodies specific to one of the mentioned cytokines. Bound cytokine is then detected via the addition of PE-conjugated detection reagents and compared to known standard concentrations on a FACSArray using FCAPArray software (BD Biosciences).

2.13 STATISTICAL ANALYSIS

Statistical analyses were performed with Graphpad Prism version 5. For comparisons between 2 groups a t-test or Mann Whitney U test (for non-parametric data) was used. A One Way ANOVA with a Tukey's or Dunnett's post test was applied for parametric data containing more than two groups. In addition, where appropriate, a Two Way ANOVA with Bonferroni post test was applied. For all non-parametric analyses containing more than two groups a Kruskal-Wallis test and Dunn's post test were applied. Differences were considered significant at $p<0.05$ and marked with *. ** designates $p<0.005$ and *** $p<0.001$.

CHAPTER THREE

Characterisation of IFNγ conditional knock-out mice

3.1 INTRODUCTION

The role of IFNγ in a myriad of diseases, as well as during homeostasis, is well documented. However, as several cell types are capable of responding to IFNγ it isn't clear *in vivo* which cells are responsible for the different actions of the cytokine.

The ability to generate conditional knock-out mice, where a gene is ablated in a specific cell type or organ, has come to the forefront in the last decade. There is now the existence of a Cre 'zoo' database containing over 100 different Cre expressing lines (Nagy *et al.*, 2009). Therefore, once created, a mouse containing a 'floxed' target gene enables the conditional deletion of the gene, in almost any cell type, by crossing the floxed mouse to the appropriate Cre mouse. This method allows the intricate dissection *in vivo* of the role of the gene of interest.

The creation of a conditionally expressed IFNγ receptor will allow the investigation of the cells responsible for the downstream actions of IFNγ signalling. This project was instigated by a previous member of Werner Muller's lab (at the Helmholtz Institute for Infection Research, Braunschweig) who generated the IFNγR2 targeting vector, transfected the plasmid into embryonic stem cells, injected the clones which had undergone homologous recombination into blastocysts and selected mice which had undergone germline transmission (Fleige, 2006). The work described in this thesis continues on from this work which generated IFNγR2$^{fl/wt}$neo^{+} and IFNγR2$^{\Delta/wt}$ mice.

Aims

Therefore, the aims of this chapter are as follows:

1. Generate and characterise an IFNγR2$^{fl/fl}$ mouse
2. Cross this IFNγR2$^{fl/fl}$ mouse to a deleter Cre line to generate a complete knock-out mouse as well as crossing to the CD4-Cre and LysM-Cre mice to create T cell and macrophage/granulocyte conditional knock-out mice.
3. Confirm in each IFNγR2$^{fl/fl}$ x Cre line that the mice are unresponsive to IFNγ in the appropriate cell(s).

4. Characterise the phenotype of the IFNγR2$^{\Delta/\Delta}$ mice.

3.2 RESULTS

3.2.1 Breeding of conditional IFNγR2 mutant mice

The generation of the IFNγR2 conditional knock-out mouse was initiated at Prof Muller's lab at the Helmholtz Institute for Infection Research, Braunschweig, Germany (Fleige, 2006).

In order to obtain mice with a ubiquitous deletion of IFNγR2 an IFNγR2$^{fl/wt}$ male was mated with a K14-Cre^{+} female. Breeding with K14-Cre induces deletion of floxed sequences in the epidermis, tongue and thymic epithelium when Cre is inherited from the father. However, when the Cre is inherited from the mother ubiquitous deletion of loxP flanked target sequences occurs due to activity of Cre in murine oocytes (Hafner *et al.*, 2004). This cross was performed at the Helmholtz Centre for Infection Research prior to transfer of the animals to the facility at the University of Manchester. However, the genotyping of these mice was performed at the University of Manchester on tail samples sent from Braunschweig. The mice were genotyped using two PCRs, designed as part of the work contained within this thesis – one to detect the IFNγR2 delta allele (Fig 3.2A) and one to detect the presence of a wild type IFNγR2 allele (Fig 3.2B). IFNγR2$^{fl/wt}$neo^{-} and IFNγR2$^{\Delta/wt}$ mice were shipped from Braunschweig and subsequently breed to become homozygous at the University of Manchester.

In order to remove any complications that have been shown to arise from the presence of a selectable marker, in this case the neomycin resistance cassette, IFNγR2$^{fl/fl}$neo^{+} mice were breed with FLP deleter mice to remove the FRT – flanked neomycin cassette (see Fig1.2B for overview of the 2loxP 2FRT method). Mice having successfully under gone recombination between the two FRT sites, and therefore deletion of the cassette, were screened by a PCR designed to recognise a section of the neomycin resistance gene (Fig 3.2C). These IFNγR2$^{fl/wt}$neo^{-} mice were subsequently crossed to obtain homozygous IFNγR2$^{fl/fl}$ mice. The detection of the floxed gene was determined using a three primer PCR strategy. This PCR allows the

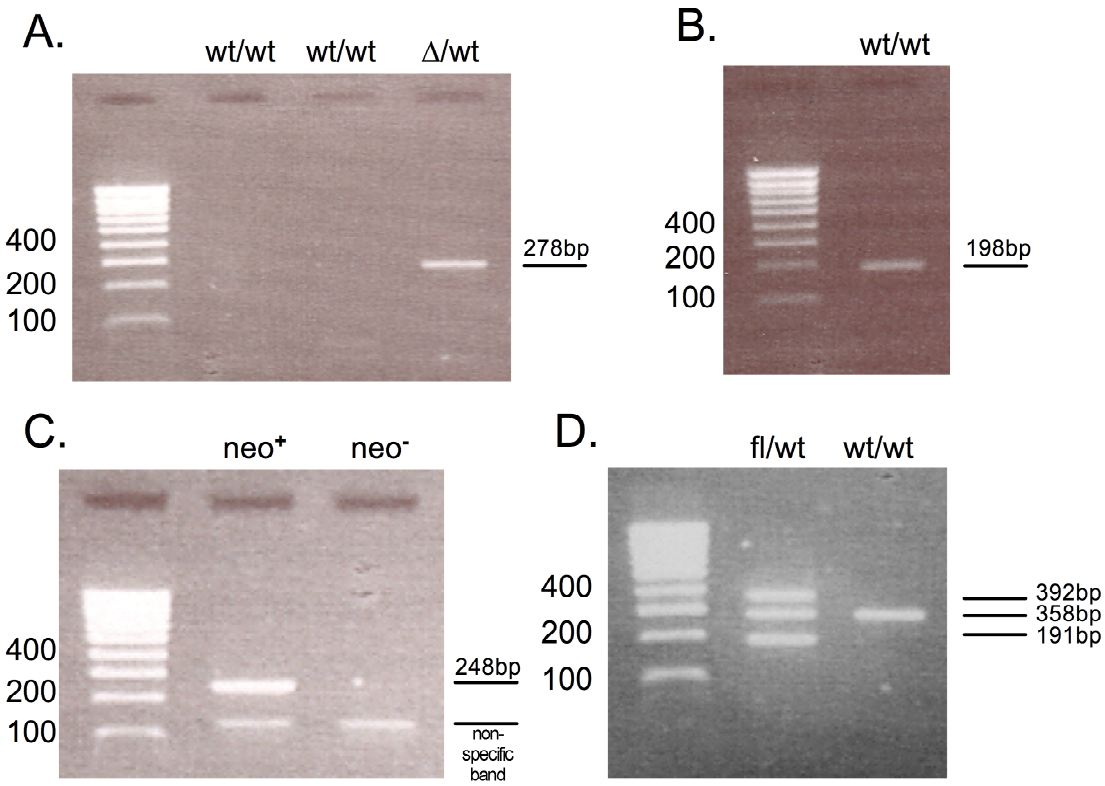

Fig 3.1 Genotyping PCRs for detecting the A. delta allele B. wild type IFNγ allele C. neomycin resistance casette and D. floxed allele. Mouse genomic DNA was extracted from tail or ear biopsies, PCRs performed with the appropriate primers and visualised on a 2% agarose gel. The neomycin resistance casette (C) PCR produces a second non-specific band at ~120bp. The PCR to detected the floxed allele (D) utilises a three primer approach resulting in a band at 358bp with the wildtype allele and bands at 392bp and 191bp with the floxed allele.

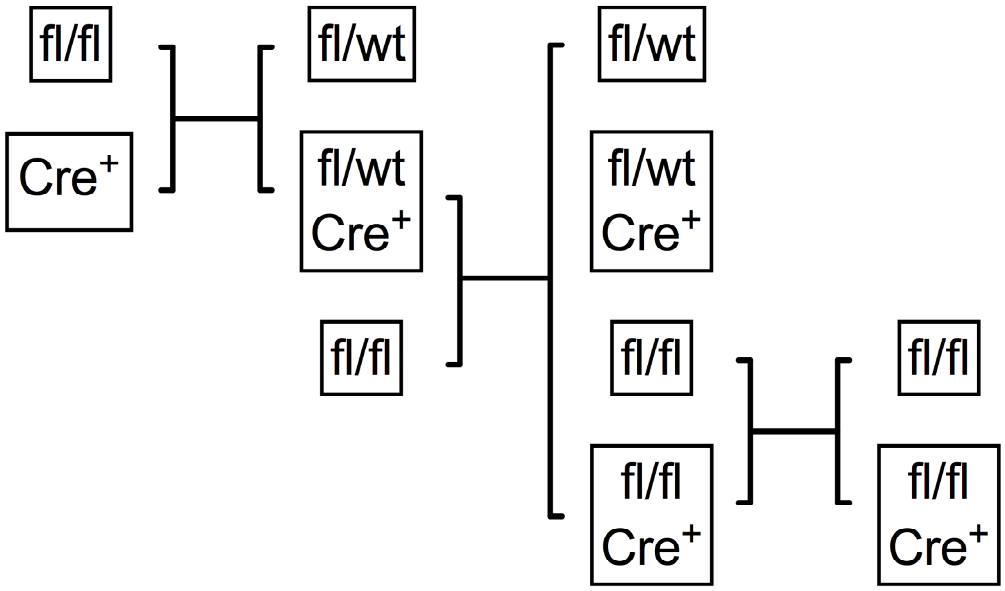

Fig 3.2 Breeding scheme used to obtain conditional knock-out mice. IFNγR2$^{fl/fl}$ mice were crossed with either CD4 Cre^{+} or LysM Cre^{+} mice to produce IFNγR2$^{fl/wt}$Cre^{+} mice. These were crossed again to IFNγR$^{fl/fl}$ mice and the IFNγR2$^{fl/fl}$Cre^{+} offspring maintained by breeding with IFNγR2$^{fl/fl}$ mice. For all experimental work IFNγR2$^{fl/fl}$Cre^{+} mice from these breedings were used and the IFNγR2$^{fl/fl}$Cre^{-} littermates used as controls

easy detection of the insertion of the 23bp loxP fragment. One primer spans the loxP site creating 3 bands in the presence of both a floxed allele and a wild-type allele, 2 bands in the presence of only floxed alleles and only 1 band in the presence of only wild-type alleles (Fig3.2D).

In order to obtain mice with a specific deletion of IFNγR2 in T-cells or myeloid cells the IFNγR2$^{fl/fl}$ mice were mated with CD4-Cre^{+} (Lee *et al.*, 2001) or LysM-Cre^{+} (Clausen *et al.*, 1999) mice and the IFNγR2$^{fl/wt}$Cre^{+} offspring detected by PCR. These IFNγR2$^{fl/wt}$Cre^{+} mice were then crossed again to IFNγR2$^{fl/fl}$ mice and the resultant IFNγR2$^{fl/fl}$Cre^{+} mice used for experiments and further breeding as shown in the breeding scheme (Fig 3.1). Cre genotyping was performed using primers specific for either CD4-Cre or LysM-Cre (sequences courtesy of A. Roers). IFNγR2$^{fl/fl}$LysMCre^{+} mice were subsequently crossed to the IFNγR2$^{fl/fl}$CD4Cre^{+} mice to give double conditional knock-out - IFNγR2$^{fl/fl}$LysMCre^{+}CD4Cre^{+} mice.

As all the mutant mice used during this thesis were all on a mixed B6 and 129 background, Cre^{-} littermates were used as controls in every experiment. Backcrossing of the IFNγR2$^{fl/fl}$ mice to B6 was conducted simultaneously and mice on a predominantly B6 background, which have undergone a minimum of 8 backcrosses, are now available.

3.2.2 Confirmation of abrogation of responsiveness to IFNγ

To verify the efficiency of IFNγR2 deletion we initially analysed the complete knock-out mice. Whole splenocytes were harvested from IFNγR2$^{\Delta/\Delta}$, IFNγR2$^{fl/fl}$ control mice and B6 mice and stimulated with IFNγ or IL-6 for 20mins. Cell lysates were run on a gel, blotted onto PVDF membrane and probed for the presence of phosphorylated STAT1, total STAT1 and β-actin protein. IFNγR2$^{fl/fl}$ mice remain responsive to IFNγ, as evident through the STAT1 phosphorylation observed after stimulation with either IFNγ or IL-6 (Fig 3.3). In contrast, IFNγR2$^{\Delta/\Delta}$ mice were not responsive to IFNγ with no STAT1 phosphorylation detected (Fig 3.3). The IFNγR2$^{\Delta/\Delta}$ mice did not have a defect in the STAT1 phosphorylation pathway as

stimulation with IL-6 still resulted in the phosphorylation of STAT1 (Fig 3.3). This data demonstrates that the IFNγR2$^{fl/fl}$ mice have normal IFNγ signalling whereas in the IFNγR2$^{\Delta/\Delta}$ mice IFNγ responsiveness has successfully been abrogated.

To verify that deletion of IFNγR2 in IFNγR2$^{fl/fl}$CD4Cre^{+} and IFNγR2$^{fl/fl}$LysMCre^{+} mice occurs efficiently and is cell-specific, isolated cell populations were analysed. T cells were isolated using magnetic cell sorting from a mixed population of splenocytes and peripheral lymph node cells. The sorted T cell and non-T cell populations were then stimulated with IFNγ and cell lysates analysed by western blot for STAT1 phosphorylation. The T cell populations from both the IFNγR2$^{fl/fl}$CD4Cre^{+} (boxed population in Fig 3.4) and IFNγR2$^{\Delta/\Delta}$ mice were unresponsive to IFNγ with no STAT1 phosphorylation detected (Fig 3.4). In contrast, the non-T cell population in the IFNγR2$^{fl/fl}$CD4Cre^{+} mice (second boxed population) was responsive to IFNγ and able to phosphorylate STAT1 (Fig 3.4). This demonstrated the successful and specific abrogation of IFNγ signalling in T cells in these mice. Moreover, both the T cell and non-T cell populations in the IFNγR2$^{fl/fl}$LysMCre^{+} mice were responsive to IFNγ (Fig 3.4). However, the non-T cell population, containing the macrophages and granulocytes, had lower STAT1 phosphorylation levels than the IFNγR2$^{fl/fl}$ control mice following stimulation with IFNγ (Fig 3.4). The lower phosphorylation is consistent with these mice having deleted IFNγR2 on their macrophages / granulocytes.

Bone-marrow derived macrophages from IFNγR2$^{fl/fl}$LysMCre^{+} mice were analysed by Western Blot for STAT1 phosphorylation following IFNγ stimulation. However, we were unable to get a macrophage purity of more than 80% therefore, we decided to analyse STAT1 phosphorylation at a single cell level by FACS using a phosphorylated-STAT1 antibody. Peritoneal macrophages isolated from mutant mice were stimulated with IFNγ and analysed gated on CD11b^{+}F4/80^{+} double positive cells. In the IFNγR2$^{fl/fl}$LysMCre^{+} positive and IFNγR2$^{\Delta/\Delta}$ mice this population was unresponsive to IFNγ, with no STAT1 phosphorylation. Control IFNγR2$^{fl/fl}$ mice did respond to IFNγ stimulation with an increase in STAT1 phosphorylation (Fig 3.5).

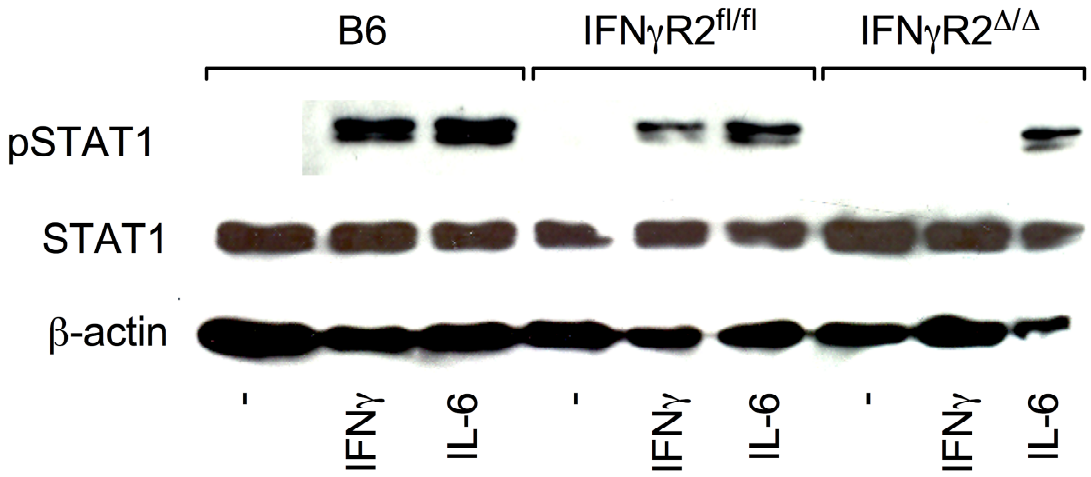

Fig 3.3 Splenocytes from B6, IFNγR2$^{fl/fl}$ or IFNγR2$^{\Delta/\Delta}$ mice stimulated with IFNγ or IL-6 and probed for total and phosphorylated STAT1. Spleen cells were stimulated for 20mins with 10ng/ml IFNγ or IL-6 and then lysed. Cell lysates were run on a 10% acrylamide gel, blotted onto a PVDF membrane and probed for phosphorylated STAT1, total STAT1 or β-actin protein. Data is representative of three repeats.

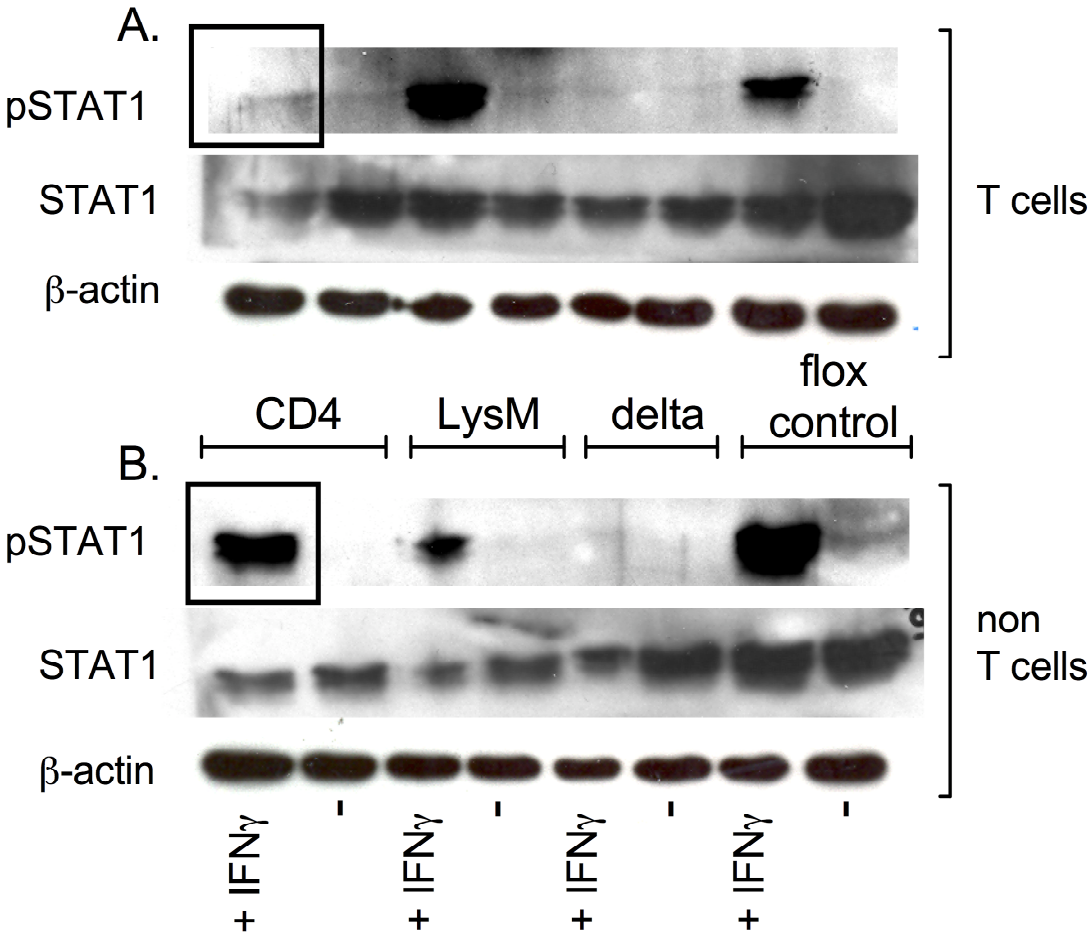

Fig 3.4A. T cells and B. non-T cell populations from IFNγR2 conditional and global knock-out mice stimulated with IFNγ and probed for total and phosphorylated STAT1. Pooled spleen cells and peripheral lymph node cells were sorted using MACS pan-T cell beads. The T cell and non-T cell populations were stimulated for 20mins with 10ng/ml IFNγ and then lysed. Cell lysates were run on a 10% acrylamide gel, blotted onto a PVDF membrane and probed for phosphorylated STAT1, total STAT1 or β-actin. Box indicates key cell populations: T cells and non-T cells from IFNγR2$^{fl/fl}$CD4Cre^{+} mice stimulated with IFNγ. Data is representative of three repeats.

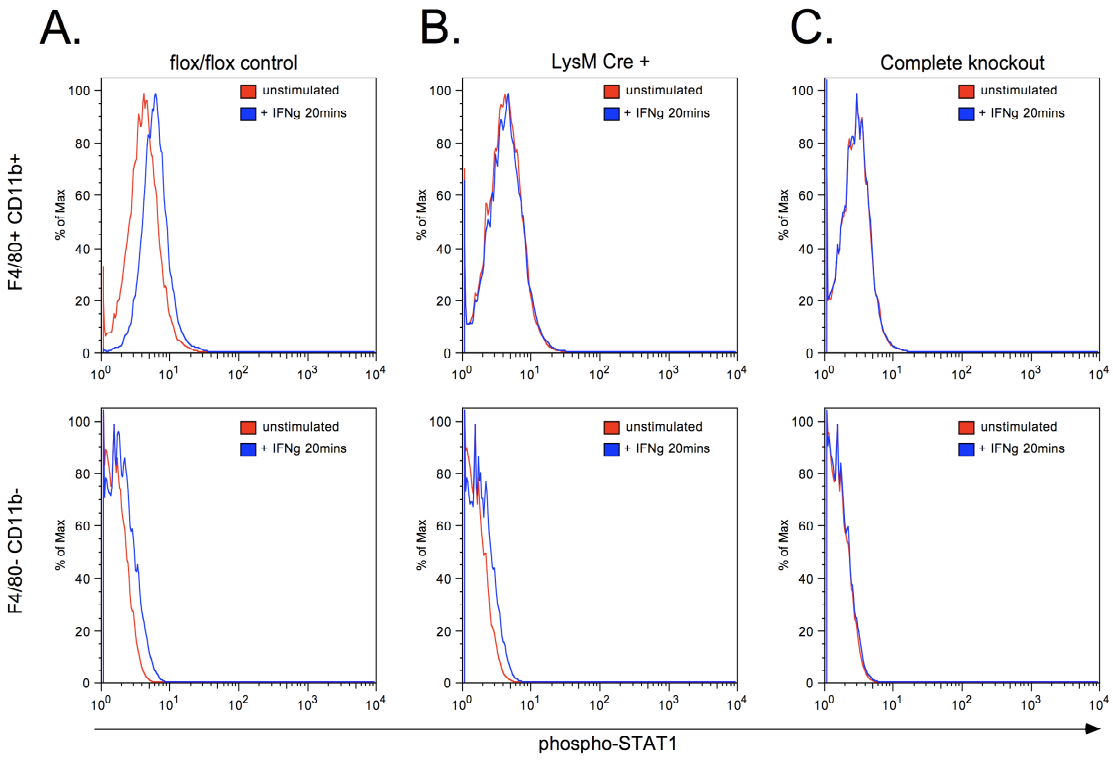

Fig 3.5 STAT1 phosphorylation of CD11b^{+}F4/80^{+} and CD11b^{-}F4/80^{-} cells from A. IFNγR2$^{fl/fl}$ B. IFNγR2$^{fl/fl}$xLysMCre^{+} and C. IFNγR2$^{\Delta/\Delta}$ mice stimulated with IFNγ. Peritoneal lavage cells were stimulated for 20mins with 10ng/ml IFNγ. Cells were fixed, permeabilised and stained with Alexa 488-phosphorylated STAT1, PE-CD11b and APC-F4/80. Cells were acquired on a LSR-II and data analysed using FlowJo. Data shown is gated on either CD11b^{+}F4/80^{+} or CD11b^{-}F4/80^{-} cells and is representative of 3 repeats.

Furthermore, the non-macrophage population ($F4/80^{-}CD11b^{-}$) from both the $IFN\gamma R2^{fl/fl}$ and $IFN\gamma R2^{fl/fl}LysMCre^{+}$ mice was responsive to IFNγ. In contrast, as expected, the non-macrophage population in $IFN\gamma R2^{\Delta/\Delta}$ mice was unresponsive to IFNγ stimulation (Fig 3.5)

Thus the inactivation of the IFNγR2 gene in $IFN\gamma R2^{\Delta/\Delta}$, $IFN\gamma R2^{fl/fl}LysMCre^{+}$ and $IFN\gamma R2^{fl/fl}CD4Cre^{+}$ mice appears to be occurring in the expected cell-types.

3.2.3. Complete deletion of IFNγR2 does not alter the leukocyte percentages in lymph nodes or spleen

Previous work has identified a decrease in CD4:CD8 T cell ratio and a slight increase in B cell proportions in the blood of IFNγR1 deficient mice (Frischmann & Müller, 2006). To determine if the same is true in our $IFN\gamma R2^{\Delta/\Delta}$ mice we analysed the composition of leukocytes in blood, mesenteric lymph nodes, peripheral lymph nodes and the spleen. In the $IFN\gamma R2^{\Delta/\Delta}$ mice we saw no significant changes in the CD4:CD8 ratio in the blood, peripheral lymph nodes, mesenteric lymph nodes or spleen compared to $IFN\gamma R2^{fl/fl}$ mice (Fig 3.6). In contrast, similarly to in the study by Frischmann and Müller, we observed an increase in B cells in the $IFN\gamma R2^{\Delta/\Delta}$ mice compared to the $IFN\gamma R2^{fl/fl}$ mice (Fig 3.7). However, this was only statistically significant in the peripheral lymph nodes isolated from female mice (Fig 3.7B), and there was no increase in comparison to B6 mice suggesting this may be a product of the mixed genetic background of these mice. Moreover, there were no other alterations in leukocyte composition analysed (mature and immature B cells, monocytes, neutrophils or NK cell percentage) from blood, peripheral lymph nodes, mesenteric lymph nodes or spleen between the different genotypes or sexes (Table 3.1).

3.2.4 Abrogation of IFNγ signalling through the IFNγR2 chain alters responsiveness to IFNα

It has previously been described that the deletion of IFNαR2 can decrease

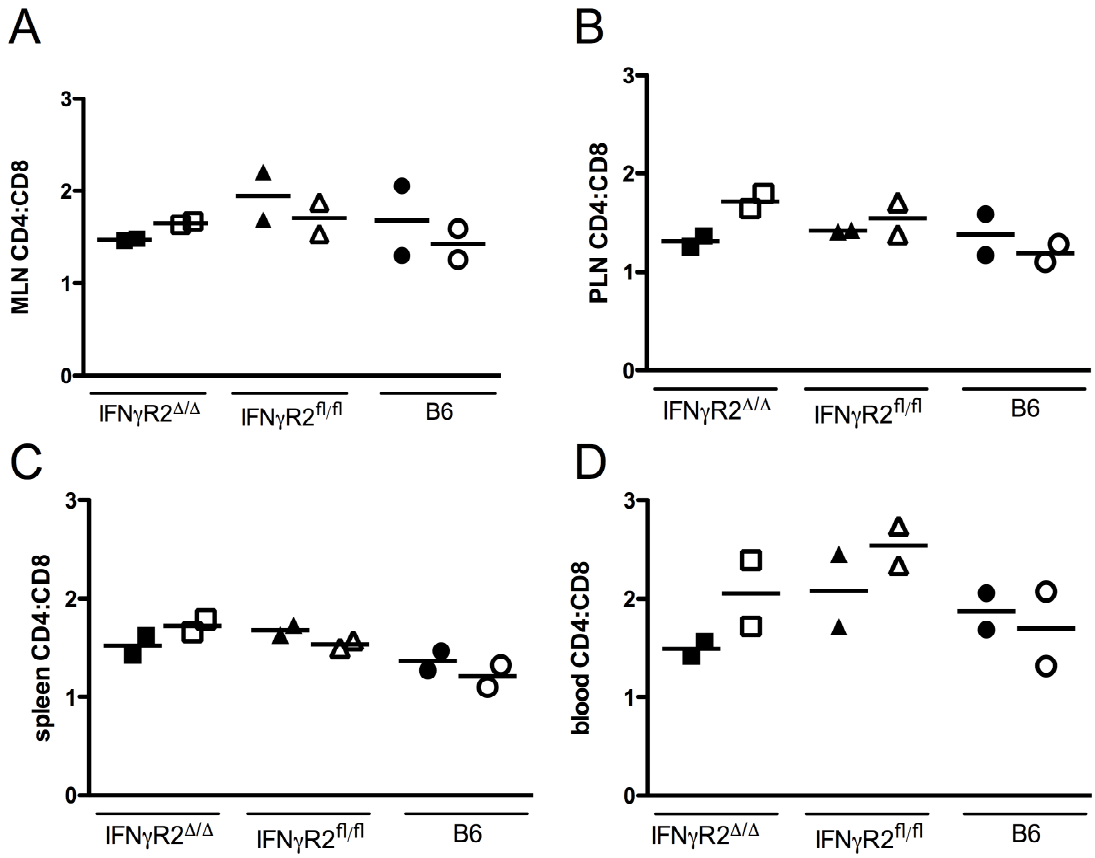

Fig 3.6 Analysis of CD4:CD8 T cell ratio in A. MLN cells B. PLN cells C. spleen cells and D. blood. Cells were isolated from IFNγR2$^{\Delta/\Delta}$, IFNγR2$^{fl/fl}$ or B6 mice as indicated and stained with PE-Cy5-CD4 and PE-Cy5-CD8. Cells were acquired on a FACSCalibur and data analysed using FlowJo software. Line indicates mean of group. Closed symbols - males, open symbols - females, n=2.

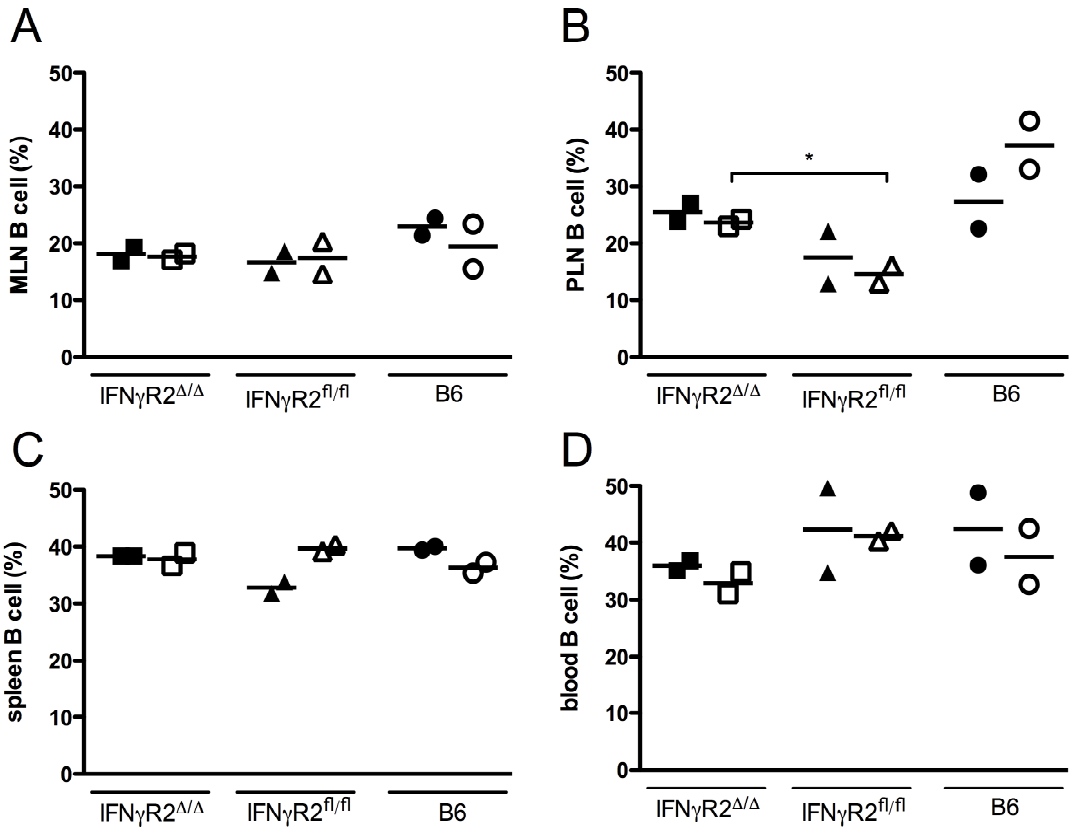

Fig 3.7 Analysis of B cell percentage in A. MLN cells B. PLN cells C. spleen cells and D. blood. Cells were isolated from IFNγR2$^{\Delta/\Delta}$, IFNγR2$^{fl/fl}$ or B6 mice as indicated and stained with APC-CD19. Cells were acquired on a FACS Calibur and data analysed using FlowJo. Line indicates mean of group *$p<0.05$ statistically significant data. Closed symbols - males, open symbols - females, n=2.

Mesenteric Lymph Node					
	IgM+ B cells	Igm+IgD+ B cells	Monocytes	Neutrophils	NK cells
IFNγR2 KO M	2.9 ± 0.5	14.8 ± 0.9	8.6 ± 2.3	1.7 ± 0.2	0.3 ± 0.0
IFNγR2 KO F	2.0 ± 0.1	14.6 ± 0.6	6.0 ± 1.4	1.1 ± 0.1	0.3 ± 0.0
IFNγR2 floxed M	2.1 ± 0.2	13.7 ± 2.0	6.6 ± 1.4	1.1 ± 0.1	0.3 ± 0.1
IFNγR2 floxed F	2.6 ± 0.5	13.7 ± 1.9	6.2 ± 0.2	0.9 ± 0.2	0.3 ± 0.0
B6 M	2.7 ± 0.0	19.5 ± 0.9	5.0 ± 0.0	1.6 ± 0.1	0.4 ± 0.0
B6 F	3.0 ± 0.9	15.4 ± 2.5	10.9 ± 1.0	1.4 ± 0.7	0.6 ± 0.1

Peripheral Lymph Node					
	IgM+ B cells	Igm+IgD+ B cells	Monocytes	Neutrophils	NK cells
IFNγR2 KO M	3.0 ± 0.1	22.2 ± 1.7	10.8 ± 0.8	1.4 ± 0.1	0.3 ± 0.0
IFNγR2 KO F	2.9 ± 0.1	20.0 ± 0.8	10.0 ± 1.1	1.2 ± 0.0	0.3 ± 0.0
IFNγR2 floxed M	2.2 ± 0.2	15.1 ± 4.2	15.1 ± 0.4	1.5 ± 0.3	0.5 ± 0.0
IFNγR2 floxed F	2.0 ± 0.2	12.3 ± 1.4	14.6 ± 0.4	0.7 ± 0.2	0.4 ± 0.1
B6 M	3.1 ± 0.1	23.8 ± 4.7	12.2 ± 2.2	1.8 ± 0.2	0.7 ± 0.0
B6 F	4.0 ± 0.1	33.1 ± 4.3	15.3 ± 5.8	1.2 ± 0.2	0.5 ± 0.1

Blood					
	IgM+ B cells	Igm+IgD+ B cells	Monocytes	Neutrophils	NK cells
IFNγR2 KO M	8.6 ± 0.5	26.6 ± 0.5	12.4 ± 2.3	1.1 ± 0.1	4.3 ± 0.1
IFNγR2 KO F	6.6 ± 2.0	24.1 ± 0.5	2.4 ± 1.2	1.1 ± 0.0	7.9 ± 1.2
IFNγR2 floxed M	9.3 ± 2.0	30.2 ± 5.6	2.9 ± 0.2	0.7 ± 0.4	13.1 ± 1.5
IFNγR2 floxed F	10.2 ± 0.8	27.6 ± 1.4	1.7 ± 0.9	0.8 ± 0.1	9.3 ± 1.6
B6 M	9.1 ± 1.5	31.5 ± 5.1	2.4 ± 0.3	1.0 ± 0.2	6.7 ± 0.6
B6 F	10.1 ± 0.5	24.3 ± 5.3	3.5 ± 1.0	4.2 ± 2.2	9.5 ± 0.0

Spleen					
	IgM+ B cells	Igm+IgD+ B cells	Monocytes	Neutrophils	NK cells
IFNγR2 KO M	8.3 ± 0.3	28.8 ± 0.6	23.5 ± 0.3	0.8 ± 0.1	2.0 ± 0.3
IFNγR2 KO F	9.6 ± 0.7	26.9 ± 2.2	22.3 ± 0.0	0.6 ± 0.1	2.2 ± 0.6
IFNγR2 floxed M	7.5 ± 0.3	23.8 ± 1.2	20.7 ± 0.3	0.9 ± 0.1	3.1 ± 0.2
IFNγR2 floxed F	11.0 ± 0.3	26.7 ± 1.0	18.4 ± 1.2	0.8 ± 0.2	2.0 ± 0.1
B6 M	7.2 ± 1.2	30.7 ± 1.6	17.5 ± 0.2	0.6 ± 0.2	2.5 ± 0.1
B6 F	7.8 ± 0.6	26.7 ± 0.3	18.9 ± 0.7	1.3 ± 0.1	3.4 ± 0.2

Table 2.1 Analysis of IgM^+, IgM^+IgD^+ B cell, monocyte, neutrophil and NK cell percentage in MLN cells, PLN cells, spleen cells and blood. Cells were isolated from $IFN\gamma R2^{\Delta/\Delta}$ (KO), $IFN\gamma R2^{fl/fl}$ (floxed) or B6 mice as indicated and stained with CD4 Pe-Cy5, CD8 PE-Cy5, CD19 APC, IgM PE, IgD FITC, F4/80 PE, CD49b FITC, Gr-1 PE, Gr-1 FITC and PI. Cells were acquired on a FACS Calibur and data analysed using FlowJo. Monocytes were defined as $CD19^-CD4^-CD8^-F4/80^+$ neutrophils as $CD19^-CD4^-CD8^-Gr1^+$ and NK cells as $CD19^-CD4^-CD8^-CD49b^+$. Data shown as mean ± standard error n=2.

responsiveness to IFNγ (Takaoka *et al.*, 2000); therefore, we set out to determine if the converse is true. Splenocytes from IFNγR2$^{\Delta/\Delta}$ mice were stimulated with IFNα and STAT1 phosphorylation analysed. This demonstrated that upon stimulation with 10^4 U/ml of IFNα there was a decrease in STAT1 phosphorylation in IFNγR2$^{\Delta/\Delta}$ mice compared to IFNγR2$^{fl/fl}$ mice (Fig 3.8). At higher levels of IFNα stimulation (10^5 or 10^6 U/ml) in IFNγR2$^{fl/fl}$ mice there was a decrease in total STAT1 levels which wasn't seen in the IFNγR2$^{\Delta/\Delta}$ mice. This was mirrored by a decrease in Jak1 levels in IFNγR2$^{fl/fl}$ mice at 10^5 or 10^6 U/ml IFNα that was only observed at 10^6 U/ml IFNα in IFNγR2$^{\Delta/\Delta}$ mice (Fig 3.8).

The changes observed in IFNα responsiveness are relatively minor compared to the changes previously demonstrated in response to IFNγ in IFNαR2 deficient mice (Takaoka *et al.*, 2000). Nevertheless, we have demonstrated a clear difference in IFNα responses, which needs to be further investigated.

3.2.5. Macrophage activation in complete IFNγR2 knock-out mice

Macrophages can be broadly classified into classical and alternatively activated macrophages. Classically activated macrophages require IFNγ for activation and are characterised by the production of nitric oxide. In contrast, alternatively activated macrophages can be activated by other stimuli including IL-4 and are characterised by the production of arginase-1 (Gordon, 2003).

Simulation of peritoneal macrophages from IFNγR2$^{\Delta/\Delta}$ or IFNγR2$^{fl/fl}$ mice with IFNγ + LPS (classical activation) or IL-4 + LPS (alternative activation) allowed the analysis of the potential to generate the two classes of macrophages. IFNγR2$^{fl/fl}$ mice stimulated with IFNγ or LPS produced nitric oxide and the combination of IFNγ + LPS resulted in a synergistic increase in nitric oxide production (Fig 3.9A). In contrast IFNγR2$^{\Delta/\Delta}$ mice produced significantly more nitric oxide than IFNγR2$^{fl/fl}$ mice when stimulated with LPS but, as expected, produced no nitric oxide in response to IFNγ. Additionally, IFNγR2$^{\Delta/\Delta}$ mice produced significantly less nitric oxide in comparison to IFNγR2$^{fl/fl}$ mice following stimulation with IFNγ + LPS, with

no elevation in nitric oxide production compared to stimulation with LPS alone (Fig 3.9A). In contrast, IFNγR2$^{\Delta/\Delta}$ mice produced significantly higher levels of arginase-1, than IFNγR2$^{fl/fl}$ mice, under baseline conditions. Moreover, when stimulated with either LPS or IL-4 IFNγR2$^{\Delta/\Delta}$ mice had significantly increased arginase-1 activity compared to IFNγR2$^{fl/fl}$ mice (Fig 3.9B). In both IFNγR2$^{\Delta/\Delta}$ and IFNγR2$^{fl/fl}$ mice arginase-1 production was increased following the combined stimulation of LPS + IL-4 but there was no difference between the IFNγR2$^{fl/fl}$ and IFNγR2$^{\Delta/\Delta}$ mice (Fig 3.9B).

This data demonstrates that the deletion of IFNγR2 alters the *in vitro* activated macrophage phenotype, with decreased nitric oxide production and increased arginase activity, suggesting a shift towards an alternatively activated phenotype.

As well as the changes reported in this chapter other important phenotypes have been demonstrated in the IFNγ, IFNγR1 or IFNγR2 deficient mice. This includes the inability of B cells to switch from antibody production of IgM to IgG2$_{a/c}$ (Finkelman *et al.*, 1988; Huang *et al.*, 1993) and an impaired T helper 1 development (Dighe *et al.*, 1995; Lu *et al.*, 1998). These characteristics will be analysed in our IFNγR2$^{\Delta/\Delta}$ mice in Chapter 5 using the *in vivo* model of *Trichuris muris*. The phenotypes described in this results chapter will be further dissected in the following discussion.

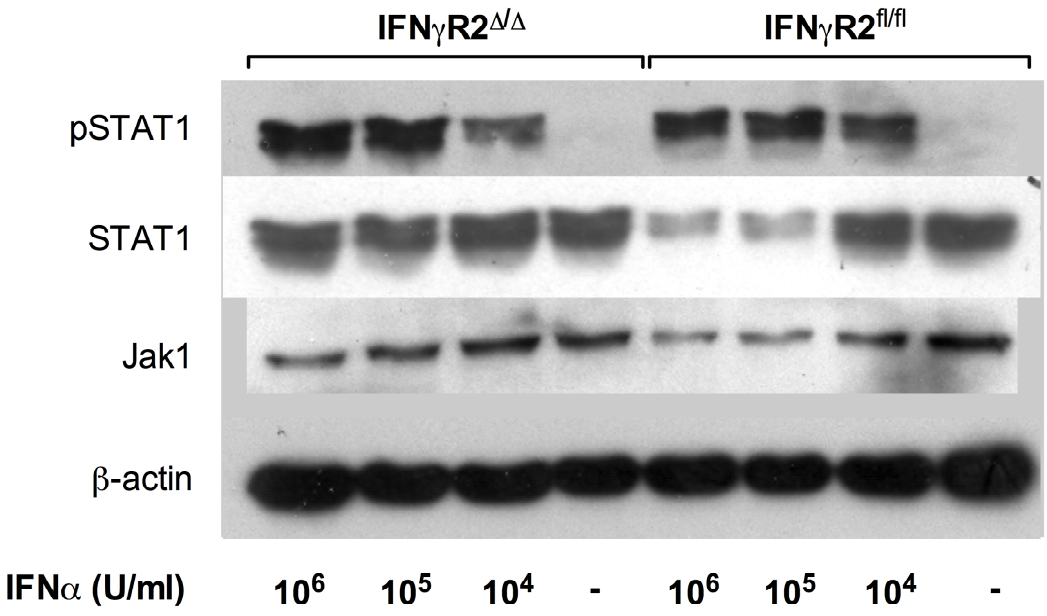

Fig 3.8 Splenocytes from IFNγR2$^{fl/fl}$ or IFNγR2$^{\Delta/\Delta}$ mice stimulated with IFNα and probed for total STAT1, phosphorylated STAT1, Jak1 and β-actin. Spleen cells were stimulated for 20mins with 0, 10^4, 10^5 or 10^6 U/ml IFNα and then lysed. Cell lysates were run on a 10% acrylamide gel, blotted onto a PVDF membrane and probed for phosphorylated STAT1, total STAT1, Jak1 or β-actin protein. Data is representative of three repeats.

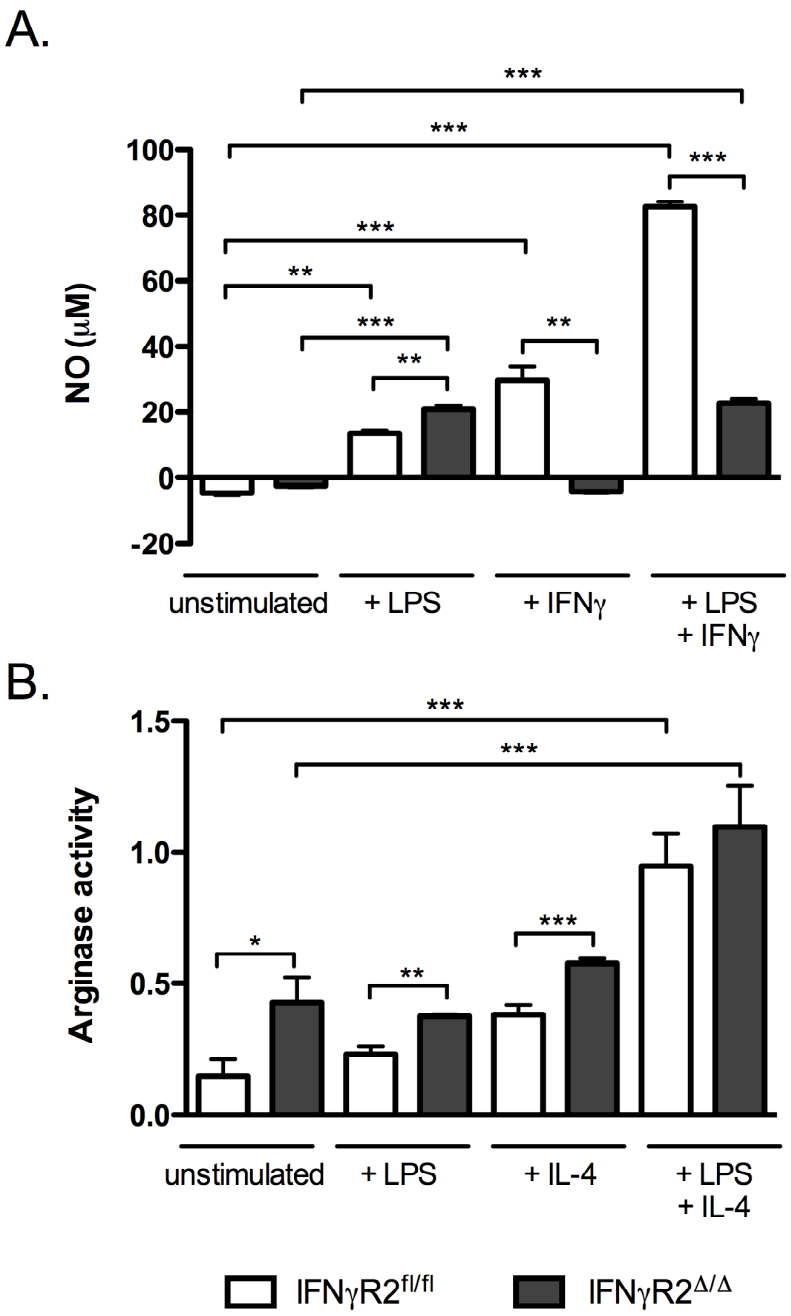

Fig 3.9 Peritoneal macrophages from IFNγR2$^{fl/fl}$ or IFNγR2$^{\Delta/\Delta}$ mice stimulated with A. LPS ± IFNγ for 24 hours and NO production measured or B. LPS ± IL-4 and arginase activity measured. Peritoneal lavage cells were left for 2 hours to adhere to plates and the non adherent cells removed. Adherent cells were stimulated with LPS, IFNγ or IL-4 (alone or in combination) for 24 hours. Cell supernatants were measured for NO production using the Griess reaction. Cells were lysed and arginase activity measured through the ability of cells lysates to convert arginine to urea. Data is presented a mean ± s.e, n=6. * $p<0.05$, ** $p<0.01$, *** $p<0.001$ statistically significant data

3.3 DISCUSSION

3.3.1 The Cre-loxP system of conditional gene inactivation

The Cre-loxP system of conditional gene inactivation has been widely used since it was first described over 15 years ago. The main complication that needs to be monitored, when using this system, is variability in recombination efficiency. This variability can be due to certain tissue-specific promoters not expressing the Cre proteins at high enough levels to guarantee efficient deletion or problems with accessibility of loxP sites. Indeed, some areas of genomic DNA yield low recombination efficiency even with high levels of Cre expression and this may be due to the local chromatin structure (Castrop, 2010; Vooijs *et al.*, 2001). Therefore, even if a specific Cre line has been reported to result in efficient deletion, this has to be re-analysed with each cross performed.

In our mice we saw efficient recombination in macrophages and T cells, following the cross of the floxed mice to the LysM cre or CD4 cre lines respectively. Although we analysed the deletion of the floxed gene in macrophages from LysM Cre^{+} mice, Cre is expressed in all cells of a myeloid lineage. Indeed, it has previously been reported that deletion is seen in neutrophils and monocytes/macrophages, but does not occur in the majority of peripheral dendritic cells (Clausen *et al.*, 1999). Therefore, although the IFNγ$R2^{fl/fl}$LysMCre^{+} mice are referred to as a macrophage conditional mutant, for ease in this thesis, further experiments need to be performed to examine deletion in other cells types including granulocytes and dendritic cells.

The Cre-loxP system is particularly valuable as, using the same floxed mouse, it is now possible to investigate the role of IFNγR2 in other cells types through crossing with other Cre lines. It is also possible to analyse the importance of temporal inactivation of a gene, through crossing with Cre-ER^{T} mice. The Cre-ER^{T} inducible system allows the expression of Cre to be switched on in a specific cell type: by giving the mice tamoxifen (Feil *et al.*, 1996). To further investigate a phenotype seen using the conditional inactivation of IFNγR2, the floxed mice could be crossed to an inducible Cre line. The receptor can then be inactivated at different time points

throughout the course of infection or treatment to analyse the role of IFNγ signalling in disease onset, maintenance or recovery.

As IFNγ has been demonstrated to have an important role in multiple diseases and organs, the use of the IFNγR2 conditional knock-out mouse is an important tool which will enable the elucidation of the cytokine network and clarify the role of IFNγ in multiple systems.

3.3.2. Analysis of the phenotype of unchallenged IFNγR2 deficient mice

The IFNγR2 complete knock-out mice develop normally and are fertile, as was expected from reports with IFNγ deficient mice (Huang *et al.*, 1993). We therefore analysed other parameters previously investigated in IFNγR1 or IFNγ deficient mice including the make-up of the resting lymphocyte population, responsiveness to IFNα and the macrophage phenotype.

3.3.2.1. Analysis of lymphocyte population in unchallenged IFNγR2 deficient mice

Previous work suggested that IFNγR1 deficient mice have altered lymphocyte proportions in the blood. The most striking difference observed was an elevated proportion of $CD8^+$ cells, changing the CD8:CD4 ratio from approximately 1:2 in B6 mice to 1:1 in the IFNγR1 deficient mice. These changes are accompanied by a lower percentage of neutrophils than B6 control mice and a higher levels of B cells in males than females (Frischmann & Müller, 2006). In contrast, our analysis of the complete IFNγR2 deficient mice showed no changes in CD8:CD4 ratio in the blood, mesenteric lymph nodes, peripheral lymph nodes or spleen compared to $IFN\gamma R2^{fl/fl}$ or B6 control mice. Moreover, the ratio of CD8:CD4 cells in the blood, independently of genotype, was comparable to that seen in B6 mice in the previous experiment. Similarly, no major changes in B cell or neutrophil percentage was seen in comparison to the control mice, except for a slight, statistically significant increase in B cell percentage in the peripheral lymph nodes of female $IFN\gamma R2^{\Delta/\Delta}$ mice compared to female $IFN\gamma R2^{fl/fl}$ mice. As both experiments were performed using the same method and the control mice display similar characteristics experimental

differences are unlikely to be the cause of these discrepancies. Our data is consistent with other reports which show no alterations in monocytes/macrophages, neutrophils or lymphocyte populations in the spleens of IFNγR1 deficient mice, although CD4:CD8 ratios were not analysed (Matthys *et al.*, 1999). A subsequent experiment with IFNγ deficient mice analysed the ratio of CD4:CD8 cells in lymph nodes but, similarly to our data, saw no change compared to control mice (Cornish *et al.*, 2003). Interestingly, in the study by Cornish and colleagues an equal ratio of CD4:CD8 cells was observed in IFNγ$^{-/-}$SOCS1$^{-/-}$ mice, similar to the ratio reported by Frischmann and Müller in IFNγR1 deficient mice. In the double IFNγ and SOCS1 knock-out mice the altered T cell ratio is attributed to altered responses to cytokines such as IL-12, IL-7 and IL-15. It will therefore be interesting to analyse the CD4:CD8 ratio and cytokine levels during inflammation, to determine if there is an altered cytokine response and/or preferential expansion of the CD8^{+} T cell subset during inflammation.

Although this data suggests there are no clear changes in the leukocyte population this experiment was performed with very few mice and used mice of a mixed genetic background. To be confident that this data is robust, it will be important to repeat the experiment with a larger group size and with mice that have been backcrossed onto a B6 background.

3.3.2.2. Analysis of IFNα responsiveness in IFNγR2 deficient mice

Takaoka and colleagues have previously demonstrated that mice deficient in IFNαR1 display a decreased sensitivity to IFNγ. They also performed the converse study with IFNγR1 deficient mice and demonstrated these mice display equal sensitivity to IFNα compared to wild type mice (Takaoka *et al.*, 2000). As the proposed mechanism for the cross-talk between the IFNγ and IFNα signalling pathways is through an association between IFNαR1 and IFNγR2 (Takaoka *et al.*, 2000), we analysed the impact of IFNγR2 deficiency on IFNα signalling. In contrast to IFNγR1 deficiency, IFNγR2 deficiency results in a decreased sensitivity to IFNα. It is thought that a constitutive sub-threshold level of IFNα signalling strengthens the association of IFNαR1 and IFNγR2 and maintains the docking site for STAT1 on

IFNαR1. These associations are proposed to aid the clustering of receptors in the caveolar membrane fractions, to increase the efficiency of signalling (Takaoka *et al.*, 2000). It will be of interest to verify if the deletion of IFNγR2 alters the clustering of receptors seen in wild-type mice and if this is responsible for the reduction in IFNα responsiveness seen in the IFNγR2 deficient mice.

Our experiments also demonstrated a decrease in STAT1 and Jak1 protein at high levels of IFNα stimulation in IFNγR2$^{fl/fl}$ but not IFNγR2$^{\Delta/\Delta}$ mice. This could be part of a negative feedback loop, as IFNα stimulation is known to cause a state of refractoriness following stimulation (Larner *et al.*, 1986). One potential method for decreasing the levels of Jak1 and STAT1 protein could be through the ubiquitin-proteasome pathway, which has previously been implicated in Jak-STAT signalling pathways (for review see (Shuai & Liu, 2003)). The ubiquitin-proteasome pathway controls the degradation of regulatory proteins, through the conjugation of ubiquitin to the substrate. Polyubiquitinated proteins are then recognised by the 19S complex of the 26S proteasomes and are degraded into short peptides (for a more detailed overview of the pathway see (Nandi *et al.*, 2006)). For example, following IFNγ signalling it has been demonstrated that Jak2 (Ungureanu *et al.*, 2002) and STAT1 (Kim & Maniatis, 1996) undergoes ubiquitin-proteasome-mediated degradation. Moreover, it has been demonstrated that IFNα induces the expression of ubiquitin cross-reactive protein and ubiquitin-conjugating enzymes which are both involved in protein degradation by the ubiquitin system (Nyman *et al.*, 2000). The increased protein degradation seen following higher concentrations of the IFNα stimulation may be due to the increased levels of phosphorylated protein, as both STAT and Jak ubiquitination occurs following protein phosphorylation (Kim & Maniatis, 1996; Ungureanu *et al.*, 2002).

Our data demonstrates a slight decrease in STAT1 phosphorylation in IFNγR2$^{\Delta/\Delta}$ mice with a clear decrease in total STAT1 and Jak1 protein levels. The effect of the decreased sensitivity to IFNα needs to be investigation to determine if this has any functional significance. It will also be of interest to determine if the decreased

protein degradation seen in the IFNγR2$^{\Delta/\Delta}$ mice has an impact on the refractory period normally observed following IFNα signalling (Larner *et al.*, 1986)

3.3.2.3. Analysis of macrophage phenotype in IFNγR2 deficient mice

Macrophages display heterogeneity in their cell surface markers, location, and function and have been classified into two broad subtypes – classically activated or M1 and alternatively activated or M2. Classically activated M1 macrophages are induced by IFNγ alone or in combination with microbial stimuli (e.g. LPS) or cytokines (e.g. TNF). Alternatively activated or M2 macrophages are induced by IL-4 or IL-13, but can also be induced by exposure to immune complexes, IL-10 or hormones (Gordon, 2003; Mantovani *et al.*, 2004; Martinez *et al.*, 2008). It has previously been reported that IFNγ andd IFNγR deficient mice have an elevation in the number of alternatively activated macrophages following infection (Arora *et al.*, 2005; Gangadharan *et al.*, 2008). However, to our knowledge, there are no studies investigating the potential of macrophages to differentiate into alternatively activated macrophages in IFNγ or IFNγR-deficient naïve mice. In contrast, as expected with the role of IFNγ in classical macrophage activation, it has been demonstrated that IFNγ unresponsiveness reduces classical macrophage effector function as measured by nitric oxide production (Dighe *et al.*, 1995).

Our data corroborates the previous results by Dighe and colleagues with decreased nitric oxide production following activation of macrophages with LPS + IFNγ. Interestingly, unstimulated macrophages from naïve IFNγR2 deficient mice display an increased Arginase 1 activity, which is also seen following stimulation with IL-4. This suggests these mice not only have a decrease in the classical M1 effector function, but also demonstrate a shift towards the macrophage M2 phenotype following *in vitro* stimulation.

Classically activated macrophages are thought to play a key role in cellular immunity and immunodeficiency. It has recently been demonstrated that macrophages from mice with "macrophages insensitive to interferon-γ" (MIIG mice) are, as we have demonstrated, unable to produce nitric oxide. These mice also have an impaired

ability to control pathogens with an intracellular phase in their life cycle, due to the inability to generate classically activated macrophages (Lykens *et al.*, 2010). In contrast, alternatively activated macrophages are thought to be involved in allergic, cellular, and humoral responses to parasitic and extracellular pathogens. It will be interesting to investigate if complete IFNγR2 deficient or IFNγR2$^{fl/fl}$LysMCre^{+} mice are more resistant to these challenges.

3.4 CONCLUSION

The results present in this chapter demonstrate:

1. The generation and characterisation of a complete IFNγR2 deficient mice and IFNγR2$^{fl/fl}$ mice
2. The generation and confirmation of the abrogation of IFNγ signalling, in the appropriate cell type, in T cell and macrophage specific IFNγR2 deficient mice
3. IFNγR2$^{fl/fl}$ mice will allow for subsequent crosses with different Cre expressing lines to enable the analysis of the role of IFNγ signalling in further cell types
4. The complete IFNγR2 deficient mice display no clear alterations in leukocyte populations but have a decreased responsiveness to IFNα and demonstrate a shift towards an alternatively activated (M2) macrophage phenotype following *in vitro* stimulation.

CHAPTER FOUR

Characterisation of the role of IFNγ in DSS-induced colitis

4.1 INTRODUCTION

The induction of colitis using dextran sodium sulphate is a well-established, reproducible model which has been used for over 20 years (Okayasu *et al.*, 1990). In the acute phase of colitis it is thought that inflammation is driven by the innate immune system, as experiments with SCID mice suggest that adaptive immunity is dispensable (Dieleman *et al.*, 1994; Melgar *et al.*, 2005). Importantly, DSS induced colitis has also been shown to be a relevant model for the translation of data from mice to humans (Melgar *et al.*, 2008). Therefore, understanding the mechanisms underlying DSS induced colitis may aid in understanding the mechanisms underlying IBD in humans.

It has previously been demonstrated that the ablation of IFNγ results in protection from DSS induced intestinal inflammation (Ito *et al.*, 2006; Xu *et al.*, 2008). However, the mechanism through which this protection is achieved is largely unknown. It has been proposed that IFNγ-induced chemokines aids the accumulation of leukocytes in the intestine and therefore, blockade of IFNγ reduces this influx (Ito *et al.*, 2006). The availability of conditional IFNγ receptor deficient mice should help to elucidate whether this is an important mechanism and, if so, which are the key IFNγ-responding cells that produce these chemokines.

Aims

Therefore, the aims are as follows:

1. Establish the dose of DSS which induces colitis in wild type mice
2. Confirm the previously published phenotype in which the abrogation of IFNγ signalling is protective in DSS-induced colitis
3. Using the conditional IFNγ knock-out mice determine which cell type(s) play a role in protection from DSS-induced colitis

4.2 RESULTS

4.2.1. Induction of colitis with dextran sodium sulphate

It has previously been demonstrated that the gut microflora plays an important role in the development of intestinal inflammation and DSS-induced colitis (Tlaskalova-Hogenova et al 2005). The mice in our animal facility were imported from the Helmholtz Centre of Infection Research, Braunschweig, where all mice are maintained with a Charles River altered Schaedler flora (CRASF®). This gut flora is composed of eight 'altered Schaedler flora' strains and has been demonstrated to remain stable in mice maintained in individually ventilated cages for several years, therefore, we are confident that the mice used in our experiments maintain this flora (Stehr *et al.*, 2009). This CRASF® microflora is more restricted than gut flora found in conventional animal units and, as a result, the dose of DSS needed to induce colitis may be different to other facilities. To determine the optimum DSS concentration for colitis induction, prior to the initiation of studies with the mutant mice, we titrated the level of DSS needed to induce colitis in B6 mice.

Initially, we treated B6 mice with 0%, 2%, 2.5% or 3% DSS in their drinking water for 7 days followed by 2 days of normal water. During the entire experiment, bodyweight and clinical symptoms were assessed daily. Until day 3 no clinical symptoms of colitis were observed. From day 4 onwards loss of body weight was observed in the groups being treated with 2.5% and 3% DSS, with a significant loss of weight, compared to the 0% DSS group, observed on day 5 in the 3% DSS group and day 6 in the 2.5% DSS group. The mice treated with 2% DSS subsequently started to lose weight at day 5, reaching significance at day 8 (Fig 4.1A).

By day 8, the mice treated with 3% DSS were showing severe signs of colitis including apathy, diarrhoea and evidence of blood in their stools (Fig 4.1B). Moreover, the mice and had lost approximately 20% of their bodyweight compared to their initial starting weight (Fig 4.1A). Therefore, these mice were euthanised, in accordance with the guidelines in our Home Office project licence. Mice in all other groups were euthanised at day 9. At the time of autopsy, colitis was evident in all

groups of mice treated with DSS with a dose dependent shortening of colon length observed. This change in colon length reached significance in the 3% DSS treatment group compared to 0% DSS treated controls (Fig 4.1C). Furthermore, all treated mice were demonstrating clinical manifestations of colitis with diarrhoea and blood present in the faeces of all mice. In some animals behavioural alterations including piloerection, hunching and apathy was also observed, although this was not significantly different to the control animals (Fig 4.1B).

Histologically, severe ulceration and crypt ablation was observed throughout the colon of mice treated with 3% DSS (Fig 4.2). Less severe inflammation and ulceration was observed in the 2.5% DSS treatment group with the proximal colon relatively unaffected but severe ulceration still evident in the distal colon. Finally, treatment with 2% DSS resulted in milder inflammation with only occasional areas of complete ulceration, all located in the distal colon (Fig 4.2).

Analysis of the systemic cytokine profile was performed in all groups except the 3% DSS treatment group. This group wasn't analysed due to the unplanned euthanasia prior to the end of the experiment. Serum was analysed using the CBA multiplex analysis and demonstrated evidence of systemic inflammation in all DSS treated animals, with elevated levels of the cytokine IL-6 and chemokine MCP-1 (CCL-2) (Fig 4.1D,E). This appears to be a dose-dependent increase, with higher levels seen in the 2.5% DSS treatment group than the 2% DSS group.

A dose of 2.5% DSS was chosen for subsequent experiments as an unambiguous colitic phenotype developed, providing a clear window in which to analyse the expected protective effect of IFNγR2 deficiency.

4.2.2. Comparison of IFNγR2$^{fl/fl}$ and IFNγR2$^{\Delta/\Delta}$ mice – 2.5% DSS colitis

To determine the role of IFNγR2 in the development of DSS induced colitis IFNγR2$^{\Delta/\Delta}$ and IFNγR2$^{fl/fl}$ mice were treated with 0% or 2.5% DSS in their drinking water for 7 days, followed by a 3 day period of drinking water with no additives. Surprisingly, at day 3 the IFNγR2$^{\Delta/\Delta}$ mice treated with DSS had an increased

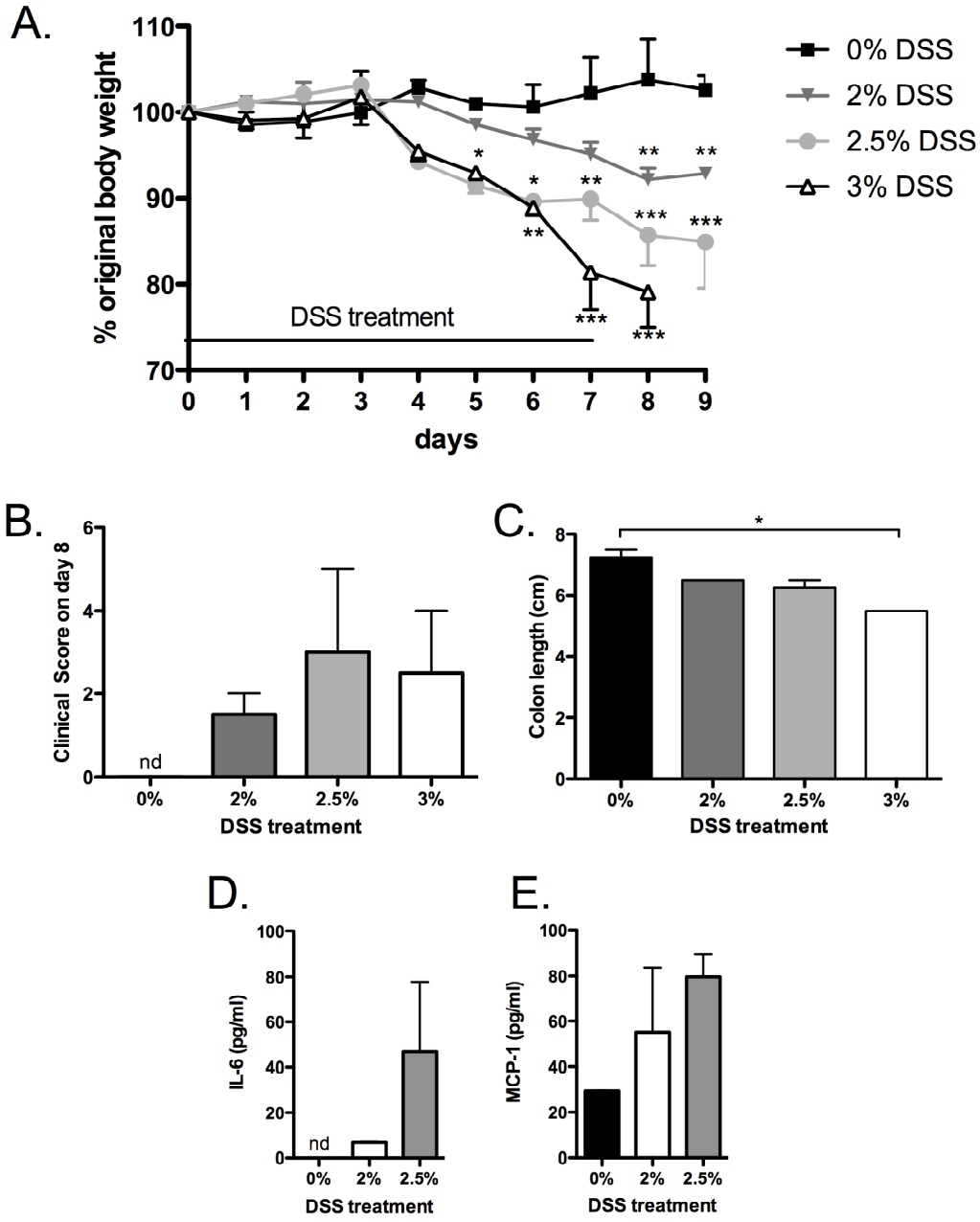

Fig 4.1 DSS-induced colitis phenotype in wild-type (B6) mice. Colitis was induced through the addition of varying concentrations of DSS in drinking water for 7 days. On day 7 water with no additives was given to the mice. **A.** body weight and **B.** clinical symptoms were monitored daily. Upon necrospy **C.** colon length was measured. Blood was harvested from individual mice and serum analysed by CBA for cytokine levels including **D.** IL-6 and **E.** MCP-1 levels. There was no detectable levels of IL-10, IL-17, IL-4, IFNγ, TNF or IL-13. Results are presented as mean ± s.e. per group, n=2 per group. *p<0.05. **p<0.01, ***p<0.001 statistically significant compared to 0% DSS treatment. nd=none detected

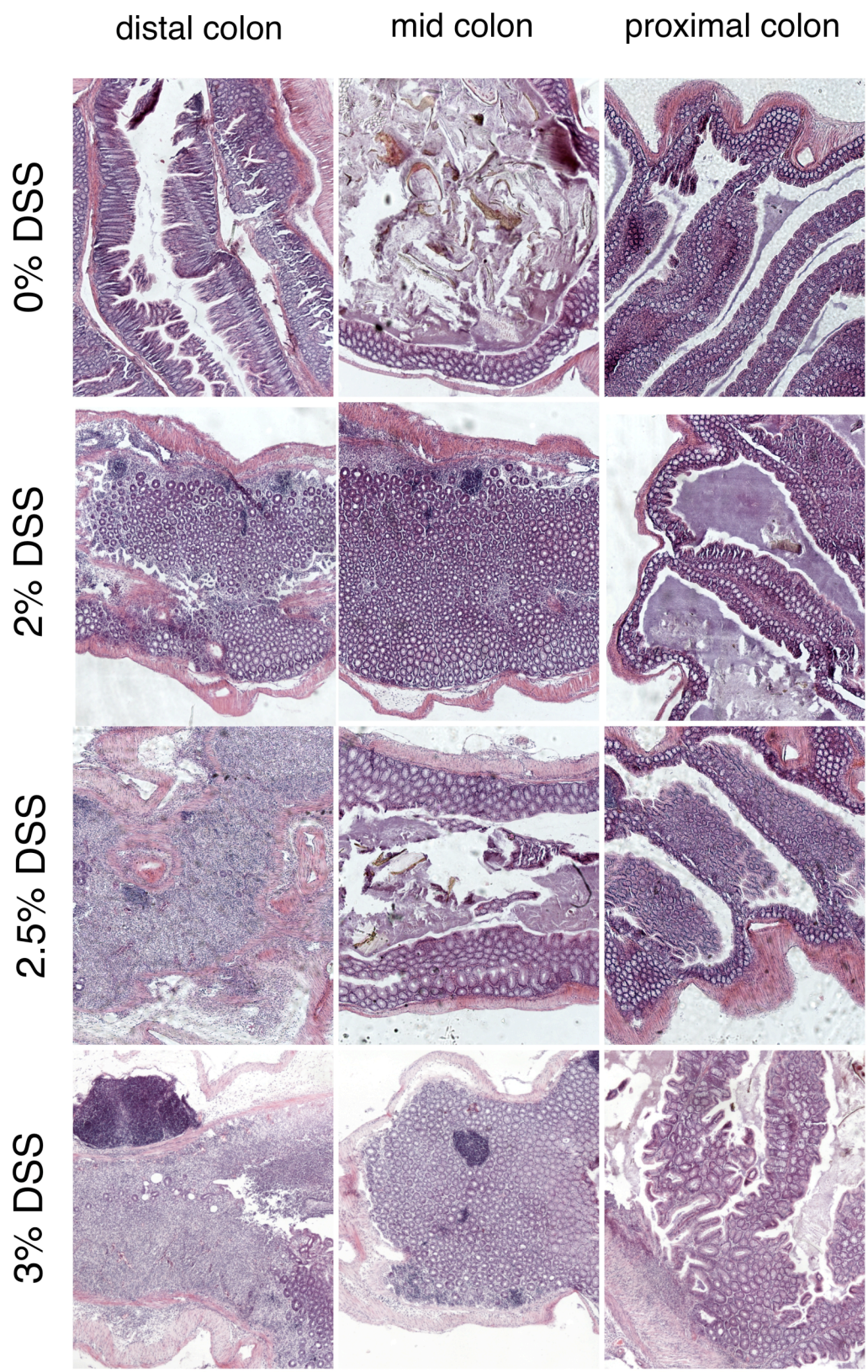

Fig 4.2 DSS-induced histological inflammation in wild-type (B6) mice. Colitis was induced through the addition of varying concentrations of DSS in drinking water for 7 days. On day 7 water with no additives was given to the mice. Histological changes were analysed from longitudinal H&E stained sections. Sections displayed are representative of each group, n=2 per group

bodyweight compared to the untreated IFNγR2$^{\Delta/\Delta}$ mice. However, by day 6 the bodyweight of DSS treated IFNγR2$^{\Delta/\Delta}$ mice had significantly decreased in comparison to the untreated IFNγR2$^{\Delta/\Delta}$ mice (Fig 4.3A). Similarly, the DSS treated IFNγR2$^{fl/fl}$ mice demonstrated a significantly decreased bodyweight compared to untreated IFNγR2$^{fl/fl}$ control mice from day 5 onwards (Fig 4.3A). Unexpectedly, by day 7 the IFNγR2$^{\Delta/\Delta}$ mice treated with DSS were showing very severe signs colitis including diarrhoea, piloerection and up to 20% bodyweight loss compared to day 0 (Fig 4.3A,B). As the control IFNγR2$^{fl/fl}$ mice treated with DSS were also displaying 10-15% bodyweight loss compared to their starting weight (Fig 4.3A) the experiment was terminated early, at day 7.

Upon necropsy it was apparent that both groups treated with DSS showed a significant shortening of the colon (Fig 4.3C), a typical sign of acute intestinal inflammation. Furthermore, a significant decrease in colon length was seen in the IFNγR2$^{\Delta/\Delta}$ DSS treated mice compared to the IFNγR2$^{fl/fl}$ treated animals, despite similar colon lengths in untreated mice (Fig 4.3C). Moreover, both the DSS treated groups displayed swelling of the colon wall with an absence of faecal pellets evident through visual inspection of the colon.

To determine the pathological basis of the clinical symptoms of colitis, we examined the histology in the intestinal tract of DSS-treated and control animals. There were prominent changes following DSS treatment with severe ulceration, loss of morphology and crypt architecture, loss of the epithelial layer and inflammatory cell infiltration. These changes were statistically significant and observed throughout all sections of the colon in IFNγR2$^{\Delta/\Delta}$ DSS treated mice (Fig 4.4A,B). By contrast, although DSS treated IFNγR2$^{fl/fl}$ mice also showed severe ulceration, loss of morphology and inflammatory cell infiltration in the distal colon, other areas of the colon were less severely affected (Fig 4.4A). In the mid colon there were patches of ulceration, but this was not continual with some areas of intact epithelium and the proximal colon had mild – medium inflammation with less ulceration than seen in the other sections of the colon and areas of normal crypt architecture. However, none

of the changes observed in the IFNγR2$^{fl/fl}$ mice, when scored, were significantly different to IFNγR2$^{fl/fl}$ untreated animals (Fig 4.4A,B).

Systemically there were no significant changes in cytokine levels with no IL-10, IL-17A, IL-4, TNF or IL-13 detected in the serum. In both IFNγR2$^{fl/fl}$ and IFNγR2$^{\Delta/\Delta}$ DSS treated mice there was an elevation in systemic IL-6 levels (Fig 4.4C), however this didn't reach significance. Moreover, systemic IFNγ was detected in 2 of the IFNγR2$^{fl/fl}$ mice treated with DSS but in no other treatment groups. However, in both mice the levels of IFNγ were very low (below 5pg/ml) and this wasn't statistically significant (Fig 4.4E).

Differences in clinical scores and histological changes, particularly in the proximal colon, between the IFNγR2$^{\Delta/\Delta}$ and IFNγR2$^{fl/fl}$ mice suggest that the IFNγR2$^{\Delta/\Delta}$ animals appear more susceptible to DSS than control animals. However, there was not a clear difference, between the genotypes, and therefore the experiment was repeated with a milder DSS treatment to allow the experiment to run to completion.

4.2.3. Comparison of IFNγR2$^{fl/fl}$ and IFNγR2$^{\Delta/\Delta}$ mice – 2% DSS colitis

Similarly to the previous experiment (2.5% DSS), IFNγR2$^{\Delta/\Delta}$ and IFNγR2$^{fl/fl}$ mice were treated with 0% or 2.0% DSS in their drinking water for 7 days, followed by a 3 day period of drinking water with no additives. Despite the milder DSS regime weight loss was evident in both groups treated with DSS by day 5. In both the IFNγR2$^{\Delta/\Delta}$ and IFNγR2$^{fl/fl}$ DSS treated mice the weight loss was significant in comparison to untreated controls of the same genotype by day 7 (Fig 4.5A). Furthermore, the experiment was ended early, on day 9, due to the significant weight loss and clinical manifestations of colitis evident in the mice. The clinical symptoms were significantly worse in the DSS treated IFNγR2$^{\Delta/\Delta}$ mice compared to the DSS treated IFNγR2$^{fl/fl}$ mice, although both groups had significantly increased clinical scores compared to untreated mice (Fig 4.5B). This was mirrored with the bodyweight data as an increased weight loss was observed in the DSS treated IFNγR2$^{\Delta/\Delta}$ mice compared to the DSS treated IFNγR2$^{fl/fl}$ mice, although this didn't reach significance (Fig 4.5A).

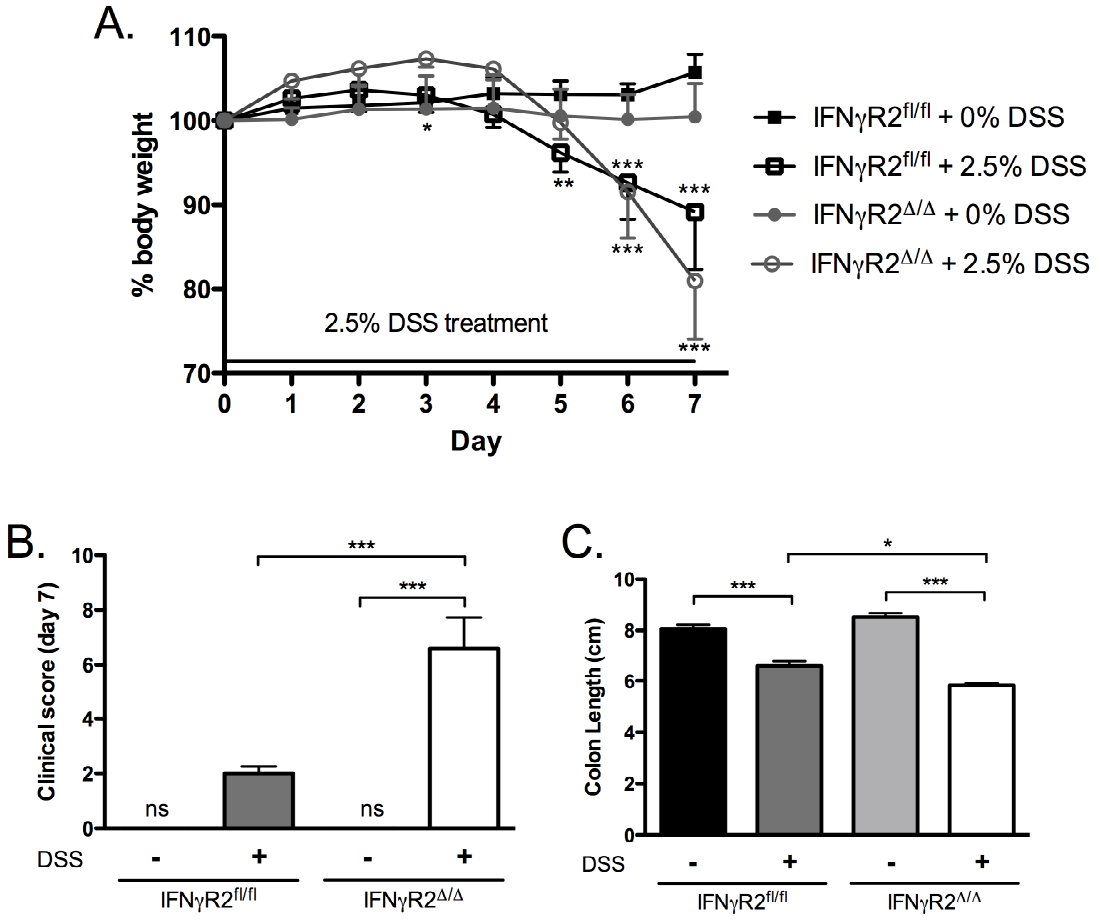

Fig 4.3 Colitis in IFNγR2$^{fl/fl}$ and IFNγR2$^{\Delta/\Delta}$ mice induced by 2.5% DSS. Colitis was induced through the addition of 2.5% DSS in drinking water for 7 days. **A.** Body weight and **B.** Clinical symptoms were monitored daily. Upon necrospy **C.** colon length was measured. Results are prsentented as mean ± s.e. per group. *p<0.05. **p<0.01, ***p<0.001 statistically significant compared to 0% DSS treatment or as indicated, ns= no score. n=5 for IFNγR2$^{\Delta/\Delta}$ groups, n=6 for IFNγR2$^{fl/fl}$ + 2.5% DSS and n=4 for IFNγR2$^{fl/fl}$ untreated mice.

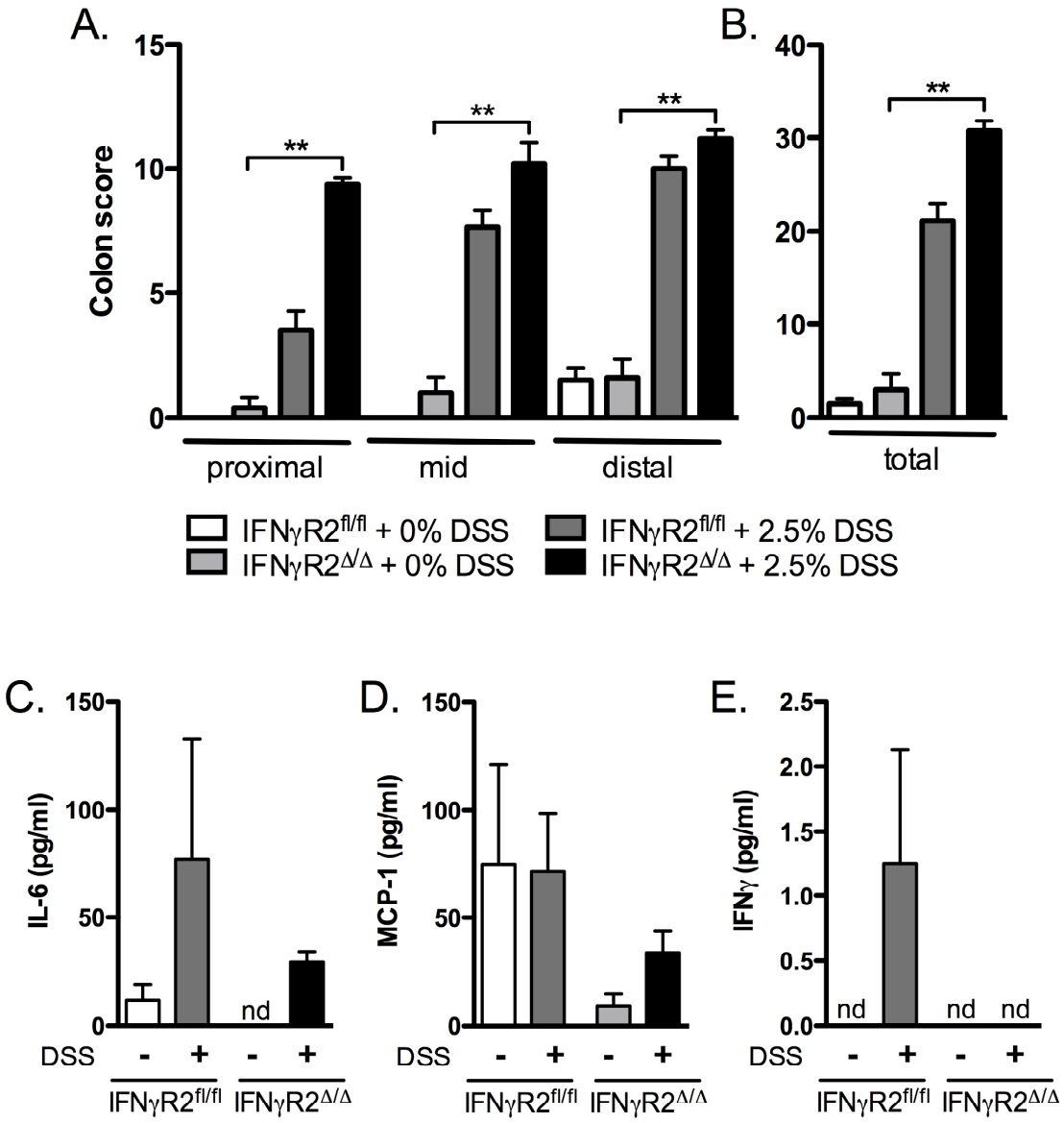

Fig 4.4 Quantification of histological changes and alterations in inflammatory mediators in IFNγR2$^{fl/fl}$ and IFNγR2$^{\Delta/\Delta}$ mice induced by 2.5% DSS. Colitis was induced through the addition of 2.5% DSS in drinking water for 7 days. Longitudinal histological sections were stained with haematoxylin and eosin and visualised on a light microscope. Histological alterations were quantificatied in **A.** colon sections and **B.** total colon. Upon necrospy blood was harvested from individual mice and serum analysed by CBA for cytokine levels including **C.** IL-6, **D.** MCP-1 and **E.** IFNγ levels. There were no detectable levels of IL-10, IL-17A, IL-4, TNF or IL-13. Results are presented as mean ± s.e. per group *p<0.05. **p<0.01, ***p<0.001 statistically significant compared to 0% DSS treatment. nd=none detected. n=5 for IFNγR2$^{\Delta/\Delta}$ groups, n=6 for IFNγR2$^{fl/fl}$ + 2.5% DSS and n=4 for IFNγR2$^{fl/fl}$ untreated mice.

Upon necropsy DSS treated animals had macroscopically evident colitis, characterised by significantly shortened colons with a lack of visible faecal pellets (Fig 4.5C), although there were no differences between the genotypes. To enable more detailed investigation, instead of using the whole colon for longitudinal histological analysis, transverse gut samples were taken from the caecum, proximal, mid and distal colon. Sections were also taken from the distal colon for RNA analysis.

Upon histological analysis only sections of the proximal colon and caecum could be analysed for crypt length. This was due to a complete ablation of all crypt architecture in both the mid and distal colon of DSS treated animals (Fig 4.6). In the proximal colon there was evidence of a trend towards crypt hyperplasia in the DSS-treated IFNγR2$^{\Delta/\Delta}$ mice with no changes evident in the IFNγR2$^{fl/fl}$ mice, however, this did not achieve significance (Fig 4.7B). Conversely, in the caecum significant crypt hyperplasia was observed in the IFNγR2$^{fl/fl}$ DSS treated mice compared to untreated IFNγR2$^{fl/fl}$ animals. However, no clear changes in crypt architecture was evident in the caecum of the IFNγR2$^{\Delta/\Delta}$ DSS treated mice (Fig 4.7C). As well as measurements of crypt length evidence of ulceration, inflammation and oedema was scored for each section. This revealed significantly increased histological alterations in the DSS treated IFNγR2$^{\Delta/\Delta}$ mice in all sections of the colon and the caecum with the largest changes evident in the distal colon. Similarly, significant changes were seen in the DSS treated IFNγR2$^{fl/fl}$ mice in the mid and distal colon and the caecum but there were no significant differences between the genotypes in any area (Fig 4.7A).

Systemically, low levels of the cytokines IL-17A, IL-4 and TNF were detectable in the serum of IFNγR2$^{\Delta/\Delta}$ DSS treated mice, but not in any of the other treatment groups, however none of these increases were significant (Fig 4.8A,C,F). Systemic levels of IFNγ and MCP-1 were also detected, however, they were present across all groups, including untreated animals, and showed no clear trends (Fig 4.8B,E). The only other cytokine tested that was detected systemically was IL-6. This displayed a

trend towards increased levels in both IFNγR2$^{fl/fl}$ and IFNγR2$^{\Delta/\Delta}$ DSS treated animals, however, in neither genotype did this reach significance (Fig 4.8D)

Analysis of mRNA transcripts from the colons of treated mice demonstrated no increase of IFNγ message in IFNγR2$^{fl/fl}$ or IFNγR2$^{\Delta/\Delta}$ mice following DSS treatment (Fig 4.9D). Furthermore, there were no changes in IFNγ-responsive genes including iNOS, IP-10 and ifi205 (Gough *et al.*, 2007) (Fig 4.9A-C). Interestingly, there appears to be a trend towards an increase in IFNγ-responsive gene (iNOS, IP-10, ifi205) message in untreated IFNγR2$^{\Delta/\Delta}$ mice, compared to untreated IFNγR2$^{fl/fl}$ mice. Furthermore, levels of IL-10 transcript was slightly, but not significantly, increased in IFNγR2$^{\Delta/\Delta}$ mice compared to IFNγR2$^{fl/fl}$ mice independently of DSS treatment. The most significant difference in mRNA levels was seen in SOCS1 message which was significantly elevated upon DSS treatment, with a 40-fold and 80-fold increase seen in DSS treated IFNγR2$^{fl/fl}$ and IFNγR2$^{\Delta/\Delta}$ mice respectively. There is also an approximately 7-fold increase in resting levels of SOCS1 transcript in IFNγR2$^{\Delta/\Delta}$ mice compared to IFNγR2$^{fl/fl}$ mice (Fig 4.9F).

4.2.4. Comparison of IFNγR2$^{fl/fl}$ and IFNγR2$^{\Delta/\Delta}$ mice – 1.5% DSS colitis

To confirm the reason we were unable to see a clear phenotype was not due to the severity of the colitis a further experiment was performed, this time with a DSS concentration of 1.5%.

As with the previous experiments, IFNγR2$^{\Delta/\Delta}$ and IFNγR2$^{fl/fl}$ mice were treated with 0% or 1.5% DSS in their drinking water, this time for 5 days followed by a period of drinking water with no additives. Unexpectedly, despite the decrease in DSS percentage, both IFNγR2$^{fl/fl}$ and IFNγR2$^{\Delta/\Delta}$ treated mice displayed a significant decrease in bodyweight on day 6. By day 7 this had reached a 15-20% loss of bodyweight (Fig 4.10A), and was significantly greater in IFNγR2$^{fl/fl}$ mice compared to IFNγR2$^{\Delta/\Delta}$ mice. The animals were euthanised on day 7 to prevent any more suffering as there was already a statistically significant increase in clinical symptoms of colitis including diarrhoea and bloody stools in both DSS treated groups (Fig 4.10B). Upon necropsy DSS treated animals had macroscopically evident colitis

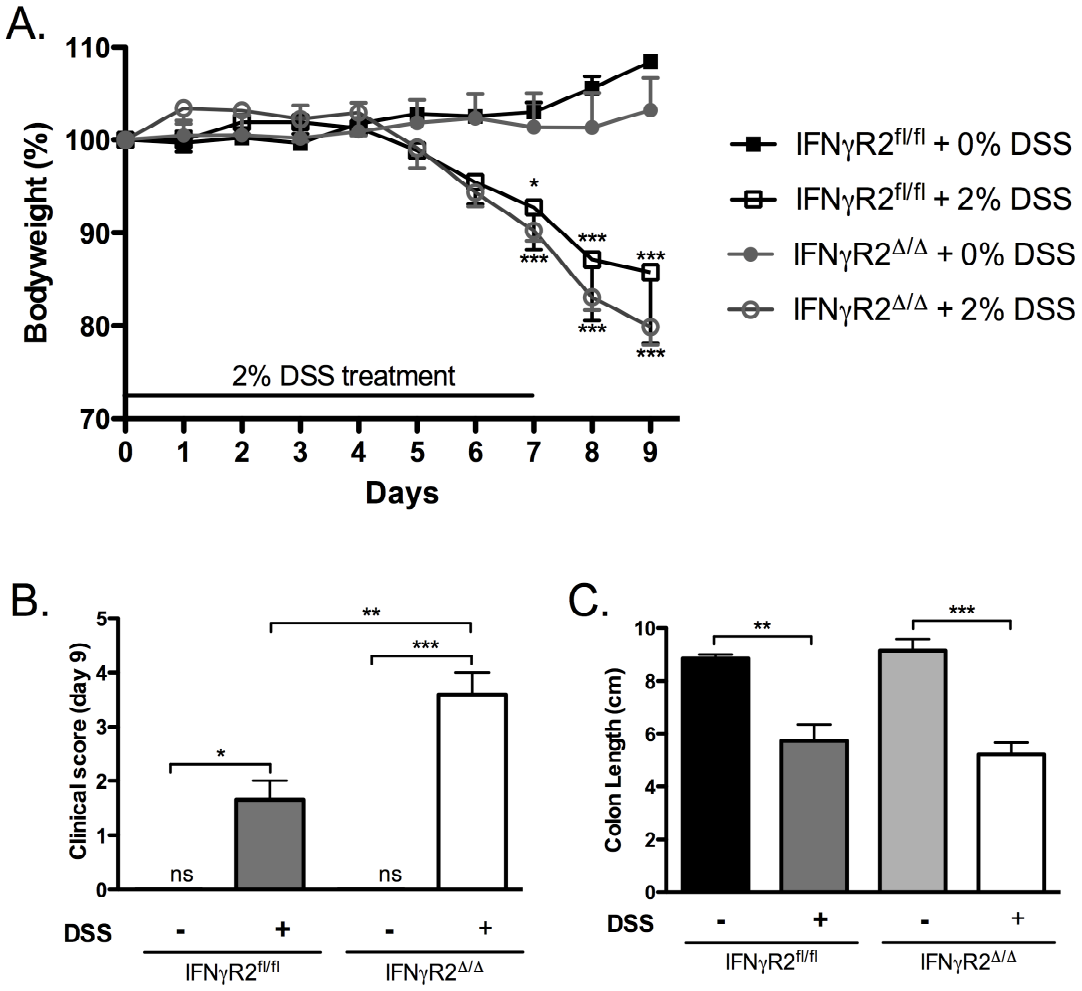

Fig 4.5 Colitis in IFNγR2$^{fl/fl}$ and IFNγR2$^{\Delta/\Delta}$ mice induced by 2.0% DSS. Colitis was induced through the addition of 2.0% DSS in drinking water for 7 days. **A.** Body weight and **B.** Clinical symptoms were monitored daily. Upon necrospy **C.** colon length was measured. Results are presented as mean ± s.e. per group. *p<0.05. **p<0.01, ***p<0.001 statistically significant compared to 0% DSS treatment or as indicated. ns=no score / scored 0. n=4 for 0% DSS treatment groups, n=3 for IFNγR2$^{fl/fl}$ + 2% DSS and n=5 for IFNγR2$^{\Delta/\Delta}$ + 2% DSS

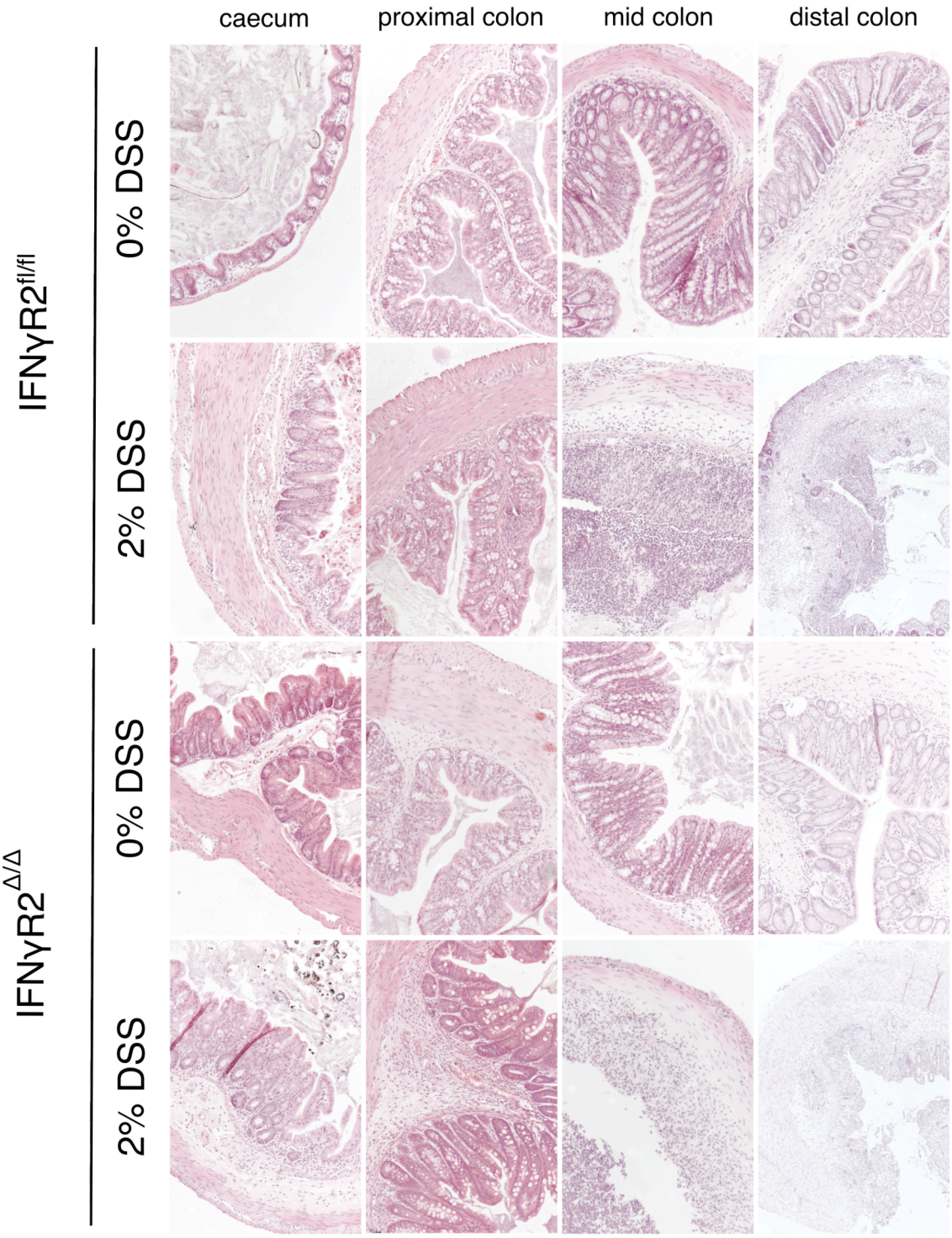

Fig 4.6 DSS-induced histological inflammation in IFNγR2$^{fl/fl}$ and IFNγR2$^{\Delta/\Delta}$ mice treated with 0 or 2% DSS. Colitis was induced through the addition of 2% DSS in drinking water for 7 days. On day 7 water with no additives was given to the mice. Histological changes were analysed from transverse H&E stained sections. Sections displayed are representative of each group.

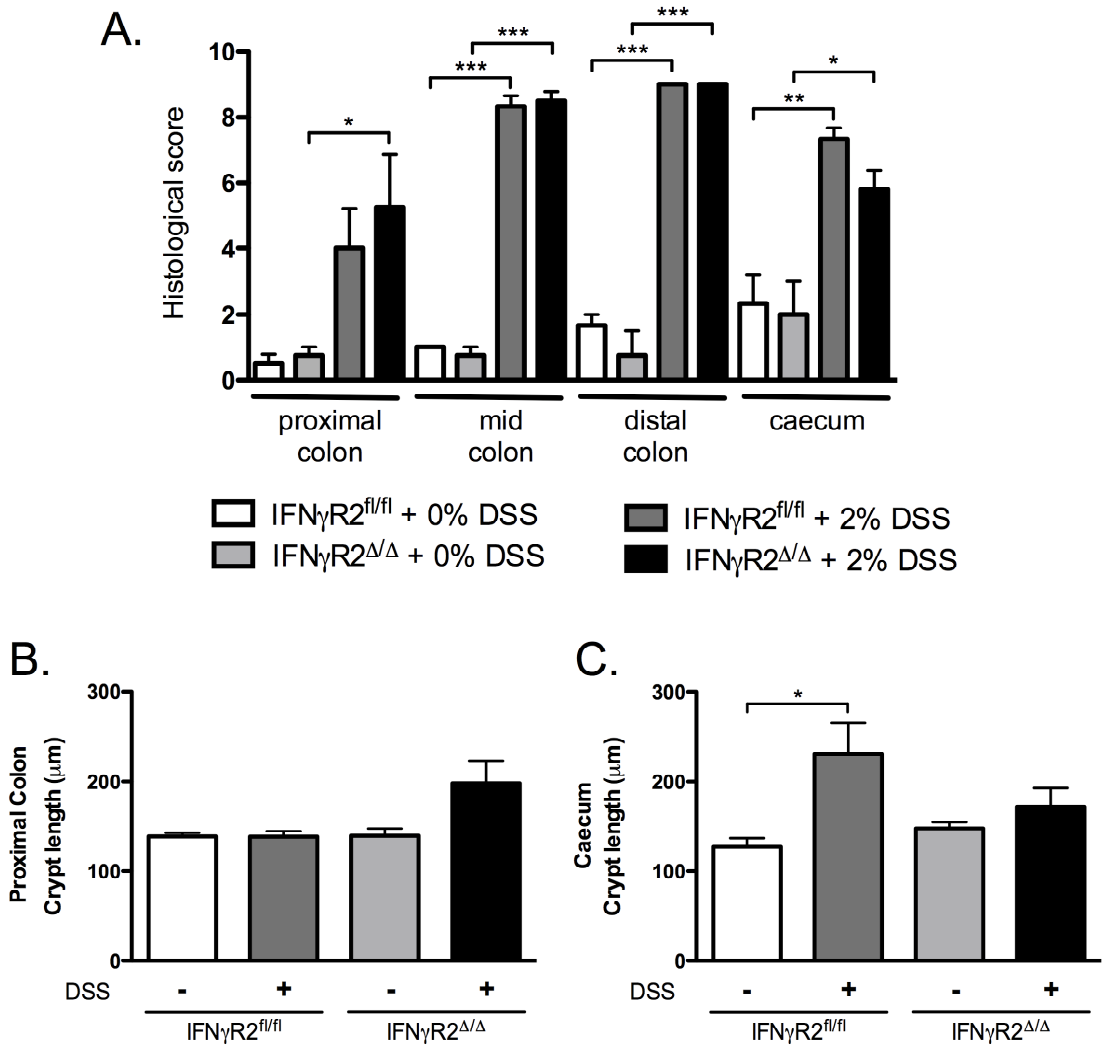

Fig 4.7 Quantification of histological changes in IFNγR2$^{fl/fl}$ and IFNγR2$^{\Delta/\Delta}$ mice induced by 2.0% DSS. Colitis was induced through the addition of 2.0% DSS in drinking water for 7 days. Transvere histological sections were stained with haematoxylin and eosin and visualised on a light microscope. **A.** Histological alterations were quantified and crypt lengths were measured using Image J® software in **B.** proximal colon and **C.** the caecum. Results are prsentented as mean ± s.e. per group. *p<0.05. **p<0.01, ***p<0.001 statistically significant compared to 0% DSS treatment. n=4 for 0% DSS treatment groups, n=3 for IFNγR2$^{fl/fl}$ + 2% DSS and n=5 for IFNγR2$^{\Delta/\Delta}$ + 2% DSS

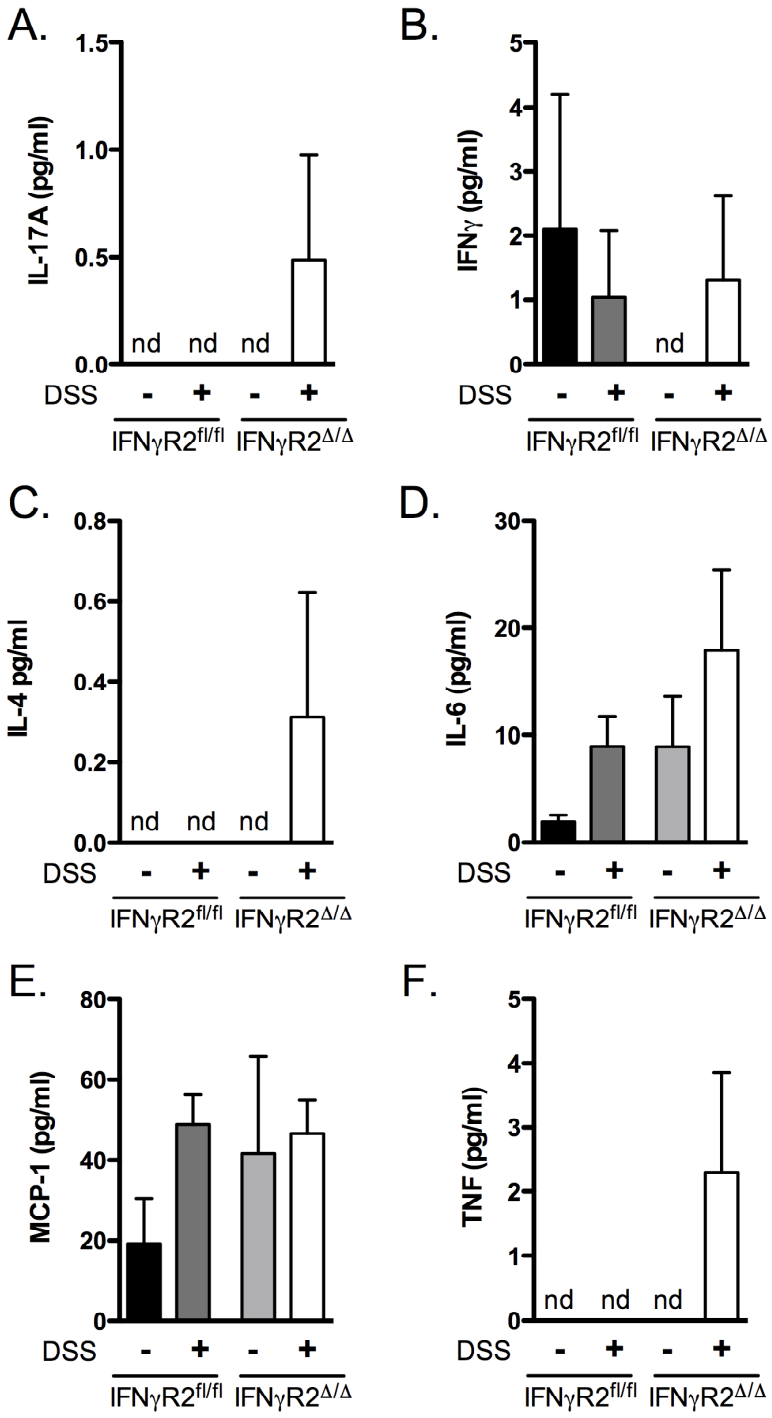

Fig 4.8 Alterations in serum cytokine levels in IFNγR2$^{fl/fl}$ and IFNγR2$^{\Delta/\Delta}$ mice induced by 2.0% DSS. Colitis was induced through the addition of 2.0% DSS in drinking water for 7 days. On day 7 water with no additives was given to the mice. Blood was harvested from individual mice and serum analysed by CBA for cytokine levels including **A.** IL-17A **B.** IFNγ **C.** IL-4 **D.** IL-6 **E.** MCP-1 and **F.** TNF levels. There were no detectable levels of IL-10 or IL-13. Results are prsentented as mean ± s.e. per group. nd = none detected. n=4 for 0% DSS treatment groups, n=3 for IFNγR2$^{fl/fl}$ + 2% DSS and n=5 for IFNγR2$^{\Delta/\Delta}$ + 2% DSS

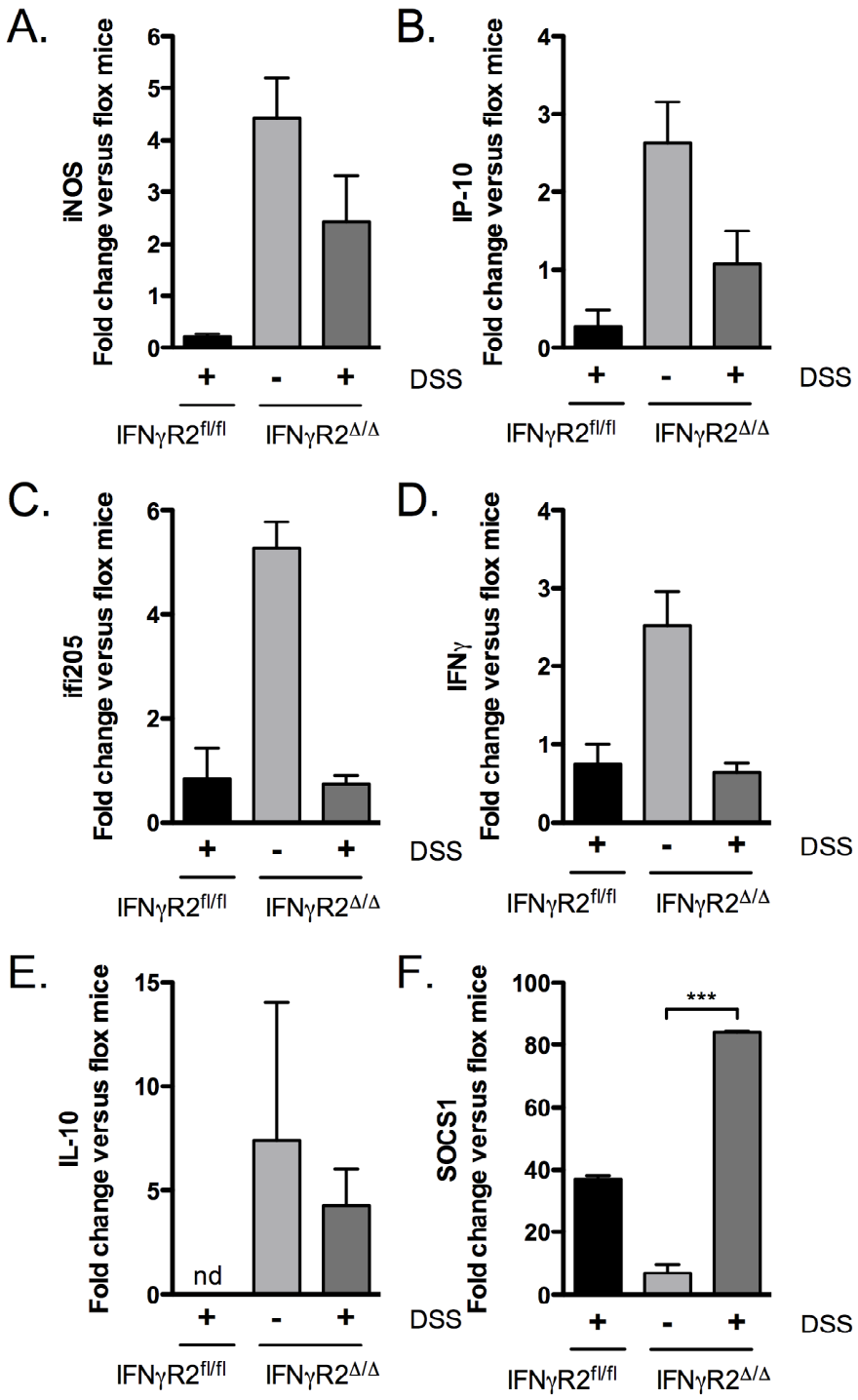

Fig 4.9 Relative-fold change in A. iNOS B. IP-10 C. ifi205 D. IFNγ E. IL-10 and F. SOCS1 in the colon of IFNγR2$^{fl/fl}$ and IFNγR2$^{\Delta/\Delta}$ mice treated with 2.0% DSS. Colitis was induced through the addition of 2.0% DSS in drinking water for 7 days. On day 7 water with no additives was given to the mice. Upon sacrifice a portion of the colon was snap frozen in trizol, the RNA extracted and reverse transcribed to cDNA, which was quantified using SYBR green qPCR. Results were normalised to HPRT and expressed as fold change compared to IFNγR2$^{fl/fl}$ mice give 0% DSS, via the ΔΔCt method. Results are prsentented as mean ± s.e. per group. *p<0.05. **p<0.01, ***p<0.001 statistically significant compared to 0% DSS treatment, nd=no difference. n=4 for 0% DSS treatment groups, n=3 for IFNγR2$^{fl/fl}$ + 2% DSS and n=5 for IFNγR2$^{\Delta/\Delta}$ + 2% DSS

exemplified by significantly shortened colons. DSS treated IFNγR2$^{\Delta/\Delta}$ mice had shorter, but not significantly so, colons than the DSS treated IFNγR2$^{fl/fl}$ mice (Fig 4.10C).

Upon histological analysis IFNγR2$^{\Delta/\Delta}$ mice displayed a complete ulceration of the distal and mid section of the colon, which was statistically significant. Less severe ulceration was evident in the proximal section but this didn't reach significance, in comparison to untreated IFNγR2$^{\Delta/\Delta}$ mice (Fig 4.11A, B). Similarly, IFNγR2$^{fl/fl}$ mice displayed increasing ulceration when moving up from the distal to the proximal colon sections. These histological alterations were significantly increased compared to the IFNγR2$^{fl/fl}$ untreated mice in the distal and mid colon but did not reach significance over the total colon (Fig 4.11A,B).

Similar systemic inflammation as the previous DSS experiments, was observed with a trend towards increased IL-6 levels in the DSS treated animals, independently of genotype (Fig 4.11F). Detectable levels of circulating MCP-1 and TNF were observed but displayed no clear trends (Fig 4.11E,G) and elevated IL-17A and IFNγ levels were seen in DSS treated IFNγR2$^{\Delta/\Delta}$ or IFNγR2$^{\Delta/\Delta}$ and IFNγR2$^{fl/fl}$ mice respectively (Fig 4.11C,D).

These results demonstrate that the phenotype of IFNγR2$^{\Delta/\Delta}$ mice in the DSS-induced colitis appears to be slightly more severe than the colitis observed in the DSS treated IFNγR2$^{fl/fl}$ mice. This is evident through the increased weight loss and severity of histological alterations when subjected to 2.5% or 2.0% DSS. However, these changes are not all statistically significant. Nevertheless, it can be conclusively stated that our IFNγR2$^{\Delta/\Delta}$ mice do not appear to be protected from the effects of DSS-induced colitis. Due to the absence of a clear distinguishable phenotype between the DSS treated IFNγR2$^{\Delta/\Delta}$ mice and DSS treated IFNγR2$^{fl/fl}$ mice no further experiments, utilising the conditional IFNγR2 knock-out mice, were performed.

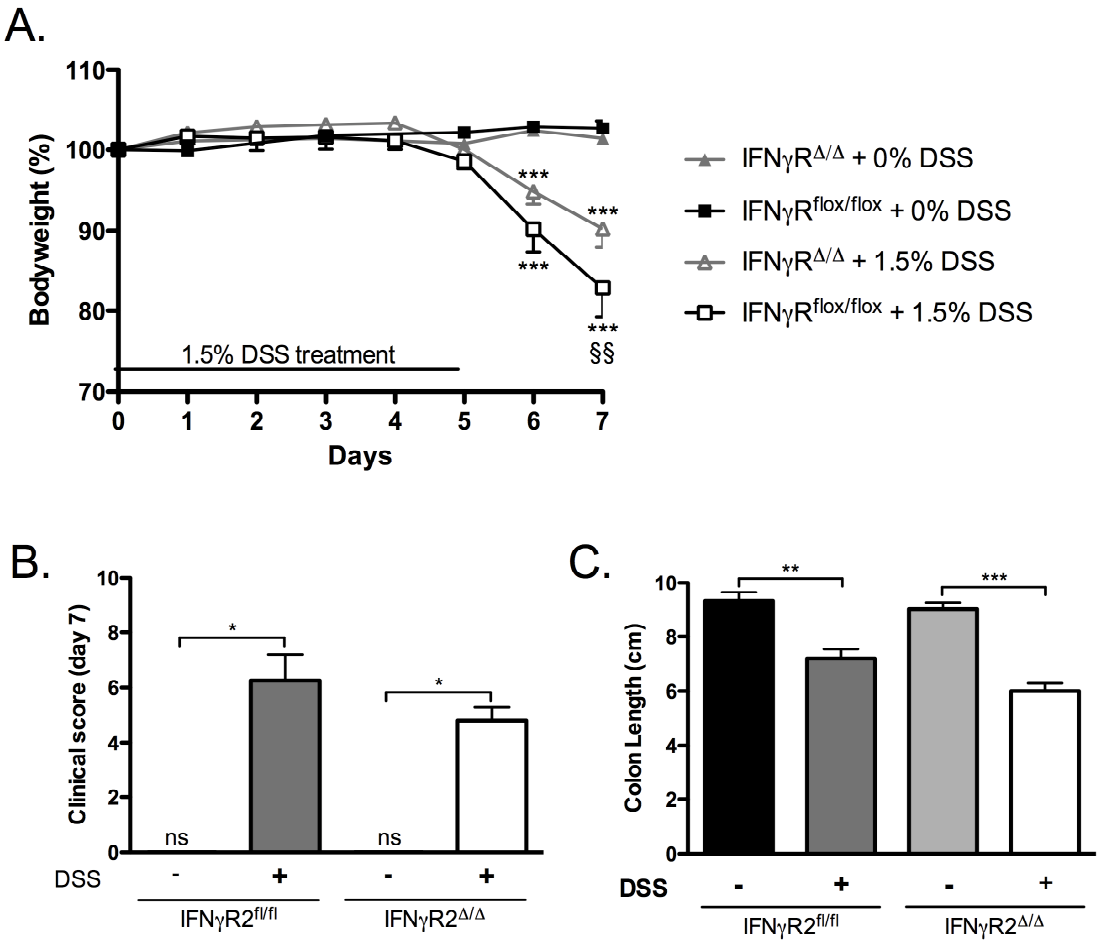

Fig 4.10 Colitis in IFNγR2$^{fl/fl}$ and IFNγR2$^{\Delta/\Delta}$ mice induced by 1.5% DSS. Colitis was induced through the addition of 1.5% DSS in drinking water for 5 days following by water with no additives for 2 days **A.** Body weight and **B.** Clinical symptoms were monitored daily. Upon necrospy **C.** colon length was measured. Results are presented as mean ± s.e. per group. *p<0.05. **p<0.01, ***p<0.001 statistically significant compared to 0% DSS treatment or as indicated, §p<0.05, §§p<0.01, §§§p<0.001 compared to IFNγR2$^{fl/fl}$ mice. ns= no score / scored zero. n=4 for IFNγR2$^{fl/fl}$ groups, n=5 for IFNγR2$^{\Delta/\Delta}$ + 1.5% DSS and n=6 for IFNγR2$^{\Delta/\Delta}$ + 0% DSS

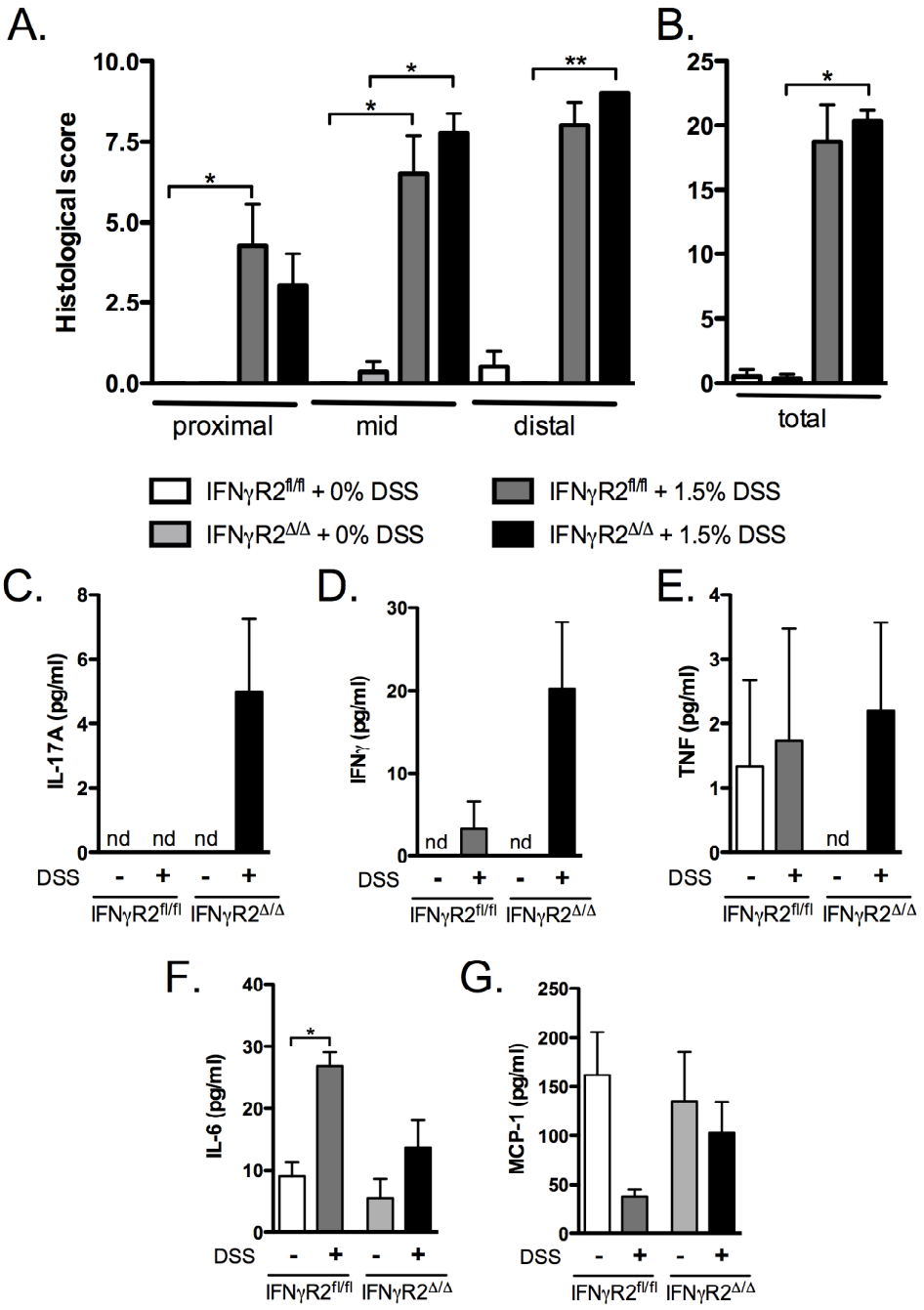

Fig 4.11 Quantification of histological changes and alterations in inflammatory mediators in IFNγR2$^{fl/fl}$ and IFNγR2$^{\Delta/\Delta}$ mice induced by 1.5% DSS. Colitis was induced through the addition of 1.5% DSS in drinking water for 5 days following by water with no additives for 2 days. Longitudinal histological sections were stained with haematoxylin and eosin and visualised on a light microscope. Histological alterations were quantificatied in **A.** colon sections and **B.** total colon. Upon necrospy blood was harvested from individual mice and serum analysed by CBA for cytokine levels including **C.** IL-17A, **D.** IFNγ, **E.** TNF, **F.** IL-6 and **G.** MCP-1 levels. There were no detectable levels of IL-10, IL-4 or IL-13. Results are presented as mean ± s.e. per group *p<0.05. **p<0.01, ***p<0.001 statistically significant compared to 0% DSS treatment. nd=none detected. n=4 for IFNγR2$^{fl/fl}$ groups, n=5 for IFNγR2$^{\Delta/\Delta}$ + 1.5% DSS and n=6 for IFNγR2$^{\Delta/\Delta}$ + 0% DSS

4.3 DISCUSSION

DSS-induced colitis is a well-established model of acute, innate-driven intestinal inflammation (Dieleman *et al.*, 1994; Okayasu *et al.*, 1990). Increasing the percentage of DSS administered in the drinking water of mice gives a dose-dependent increase in colitis pathology. There is also some, slightly contradicting, data on the importance of water intake and thus the total DSS dose administered. Some experiments show it is the concentration of DSS administered, and not the total DSS dose consumed, that is the key factor in the severity of the colitis phenotype observed. Therefore, a minor change in fluid consumption, either between treatment groups or between different mice within a group, does not affect the severity of colitis observed (Egger *et al.*, 2000). However, other experiments demonstrate a decrease in water consumption at high DSS concentrations and a correlation between total DSS dose (incorporating both water consumption and DSS concentration) and colitis (Vowinkel *et al.*, 2004). Nevertheless, in the pilot study we performed, despite not monitoring water intake, a clear dose dependent increase in pathology was observed in wild-type mice treated with DSS in their drinking water.

Previous studies have demonstrated that deletion of IFNγ results in protection against (Ito *et al.*, 2006) or reduced severity (Nava *et al.*, 2010; Xu *et al.*, 2008) of DSS-induced colitis. This is in stark contrast to our results, which suggest no protection against colitis and, if anything, a slight increased severity observed in IFNγR2$^{\Delta/\Delta}$ mice. However, in our experiments the IFNγR2$^{fl/fl}$ mice treated with DSS had no significant elevation in either intestinal or systemic levels of IFNγ. Therefore, the absence of a phenotype in IFNγR2$^{\Delta/\Delta}$ mice is expected. Conversely, in previous experiments a significant elevation of IFNγ levels in the colon is observed following DSS treatment (Ito *et al.*, 2006; Nava *et al.*, 2010). Several discrepancies in experimental protocol could underlie the differences observed between the different experiments including: background strain or gut flora of mice and the molecular weight of the DSS used for colitis induction.

4.3.1. Molecular weight of DSS could result in differences seen in the colitic phenotype of IFNγ deficient mice.

It has been demonstrated that altering the molecular weight of DSS used for the induction of colitis in mice can impact both the severity and primary location of colitis observed. Mice given 5kD DSS develop a colitis predominantly observed in the caecum and upper colon, where as mice given 40kD DSS develop a colitis which is predominant in the lower colon and is more severe than the colitis induced by 5kD DSS (Kitajima *et al.*, 2000). Ito *et al.* used DSS with a molecular weight of 5kDa, but neither Xu *et al.* nor Nava *et al.* state the molecular weight of the DSS used in their experiments. For our experiments we used DSS with a molecular weight of 36-50kDa, and in keeping with observations of Kitajima *et al.*, we detected the most severe inflammation in the lower colon. In the experiment performed by Ito *et al.,* where total protection against DSS is observed in the absence of IFNγ, the histological alterations aren't divided into segments of the colon; therefore it cannot be determined if the colitis predominated in the upper colon or the lower colon. Nevertheless, given the alterations in both severity and location previously reported, the lower molecular weight DSS may be driving inflammation through an altered mechanism which, in turn, could be driving the significant elevation of IFNγ seen in this model.

4.3.2. Background strain of mice could result in differences in colitic phenotypes.

It has been extensively documented that the background strain of mice is a key factor in determining the severity of colitis observed following DSS treatment. Mahler *et al.* analysed acute DSS-colitis in nine inbred strains and observed the pattern and severity of colitis. C3H/HeJ mice were most susceptible to colitis with a colonic ulceration frequency of 88%. In contrast, no ulcerations were observed DBA/2J mice. In this study by Mahler *et al.*, both B6 and 129/Sv mice were highly susceptible to colitis, with severe inflammation observed in the colon. Interestingly, despite similar colonic pathology B6 mice had significantly increased inflammation in the caecum compared to 129/Sv mice (Mahler *et al.*, 1998). In previous experiments using IFNγ deficient mice, animals used were fully backcrossed onto a

B6 line (Ito *et al.*, 2006; Nava *et al.*, 2010; Xu *et al.*, 2008). However, the mice we used for these experiments were on a mixed genetic background of B6 and 129/Sv. Although these two lines appear to have relatively similar inflammatory response to DSS (Mahler *et al.*, 1998), it is important to also recognise that knowing the phenotype of parental strains doesn't always define the range of responses in animals derived from their crossing. It has been demonstrated that epistatic interactions can occur between two strains resulting in a phenotype in offspring unlike the phenotype seen in either of the parental strains (Miner, 1997). This could explain the high sensitivity to the DSS-induced colitis seen in our IFNγR2$^{fl/fl}$ mice. These mice succumbed to severe colitis at low DSS concentrations when compared to the colitis observed B6 mice used in the pilot study. However, the genetic strain is unlikely to underlie the different phenotype of the IFNγR2 deficient mice in comparison to the IFNγ deficient mice of previous studies as both the IFNγR2$^{\Delta/\Delta}$ and IFNγR2$^{fl/fl}$ mice were on the same mixed background.

4.3.3. Gut flora of mouse colonies could influence the colitic phenotype of IFNγ deficient mice.

There is increasing evidence that normal enteric bacteria can play an important role in the intestinal inflammation see in both human IBD and in experimental colitis models. The association of enteric bacteria with inflammation in DSS-colitis is well described. Okayasu *et al*. reported alterations in the balance of enteric bacteria following acute DSS colitis, with increases in *Bacteroides, Enterobacter* and *Clostridium* but decreases in *Eubacterium spp.* and *Enterococcus spp* (Okayasu *et al.*, 1990).

It has recently been demonstrated in DSS-induced colitis that the inner mucus layer of the colon, which is normally devoid of bacteria, becomes penetrated with bacteria following DSS treatment. Moreover, this occurs prior to the observation of any intestinal inflammation (with 24 hours of DSS administration) and therefore could be one of the mechanisms through which DSS induces colitis (Johansson *et al.*, 2010). This is supported through experiments demonstrating that treatment with some antibiotics can eliminate certain bacterial strains and therefore protect against colitis.

It is important, however, to note that some commensal bacteria have stronger pro-inflammatory capabilities than others (Rath *et al.*, 2001) and some can actually be protective. Indeed, it has recently been demonstrated that germfree IL-10 deficient mice are even more susceptible to DSS induced colitis that IL-10 deficient mice maintained on CRASF® flora (Pils *et al.*, 2010a). Thus, it is thought that some commensal bacteria can have a protective effect on DSS, with other experiments demonstrating commensal or probiotic bacteria e.g. *Bifidobacterium* can attenuate the severity of DSS induced colitis (Frick *et al.*, 2007; Nanda Kumar *et al.*, 2008). Taken together, this demonstrates that the balance of commensal bacteria found in mice is vitally important to the colitic phenotype.

The mice in our animal facility are maintained with a Charles River altered Schaedler flora (CRASF®) however, previous DSS experiments performed using IFNγ deficient mice did not report a defined flora. This is important as conventional mouse facilities can contain some pathogenic bacteria e.g. *Helicobacteur hepaticus* (Bohr *et al.*, 2006) that is known to drive IFNγ-dependant intestinal inflammation in some mouse models of colitis e.g. IL-10 deficient mice (Kullberg *et al.*, 1998). Therefore, different commensal gut flora can result in different levels of intestinal IFNγ following DSS treatment. This suggests that the increased IFNγ levels seen in studies by Ito *et al.* and others could be a result of an altered or more aggressive intestinal microbiota than maintained in our animal facility. Indeed, work with peptidoglycan recognition protein (PGRP) deficient mice identified an elevation in intestinal IFNγ levels, as a result of alterations in normal bacterial flora. These bacterial flora alterations led to an increased severity of DSS in these animals (Saha *et al.*, 2010). Moreover, experiments by Saha *et al.* support the results we have generated as, wild-type mice treated with DSS display no increase in IFNγ levels or the IFNγ-responsive genes CXCL-9, -10, -11 or CCL-8. Moreover, although a role of IFNγ is implicated in PGRP deficient mice, blockade of IFNγ through neutralising antibodies does not protect the mice from colitis development but returns the severity of the disease to levels seen in control DSS-treated animals.

In conclusion, it appears that IFNγ is an important mediator in colitis when the colitis is driven by a skewed or excessively aggressive gut microbiota. Conversely, in DSS-colitis induced in an animal unit with a strictly controlled gut microbiota there is no induction of IFNγ expression in the intestine and therefore, neutralisation of IFNγ or IFNγ signalling appears to be unimportant.

4.3.4. Targeting of different genes for deletion could result in differences seen in the colitic phenotype of IFNγ deficient mice.

In previous experiments looking at the role of IFNγ in the induction of DSS colitis mice deficient in IFNγ have been used (Ito *et al.*, 2006; Xu *et al.*, 2008), whereas we have generated mice with a deficiency in IFNγR2. This may affect the phenotype seen in DSS-colitis as we have demonstrated that, as well as the abrogation of IFNγ signalling, the deletion of IFNγR2 results in a decreased sensitivity to IFNα. This could, in part, account for the trend towards increased sensitivity to DSS and elevated intestinal inflammation seen in the IFNγR2$^{\Delta/\Delta}$ mice as it has been demonstrated that mice deficient in the type I IFN receptor have an increased sensitivity to DSS. This is thought to be due to an anti-inflammatory action of IFNα/β on macrophages and a role of IFNα/β in protecting epithelial integrity (Katakura *et al.*, 2005). Thus, by decreasing sensitivity to IFNα/β there could be a detrimental effect on epithelial integrity and macrophage actions. The decreased sensitivity of the IFNγR2$^{\Delta/\Delta}$ mice to IFNα/β needs to be further investigated, therefore the relevance of this mechanism needs further dissecting.

4.3.5. Future experiments to investigate the contribution of IFNγ in colitis

To confirm that the gut flora of these mice is the key contributing factor to the altered phenotype of the IFNγR2$^{\Delta/\Delta}$ mice, compared to previously published results the experiment needs to be repeated in fully backcrossed mice housed both with the CRASF® flora and in a more conventional animal house.

It has previously be demonstrated that the spontaneous colitis development observed in IL-10 deficient mice, maintained in conventional animal facilities, is associated

with increased levels of IFNγ production by CD4 T cells (Berg *et al.*, 1996; Mahler & Leiter, 2002). Moreover, the enterocolitis development in these mice is preventable when mice are treated with anti-IL-12 or anti-IFNγ antibodies (Berg *et al.*, 1996; Davidson *et al.*, 2000). However, if treated once disease is established the anti-IFNγ antibodies are unable to reduce the severity of colitis (Berg *et al.*, 1996). Therefore it will be interesting to cross the global and conditional IFNγR2 deficient mice to the IL-10 deficient background and to determine if IFNγR2 deficiency on the IL-10 deficient background protects against the development of colitis. If IFNγR2 deficiency is protective it will be interesting to determine the key IFNγ responding cells in this setting using the conditional IFNγR2 deficient mice crossed to IL-10 deficient mice. This will be particularly relevant, as clinically it has been demonstrated that IL-10 receptor deficient patients can develop severe, early-onset IBD (Glocker *et al.*, 2009).

These mice could also be used to investigate the IFNγ-driven intestinal inflammation seen in *H. hepaticus*. *H. hepaticus* infected IL-10 deficient mice are protected from colitis development when treated with anti-IFNγ antibodies (Kullberg *et al.*, 1998). These experiments could be performed in our animal facility where, due to the maintenance of animals on the CRASF® flora, spontaneous colitis development doesn't occur in IL-10 deficient mice(Pils *et al.*, 2010a).

4.4 CONCLUSION

The results presented in this chapter demonstrate

1. IFNγR2$^{\Delta/\Delta}$ mice are not resistant to DSS-induced colitis, under the conditions used in our experiments, and IFNγR2$^{fl/fl}$ mice do not show an up-regulation of IFNγ either locally or systemically following DSS treatment.
2. IFNγR2$^{\Delta/\Delta}$ and IFNγR2$^{fl/fl}$ mice on a mixed B6 and 129/Sv background appeared to display increased sensitivity to DSS-induced colitis compared to the B6 mice used to titrate the initial DSS dose.
3. Future experiments to investigate the role of IFNγR2 in colitis include crossing the complete and conditional IFNγR2 knock-out mice with IL-10

deficient animals and monitoring either spontaneous colitis development in a conventional animal facility or *H. hepaticus* driven intestinal inflammation.

CHAPTER FIVE

Characterisation of the role of IFNγ in *Trichuris muris* infection

5.1 INTRODUCTION

It has already been established that IFNγ is an important mediator of susceptibility to *T. muris*, as antibody depletion of IFNγ can confer resistance to a normally susceptible mouse (Else *et al.*, 1994) and mice deficient in IFNγ or IFN-γ receptor 1 expel the parasite more rapidly than wild type animals (unpublished observation in review by (Grencis, 2001)). However, the cells that are important in responding to IFNγ and conferring susceptibility are unknown.

Our conditional IFNγR2 system under the control of Cre-LoxP, as described in Chapter 3, enables us to investigate this mechanism in more detail. Given the importance of T cells in resistance to *T. muris* (Lee *et al.*, 1983) and the prototypic role of IFNγ in Th1 skewed T cells, it is of interest to determine if the role of IFNγ is due to its actions on the T cell compartment. Alternatively, as there is a large accumulation of macrophages in the intestines of infected mice and, given the importance of IFNγ for macrophage activation, the action of IFNγ on macrophages may underlie the importance of IFNγ in susceptibility. The mice we have generated with the conditional inactivation of IFNγ on T cells and macrophages as described in Chapter 3 provides an elegant method for dissecting the role of IFNγ during *T. muris* infection.

Aims

Therefore, the aims are as follows:

1. To verify if complete IFNγR2 deficient mice are resistant to a low dose *Trichuris muris* infection
2. To determine if the absence of IFNγR2 on T cells and/or macrophages will mimic the resistant phenotype expected in the complete IFNγR2 knock-out mice
3. Confirm the characterisation of IFNγ as a IgG2a switch inducing factor through the analysis of the antibody response in complete IFNγR2 deficient mice

4. To analyse the role of IFNγR2 in the differentiation of naïve T cells to Th1 or Th2 cells, during *T. muris* infection.

5.2 RESULTS

5.2.1 Lack of responsiveness to IFNγ is sufficient to render a mouse resistant to *T. muris*

To determine the importance of IFNγ signalling during the expulsion of *T. muris*, complete IFNγR2 knock-out mice ($IFN\gamma R2^{\Delta/\Delta}$) and control $IFN\gamma R2^{fl/fl}$ mice (generated as described in Chapter 3) were infected with a low dose of *T. muris* and worm burden was assessed at day 35 p.i.. As anticipated, $IFN\gamma R2^{\Delta/\Delta}$ mice were resistant to the infection having completely expelled their parasites, in contrast to $IFN\gamma R2^{fl/fl}$ mice which were susceptible to infection, all harbouring adult worms (Fig 5.1). This was not due to initial differences in infectivity, as at day 12 p.i. there were no differences between the two experimental groups (data not shown).

Analysis of the antibody responses demonstrated the *T. muris* infected $IFN\gamma R2^{fl/fl}$ mice mounted a mixed parasite-specific IgG1 and $IgG2_{a/c}$ response, consistent with the mixed Th1 / Th2 response expected in B6 mice (Fig 5.2). In contrast, the infected $IFN\gamma R2^{\Delta/\Delta}$ mice mounted a slightly, but not significantly, stronger IgG1 response (Fig 5.2), with no detectable parasite specific $IgG2_{a/c}$ (Fig 5.2). This lack of $IgG2_{a/c}$ was expected as IFNγ has previously been described as an $IgG2_{a/c}$ switch inducing factor (Finkelman *et al.*, 1988). Thus, the absence of an $IgG2_{a/c}$ response is not indicative of the absence of a Th1 response, but the inability for B cells to undergo class switching to $IgG2_{a/c}$.

Histological adaptations in crypt length were significantly different between the genotypes of infected mice, with infected $IFN\gamma R2^{fl/fl}$ mice showing significant crypt hyperplasia at day 35 p.i. compared to naïve $IFN\gamma R2^{fl/fl}$ mice. In contrast, infected $IFN\gamma R2^{\Delta/\Delta}$ mice had a similar crypt length to naïve $IFN\gamma R2^{\Delta/\Delta}$ mice (Fig 5.3). A significant goblet cell hyperplasia was also seen in infected $IFN\gamma R2^{fl/fl}$ mice

compared to naïve IFNγR2$^{fl/fl}$ mice (Fig 5.4). Interestingly, although no goblet cell hyperplasia was observed in infected IFNγR2$^{\Delta/\Delta}$ mice compared to naïve IFNγR2$^{\Delta/\Delta}$ mice, uninfected IFNγR2$^{\Delta/\Delta}$ mice had significantly more goblet cells than uninfected IFNγR2$^{fl/fl}$ mice (Fig 5.4). As well as increased crypt length and goblet cells the infected IFNγR2$^{fl/fl}$ mice had a significant increase in CD3^{+} cells at d21 and d35 p.i. compared to naïve IFNγR2$^{fl/fl}$ mice. In contrast, infected IFNγR2$^{\Delta/\Delta}$ mice had a significant increase in CD3^{+} cells at d21 compared to naïve IFNγR2$^{\Delta/\Delta}$ mice, but this was no longer significant by d35 p.i. (Fig 5.5, 5.6). The influx of F4/80^{+} cells in IFNγR2$^{fl/fl}$ mice was slightly delayed in comparison to CD3^{+} cells, with no increase at d21 compared to naïve IFNγR2$^{fl/fl}$ mice but an elevation at d35 p.i., which was accompanied by an increase in Arg1^{+} cells. In the infected IFNγR2$^{\Delta/\Delta}$ mice a similar trend was observed in the F4/80^{+} cells as in the CD3^{+} cells, with a significant increase compared to the naïve IFNγR2$^{\Delta/\Delta}$ mice at d21 p.i. but a return to baseline levels by d35 p.i. (Fig 5.5, 5.6).

Taken together, it can be seen that the deletion of IFNγR2 resulted in the abrogation of the parasite-specific IgG2$_{a/c}$ response, a trend towards elevated parasite-specific IgG1 titres and expulsion of the parasite. This is accompanied by an elevation in inflammatory cells at d21 p.i. which returns to levels comparable to naïve mice by d35 p.i..

5.2.2 Conditional inactivation of IFNγR2 on T cells or macrophages is insufficient to impart a resistant phenotype

To determine the responding cells important in imparting the resistant phenotype to *T. muris* seen in complete IFNγR2 knock-out mice, T-cell deficient (IFNγR2$^{fl/fl}$CD4Cre^{+}) and macrophage deficient (IFNγR2$^{fl/fl}$LysMCre^{+}) mice, as described in Chapter 3, were infected with a low dose of *T. muris* and worm burden was assessed at day 35 p.i.. However, no significant differences in worm burden were seen in the conditional knock-out mice compared to the IFNγR2$^{fl/fl}$ control mice and all mice harboured chronic infections (Fig 5.7).

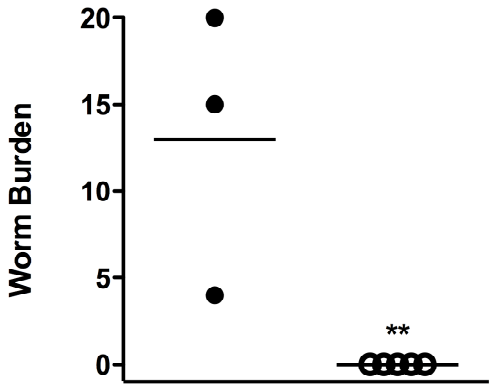

Fig 5.1 Worm burden recovered from IFNγR2$^{\Delta/\Delta}$ (knock-out) and IFNγR2$^{fl/fl}$ (control) mice on day 35 post infection with *T. muris*. Mice were infected with 20 *T. muris* eggs on day 0 and worm burdens assessed on day 35 post infection. Line indicates mean of each group. n= 3 (infected IFNγR2$^{fl/fl}$); n=5 (infected IFNγR2$^{\Delta/\Delta}$) ** significantly different between IFNγR2$^{\Delta/\Delta}$ and IFNγR2$^{fl/fl}$ mice ($p \leq 0.01$) ● IFNγR2$^{fl/fl}$ + T. muris
○ IFNγR2$^{\Delta/\Delta}$ + T. muris

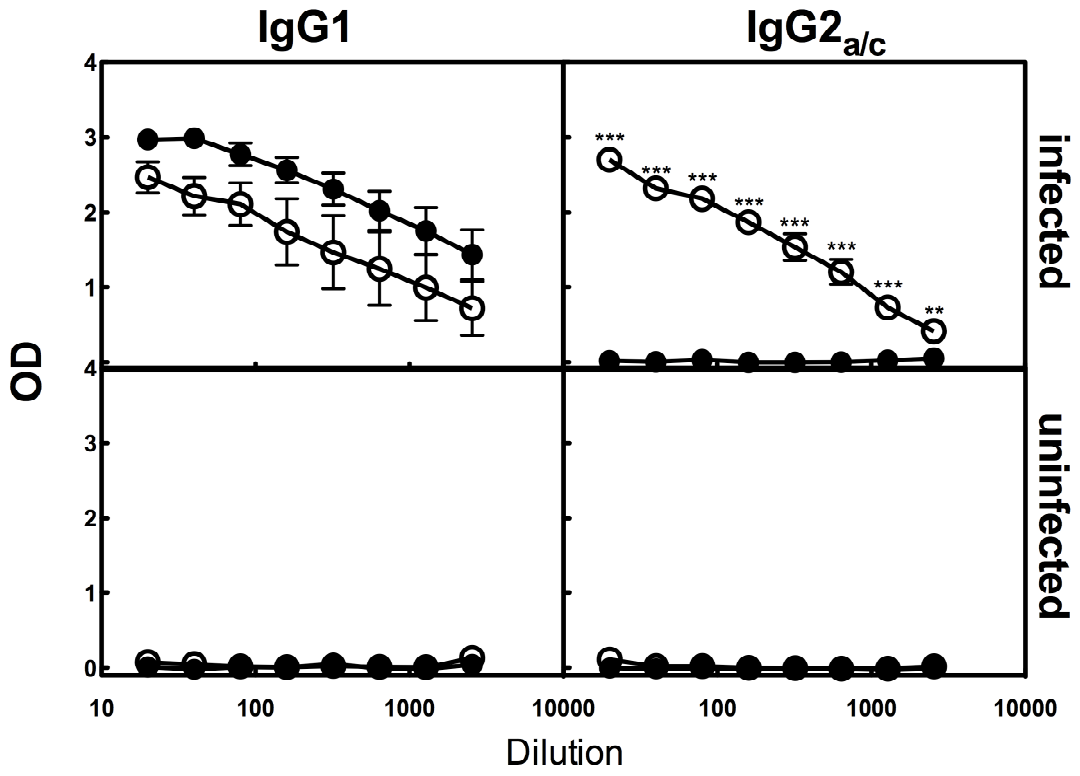

Figure 5.2 Serum parasite-specific IgG1 and IgG2$_{a/c}$ responses at day 35 p.i. from IFNγR2$^{Δ/Δ}$ (knock-out) and IFNγR2$^{fl/fl}$ (control) *T. muris* infected mice. Mice were infected with 20 *T. muris* eggs on day 0. Blood was removed from individual mice upon sacrifice and serum analysed by parasite-specific ELISA. Results are presented as mean ± s.e, n=3 (IFNγR2$^{Δ/Δ}$ uninfected, IFNγR2$^{fl/fl}$ infected mice), n= 4 (IFNγR2$^{fl/fl}$ infected mice) or n=5 (IFNγR2$^{Δ/Δ}$ infected mice) **p≤0.01 ***p≤0.001 significantly different between IFNγR2$^{Δ/Δ}$ and IFNγR2$^{fl/fl}$ mice ⊖ IFNγR2$^{fl/fl}$ mice ● IFNγR2$^{Δ/Δ}$ mice

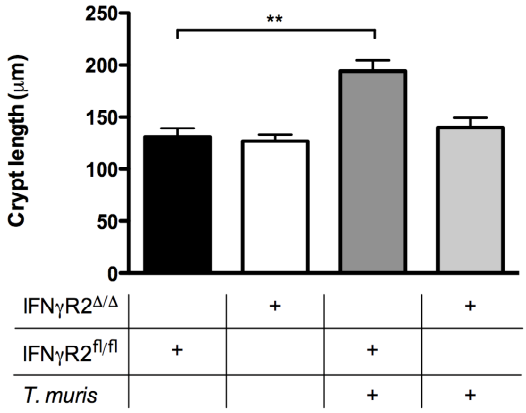

Fig 5.3 Crypt lengths in IFNγR2$^{\Delta/\Delta}$ (knock-out) and IFNγR2$^{fl/fl}$ (control) mice on day 35 post infection with *T. muris*. Mice were infected with 20 *T. muris* eggs on day 0. Histological sections were stained with haematoxylin and eosin before crypt lengths were visualised on a light microscope and measured using ImageJ® software. Results are presented as mean ± s.e. per group, n=3 (IFNγR2$^{\Delta/\Delta}$ uninfected, IFNγR2$^{fl/fl}$ infected mice), n= 4 (IFNγR2$^{fl/fl}$ infected mice) or n=5 (IFNγR2$^{\Delta/\Delta}$ infected mice) ** statistically significant compared to IFNγR2$^{fl/fl}$ uninfected mice (p≤0.01)

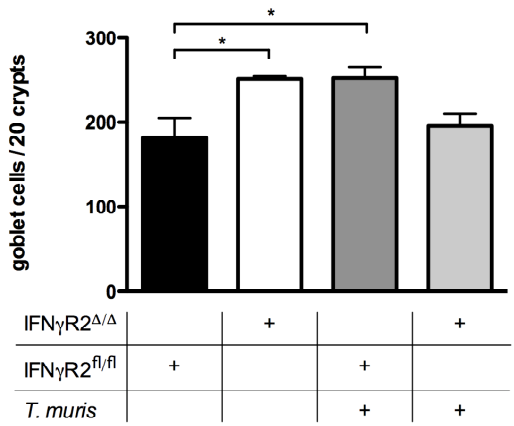

Fig 5.4 Number of intestinal goblet cells in IFNγR2$^{\Delta/\Delta}$ (knock-out) and IFNγR2$^{fl/fl}$ (control) mice on day 35 post infection with *T. muris*. Mice were infected with 20 *T. muris* eggs on day 0. Histological sections were stained with Periodic acid-Schiffs before goblet cells were enumerated in 20 randomly selected areas, sampling at least 3 non-sequental sections. Results are presentented as mean ± s.e. per group, n=3 (IFNγR2$^{\Delta/\Delta}$ uninfected, IFNγR2$^{fl/fl}$ infected mice), n= 4 (IFNγR2$^{fl/fl}$ infected mice) or n=5 (IFNγR2$^{\Delta/\Delta}$ infected mice) *statistically significant compared to IFNγR2$^{fl/fl}$ uninfected mice (p≤0.05)

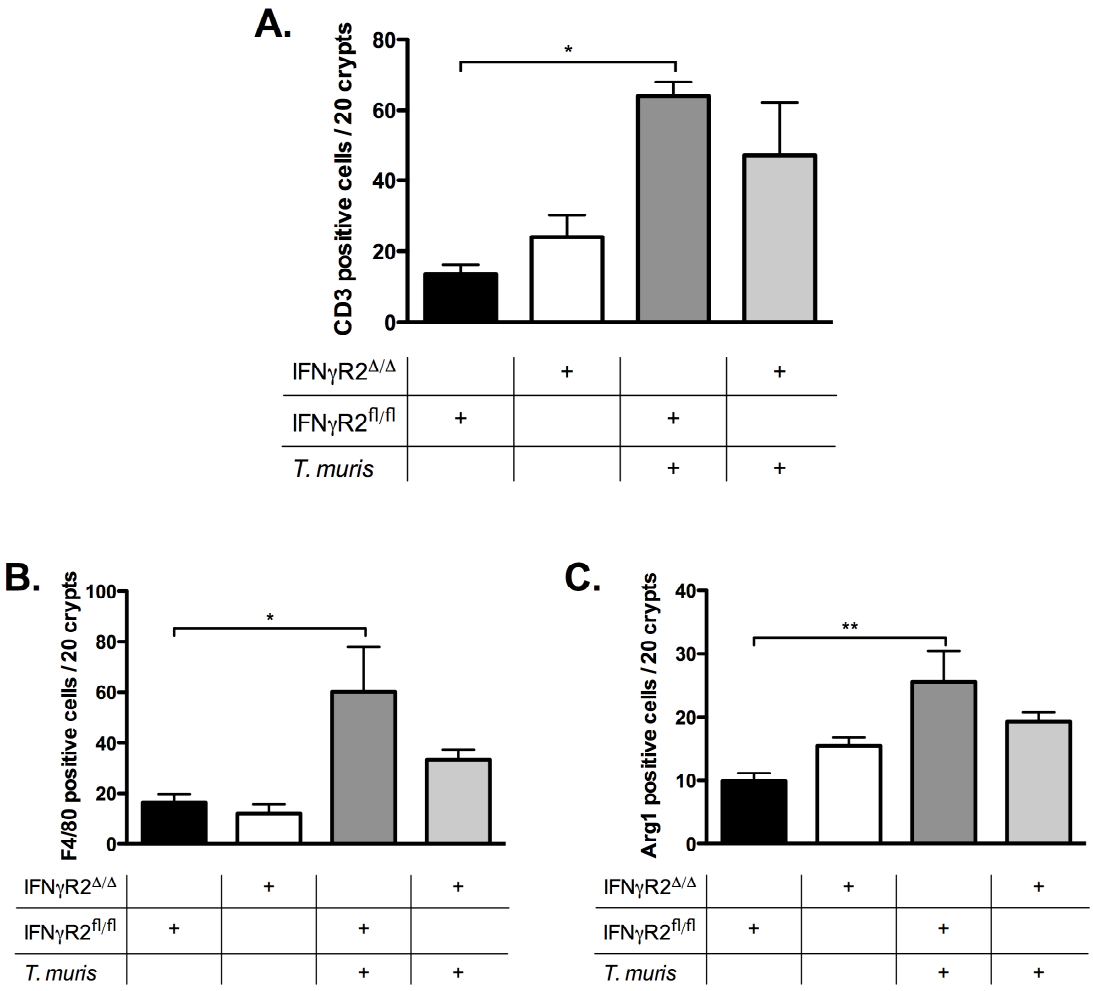

Fig 5.5 Numbers of intestinal A. CD3 positive B. F4/80 positive and C. Arg1 positive cells in IFNγR2$^{\Delta/\Delta}$ (knock-out) and IFNγR2$^{fl/fl}$ (control) mice on day 35 post infection with *T. muris*. Mice were infected with 20 *T. muris* eggs on day 0. Histological sections were stained with CD3, F4/80 or Arg1 antibodies and counterstained with haematoxylin. Positive cells were enumerated in 20 crypts, sampling at least 3 non-sequental sections. Results are presentented as mean ± s.e. per group, n=3 (IFNγR2$^{\Delta/\Delta}$ uninfected, IFNγR2$^{fl/fl}$ infected mice), n= 4 (IFNγR2$^{fl/fl}$ infected mice) or n=5 (IFNγR2$^{\Delta/\Delta}$ infected mice) *p≤0.05, **p≤0.01 statistically significant as indicated.

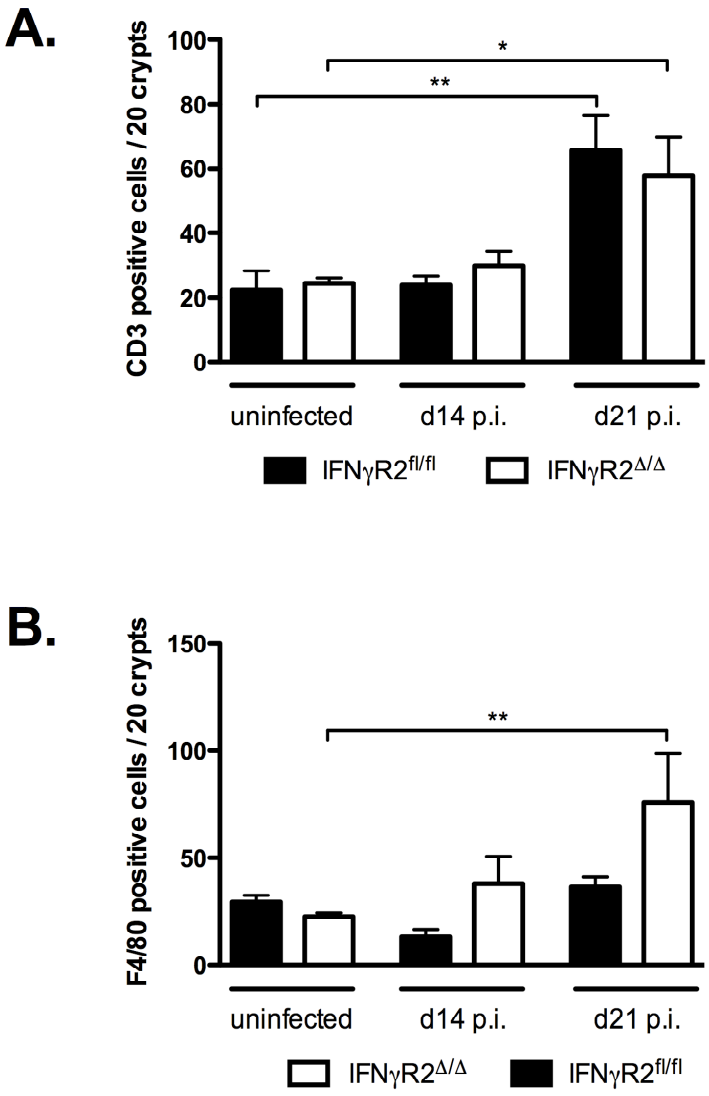

Fig 5.6 Numbers of intestinal A. CD3 positive and B. F4/80 positive cells in IFNγR2$^{\Delta/\Delta}$ (knock-out) and IFNγR2$^{fl/fl}$ (control) mice uninfected, on day 14 or day 21 post infection with *T. muris*. Mice were infected with 20 *T. muris* eggs on day 0. Histological sections were stained with CD3 or F4/80 antibodies and counterstained with haematoxylin. Positive cells were enumerated in 20 crypts, sampling at least 3 non-sequental sections. Results are presented as mean ± s.e. per group. *p≤0.05, **p≤0.01 indicates statistically significant data.

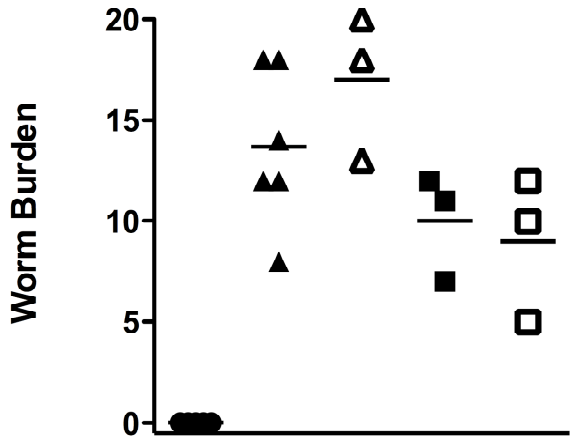

Fig 5.7 Worm burden recovered from IFNγR2$^{\Delta/\Delta}$ (knock-out), IFNγR2$^{fl/fl}$xLysMCre and IFNγR2$^{fl/fl}$xCD4Cre mice on day 35 post infection with *T. muris*. Mice were infected with 20 *T. muris* eggs on day 0 and worm burdens assessed on day 35 post infection. n=3 for Cre^{-} groups, n=3 for CD4^{+}, n= 5 for global knockout and n=6 for LysM^{+} infected. Line indicates mean of each group. Closed symbols = Cre+ Open symbols = Cre-

● IFNγR2$^{\Delta/\Delta}$ ▲ IFNγR2$^{fl/fl}$ x LysMCre ◘ IFNγR2$^{fl/fl}$ x CD4Cre

Histological alterations in crypt length were only statistically different in infected IFNγR2$^{fl/fl}$LysMCre^{+} mice, which displayed a marked crypt hyperplasia compared to naïve mice of the same genotype (Fig 5.8). However, the hyperplasia did not reach significance in comparison to IFNγR2$^{fl/fl}$LysMCre^{-} *T. muris* infected mice. Moreover, there were no significant differences between infected and uninfected IFNγR2$^{fl/fl}$CD4Cre^{+} mice or between infected IFNγR2$^{fl/fl}$CD4Cre^{+} mice and infected IFNγR2$^{fl/fl}$CD4Cre^{-} mice (Fig 5.8).

As demonstrated previously, the infected IFNγR2$^{\Delta/\Delta}$ mice mounted a strong parasite-specific IgG1 response, with no IgG2$_{a/c}$ response detected (Fig 5.2). In contrast, mice harbouring an IFNγR2 deficiency on either their T-cells or macrophages were capable of mounting a parasite-specific IgG2$_{a/c}$ response (Fig 5.9). Moreover, the infected IFNγR2$^{fl/fl}$LysMCre^{+} mice displayed a significant increase in parasite-specific IgG2$_{a/c}$ compared to infected IFNγR2$^{fl/fl}$LysMCre^{-} mice (Fig 5.9). This increase in IgG2$_{a/c}$ was not accompanied by a reciprocal decrease in IgG1, with no significant differences in antibody titre between infected LysM-Cre conditional mutant mice and infected IFNγR2$^{fl/fl}$ mice (Fig 5.9).

Analysis of antigen-specific cytokine production following MLN re-stimulation demonstrated no significant changes in IFNγ, IL- 17A, IL-10, IL-4, IL-13, IL-6, TNF or MCP-1 following *T. muris* infection (Fig 5.10, 5.11). Large variability within both uninfected and infected groups hindered analysis and could be due, in part, to the mixed genetic background of the mice. Overall, as expected in a low dose infection, the mice mounted a predominantly Th1-mediated response with high levels of IFNγ detected and low or no IL-4 detected, except in the resistant IFNγR2$^{\Delta/\Delta}$ mice. In keeping with the levels of parasite-specific IgG2$_{a/c}$, which is a marker of Th1 responses, higher levels of IFNγ were seen in IFNγR2$^{fl/fl}$LysMCre^{+} mice compared to Cre^{-} littermates, however, this was not statistically significant (Fig 5.10A).

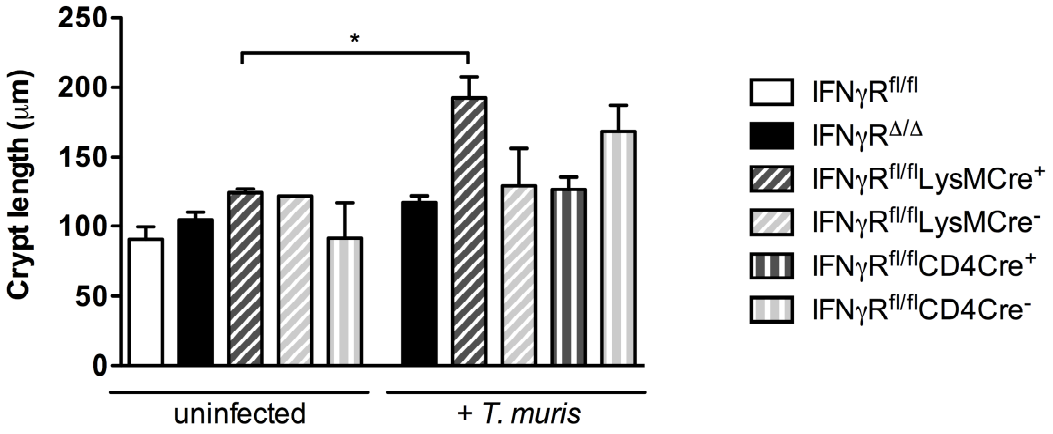

Fig 5.8 Crypt lengths in IFNγR2$^{\Delta/\Delta}$ (knock-out), IFNγR2$^{fl/fl}$xLysMCre and IFNγR2$^{fl/fl}$xCD4Cre mice on day 35 post infection with *T. muris*. Mice were infected with 20 *T. muris* eggs on day 0. Histological sections were stained with haematoxylin and eosin before crypt lengths were visualised on a light microscope and measured using ImageJ® software. Results are presented as mean ± s.e. per group. n=2 or 3 for uninfected groups; n=3 for Cre$^-$ infected groups, n=2 for CD4$^+$ infected, n= 5 for global knockout and n=6 for LysM$^+$ infected.*p≤0.05 stastically significant compared to uninfected control

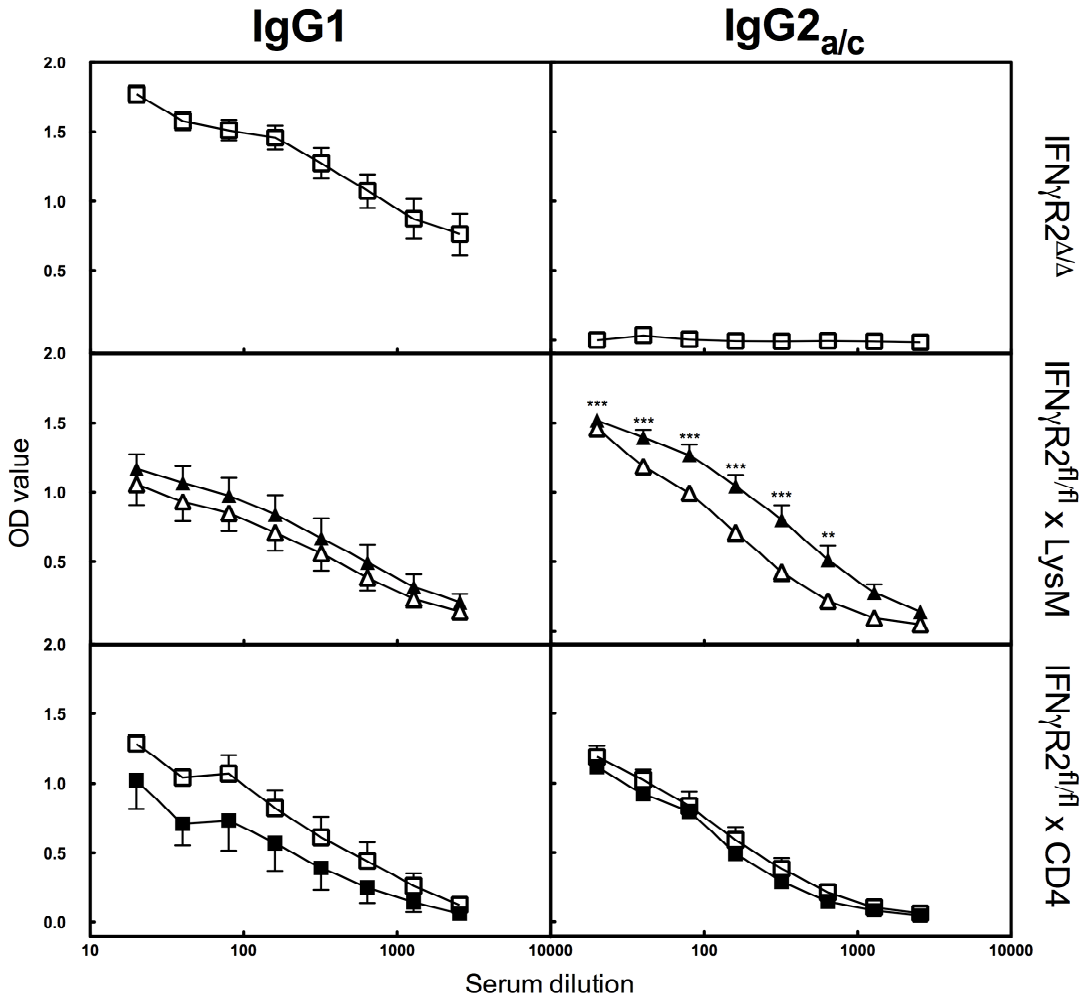

Figure 5.9 Serum parasite specific IgG1 and IgG2$_{a/c}$ responses at day 35 p.i. from IFNγR2$^{Δ/Δ}$ (knock-out), IFNγR2$^{fl/fl}$xLysMCre and IFNγR2$^{fl/fl}$xCD4Cre mice on day 35 post infection with *T. muris*. Mice were infected with 20 *T. muris* eggs on day 0. Blood was removed from individual mice upon sacrifice and serum analysed by ELISA. Results are presented as mean ± s.e. n=3 for Cre$^-$ groups, n=2 for CD4$^+$, n= 5 for global knockout and n=6 for LysM$^+$ ** p≤0.01 ***p≤0.001 statistically significant between Cre$^+$ and Cre$^-$ mice. Cre+ = closed sympbols, Cre- = open symbols

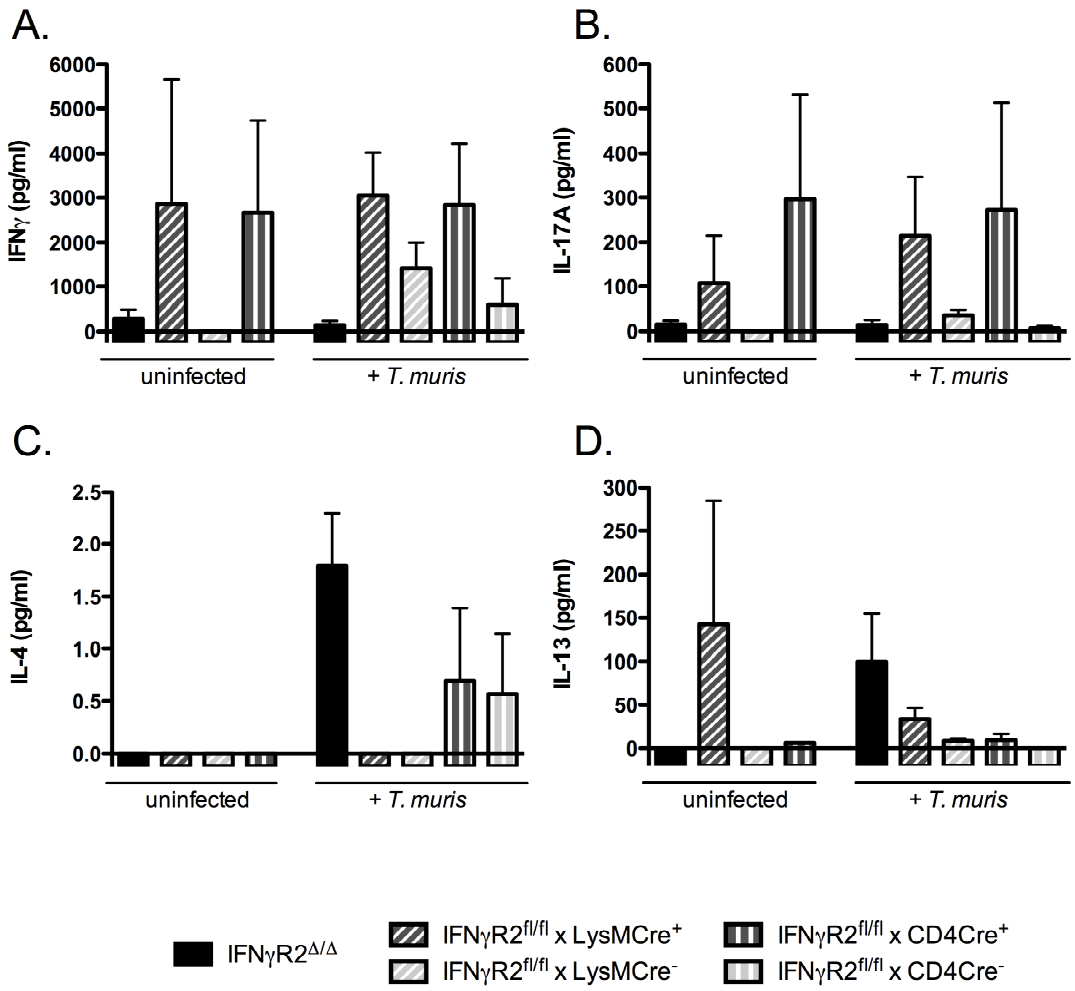

Fig 5.10 Secretion of Th1, Th17 and Th2 cytokines A. IFNγ B. IL-17A C. IL-4 and D. IL-13 Mice were infected with 20 *T. muris* egg on day 0. MLN cells were removed from individual mice, stimulated for 48 hours with E/S antigen and cell supernantants analysed by CBA. Results are presented as mean ± s.e. per group. n=2 or 3 for uninfected groups; n=3 for Cre^- infected groups, n=2 for $CD4^+$ infected, n= 5 for global knockout and n=6 for $LysM^+$ infected.

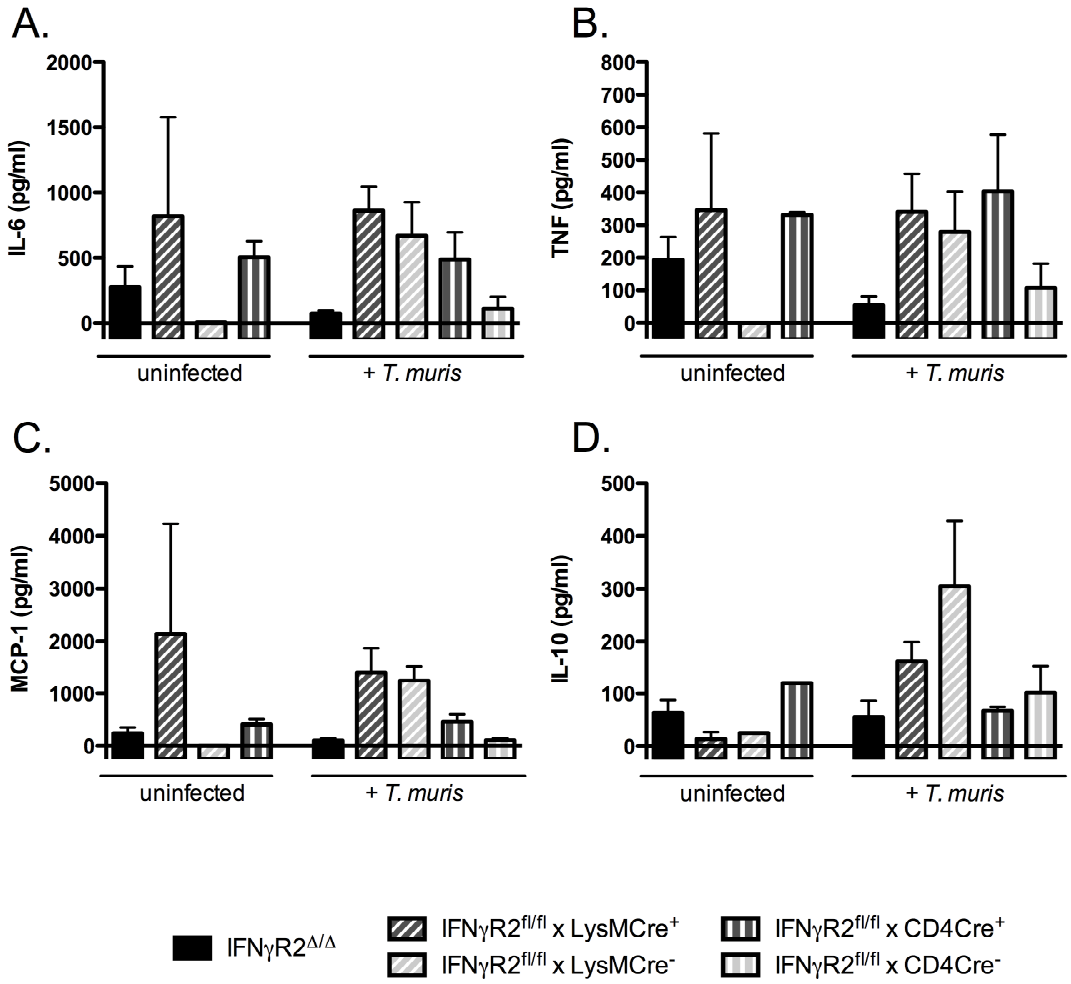

Fig 5.11 Secretion of pro-inflammatory and anti-inflammatory cytokines A. IL-6 B. TNF C. MCP-1 and D. IL-10 Mice were infected with 20 *T. muris* egg on day 0. MLN cells were removed from individual mice, stimulated for 48 hours with E/S antigen and cell supernantants analysed by CBA. Results are presented as mean ± s.e. per group. n=2 or 3 for uninfected groups; n=3 for Cre^- infected groups, n=2 for $CD4^+$ infected, n= 5 for global knockout and n=6 for $LysM^+$ infected.

Therefore, the ablation of the IFNγ response in T cells or macrophages, through the conditional inactivation of the IFNγR2 chain, is insufficient to mimic the resistant phenotype seen in the complete knock-out mice.

5.2.3. Conditional inactivation of IFNγR2 on T cells and macrophages is insufficient to consistently impart a resistant phenotype

To determine if there is redundancy in the IFNγ system the two conditional knockout lines were interbred to create a double conditional KO mouse (double KO, IFNγR2$^{fl/fl}$LysMCre^{+}CD4Cre^{+}) with the ablation of the IFNγ receptor on both T cells and macrophages. Initial experiments demonstrated the double conditional KO mice were capable of expelling a low dose infection. A trend towards a reduced worm burden in the T cell conditional knockout was also observed, although this did not reach significance (Fig 5.12). However, subsequent repeats of the experiment were unable to reproduce this phenotype with a significant increase in worms recovered from both the double conditional KO mice and the T cell specific knock-out from Experiments 2 and 3 compared to the worm burdens in Experiment 1 (Fig 5.12). Furthermore, in experiments 2 and 3 all mice were susceptible to the low dose infection with fecund adult worms present in the intestine. To determine if a subtler phenotype was being produced, in experiment 3 the length of the worms recovered from the gut at d35 p.i. were measured. However, no stunting was seen in the double conditional knockout mice. Nevertheless, there was a slight but significant stunting of worm growth in the IFNγR2$^{fl/fl}$LysMCre^{+} infected mice compared to the IFNγR2$^{fl/fl}$ infected mice (Fig 5.13).

In the initial experiment, where the double conditional knockout mice were capable of expelling the parasite, the double KO mice displayed no histological changes compared to the IFNγR2$^{fl/fl}$ infected mice across all parameters measured (crypt length; CD3^{+} cell, F4/80^{+} cell and Arg1^{+} cell influx; Fig 5.14, 5.15). In contrast, there were significant differences in the antibody response with a decreased IgG2$_{a/c}$ response in both IFNγR2$^{fl/fl}$CD4Cre^{+} and IFNγR2$^{fl/fl}$CD4Cre^{+}LysMCre^{+} infected mice compared to IFNγR2$^{fl/fl}$ infected mice (IFNγR2$^{fl/fl}$CD4Cre^{-}LysMCre^{-}) but no

changes in IgG1 response (Fig 5.17). Despite this decrease in $IgG2_{a/c}$ there was no corresponding decrease in IFNγ production following MLN re-stimulation (Fig 5.19A), although there was a trend towards elevated IL-4 levels in the infected double KO mice and a significant increase in the infected $IFN\gamma R2^{fl/fl}CD4Cre^{+}$ mice compared to the infected $IFN\gamma R2^{fl/fl}$ mice (Fig 5.19C). IL-13 cytokine levels mirrored the pattern of increased IL-4 cytokine production in the double KO and $IFN\gamma R2^{fl/fl}CD4Cre^{+}$ mice, although this did not reach significance in any of the groups (Fig 5.19C, D). Therefore, the resistance to *T. muris* infection in the double conditional knockout mice appears to be accompanied by a slight shift in the Th1-Th2 balance compared to $IFN\gamma R2^{fl/fl}$ mice, although this change was very subtle.

To investigate the differences between the three experiments, in order to determine the mechanisms behind the different expulsion profiles, the histological adaptations in the intestine was examined. No significant differences in crypt length was observed between the genotypes within each experiment or across the across the experiments within each genotype (Fig 5.14). However, in the final experiment there appeared to be a significant increase in $CD3^{+}$ cell influx in the intestine and a trend towards increased $F4/80^{+}$ cell influx across all genotypes (Fig 5.15A,B). The validity of this data is uncertain as in the final experiment the tissue sections were fixed using a slightly difference method, therefore the elevation in positive cells could be a staining artefact. Nevertheless, the consistency of the $Arg1^{+}$ cell numbers in comparison to the previous experiments (Fig 5.15C) and the elevated levels of MCP-1 and TNF following MLN re-stimulation suggests that this may be a real result due to an increased inflammatory response (Fig 5.20B,C).

Analysis of parasite specific IgG1 and $IgG2_{a/c}$ responses at day 35 p.i. demonstrated no significant differences between experiments in infected $IFN\gamma R2^{fl/fl}$ and $IFN\gamma R2^{fl/fl}CD4Cre^{+}$ mice (Fig 5.17A,C; 5.18A,C). However, in the initial experiment the double conditional knock-out mice mounted a significantly increased IgG1 response compared to experiments 2 and 3 (Fig 5.17B). This elevated Th2 response was accompanied by a decreased Th1 response with a diminished $IgG2_{a/c}$ response compared to the subsequent experiments (Fig 5.18B). Additionally, in the initial

experiment the macrophage specific knock-out mice mounted a significantly reduced IgG1 response compared to subsequent experiments (Fig 5.17C). Conversely to the double conditional knock-out, this reduction in IgG1 levels was not accompanied by a change in $IgG2_{a/c}$ levels, with no differences between the experiments (Fig 5.18C).

On examination, the Ag-specific cytokine production following MLN re-stimulation demonstrated a similar trend to the antibody data. In the double conditional knockouts there was an increase in levels of the type 2 cytokines IL-4 and IL-13 in experiment 1 compared to the subsequent experiments (Fig 5.19C,D) with a concurrent decrease in IFNγ and IL-17A secretion (Fig 5.21A,B). However, these changes did not reach significance. Interestingly there appeared to be an increase in both IL-6 (Fig 5.20A) and TNF (Fig 5.20B) levels between the experiments with significantly higher levels of IL-6 seen in both experiments 2 and 3 when compared to the initial experiment and significantly higher levels of TNF in experiment 3 across all of the genotypes.

Therefore, the expulsion of the parasite seen in the double conditional knock-out mice in the initial experiment is associated with an increased Th2 response demonstrated by an elevation of antigen specific IgG1 and a trend towards increased IL-4 and IL-13 levels. This increased Th2 response is associated with a decreased Th1 response with lowered antigen specific $IgG2_{a/c}$ levels and a trend towards decreased IFNγ levels. However, the expulsion cannot be consistently repeated with subsequent experiments unable to replicate the resistant phenotype.

The potential mechanisms behind the expulsion seen in the complete IFNγR2 deficient mice and the discrepancies in the phenotype of the conditional knockout mice is dissected in the following discussion.

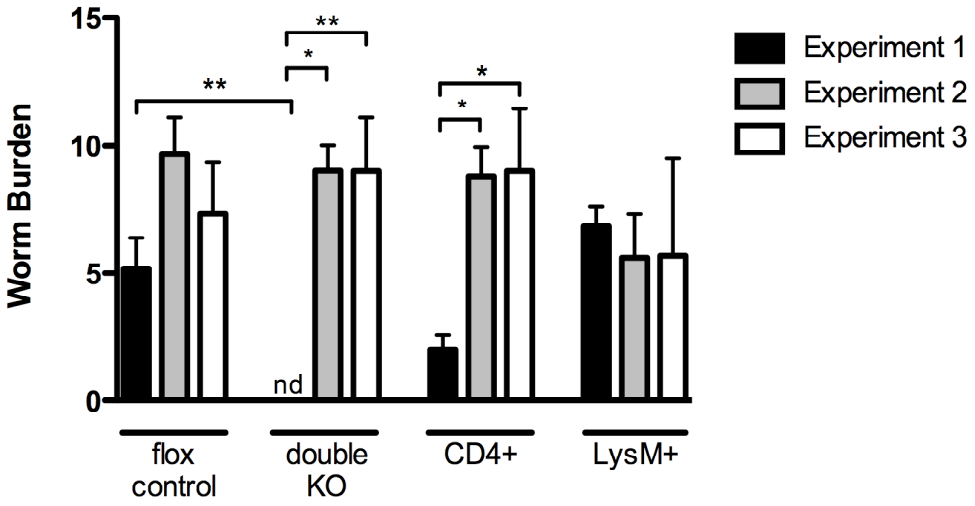

Fig 5.12 Worm burden recovered from IFNγR2 conditional knock-out and IFNγR2$^{fl/fl}$ (control) mice on day 35 post infection with *T. muris*. Mice were infected with 20 *T. muris* eggs on day 0 and worm burdens assessed on day 35 post infection. Results are presented as mean ± s.e. n = 3-5 for all groups except experiment 2 double KO (n=2) and experiment 1 LysM^{+} (n=6) * p≤0.05 ** p≤0.01 statisitically significant as indicated

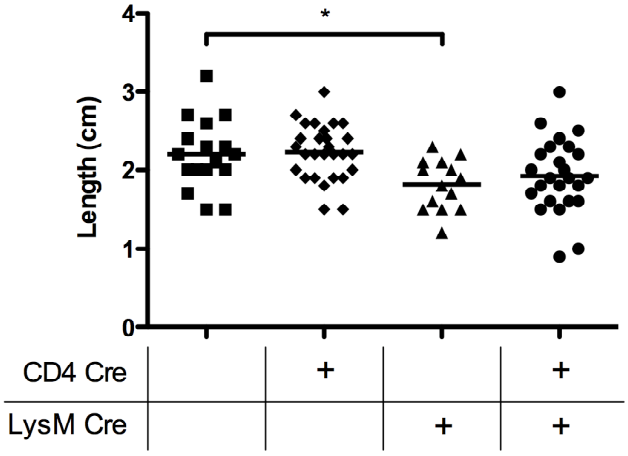

Fig 5.13 Worm length of worms recovered from IFNγR2 conditional knock-out and IFNγR2$^{fl/fl}$ (control) mice on day 35 post infection with *T. muris*. Mice were infected with 20 *T. muris* egg on day 0 and worm length measured from recovered worms of Experiment 3 on day 35 post infection. A minimum of 14 worms were counted in each group. Line indicates mean of group. * p≤0.05 statisitically significant compared to worms retrieved from IFNγR2$^{fl/fl}$ mice.

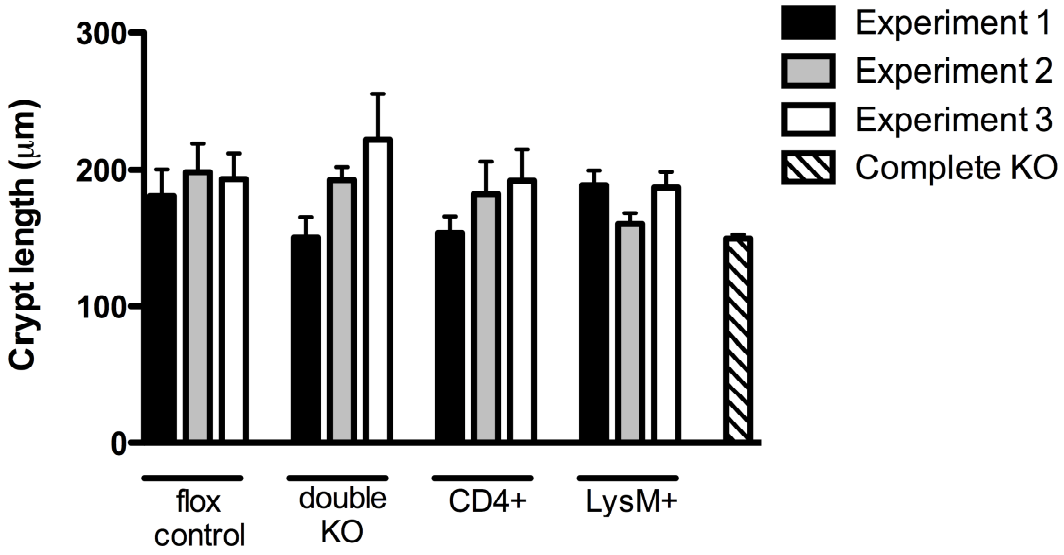

Fig 5.14 Crypt lengths in IFNγR2 conditional knock-out and IFNγR2$^{fl/fl}$ (control) mice on day 35 post infection with *T. muris*. Mice were infected with 20 *T. muris* egg on day 0. Histological sections were stained with haematoxylin and eosin before crypt lengths were visualised on a light microscope and measured using ImageJ® software. n = 3-5 for all groups except experiment 2 double KO (n=2) and experiment 1 LysM^{+} (n=6). Results are presented as mean ± s.e. per group.

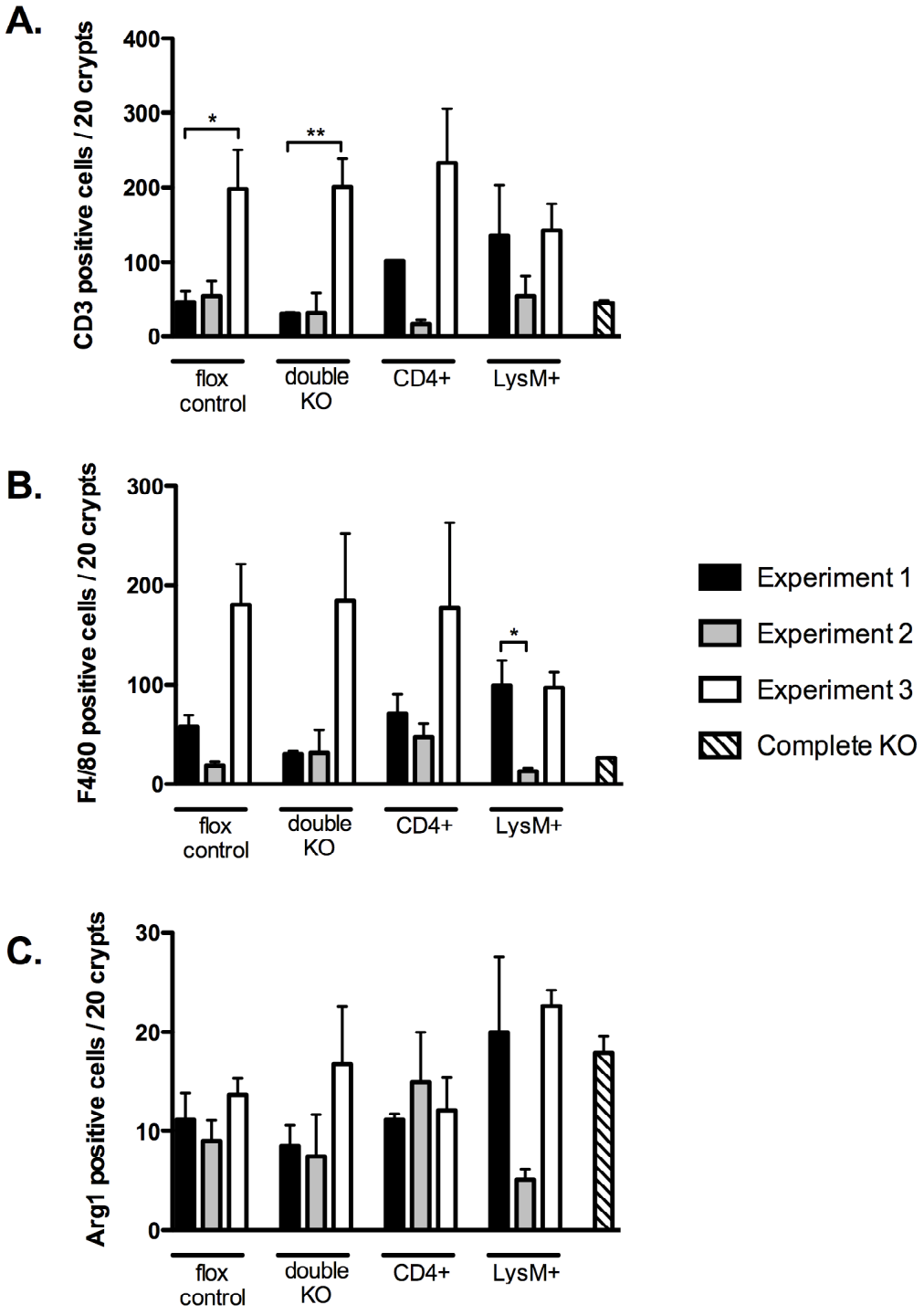

Fig 5.15 Numbers of intestinal A. CD3 positive B. F4/80 positive and C. Arg1 positive cells in IFNγR2 conditional knock-out and IFNγR2$^{fl/fl}$ (control) mice on day 35 post infection with *T. muris*. Mice were infected with 20 *T. muris* egg on day 0. Histological sections were stained with CD3, F4/80 or Arg1 antibodies and counterstained with haematoxylin. Positive cells were enumerated in 20 crypts, sampling at least 3 non-sequental sections. n = 3-5 for all groups except experiment 2 double KO (n=2) and experiment 1 LysM^{+} (n=6). Sections in Experiment 3 were fixed using adapted NBF fixative, sections in Experiments 1 and 2 were fixed in NBF. Results are presentented as mean ± s.e. per group. * p≤0.05, **p≤0.01 statistically significant as indicated.

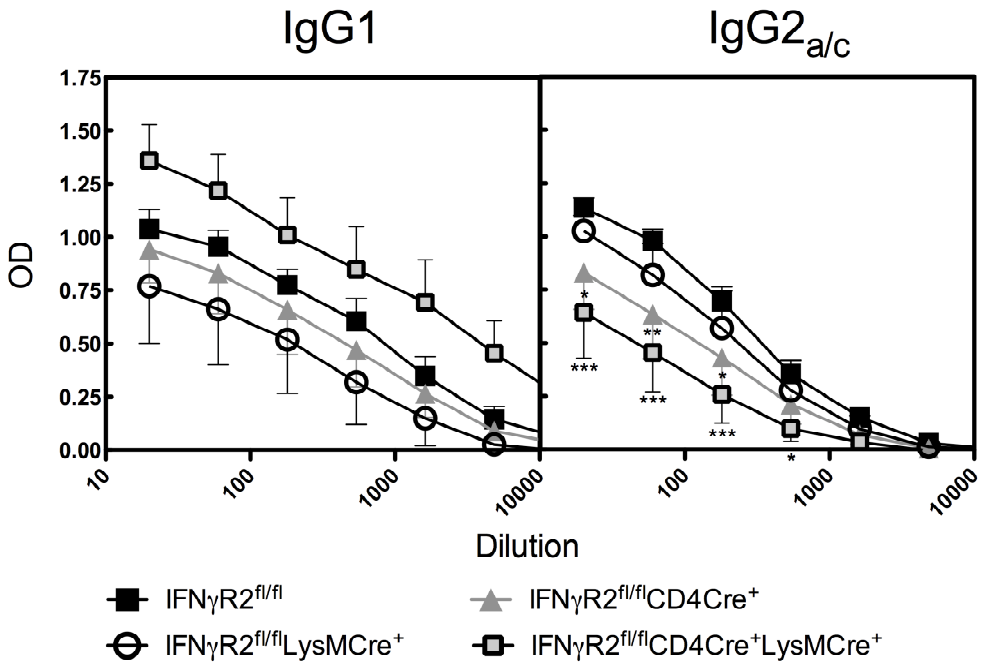

Fig 5.16 Serum parasite specific IgG1 and IgG2a/c responses in IFNγR2$^{fl/fl}$ (control), IFNγR2$^{fl/fl}$LysMCre^{+}CD4Cre^{+} (double KO), IFNγR2$^{fl/fl}$LysMCre^{+} and IFNγR2$^{fl/fl}$CD4Cre^{+} mice. Mice were infected with 20 *T. muris* eggs on day 0. Blood was removed from individual mice upon sacrifice and serum analysed by ELISA. Results are presented as mean ± s.e. per group. n= 3 (CD4^{+}), 4 (double KO), 5 (control) or 6 (LysM^{+}) *p≤0.05, **p≤0.01, ***p≤0.001 stastically significant compared to IFNγR2$^{fl/fl}$.

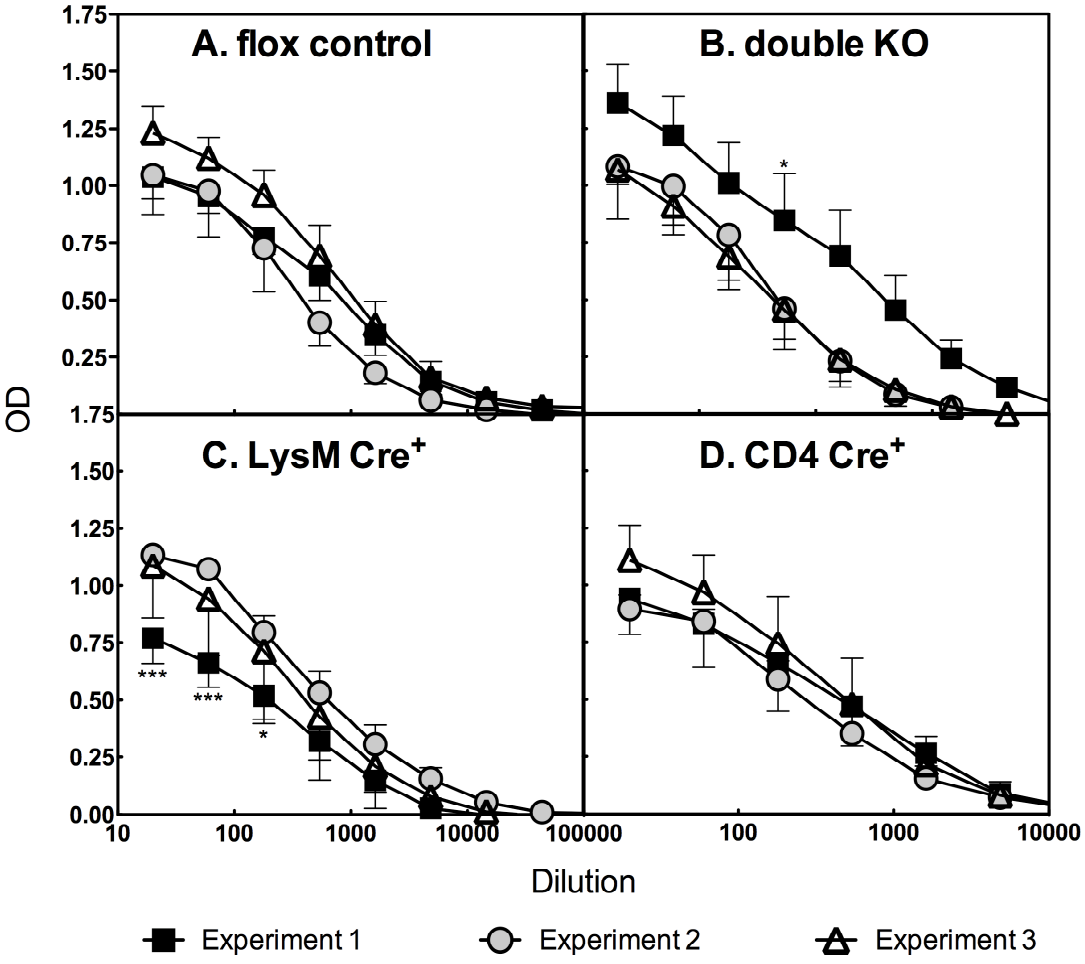

Fig 5.17 Serum parasite specific IgG1 responses in A. IFNγR2$^{fl/fl}$ (control) B. IFNγR2$^{fl/fl}$LysMCre^{+}CD4Cre^{+} (double KO) C. IFNγR2$^{fl/fl}$LysMCre^{+} and D. IFNγR2$^{fl/fl}$CD4Cre^{+} mice. Mice were infected with 20 *T. muris* eggs on day 0. Blood was removed from individual mice upon sacrifice and serum analysed by parasite specific ELISA. Results are presented as mean ± s.e. per group. n = 3-5 for all groups except experiment 2 double KO (n=2) and experiment 1 LysM^{+} (n=6) *p≤0.05, **p≤0.01, ***p≤0.001 stastically significant compared to Experiment 2.

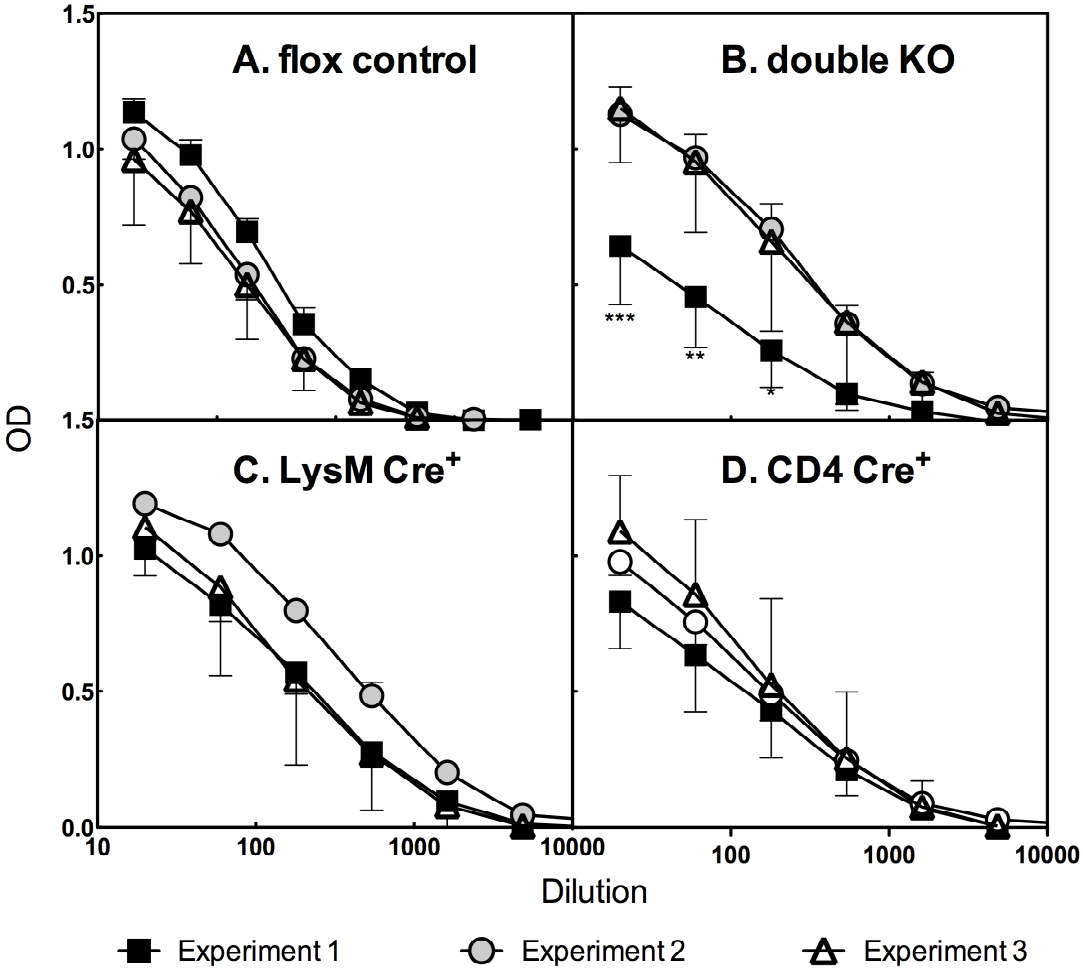

Fig 5.18 Serum parasite specific IgG2a/c responses in A. IFNγR2$^{fl/fl}$ (control) B. IFNγR2$^{fl/fl}$LysMCre^{+}CD4Cre^{+} (double KO) C. IFNγR2$^{fl/fl}$LysMCre^{+} and D. IFNγR2$^{fl/fl}$CD4Cre^{+} mice. Mice were infected with 20 *T. muris* eggs on day 0. Blood was removed from individual mice upon sacrifice and serum analysed by parasite specific ELISA. Results are presented as mean ± s.e. per group. n = 3-5 for all groups except experiment 2 double KO (n=2) and experiment 1 LysM^{+} (n=6) *p≤0.05, **p≤0.01, ***p≤0.001 stastically significant compared to Experiment 3.

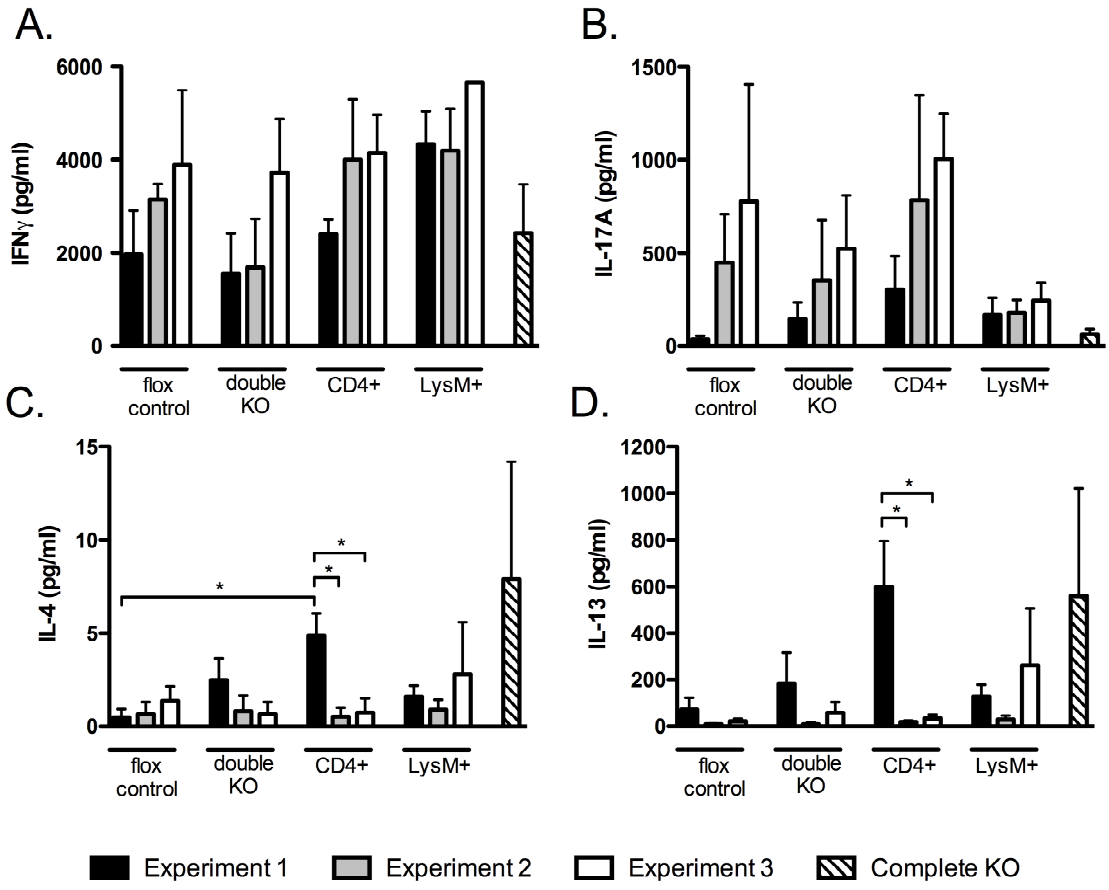

Fig 5.19 Secretion of Th1, Th17 and Th2 cytokines A. IFNγ B. IL-17A C. IL-4 and D. IL-13 by antigen stimulated MLN cells in IFNγR2 conditional knock-out and IFNγR2$^{fl/fl}$ (control) mice on day 35 post infection with *T. muris*. Mice were infected with 20 *T. muris* eggs on day 0. MLN cells were removed from individual mice, stimulated for 48 hours with E/S antigen and cell supernantants analysed by CBA. Results are presented as mean ± s.e. per group. n = 3-5 for all groups except experiment 2 double KO (n=2) and experiment 1 LysM^{+} (n=6) * p≤0.05 ** p≤ 0.01 statisitically significant as indicated

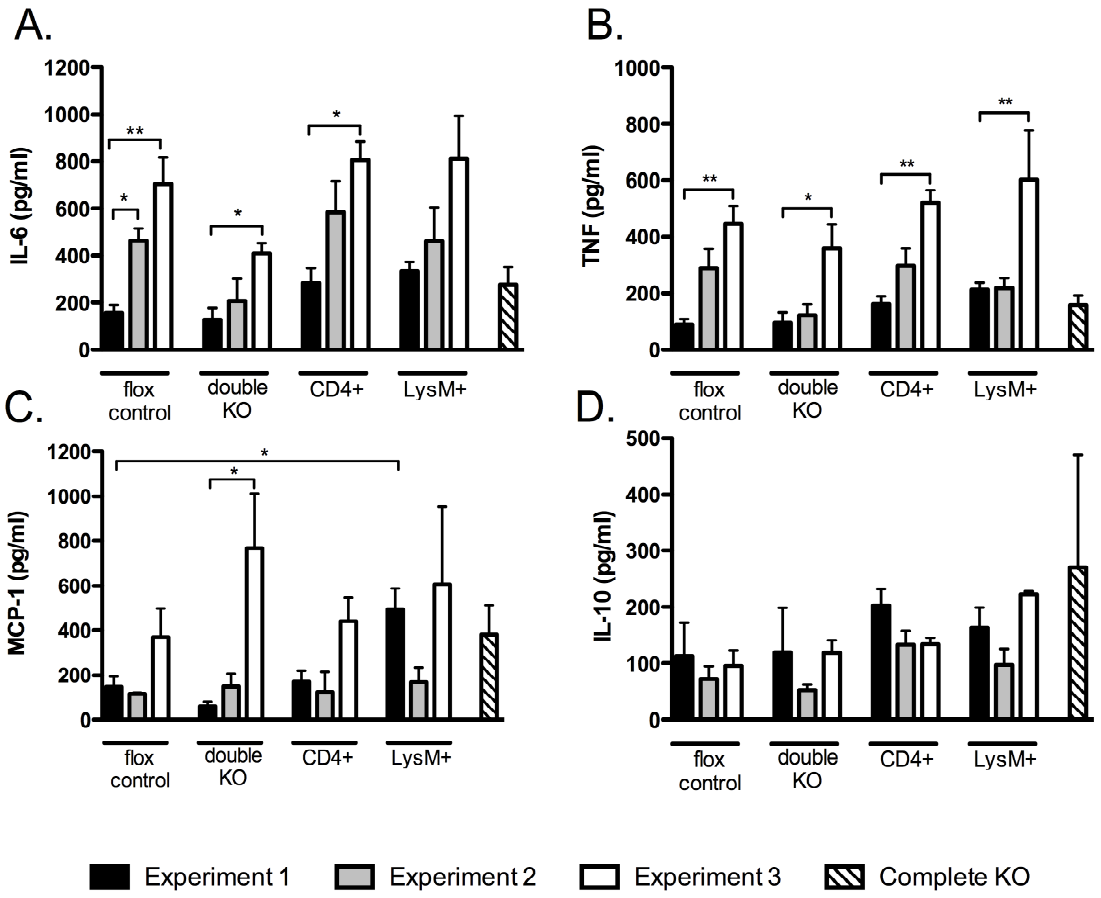

Fig 5.20 Secretion of pro-inflammatory and anti-inflammatory cytokines A. IL-6 B. TNF C. MCP-1 and D. IL-10 by antigen stimulated MLN cells in IFNγR2 conditional knock-out and IFNγR2$^{fl/fl}$ (control) mice on day 35 post infection with *T. muris*. Mice were infected with 20 *T. muris* eggs on day 0. MLN cells were removed from individual mice, stimulated for 48 hours with E/S antigen and cell supernantants analysed by CBA. Results are presented as mean ± s.e. per group. n = 3-5 for all groups except experiment 2 double KO (n=2) and experiment 1 LysM^{+} (n=6) * p≤0.05 ** p≤ 0.01 statisitically significant as indicated

5.3 DISCUSSION

Previous studies have demonstrated that mice harbouring the deletion of IFNγ or the receptor for IFNγ can expel a high dose *T. muris* infection more rapidly than control animals (unpublished observation in review by (Grencis, 2001)). The results of this chapter have extended this data to demonstrate that the deletion of IFNγ receptor 2 is sufficient to impart resistance to a low dose infection.

As most cells express IFNγ receptors, and are therefore capable of responding to IFNγ, it can be very difficult to dissect the *in vivo* actions of the cytokine (Bach *et al.*, 1997). Therefore, the conditional Cre-loxP system is extremely powerful in elucidating the mechanism through which resistance to *T. muris* is mediated. The analysis of the *in vivo* infection of conditional knock-out mice has demonstrated that the action of IFNγ, contrary to our hypotheses, is not dependent on T cells or macrophages, as CD4- and LysM- Cre conditional knockout mice remain susceptible to a low dose *T. muris* infection. However, there is some evidence that in certain circumstances the abrogation of IFNγ signalling in both T cells and macrophages is sufficient to reinstate the resistant phenotype seen in complete knock-out animals.

5.3.1 The role of IFNγ-responsive cells in the generation of a Th1 response

After infection with *T. muris* it is well documented that mouse strains either mount a Th1 response and become susceptible, with infections reaching chronicity; or they develop a Th2 response and expel their parasites. This T cell response is known to play a pivotal role in the mechanism of *T. muris* expulsion, as the depletion of $CD4^+$ cells results in susceptibility to the parasite in normally resistant strains of mice (Koyama *et al.*, 1995). Mice given a low dose infection, even if they are normally resistant to *T. muris*, will become susceptible (Wakelin, 1973). As susceptibility is accompanied by the inappropriate mounting of a Th1 response this model, of low-dose *T. muris* infection, allows us to investigate the importance of IFNγ-responsiveness in the generation of a Th1 response.

Previous experimental work has established that although IFNγ is not vital for the development of a Th1 response, it enhances responsiveness to IL-12 in naïve T cells thus increasing Th1 development (Wenner *et al.*, 1996). Indeed, other experiments with IFNγR2 knock-out mice have shown a decreased Th1 polarisation, when IFNγ signalling is abrogated, due to a down-regulation of IL-12Rβ2 (Lu *et al.*, 1998). However, in our model using a low dose *T. muris* infection to drive a Th1 response, we see no significant differences in IFNγ production between control mice and mice harbouring a complete knock-out of IFNγR2 when lymph node re-stimulations are analysed.

A potential reason for the discrepancies in results is the different *in vivo* models used to investigate the Th1 polarisation. Lu *et al* immunised their mice with keyhole limpet hemocyanin (KLH) in FCA and analysed the immune responses following KLH re-stimulation of the draining lymph node cells at day 10 post immunisation. They observe a functional Th1 response in the IFNγR2$^{\Delta/\Delta}$ mice but it is significantly muted compared to the control mice. This experiment looks at a very early time point in the adaptive immune response and potentially the IFNγR2$^{\Delta/\Delta}$ mice take longer to mount a full Th1 response, so by day 35 post infection with *T. muris* we don't see any significant differences between IFNγR2$^{fl/fl}$ and IFNγR2$^{\Delta/\Delta}$ mice.

Moreover, experiments using the over-expression of a cytoplasmically-truncated dominant negative IFNγR1 on either T cells or macrophages demonstrated that macrophages made unresponsive to IFNγ fail to produce IL-12 and therefore a decrease in Th1 polarisation is observed. In contrast, mice in which T cells are unresponsive to IFNγ show normal Th1 polarisation (Dighe *et al.*, 1995). However, our data suggests that both the IFNγR2$^{fl/fl}$LysMCre^{+} and IFNγR2$^{fl/fl}$CD4Cre^{+} mice are capable of mounting a Th1 response, with comparable levels of IFNγ produced, upon re-stimulation of lymph nodes with E/S antigen, as produced by IFNγR2$^{fl/fl}$ mice. Again, the different models used can explain the discrepancies in the data. The method of using the over-expression of a dominant negative receptor is a less specific method of gene inactivation. The high expression levels of the non-endogenous mutant receptor can potentially have adverse effects, including the

mutation altering specificity for the original target or the physical-chemical properties of the receptor (Lagna & Hemmati-Brivanlou, 1998). Furthermore, the *in vitro* system used to analyse the generation of a Th1 response greatly simplifies the actions occurring *in vivo*, where the decreased IL-12 production from non-responsive macrophages could be compensated for by other cell types in the IFNγR2$^{fl/fl}$LysMCre^{+} mice; for instance dendritic cells.

5.3.2. The role of IFNγ responsive cells in mediating *T. muris* – induced intestinal inflammatory changes

During *T. muris* infection an accumulation of lymphocytes is observed in the epithelium and lamina propria of the large intestine (Little *et al.*, 2005). In resistant mice it has been demonstrated that inflammation is dominated by CD4^{+} intraepithelial lymphocytes and F4/80^{+} lamina propria leukocytes, which peaks at the time of worm expulsion. In contrast, susceptible mice have a peak of infiltrating cells during the chronic phase of the infection and the infiltrate is dominated by CD8^{+} intraepithelial lymphocytes and F4/80^{+} lamina propria leukocytes. Alongside the influx of inflammatory cells there are also changes in gut architecture with the generation of crypt hyperplasia, thought to be a hallmark of chronic infection (Artis *et al.*, 1999).

5.3.2.1. The role of IFNγ-responsive cells in mediating alterations in crypt length following *T. muris* infection.

Intestinal epithelial cells undergo a continuous turnover and renewal with pluripotent stem cells at the base of crypts giving rise to daughter cells, which migrate luminally. As these enterocytes migrate they proliferate, differentiate and mature before undergoing programmed cell death and are extruded into the intestinal lumen (Potten, 1998). This process of epithelial cell turnover, in combination with the rate of epithelial cell proliferation, determines the length of crypts in the intestine.

An elevation in the rate of epithelial cell turnover is an effector mechanism by which *T. muris* is expelled from the gut. In the Th2-dominated environment of a resistant mouse IL-13 induces an increase in the 'epithelial escalator', physically pushing the

parasites out of their niche environment (Cliffe *et al.*, 2005). In contrast, in a Th1 dominated environment IFNγ induces the chemokine CXCL-10 which has opposing actions to IL-13 and slows the rate of epithelial cell turnover (Cliffe *et al.*, 2005). As well as altering epithelial turnover IFNγ can also increase crypt length by inducing epithelial hyper-proliferation (Artis *et al.*, 1999). These two effects of IFNγ synergistically lead to an increase in crypt length and the niche environment in which *T. muris* resides.

The histological data from the IFNγR2 complete knock-out mice demonstrates these mice do not undergo crypt hyperplasia during *T. muris* infection. This may be due to the expulsion of the parasite and recovery of the intestine to normal morphology, by day 35 p.i. when the analysis was performed. However, given the instrumental role of IFNγ in crypt hyperplasia, the deletion of the IFNγ receptor could be directly inhibiting epithelial hyper-proliferation and CXCL-10 induction. This would prevent crypt hyperplasia and decrease the epithelial niche in which the parasite resides, aiding parasite expulsion.

Despite the well-established role IFNγ plays in crypt hyperplasia, whether IFNγ is acting directly on the epithelial cells or via another cell type to induce these actions is unknown. It has been proposed that the increased epithelial cell proliferation seen during *T. muris* infection could be due to IFNγ acting on macrophages and the induction of mediators like nitric oxide (Artis *et al.*, 1999). Indeed, nitric oxide is a known mediator of IFNγ-induced intestinal epithelial hyper-permeability (Unno *et al.*, 1995) as well as an inducer of epithelial cell apoptosis (Kagnoff & Eckmann, 1997). However, we've demonstrated that in the IFNγR2$^{fl/fl}$LysMCre^{+} mice there is no decrease in crypt hyperplasia compared to IFNγR2$^{fl/fl}$ mice, suggesting that macrophages are not involved in the epithelial hyper-proliferation. Moreover, the lack of alterations in histological morphology in infected IFNγR2$^{fl/fl}$CD4Cre^{+} mice compared to infected IFNγR2$^{fl/fl}$ control mice suggests that T cells are also unimportant in these histological changes.

5.3.2.2. The role of IFNγ-responsive cells in the influx of $CD3^+$ T lymphocytes into the intestine following *T. muris* infection

The kinetics of lymphocyte influx into the intestine following *T. muris* infection has been demonstrated to be indicative of susceptibility to the parasite. Resistant mice show a peak in $CD4^+$ intraepithelial lymphocytes around the time of worm expulsion and then a reversion to normal levels. However, in susceptible mice the number of intraepithelial lymphocytes increases more gradually than in resistant mice, as infection progresses, and remains high during the chronic phase of infection (Little *et al.*, 2005).

In our experiments there was an increase in $CD3^+$ cells in both $IFN\gamma R2^{fl/fl}$ and $IFN\gamma R2^{\Delta/\Delta}$ mice by d21 p.i. however, in the $IFN\gamma R2^{\Delta/\Delta}$ mice by day 35 p.i. this is no longer significant and appears to be returning to naïve levels. In contrast, $IFN\gamma R2^{fl/fl}$ mice at day 35 p.i. still have a significant increase in $CD3^+$ cells in the intestine compared to uninfected mice. This is consistent with previous data showing that, in susceptible mice, $CD4^+$ cells remain high during chronic infection. In contrast, there were no significant differences in the number of $CD3^+$ T cells present in the gut of infected $IFN\gamma R2^{fl/fl}CD4Cre^+$ mice compared to infected $IFN\gamma R2^{fl/fl}$ control mice at d35 p.i.. As we looked at just the $CD3^+$ population we could have missed more subtle changes in the $CD4^+$, $CD8^+$ and $CD4^-CD8^-$ sub-populations found in the large intestine. Indeed, it has previously be reported that susceptible mice, despite having a more gradual influx of $CD4^+$ cells, have more $CD8^+$ cells in the intestine (Little *et al.*, 2005), therefore, there could be no significant changes in the overall $CD3^+$ population. However, in the previous experiment high dose *T. muris* infections were given and the resistant and susceptible mice were on different genetic backgrounds (BALB/c and AKR respectively). The different genetic background may have confounding effects on the histological analysis as the mice display different levels of intraepithelial lymphocyte phenotypes in unchallenged mice, with significantly more $CD8^+$ cells present in AKR mice (Little *et al.*, 2005). Therefore, the differences in the influx of cells during in infection may be due to the strain differences and not the susceptibility to the parasite. To further clarify the importance of the influx of the

$CD3^+$ subpopulations in mediating resistance to the parasite these populations should be characterised in the $IFN\gamma R2^{\Delta/\Delta}$ (resistant) and $IFN\gamma R2^{fl/fl}$ (susceptible) mice.

5.3.2.2. The role of IFNγ-responsive cells in the influx of macrophages into the intestine following *T. muris* infection

The role of macrophages in the expulsion of *T. muris* is not fully understood, however, it has been well documented that resistant mice have more macrophages in the intestine than susceptible mice (Little *et al.*, 2005). Indeed, mice lacking the macrophage chemokine CCL2 have fewer macrophages in the gut lamina propria and fail to expel the parasite with an associated altered Th1/Th2 balance (deSchoolmeester *et al.*, 2003). In light of this data it has been proposed that macrophages may be important in the mechanism of worm expulsion from the gut (Little *et al.*, 2005).

Work with other models of helminth parasites has determined that macrophages at the site of infection primarily display an alternatively-activated phenotype (Jenkins & Allen, 2010). The numbers of circulating alternatively activated macrophages (AAMs) increase during infection with *Nippostrongylus brasiliensis* and the AAMs are thought to be responsible for infection-associated alterations in small intestine smooth muscle. Indeed, expulsion of *N. brasiliensis* is impaired after depletion of macrophages or blocking of arginase (Zhao *et al.*, 2008). Similarly, depletion of macrophages or blocking arginase activity in mice infected with *Heligmosomoides bakeri* (formerly *Heligmosomoides polygyrus*) increases parasitic burdens (Anthony *et al.*, 2006). Previous research has therefore implicated a role for AAMs as effector cells in parasitic infections and AAMs are increasingly being recognised as an important arm of the Th2 immune response (Jenkins & Allen, 2010). Moreover, a striking number of mechanisms associated with alternatively activated macrophage responses to parasitic nematode infections have been identified, although these vary from parasite to parasite and between tissues (for review see (Horsnell & Brombacher, 2010)).

In keeping with the previous *T. muris* data, our IFNγR2$^{\Delta/\Delta}$ resistant mice have a significantly increased number of macrophages in the gut by day 21 p.i. which returns to naïve levels by day 35 p.i.. The IFNγR2$^{fl/fl}$ mice, on the other hand, do not display an increased number of macrophages in the intestine until day 35 p.i.. Moreover, in IFNγR2$^{\Delta/\Delta}$ mice we have demonstrated that macrophages produce significantly less nitric oxide and more arginase *in vitro* suggesting a skewing of the macrophages towards a alternatively activated phenotype. However, *in vivo* following *T. muris* infection there is no significant increase in the number of Arg1^{+} cells in the intestine of IFNγR2$^{\Delta/\Delta}$ or IFNγR2$^{fl/fl}$LysMCre^{+} mice compared to IFNγR2$^{fl/fl}$ mice. This is in contrast to other work with IFNγ knock-out mice, which display an enhanced generation of AAMs following pulmonary *Cryptococcus neoformans* infection (Arora *et al.*, 2005). This discrepancy may be due to the model of infection used as in the low dose *T. muris* infection there is not a significant increase in levels of Th2 cytokines that drive the differentiation of AAMs. The elevation of macrophages seen during *T. muris* may not be as important as hypothesised as it has been recently demonstrated that expulsion of *T. muris* is unaffected by AAMs and arginase-1 is not essential for resistance to *T. muris* (R. Bowcutt, personal communication) and we have demonstrated efficient worm expulsion in IFNγR2$^{\Delta/\Delta}$ mice which do not develop classical macrophage effector functions. Moreover, it has recently been discovered that depletion of macrophages using CD11b-DTR mice during *T. muris* infection, does not alter worm expulsion but is important for regulating inflammation (M. Little, personal communication).

An alternative explanation for the increase in macrophages seen at d21 p.i. in the intestines of IFNγR2$^{\Delta/\Delta}$ mice is that this is unrelated to resistance to *T. muris* but due to an altered myelopoiesis and chemokine expression (Kelchtermans *et al.*, 2007; Matthys *et al.*, 1999). It has previously been demonstrated that IFNγ is normally involved in the maintenance of myelopoiesis and the removal of IFNγ signalling results in an increase in macrophage production (Matthys *et al.*, 1999). This synergises with an elevation in chemokine production e.g. MCP-1 following IFNγ deletion (Kelchtermans *et al.*, 2007), resulting in an increased infiltration of monocytes into tissues. Although following MLN stimulation there did not appear to

be an increase in MCP-1, we cannot rule out an increase in MCP-1 in the intestinal tissue.

5.3.3 Future directions to further investigate the role of IFNγ responsive cells in *T. muris* infection

The inconsistency in the IFNγR2$^{fl/fl}$CD4Cre^{+}LysMCre^{+} phenotype, in contrast to the robustness of the complete knock-out phenotype, demonstrates that although the inability to respond to IFNγ in T cells and macrophages can, under some circumstances, boost the Th2 response sufficiently to enable to expulsion of the parasite, there is another important IFNγ responding cell type or types involved in susceptibility to the *T. muris*.

The mechanism behind the differences seen between the three experiments with the double conditional knockout mice is unknown. All of the control mice had comparable worm burdens, the eggs were from the same batch and infections were performed at similar times suggesting that the level of infection or circadian interactions weren't the cause of the inconsistency. Moreover, there were no differences in the age of the mice and although in all three experiments mice of a mixed sex were used no significant differences were seen between the sexes in any of the parameters analysed. The only confounding factor between the experiments was the time of year. Indeed, it has been demonstrated in other experiments that 'circannual rhythms' can have an influence despite mice being housed temperature and light controlled environments (Loscher & Fiedler, 1996). The way mice are able detect seasonal changes despite the controlled environment is not known, but it has been proposed that the presence of an endogenous oscillator as part of a calendar system in combination with a seasonally varying environmental queue could be responsible. One environmental queue which as been hypothesised to be detectable by mice, despite maintenance in a controlled environmental, is the horizontal component of the geomagnetic field (Bartsch *et al.*, 1994). The ability of changes in circannual rhythms to impact the susceptibility of mice to *T. muris* infection is

feasible, indeed, it has recently been demonstrated that circadian rhythms can alter susceptibility (S. Otto, personal communication).

Nevertheless, there are clearly other cell types involved in the resistance seen in IFNγR2$^{\Delta/\Delta}$ mice. Potential candidates include other haemopoietic cells e.g. dendritic cells and B cells or non-haemopoietic cells e.g. epithelial intestinal cells. To clarify the potential involvement of these other cell types the following experiments, using the versatility of the Cre-loxP system, could be performed.

5.3.3.1 Generation of an IFNγR2$^{fl/fl}$ x Vav-Cre mouse would allow the role of IFNγ-responsive cells in the haemopoietic system during *T. muris* infection to be elucidated

Vav-Cre mice have been generated which drive recombination between loxP sites in the majority of haematopoietic cells and endothelial cells but in very few other somatic cells (Georgiades *et al.*, 2002). Crossing the IFNγR2$^{fl/fl}$ mice to Vav-Cre mice will allow the determination of whether the additional cells responsible for the resistant phenotype observed in IFNγR2$^{\Delta/\Delta}$ mice are part of the haemopoietic system. If this is the case, further experiments could then be performed to dissect which components of the haemopoietic system are most important. Two potential candidates are the dendritic cells and the B cells.

5.3.3.1.1. Generation of an IFNγR2$^{fl/fl}$ x CD11c-Cre mouse would allow the role of IFNγ-responsive dendritic cells during *T. muris* infection to be elucidated.

Dendritic cells (DCs) are the most important professional antigen-presenting cells, with the ability to prime naïve T cells. Immature DCs reside in peripheral tissue where they act as sentinels, capturing and processing antigens. Upon activation DCs migrate to secondary lymphoid organs where they prime antigen-specific naïve T cells (Moser & Murphy, 2000).

The importance of dendritic cell responses in the outcome of *T. muris* infection has been demonstrated through experiments showing that the kinetics and magnitude of the dendritic cell response are strikingly different between resistant and susceptible animals (Cruickshank *et al.*, 2009). Dendritic cells in mice susceptible to *T. muris* do not appear to become fully mature in contrast to dendritic cells in resistant mice, which display increased MHC class II, CCR7 and other maturation markers. Moreover, as the influx of dendritic cells occurs several days prior to the generation of an adaptive immune response, they may be key in facilitating the skewing of the immune response (Cruickshank *et al.*, 2009).

It has also been demonstrated that IFNγ is an important mediator in the maturation of dendritic cells. Using IFNγR2 knock-out mice it has been shown that IFNγ is important for the up-regulation of the co-stimulatory molecules CD54 and CD86. It is also important for the secretion of the pro-inflammatory cytokines IL-1β and IL-12p70. Furthermore, IFNγR2-deficient DCs have a decreased ability to stimulate alloreactive T cells and drive Th1 differentiation (Pan *et al.*, 2004). Therefore, the dendritic cell may be an important target for IFNγ responsiveness and could be, at least in part, responsible for the discrepancy seen between the double conditional and complete knock-out phenotype.

5.3.3.1.2. Generation of an IFNγR2$^{fl/fl}$ x CD19-Cre mouse would allow the role of IFNγ-responsive B cells during *T. muris* infection to be elucidated.

B cells upon activation will become either a memory cell or a plasma cell capable of producing a large amount of antibody. In germinal centres mature B cells can undergo class switching - changing from the production of IgM and IgD to other isotypes such as IgG and IgE (for review see (Bonilla & Oettgen, 2010)). Class switching is partly determined by the cytokine milieu e.g. IL-4 promotes class switching to IgE and IgG1 whereas IFNγ promotes class switching to IgG2a. In addition, IFNγ antagonises the effects of class switching induced by IL-4 (Hasbold *et al*., 1999). In keeping with this, it has been established that the abrogation of IFNγ

signalling results in inhibition of IgG2a secretion and the enhancement of IgG1 and IgE secretion by B cells (Finkelman *et al.*, 1988).

The investigation of IFNγR2$^{fl/fl}$ x CD19-Cre mice would allow the role of IgG2a antibodies during *T. muris* infection to be analysed. It has previously been proposed that IgG2a may act as a blocking antibody to prevent IgG1-mediated effector mechanisms. Therefore, the deletion of IFNγR2 on B cells may not only increase IgG1 levels through the removal of IFNγ antagonism of IL-4-induced IgG1 class switch but also increase the efficacy of IgG1 by the removal of functional antagonism. Parasite-specific IgG1 is known to be important to *T. muris* infection outcome as the transfer of parasite-specific IgG1, purified from the serum of resistant NIH mice, can prevent worm establishment in μMT mice (Blackwell & Else, 2001). Although anti-parasitic IgG1 responses are an attractive candidate for effector mechanisms against *T. muris* a clear role for antibody has not been demonstrate during primary infections (Blackwell & Else, 2002). This suggests that IFNγ responsive B cells are unlikely to be the cause of discrepancy between the double conditional knock-out mice and the complete knock-out mice, but the IFNγR2$^{fl/fl}$ x CD19-Cre mice present an elegant method of confirming the role of IgG2a in primary and secondary *T. muris* infections.

5.3.3.1.2 Generation of an IFNγR2$^{fl/fl}$ x Villin-Cre mouse would allow the role of IFNγ-responsive intestinal epithelial cells during *T. muris* infection to be elucidated.

Another cell type, which could be an important target for IFNγ in susceptibility to *T. muris*, is the intestinal epithelial cell. Epithelial cells have recently be recognised to play a more important role that once acknowledged in directing immune responses as demonstrated by the presence of the 'epimmunome' – a collection of molecules secreted by epithelial cells and epithelial cell surface molecules which are capable of directing the actions of immune cells (Swamy *et al.*, 2010).

T. muris resides within the epithelial cells throughout its lifetime, as following egg hatching L1 larvae invade the epithelial cells, moving through the epithelium in a syncytical tunnel. Indeed, in *T. muris* it is known that intestinal epithelial cells play a vital role in resistance to the parasite as the intestinal epithelial cell-specific deletion of IκB kinase (IKK)-β results in the development of susceptibility to a high dose infection (Zaph *et al.*, 2007). This susceptibility is associated with the failure to mount a Th2 response and the alteration of dendritic cell conditioning, suggesting that epithelial cells may be able to alter the dendritic cell response.

In addition to the role of epithelial cells in shaping the immune response following infection with *T. muris*, it has been demonstrated that epithelial cells play an important role in the effector response required for parasite expulsion. It is known that the epithelial escalator is important in the expulsion of the parasite and that this is controlled through IL-13 which enhances movement up the crypt and IFNγ-induced CXCL10 which slows movement of cells up the crypt (Cliffe *et al.*, 2005). We have demonstrated that macrophages and T cells are unlikely to be the important source of CXCL10 in the gut as, although mucosal T cells are capable of producing CXCL10 (Singh *et al.*, 2008), IFNγR2$^{fl/fl}$CD4Cre^{+} and IFNγR2$^{fl/fl}$LysMCre^{+} infected mice display similar crypt hyperplasia to IFNγR2$^{fl/fl}$ mice. It is known that gut epithelial cells are capable of responding directly to IFNγ (Baumgart *et al.*, 1998) and producing CXCL10 (Kawaguchi *et al.*, 2009) so, could be the vital source of CXCL10 during infection. Furthermore, epithelial hyper-proliferation enhances crypt hyperplasia and has been shown to be dependant on IFNγ (Artis *et al.*, 1999). Recently it has been demonstrated that IFNγ acts directly on epithelial cells to regulate intestinal epithelial homeostasis via β-catenin signalling pathways and can increase epithelial proliferation (Nava *et al.*, 2010). Given the importance of the epithelial escalator in parasite expulsion and the potential of IFNγ responding intestinal epithelial cells to alter crypt length, it would be of interest to determine if the intestinal epithelial specific deletion of IFNγR2 is sufficient to confer resistance.

5.4 CONCLUSION

The results presented in this chapter demonstrate that:

1. Complete deletion of IFNγ results in the generation of a mouse resistant to *T. muris* infection.
2. T cells and macrophages play a role in the resistance to *T. muris* but there are other cell types that are also important.
3. Complete, T cell specific or macrophage specific deletion of IFNγR2 does not impede the development of a Th1 response following *T. muris* infection.
4. Complete deletion of IFNγR2 stops B cells being able to class switch to produce $IgG2_{a/c}$ antibodies.
5. The generation of further conditional knock-out mice will allow more detailed dissection of the role IFNγ plays during *T. muris* infection.

CHAPTER SIX

Characterisation of the role of IFNγ in Experimental Autoimmune Encephalomyelitis

6.1 INTRODUCTION

Experimental autoimmune encephalomyelitis (EAE) is currently the most commonly used animal model for the study of multiple sclerosis. The role of IFNγ in the pathogenesis of CNS inflammation in both MS and EAE has been controversial with data pointing to both a detrimental and protective function.

For many years the IFNγ-secreting Th1 cells were believed to be the pathogenic population central EAE. However, following the initial experiment by Billiau and colleagues, which produced the unexpected result that treatment of mice with neutralising monoclonal antibodies against IFNγ enhanced the severity of EAE (Billiau *et al.*, 1988), the role of IFNγ during EAE has remained fairly controversial. Further experiments using mutant mice confirmed the studies with neutralising antibodies as IFNγR1 deficient mice on a 129/Sv background developed EAE with high morbidity and mortality compared to wild type mice (Willenborg *et al.*, 1996). Multiple studies have now been performed using both IFNγR1 and IFNγ deficient mice, in both acute EAE and adoptively transferred EAE, all of which demonstrate an increased susceptibility and more severe symptoms in the mutant mice (Chu *et al.*, 2000; Ferber *et al.*, 1996; Krakowski & Owens, 1996; Willenborg *et al.*, 1999). More recent studies have suggested that IFNγ deficiency results in a shift from classical EAE symptoms – with ascending paralysis and inflammation in the spinal cord to a non-classical or atypical EAE with axial rotatory movement, disequilibrium, and ataxia (Wensky *et al.*, 2005).

Atypical EAE in IFNγ deficient mice has been demonstrated to result in a large eosinophil accumulation in the brainstem and cerebellum. It was hypothesised that the eosinophilia could be responsible for the atypical symptoms (Wensky *et al.*, 2005), however, further work has demonstrated that mice backcrossed onto an IL-5 deficient background still display atypical symptoms but there is an absence of eosinophilia (Wensky *et al.*, 2005). Therefore, the location of inflammation rather than the make up of the inflammatory cell infiltrate is thought to determine the EAE phenotype, however, it is still to be elucidated what the mechanisms are behind these alterations. Several reasons have been proposed for the atypical symptoms observed

in IFNγ or IFNγR1 deficient mice including a decreased chemokine expression or altered lineage commitment of cells i.e. IFNγ has been shown to inhibit Th17 development *in vitro* through the down-regulation of the IL-23 receptor (Harrington *et al.*, 2005).

It has been demonstrated that the generation of an atypical pathology in IFNγ or IFNγR1 deficient mice is associated with the influx of inflammatory cells into the cerebellum and brain stem (Wensky *et al.*, 2005) rather than the spinal cord as seen in classical EAE. This has also been demonstrated in the adoptive transfer model of EAE as the transfer of wild-type T cells into wild-type mice results in spinal cord inflammation; but the transfer of wild-type cells into IFNγR1 deficient mice results in brain inflammation. Interestingly, the transfer of IFNγ deficient T cells into wild-type mice also results in brain, rather than spinal cord, inflammation and an atypical phenotype (Lees *et al.*, 2008). Given these results it has been proposed that IFNγ signalling in the spinal cord is required for inflammation but IFNγ signalling in the brain inhibits inflammation (Lees *et al.*, 2008). This is not fully understood as, in contrast to this hypothesis, it has been shown that IFNγ has several pro-inflammatory actions in the CNS including activation of resident microglia and infiltrating macrophage cells, induction of MHC class II and co-stimulatory molecule expression in astrocytes (Nikcevich *et al.*, 1997), all culminating in increased tissue injury (Goverman, 2009; Krakowski & Owens, 1996). Indeed, IFNγ expression in the mature CNS under the control of an oligodendrocyte specific promoter resulted in the development of demyeliniation, gliosis and inflammation (Horwitz *et al.*, 1997). In light of this data an alternative hypothesis has been suggested which proposes that it is an altered influx of cells which is important for the different phenotypes observed and that IFNγ is important in inhibiting the influx of T cells into the brain. Indeed, IFNγ deficient mice displaying atypical symptoms have no detectable CNS expression of the chemokines CXCL9 and CXCL10 (Lees *et al.*, 2008). Moreover, it has been shown that the receptor for these chemokines, CXCR3, plays an important role in retaining T cells in the perivasculature space of the cerebellum and therefore, preventing atypical disease development (Muller *et al.*, 2007).

An alternative proposed mechanism for the altered location of inflammatory cells is the CD4 T cell subset developed in the mice. Recent experiments have demonstrated the T cells specific for different epitopes of MOG preferentially induce inflammation in different areas e.g. MOG_{97-114} preferentially induces brain inflammation and an atypical phenotype whereas MOG_{35-55} and MOG_{79-90} preferentially induces spinal cord inflammation and a classical phenotype. In this system T cells infiltrated the brain and spinal cord meninges at a comparable rate for all three epitopes but brain inflammation was only observed in mice where the number of Th17 cells was equal or higher to the number of Th1 cells in the brain meninges. This observation lead to the proposal that the balance of Th17 and Th1 cells, in the infiltrating population, is the crucial factor in determining inflammatory cell infiltration in the brain. As it has been shown that inhibition of IFNγ can increase IL-17 producing cells (Harrington *et al.*, 2005), in IFNγ deficient mice an increased ratio of Th17 cells to Th1 cells could be the cause of the atypical phenotype seen in the mutant mice. However, experiments performed at the University of Zurich demonstrate that the cause of the preferential influx into the cerebellum and brain stem is not due to an increase in IL-17 expressing cells, as IL-17, IFNγ double deficient animals still develop an atypical disease (V. Toveski, personal communication).

It is apparent that, despite multiple groups establishing an altered site of inflammation influx in IFNγ deficient animals with atypical EAE, more research is necessary to understand the mechanisms underlying this process. Through a collaboration with Professor Burkhard Becher at the University of Zurich we were able to investigate, for the first time, the role of IFNγR2 during EAE. Mice from our facility at the University of Manchester were shipped to the animal facility at the University of Zurich, and the EAE experiments were performed in Zurich. Future work utilising the conditional inactivation of the gene through the Cre-LoxP system may finally clarify the role of IFNγ in this model.

6.2 EXPERIMENTAL SETUP

The experiments were performed according to the scheme shown in Fig 6.1. Briefly, for the initial experimental (Experiment 1) mice were shipped from the Biological Services Unit at the University of Manchester to the experimental animal facility at the University of Zurich. These mice were then left to acclimatise for 1 week prior to immunisation with MOG-CFA and pertussis toxin on day 0 (for details see Section 2.2.3). Mice were subjected to a second dose of pertussis toxin on day 2 p.i.. Mice were monitored daily for clinical symptoms and from day 7 p.i. were weighed daily until the termination of the experiment at day 21 p.i.. B6 mice, bred and maintained at the University of Zurich experimental animal facility, were immunised simultaneously and used as controls.

Minor alterations were made to the experimental procedure prior to the start of the subsequent experiment (experiment 2) (see Fig 6.1). The primary change was an

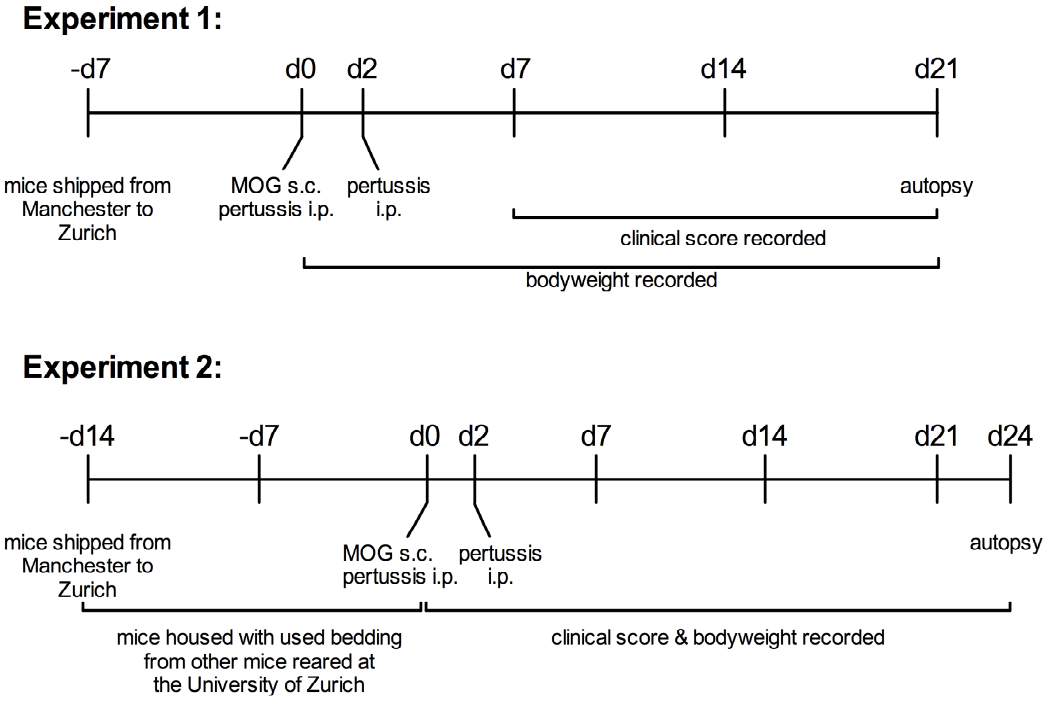

Fig 6.1 Scheme illustrating the experimental setup followed for EAE experiments. In Experiment 1 mice were shipped from Manchester to Zurich seven days prior to immunisation and autopsied on day 21 post immunisation. In Experiment 2 mice had a two week acclimitisation period with used bedding from other cages prior to immunisation. Mice were subsequently autopsied at day 24 post immunisation

increase in the acclimatisation time following the shipping of animals to Zurich, from one week to two weeks. During this period the mice were exposed to dirty bedding from mice, which had been reared at the University of Zurich experimental animal facility. For this experiment bodyweight was measured from day 0 and the experiment was continued until day 24 p.i..

6.3 RESULTS

6.3.1. Induction of EAE in IFNγR2$^{fl/fl}$ and IFNγR2$^{\Delta/\Delta}$ mice

Experiment 1: EAE disease penetrance was poor with 3/9 IFNγR2$^{\Delta/\Delta}$ mice and 1/9 IFNγR2$^{fl/fl}$ mice displaying clinical symptoms by day 21 p.i. (Fig 6.2B). Furthermore, mice which did display clinical symptoms only had a mild phenotype e.g. the sole IFNγR2$^{fl/fl}$ mouse which displayed clinical symptoms only suffered from tail paralysis with no involvement of the hind or fore limbs (Fig 6.2B). Furthermore, neither group appeared to undergo a significant weight loss (Fig 6.2A). There was a greater increase in weight d11-13p.i. in the IFNγR2$^{\Delta/\Delta}$ mice in comparison to IFNγR2$^{fl/fl}$ mice, however this was not maintained for the duration of the experiment (Fig 6.2A).

In both IFNγR2$^{fl/fl}$ and IFNγR2$^{\Delta/\Delta}$ mice severe ulceration at the point of MOG-CFA immunisation was observed (Fig 6.3). It has previously been recognised that the subcutaneous immunisation of CFA-containing adjuvants can cause ulceration (Broderson, 1989). However, the penetrance and severity of ulceration in the mice was more severe than normally observed in mice at the University of Zurich (B. Becher, personal communication). Moreover, B6 control mice had good EAE penetrance and no ulcerations at the injection site (data not shown). Therefore, one hypothesis was that a difference between animal units could be the cause of the low penetrance and ulceration. As one of the main differences in the mouse colonies at the University of Manchester and the University of Zurich is the gut flora the mice are maintained on, the experiment was repeated but upon arrival at the University of Zurich mice were house in cages with dirty bedding. The mice were then left to

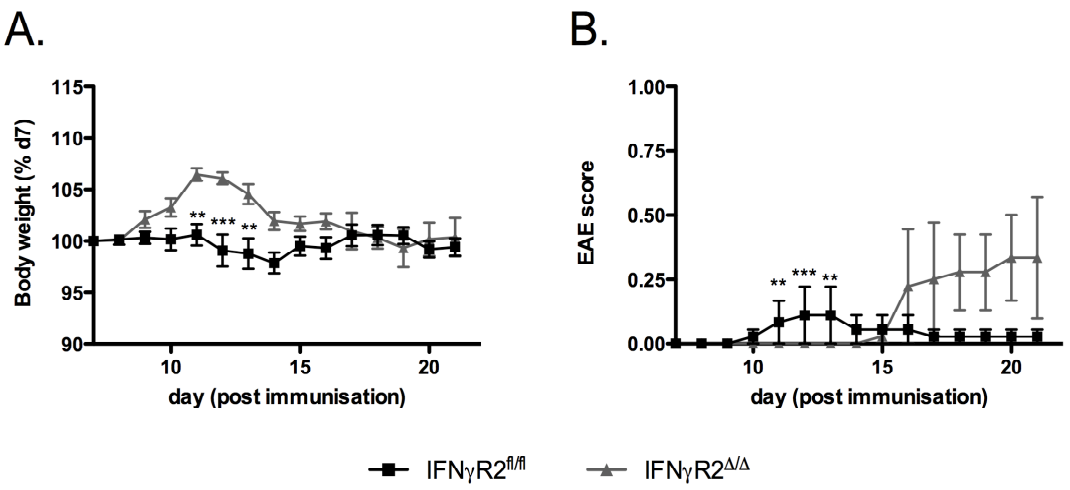

Fig 6.2 EAE in IFNγR2$^{fl/fl}$ and IFNγR2$^{\Delta/\Delta}$ mice induced by MOG/CFA immunisation. EAE was induced through the subcutanous injection of a MOG/CFA emulsion and the intraperitoneal injection of pertussis toxin on day 0 and day 2. **A.** Body weight and **B.** Clinical symptoms were monitored daily. Results are presented as mean ± s.e. per group. *p<0.05. **p<0.01, statistically significant compared to IFNγR2$^{fl/fl}$ mice; n=9.

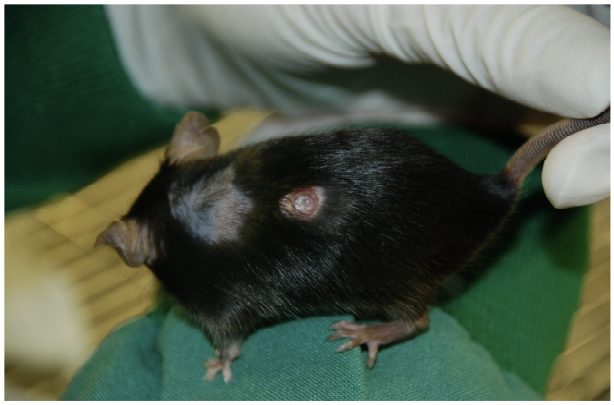

Fig 6.3 Ulcerations at the point of immunisation in IFNγR2$^{fl/fl}$ and IFNγR2$^{\Delta/\Delta}$ mice. EAE was induced through the subcutanous injection of a MOG/CFA emulsion and the intraperitoneal injection of pertussis toxin on day 0 and day 2. Ulcerations at the site of subcutanous injection were apparent in both groups from day 7 post immunisation.

acclimatise for two weeks, being maintained in cages that contained dirty bedding from other cages within the animal unit (see Fig 6.1).

6.3.2. Clinical symptoms of EAE in IFNγR2$^{fl/fl}$ and IFNγR2$^{\Delta/\Delta}$ mice

Experiment 2: Following acclimatisation, mice were immunised and clinical symptoms and bodyweight monitored daily (Fig 6.4A). No ulcerations at the site of immunisation were observed in any mice throughout the experiment. In IFNγR2$^{fl/fl}$ mice an EAE penetrance of 7/9 was observed with a decreased bodyweight evident from day 13 p.i., corresponding with the onset clinical symptoms (Fig 6.4A,B). Weight loss continued for approximately 4 days accompanied by worsening of clinical symptoms. These clinical symptoms were of a classical EAE phenotype evident initially through loss of tone in the tail and proceeding with complete tail paralysis followed by hind limb paralysis in most mice. At day 17 p.i. bodyweight began to increase, returning to baseline, and clinical symptoms decreased with recovery of hind limb and then tail function (Fig 6.4A,B). At the end of the experiment (day 24 p.i.) the mice had almost fully recovered with a slight paralysis of the tip of the tail the only evidence of any EAE in the mice (Fig 6.4B).

IFNγR2$^{\Delta/\Delta}$ mice also displayed good EAE penetrance with 6/9 mice displaying symptoms. Weight loss began at a similar time to the IFNγR2$^{fl/fl}$ mice - approximately day 13 p.i., with a corresponding onset of clinical symptoms (Fig 6.4A,B). However, in contrast to the IFNγR2$^{fl/fl}$ mice, the clinical symptoms observed in 5/6 IFNγR2$^{\Delta/\Delta}$ mice were not the classical symptoms of EAE but an alternative or atypical symptoms. These symptoms generally started with an axial rotatory movement upon tail suspension, bringing the fore-limb of one side up to the hind limb of the same side. This was followed by evidence of a head tilt that proceeded to tilting of both the head and body. These symptoms increased until the mice were unable to walk in a straight line, and instead started to travel in circles, with evidence of vertigo. In some cases the onset of symptoms in IFNγR2$^{\Delta/\Delta}$ mice was sudden, with no evidence of any EAE phenotype one day prior to the observation of severe symptoms and vertigo. Moreover, the IFNγR2$^{\Delta/\Delta}$ mice were unable to recover from these symptoms before the termination of the experiment on

day 24 p.i. and, correspondingly, had no recovery in bodyweight (Fig 6.4A). One IFNγR2$^{\Delta/\Delta}$ mouse developed classical EAE symptoms, however, unlike the IFNγR2$^{fl/fl}$ mice it had not recovered by the end of the experiment and still displayed complete hind limb paralysis. Moreover, there was evidence of both the classical paralysis and atypical symptoms with asymmetric axial rotation upon tail suspension observed, a sign of preliminary atypical disease.

Due to the poor penetrance of EAE in the initial experiment all subsequent data refers to analysis performed in mice in experiment two.

6.3.3. Histological alterations during EAE in IFNγR2$^{fl/fl}$ and IFNγR2$^{\Delta/\Delta}$ mice

To determine the cause of the EAE symptoms, inflammation in the spinal cord and cerebellum was analysed in the IFNγR2$^{\Delta/\Delta}$ and IFNγR2$^{fl/fl}$ mice. Analysis of H&E stained longitudinal sections of the spinal cord demonstrated inflammation in both the IFNγR2$^{\Delta/\Delta}$ and IFNγR2$^{fl/fl}$ mice displaying EAE symptoms, with a trend towards increased inflammation in the IFNγR2$^{fl/fl}$ mice (Fig 6.5A,B). No correlation between EAE symptoms and spinal cord inflammation was seen in IFNγR2$^{\Delta/\Delta}$ mice although, the IFNγR2$^{\Delta/\Delta}$ mice which developed classical EAE symptoms had more severe inflammation in the spinal cord than the other IFNγR2$^{\Delta/\Delta}$ mice (Fig 6.5B,C). In contrast, a clear correlation between spinal cord inflammation and classical EAE symptoms was observed in IFNγR2$^{fl/fl}$ mice (Fig 6.5D).

Analysis of H&E stained brain sections demonstrated the presence of inflammation, but in order to get a clearer picture of the inflammatory changes occurring further staining was performed by immunohistochemistry for CD45 and ionised calcium binding adaptor molecule -1 (IBA-1) positive cells. In the cerebellum a significant increase in CD45 positive cells was observed in the IFNγR2$^{\Delta/\Delta}$ mice compared to the IFNγR2$^{fl/fl}$ mice (Fig 6.6A). This became highly significant ($p=0.0004$) when the mice that didn't develop EAE were excluded from the analysis. In contrast to the spinal cord analysis, the CD45 influx in the IFNγR2$^{\Delta/\Delta}$ mice showed a correlation with maximum EAE score (Fig 6.6B) whereas, in the IFNγR2$^{fl/fl}$ mice there was no correlation between EAE score and CD45-positive cell infiltrate (Fig 6.6C). It needs

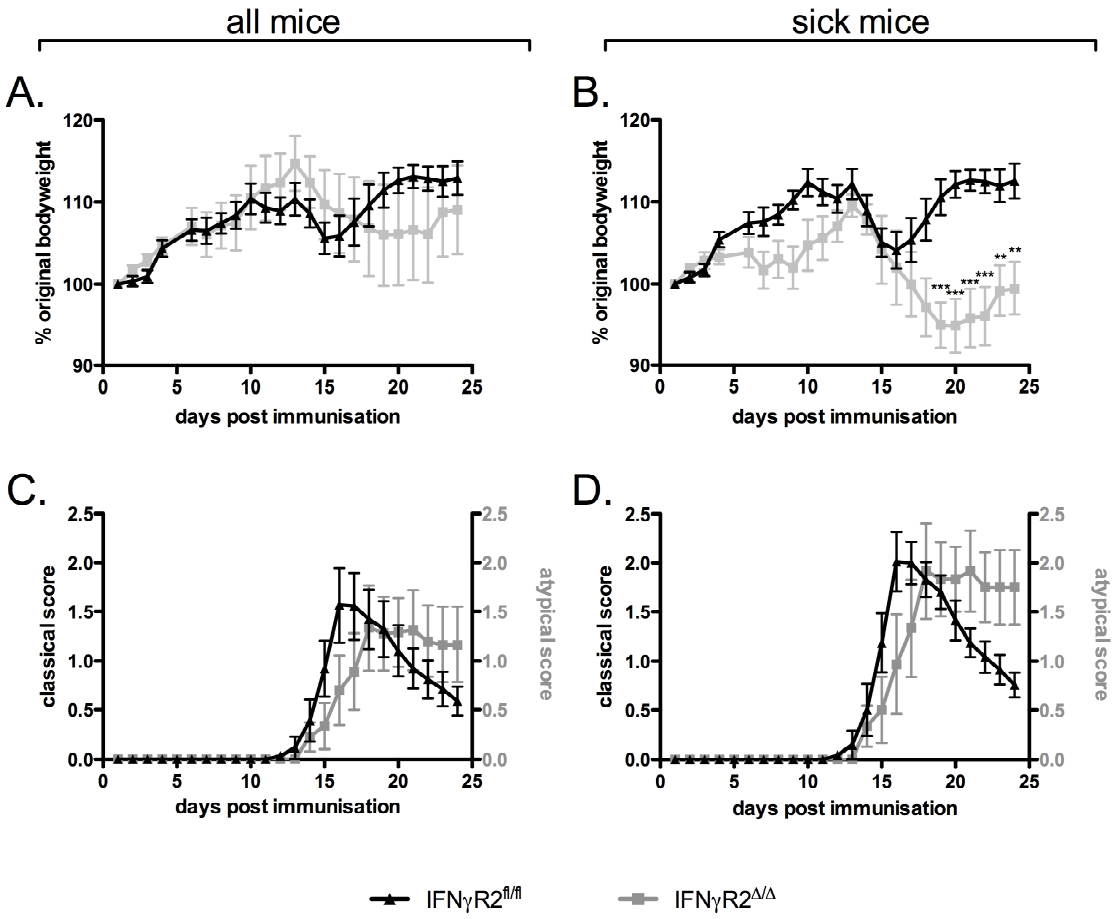

Fig 6.4 EAE in IFNγR2$^{fl/fl}$ and IFNγR2$^{\Delta/\Delta}$ mice induced by MOG/CFA immunisation. EAE was induced through the subcutanous injection of a MOG/CFA emulsion and the intraperitoneal injection of pertussis toxin on day 0 and day 2. **A.** Body weight of all mice, **B.** body weight of mice which developed EAE symptoms, **C.** Clinical sysmptoms of all mice and **D.** clinical symptoms of mice which developed EAE symptoms. Body weight and clinical symptoms were monitored daily. Results are presented as mean ± s.e. per group. *p<0.05. **p<0.01, statistically significant compared to IFNγR2$^{fl/fl}$ mice; n=9 (both groups containing all mice), n=7 IFNγR2$^{fl/fl}$ mice displaying clinical symptoms and n=6 IFNγR2$^{\Delta/\Delta}$ mice displaying clinical symptoms.

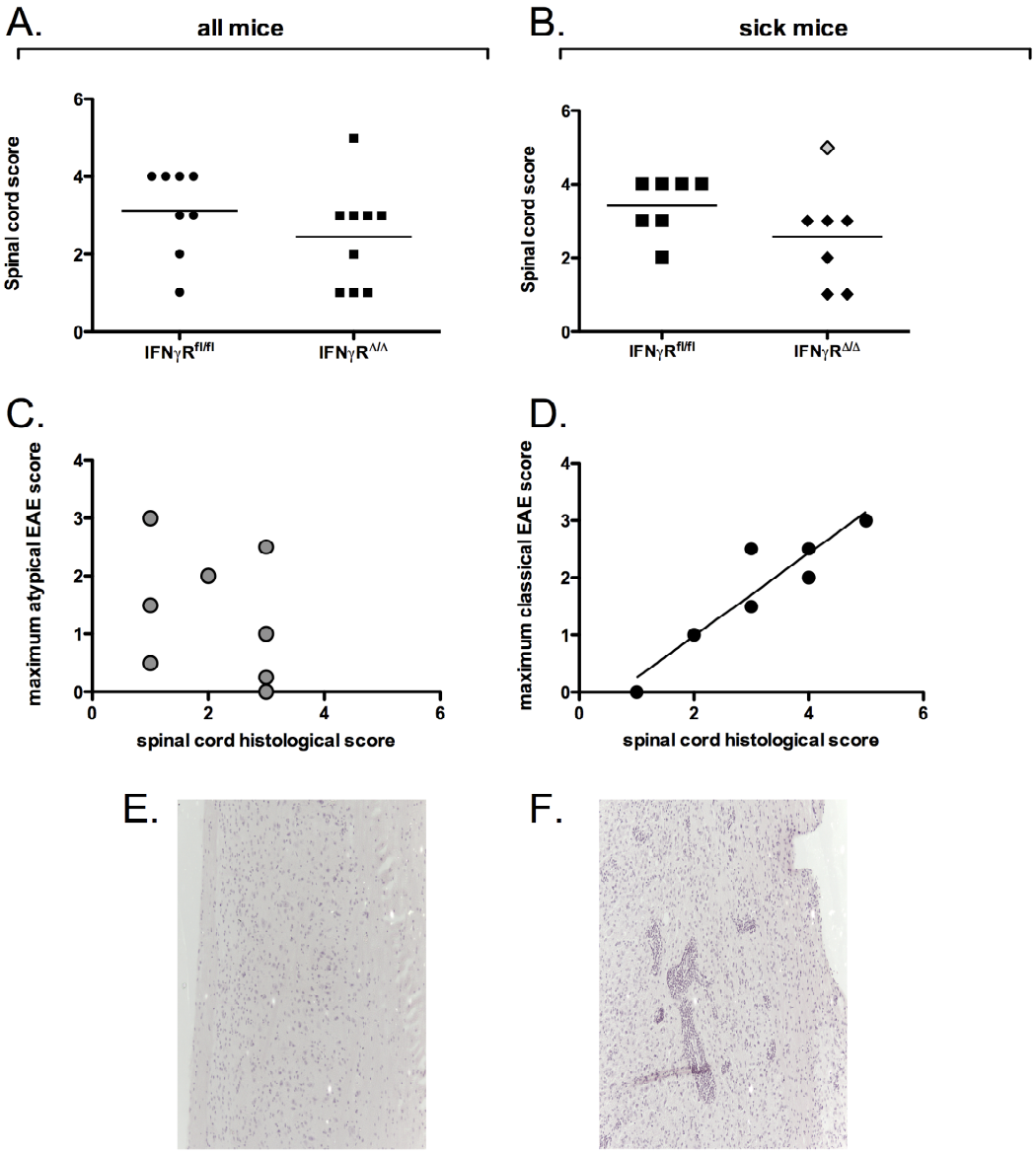

Fig 6.5 Spinal Cord inflammation in IFNγR2$^{fl/fl}$ and IFNγR2$^{\Delta/\Delta}$ mice with EAE. EAE was induced through the subcutanous injection of a MOG/CFA emulsion and the intraperitoneal injection of pertussis toxin on day 0 and day 2. Longitudinal spinal cord sections were stained with hematoxylin and eosin and visualised under a light microscope. Sections were scored for histological alterations in **A.** all mice and **B.** mice which displayed clinical symptoms (point in grey indicates IFNγR2$^{\Delta/\Delta}$ mouse which developed classical EAE symptoms). **C.** Correlation between maximum EAE symptoms and inflammation score in the spinal cord in IFNγR2$^{\Delta/\Delta}$ and **D.** IFNγR2$^{fl/fl}$ mice. **E.** x100 spinal cord section with no inflammation; score 0, **F.** x100 spinal cord section demonstrating extensive inflammation; score = 4. Results are prsentented as mean ± s.e. per group. n=9 (both groups containing all mice), n=7 IFNγR2$^{fl/fl}$ mice displaying clinical symptoms and n=6 IFNγR2$^{\Delta/\Delta}$ mice displaying clinical symptoms.

to be noted that the number of CD45 cells stained may be an under-representation of the number of CD45 cells in the brain as the brains were left in paraformaldehyde for 2 weeks prior to tissue processing.

To get a better understanding of the events occurring in the brain, sections were analysed for microglial activation. Microglia were visualised through staining with an IBA-1 antibody (Imai *et al.*, 1996) and the different activation states were analysed (see Section 2.3.5. for a description of the microglia scoring criteria). Again, due to fixation problems the staining was not as strong as typically seen and, therefore, only microglia in activation states 2-4 and not resting microglia were visualised as these states express higher levels of IBA-1 (Ito *et al.*, 2001). Despite the increased inflammatory infiltrate into the cerebellum, IFNγR2$^{\Delta/\Delta}$ mice had lower levels of microglia activation in the cerebellum compared to IFNγR2$^{fl/fl}$ mice (Fig 6.7A). The clearest difference between the IFNγR2$^{\Delta/\Delta}$ and IFNγR2$^{fl/fl}$ mice was apparent in the cerebral cortex, as IFNγR2$^{\Delta/\Delta}$ mice had significantly less activated microglia in this area compared to other areas of the brain. Moreover, in this area, the IFNγR2$^{\Delta/\Delta}$ mice had significantly less, state 2 and total, activated microglia compared to IFNγR2$^{fl/fl}$ mice (Fig 6.7C,E).

This histological data supports previously demonstrated findings that atypical symptoms correlate with inflammation in the brain whereas typical or classical EAE symptoms correlate with inflammation in the spinal cord (Wensky *et al.*, 2005).

6.3.4. FACS analysis of infiltrating cells in the brain during EAE in IFNγR2$^{fl/fl}$ and IFNγR2$^{\Delta/\Delta}$ mice

FACS analysis was performed on four IFNγR2$^{\Delta/\Delta}$ mice and two IFNγR2$^{fl/fl}$ mice, of the IFNγR2$^{\Delta/\Delta}$ mice one mouse displayed classical and not atypical EAE symptoms. Matching the histological analysis, there was an increased percentage of CD45 positive cells in IFNγR2$^{\Delta/\Delta}$ mice compared to IFNγR2$^{fl/fl}$ animals (Fig 6.8A). Moreover, within this CD45 positive population there appeared to be an trend towards an increase in 1A8 positive cells (primarily neutrophils), but only in the

IFNγR2$^{\Delta/\Delta}$ mice displaying atypical symptoms (Fig 6.8B). There was also a trend towards an increased CD4 positive population in the IFNγR2$^{\Delta/\Delta}$ mice, independently of the EAE phenotype observed (Fig 6.8C).

In summary, we have demonstrated that differences in animal unit conditions may have altered the penetrance of EAE and susceptibility of mice to ulceration. Moreover, the IFNγR2$^{\Delta/\Delta}$ mice appear to develop a severe, atypical disease with no recover that is accompanied by inflammation in the cerebellum. In contrast, the IFNγR2$^{fl/fl}$ mice develop a classical EAE disease course with almost complete recovery and spinal cord inflammation. Interestingly, despite the increased brain inflammation, lower levels of microglial activation is observed in the brains of IFNγR2$^{\Delta/\Delta}$ mice compared to IFNγR2$^{fl/fl}$ mice. These differences in the context of the existing literature will be analysed in the following discussion.

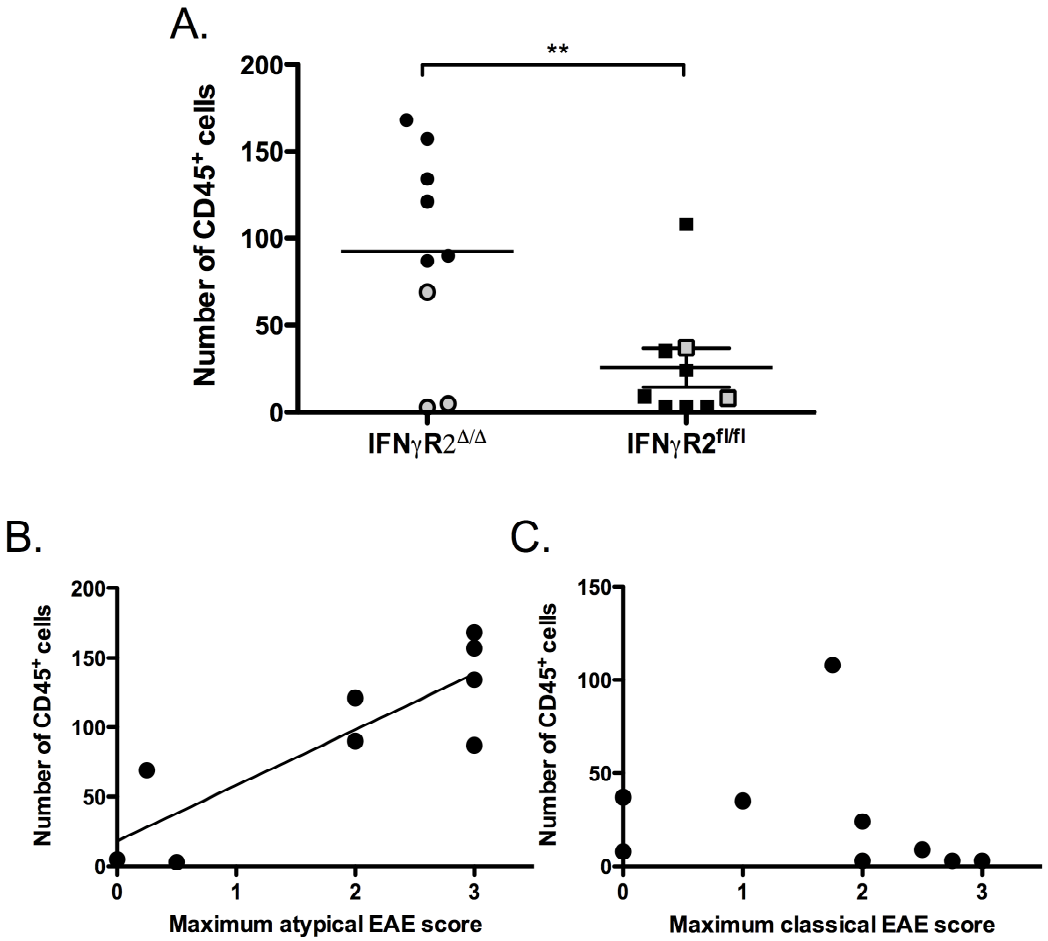

Fig 6.6 The number of CD45 positive cells in the cerebeluum of IFNγR2$^{fl/fl}$ and IFNγR2$^{\Delta/\Delta}$ mice with EAE induced by MOG/CFA immunisation. EAE was induced through the subcutanous injection of a MOG/CFA emulsion and the intraperitoneal injection of pertussis toxin on day 0 and day 2. Brain sections were stained by immunohistochemistry with a CD45 antibody and counterstained with hematoxylin. **A.** The number of CD45 positive cells was enumerated in 3 randomly selected x400 fields in the cerebellum under a light microscope. Points in grey indicate mice which did not development any clincal EAE symptoms. **B.** The maximum EAE score in IFNγR2$^{\Delta/\Delta}$ mice and **C.** IFNγR2$^{fl/fl}$ mice compared to number of CD45 positive cells in the cerebellum. Results are prsentented as mean ± s.e. per group. n=9 *p<0.05, **p<0.01 statistically significant as indicated

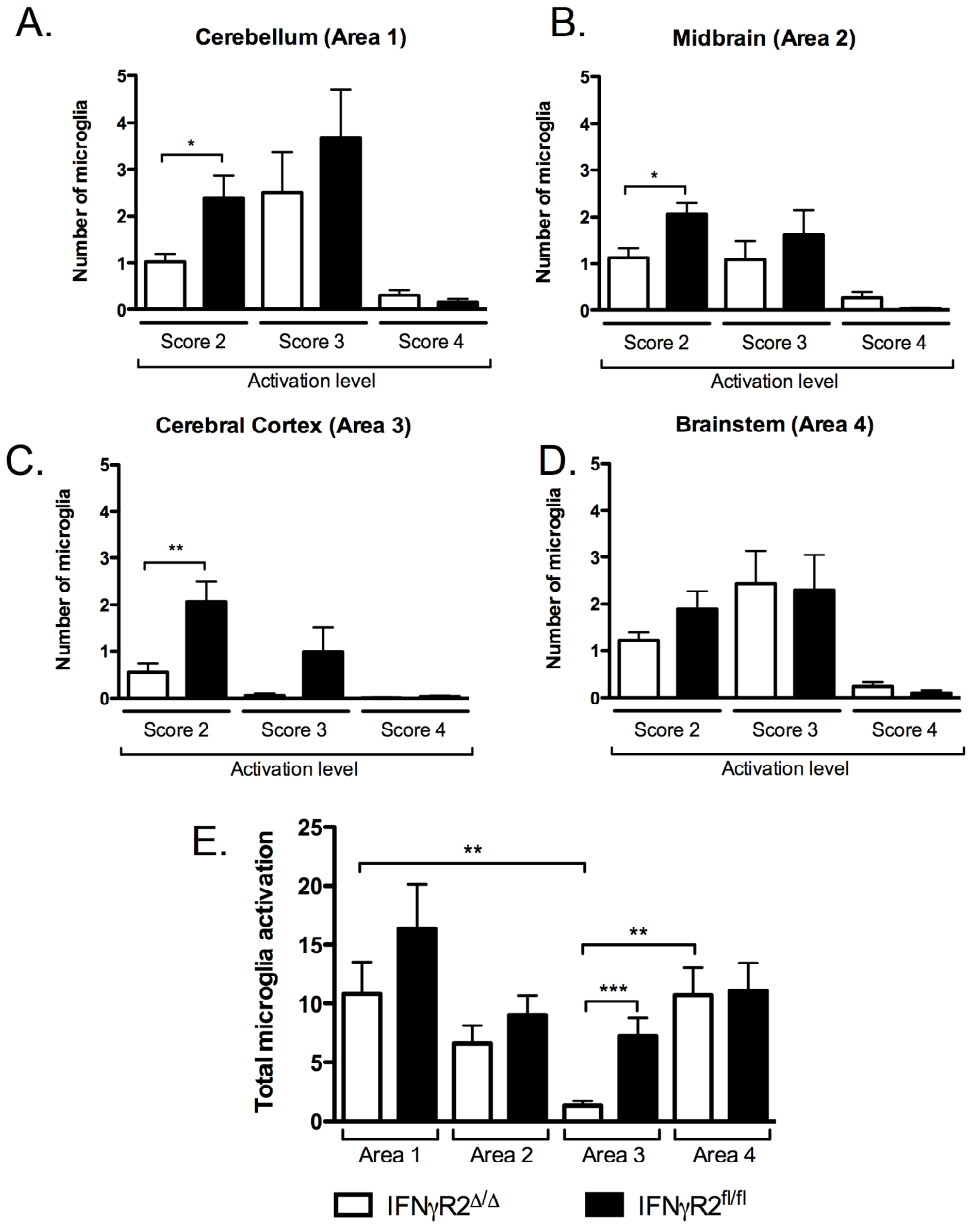

Fig 6.7 Microglia activation in the brains of IFNγR2$^{fl/fl}$ and IFNγR2$^{\Delta/\Delta}$ mice with EAE. EAE was induced through the subcutanous injection of a MOG/CFA emulsion and the intraperitoneal injection of pertussis toxin on day 0 and day 2. Brain sections were stained by immunohistochemistry with an IBA-1 antibody and counterstained with hematoxylin. The number of microglia in the different activation states were enumerated in 10 randomly selected x1000 fields in the **A.** cerebellum **B.** cerebral cortex **C.** midbrain and **D.** brainstem. **E.** Total microglia acitvation score for each section. Microglia with an activation state 1 was no visible in the sections. Results are prsentented as mean ± s.e. per group; n=9.

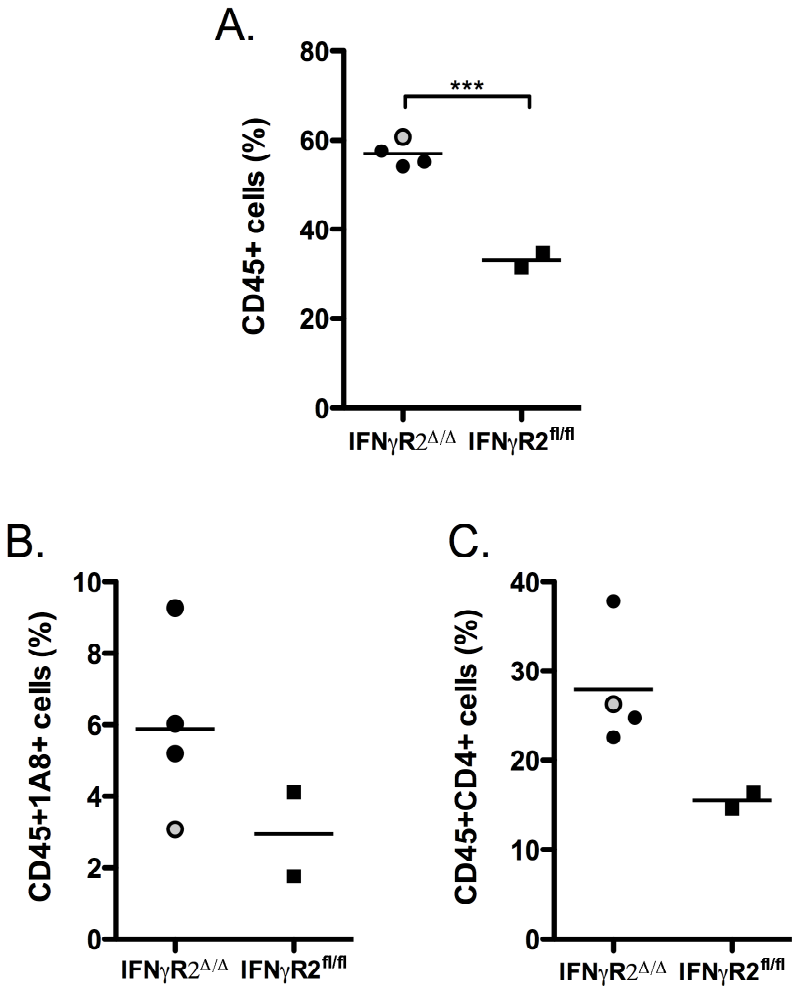

Fig 6.8 FACS analysis of the brains of IFNγR2$^{fl/fl}$ and IFNγR2$^{\Delta/\Delta}$ mice with EAE induced by MOG/CFA immunisation. EAE was induced through the subcutanous injection of a MOG/CFA emulsion and the intraperitoneal injection of pertussis toxin on day 0 and day 2. Cells were isolated from homogenised brains using Percoll and stained with CD45, CD4 and 1A8 and analysed using a FACSCanto **A.** The percentage of CD45 positive cells **B.** the percentage of CD45 1A8 double positive cells and **C.** the percentage of CD45 CD4 double positive cells. Point in grey indicates a IFNγR2$^{\Delta/\Delta}$ mouse which developed classical EAE symptoms. Results are presented as mean ± s.e. per group. n= 2 IFNγR2$^{fl/fl}$ mice and n=4 IFNγR2$^{\Delta/\Delta}$ mice.

6.4 DISCUSSION

The data contained within this chapter demonstrates that complete IFNγR2 deficient mice develop severe, atypical EAE symptoms from which they are unable to recover. To our knowledge, this is the first time that the IFNγR2 chain deficiency has been analysed in EAE and, as expected, these mice display the same phenotype as previously described in IFNγR1 deficient mice (Wensky *et al.*, 2005). The mechanism behind the altered EAE phenotype observed in IFNγ or IFNγR deficient mice is still unclear. We, and others, have shown an association between spinal cord inflammation and classical EAE symptoms, and inflammation in the cerebellum with atypical EAE symptoms (Wensky *et al.*, 2005). We have also demonstrated alterations in microglial activation in IFNγR2 deficient mice, the implications of this observation, future experiments and an examination of some of the problems and limitations of this model are discussed in the remainder of this chapter.

6.4.1. Microglial activation during EAE in IFNγR2$^{\Delta/\Delta}$ and IFNγR2$^{fl/fl}$ mice

Microglia are the key innate immune cells of the brain (Kofler & Wiley, 2010) and exhibit dynamic cell processes that appear to sample their microenvironment with projecting and retracting protrusions (Nimmerjahn *et al.*, 2005). These microglia also have similar functions to tissue macrophages including phagocytosis, antigen presentation and cytokine production (see review by (Gehrmann *et al.*, 1995)).

It is thought that microglial activation during EAE contributes to pathology through antigen presentation and pro-inflammatory cytokine secretion. Previously, it has been demonstrated that during a relapsing-remitting model of EAE a correlation was observed between loss of neuronal synapses and microglial activation (Rasmussen *et al.*, 2007). This study proposed that microglia extend their processes around the cell bodies of neighbouring neurons resulting in the loss of synaptic proteins and these microglia sustain the inflammation seen in the chronic phase of EAE. This hypothesis is supported by similar findings in primary progressive MS patients, where activated microglia are seen in association with inflammatory areas in the white matter of the brain (Kutzelnigg *et al.*, 2005). As well as loss of neuronal synapses, it is thought microglia can also play a role in demyelination and

phagocytosis of the degraded myelin (Bauer *et al.*, 1994). Furthermore, microglial cells can promote inflammation through the secretion of molecules like TWEAK (TNF like weak inducer of apoposis), and it has been demonstrated in the brains of MS patients that TWEAK-expressing microglial cells are associated with myelin loss, neuronal damage and vascular abnormalities in cortical lesions (Serafini *et al.*, 2008).

However, despite the evidence of a pathogenic role of microglia during EAE there is also evidence that microglial cells maybe beneficial. These beneficial effects occur through several mechanisms including: clearing away myelin debris and apoptotic cells, the release of protective cytokines, the recruitment of oligodendrocyte precursors and the stimulation of neurogenesis (for review see (Napoli & Neumann, 2010)). Therefore, the current hypothesis is that during EAE microglial cells can perform both neuro-destructive and neuro-protective functions, and that a switch of function from destructive to protective could be vital in preventing chronic demyelination and axonal loss.

In has been demonstrated *in vitro* that IFNγ can activate microglia and these activated microglia are capable of antigen presentation to CD4 T cells (Frei *et al.*, 1987). Therefore, it is not surprising that in IFNγR2$^{\Delta/\Delta}$ mice with EAE, despite an increased inflammatory infiltrate into the cerebellum, there is a decrease in microglia activation in comparison to IFNγR2$^{fl/fl}$ mice. It will be interesting to determine the importance of this decreased microglial activation using the IFNγR2$^{fl/fl}$LysMCre^{+} mice. Furthermore, it has been demonstrated that, similarly to macrophages, microglia may be sub-divided into different activation states – classical activation requiring IFNγ and alternative activation which is independent of IFNγ (Kofler *et al.*, 2010). Therefore, it will be of interest to analyse the microglial phenotypes in the IFNγR2$^{\Delta/\Delta}$ mice and determine if this has an influence on whether these microglia are neuro-protective or neuro-destructive during EAE.

6.4.2. Future directions to further investigate the role of IFNγ responsive cells during EAE.

A lot of research has been performed trying to define the role of IFNγ during EAE and in recent years this has focused on defining the physiological mechanisms by which IFNγ signalling alters the localisation of inflammation. However, as far as we know, this has only utilised mutant mice that are deficient in IFNγ or IFNγR1 in all cells. The existing T cell deficient IFNγR2$^{fl/fl}$CD4Cre^{+} and macrophage/granulocyte deficient IFNγR2$^{fl/fl}$LysMCre^{+} mice as well as mice which are currently being bred at the University of Zurich, by members of Prof Becher's laboratory, will allow the more precise analysis of the role of IFNγ responsive cells. The new lines being bred for these experiments include IFNγR2$^{fl/fl}$Nestin-Cre^{+} with the deletion of IFNγR2 in all macroglia and neurons (Tronche *et al.*, 1999) and IFNγR2$^{fl/fl}$CNP-Cre^{+} resulting in the deletion of IFNγR2 in oligodendrocytes (an unpublished Cre line).

The data presented in this chapter demonstrates a correlation between the location of inflammation and EAE phenotype. Future experiments will also analyse more parameters including chemokine expression, make up of inflammatory cell infiltrate and microglial phenotype. The make up of inflammatory cells will also be determined to confirm the previous reports that it is the area of inflammation, not the make-up of the inflammatory infiltrate, that plays critical key role in determining the clinical phenotype observed in the mutant mice (Wensky *et al.*, 2005). Finally the microglia phenotype will be analysed in an attempt to shed some light on the contradictory roles of these cells that is currently reported during EAE.

6.4.2.1. IFNγR2$^{fl/fl}$CD4Cre^{+} mice will allow the role of IFNγ-responsive T cells during EAE to be elucidated

T cells are well established as being vital for the pathogensis of EAE (see review by (Gutcher & Becher, 2007) for an overview of the importance of T cell polarisation during EAE). However, the importance of IFNγ acting on T cells has not been elucidated. The inactivation of IFNγR2 on T cells during EAE may result in an altered T cell polarisation, with a decrease in Th1 polarisation and a shift towards increased Th17 polarisation (Harrington *et al.*, 2005). This increased Th17

population has previously been proposed to be the cause of the atypical phenotype seen in IFNγ deficient animals. Although, IL-17, IFNγ double deficient mice still display an atypical phenotype (V. Toceski, personal communication) the importance of the Th17 population is still undetermined and the analysis of the IFNγR2$^{fl/fl}$CD4Cre^{+} mice will allow further clarity in this manner.

A second mechanism of action for IFNγ-activated T cells has also been proposed during EAE. This proposal stemmed from observations that IFNγ deficient mice have an elevation in T cell proliferation, due to the removal of the dampening of T cell responses normally provided by IFNγ signalling (Dalton *et al.*, 1993). This elevated T cell proliferation has been proposed to be a factor in the high morbidity seen in IFNγ deficient animals with EAE. Therefore, the T cell specific IFNγR2 knock out mice will be interesting to investigate to determine if an altered T cell proliferation or polarisation is observed and, if this is capable of altering the EAE disease course

6.4.2.2. IFNγR2$^{fl/fl}$LysMCre^{+} mice will allow the role of IFNγ-responsive macrophages/microglia and granulocytes during EAE to be elucidated

Macrophages and microglia are important inflammatory cells in the brain with evidence of upregulation of MHC class II and co-stimulatory molecules during EAE and MS (Martin *et al.*, 1992; Windhagen *et al.*, 1995). Importantly, these changes are thought to be due to IFNγ signalling and generate cells capable of stimulating T cell responses (Martin *et al.*, 1992). Additionally, activated macrophages / microglia are major sources of inflammatory mediators including TNF (Renno *et al.*, 1995) and NO (Tran *et al.*, 1997). These inflammatory mediators are capable of causing oligodendrocyte death which is proposed to be important in the formation of MS lesions (Merrill *et al.*, 1993). As IFNγ stimulated microglia activate multiple inflammatory pathways IFNγR2$^{fl/fl}$LysMCre^{+} mice may have a different phenotype to global IFNγ deficient mice with a less severe EAE phenotype.

IFNγ deficient mice have been shown to have decreased CXCL9 and CXCL10 expression during EAE, and this has been hypothesised to result in increased

trafficking of cells away from the perivascular space and into the parenchyma (Carter *et al.*, 2007). This altered chemokine expression has proposed to be important in the altered location of inflammation resulting in the atypical phenotype observed in these mice (Lees *et al.*, 2008). Macrophages / microglia could be key mediators of this effect as they are able to upregulate expression of CXCL9 and CXCL10 following *in vitro* stimulation with IFNγ and appear to be the only source of CXCL9 in the brains of mice with EAE (Carter *et al.*, 2007). Therefore, microglia could be involved in the atypical phenotype observed in IFNγ deficient mice.

6.4.2.3. Generation of IFNγR2$^{fl/fl}$Nestin-Cre^{+} mice will allow the role of IFNγ-responsive neuronal and glial cells during EAE to be elucidated

The importance of IFNγ-responsive brain resident cells in EAE is apparent through data that demonstrates a correlation between CNS IFNγ concentration and EAE severity (Renno et al 1995, Merrill et al 1992, Kennedy et al 1992, Owens et al 1994). This is supported by adoptive transfer studies that have shown somatic cells are important for the atypical phenotype seen in IFNγR1 deficient mice, as the transfer of wild-type cells into IFNγR1 deficient animals results in atypical disease (V. Toveski, personal communication). There are several brain somatic cells, which are potential candidates for these IFNγ-driven actions, including neuronal cells and glial cells e.g. astrocytes or oligodendrocytes.

The role of neurons in CNS inflammation is increasingly being recognised as being more important than previously acknowledged. It has recently been demonstrated that IFNγ may be important in the homeostasis of synaptic circuitry. This has been hypothesised to involve the stimulation of MHC class I expression on neurons, and there is some data showing the absence of IFNγ can result in neuronal death (Victorio *et al.*, 2010). This suggests that the deletion of IFNγR2 on neurons may be involved of the increased severity EAE seen in IFNγR2 deficient animals.

Glial cells have also been implicated in EAE, indeed astrocytes which have traditionally been seen as supplementary cells of the nervous system, have been discovered to play a more important role. They are currently thought to be important

in the structural architecture of the brain, its communication pathways, activation and plasticity (for review see (Nedergaard *et al.*, 2003)). During EAE astrocyte gliosis, with astrocyte hyperplasia and hypertrophy, has been reported (Pham *et al.*, 2009). Nevertheless, the role of astrocytes during MS and EAE is not fully understood. It is proposed that reactive astrocytes may be beneficial following demyelination but subsequently or in the presence of 'inactive' astrocytes they may inhibit remyelination (for a review of all the different effects of astrocytes in MS and animal models see (Williams *et al.*, 2007)).

Although astrocytes do not constitutively express MHC class II molecules, expression is up-regulated during active EAE. Importantly, *in vitro* incubation with IFNγ also results in MHC class II upregulation and generates astrocytes capable of priming naïve antigen-specific T cells (Nikcevich *et al.*, 1997). IFNγ can also induce astrocyte proliferation and increase the extent of trauma-initiated gliosis (Yong *et al.*, 1991). Furthermore, astrocytes have been shown to be capable of upregulating CXCL10 following stimulation with IFNγ and CXCL10 expression is seen in astrocytes surrounding inflammatory EAE lesions (Carter *et al.*, 2007). Therefore, astrocyes, either independenatly or in conjuction with microglia (as discussed in section 6.3.2.2), may play a key role in directing the location of the inflammatory infiltrate and aiding T cell activation.

Oligodendrocytes are the other key macroglial cell thought to be important in EAE. Indeed, the loss of oligodendrocytes is a hallmark of MS and EAE and is associated with neuronal dysfunction and damage resulting in the clinical manifestations of disease. It has been demonstrated *in vitro* that upon exposure to IFNγ a decrease in the number of viable oligodendrocytes is observed (Vartanian *et al.*, 1995). This has subsequently be determined to be due to the combined anti-miotic and pro-apoptotic effects of IFNγ on oligodendrocyte precursors (Horiuchi *et al.*, 2006). This data suggests that the deletion of IFNγR2 on oligodendrocytes may result in a protective effect, which could be hidden in the complete IFNγR2 deficient animals by the effects IFNγ has on other cell types. The generation of IFNγR2$^{fl/fl}$CNP-Cre^{+} mice would allow the importance of IFNγ signalling in oligodendrocytes *in vivo* to be

elucidated and determination if IFNγ can result in oligodendrocyte loss *in vivo* and, if so, what implication this has for the development of EAE.

6.4.3. Reasons for the poor penetrance and severe ulceration seen in initial EAE studies.

It has been well established that ulceration and the skin lesions are recognised side effects of injection with complete freund's adjuvant (CFA) (Broderson, 1989). In mice, following subcutaneous immunisation, these lesions have been demonstrated to be associated with moderate to severe pathological changes including granuloma formation, diffuse inflammation and fibrosis (Leenaars *et al.*, 1995; Leenaars *et al.*, 1998). In these experiments there was also evidence of acute pain including bodyweight loss and piloerection during the first few days post injection. Therefore, the ulceration observed in our initial experiment consistent with previously reported experiments in the literature, although we did not observe any evidence of acute pain. We hypothesised that the high levels of inflammation observed in the skin of immunised mice with ulcerations could be directing the inflammatory response away from the brain and spinal cord and this could be responsible for the low EAE penetrance. However, previous data from EAE induced in rats suggests this is unlikely to be the cause of the low EAE penetrance, as they observed a correlation between skin ulceration and EAE severity (Levine & Wenk, 1961).

An alternative hypothesis is that the high susceptibility to skin ulceration and the low penetrance of EAE are both a result of the different gut flora present in the animal units at the University of Manchester and the University of Zurich. Indeed, it has been demonstrated that gut flora is able to influence inflammatory responses in the skin as the administration of *Lactobacilli*, a gram positive bacteria commonly used in human probiotics, can decrease the severity of contact hypersensitivity (Chapat *et al.*, 2004). Moreover, as discussed in chapter four of this thesis, the mice at the University of Manchester are maintained on CRASF® flora. This limited gut flora with reduced exposure to pathogens may result in an immune system that is hypersensitive to bacterial challenge. Therefore, following CFA exposure an enhanced immune response could be mounted driving the severe ulcerations apparent

in the immunised mice. Furthermore, there is clear evidence that the gut flora can significantly alter the penetrance of EAE as, treatment of mice with antibiotics has been demonstrated to alter the gut flora of mice and suppress the induction of EAE (Yokote *et al.*, 2008).

This hypothesis, indicating a role of gut flora, is supported by our data demonstrating that subsequent to the longer acclimatisation period, with dirty bedding from other mice normally housed at the University of Zurich, immunised mice have no evidence of ulceration and a good disease induction. However, as we did not analyse the caecal contents from these mice we are unable to determine if there had been any alterations in gut flora or if the increased penetrance was due to another change in experimental conditions.

6.4.4. Limitations of murine EAE as a model of MS

The use of murine models of EAE and the availability of genetically modified mice has provided a lot of insight into the mechanisms involved in the pathogenesis of EAE but, nevertheless, these models also have their shortcomings (for overview see review by (Gold *et al.*, 2006)).

In contrast to the primary demyelination seen in MS most murine models of EAE have lesions characterised by massive tissue injury with both axonal and neuronal damage. Moreover, in EAE models the tissue damage is accomplished primarily by T cells and activated macrophages and, in contrast to MS, the role of demyelinating auto-antibodies is less important (see review by (Gold *et al.*, 2006)). Furthermore, the CD4+ T cell dominance seen in EAE is not reflected in MS where is there an predominance of CD8+ T cells in lesions (see (Friese & Fugger, 2005) for review). Therefore, there is a need for more CD8+ T cell based models.

A clear feature in MS is the large heterogeneity in pathological features that vary between patients and disease stage. The only way to mimic this complexity in EAE models is through the use of a large spectrum of models in different species by different sensitisation techniques (see (Gold *et al.*, 2006) for a review of different

models and the appropriateness of each model in mimicking different MS pathologies). Nevertheless, with these limitations kept in mind EAE has, and continues to, provide an important insight into the mechanisms of damage during MS.

6.5 CONCLUSION

The results presented in this chapter demonstrate that:

1. Complete deletion of IFNγR2 results in an atypical EAE phenotype
2. Atypical EAE appears to be accompanied by an inflammation predominately located in the cerebellum whereas in classical EAE inflammation predominates in the spinal cord
3. Penetrance of EAE and frequency of ulceration following Freund's adjuvant use may be altered by conditions in animal facilities
4. IFNγR2 deficiency decreases microglial activation in the brain

CHAPTER SEVEN

General Conclusions

7.1 SUMMARY

In this thesis, the generation and characterisation of a complete IFNγR2 deficient mouse, as well as a conditional macrophage/granulocyte- and T cell-specific mouse mutant has been described. The initial generation of mice with a conditional IFNγR2 allele was performed by A. Fleige (Fleige, 2006) at the Helmholtz Institute for Infection Research, Braunschweig. Subsequent deletion of the neomycin resistance cassette and breeding homozygous floxed and delta alleles was described at the start of this thesis. Characterisation of IFNγR2$^{fl/fl}$ and IFNγR2$^{\Delta/\Delta}$ mice demonstrated the IFNγR2$^{fl/fl}$ mice have a functional IFNγR2 whereas the IFNγR2$^{\Delta/\Delta}$ mice have no functional IFNγR2, as expected. Subsequent *in vitro* characterisation of the complete IFNγR2 mouse mutant demonstrates decreased STAT1 phosphorylation, following IFNα stimulation, compared to control mice and a skewing of the macrophage phenotype towards alternative activation. IFNγR2$^{fl/fl}$CD4Cre^{+} and IFNγR2$^{fl/fl}$LysMCre^{+} mice have been successfully generated and the deletion of IFNγR2 confirmed to occur in a cell-type specific manner.

The complete mutant mouse was tested in three models *in vivo* – DSS-induced colitis, *Trichuris muris* infection and EAE. Acute DSS-induced colitis is a model of the innate immune system as it can occur independently of cells of adaptive immunity (Dieleman *et al.*, 1994). Despite previous reports demonstrating IFNγ deficient mice are protected from DSS-colitis (Ito *et al.*, 2006; Xu *et al.*, 2008) our data demonstrates IFNγR2 deficient mice display an equal or more severe colitis than control mice. We hypothesise that this discrepancy is due to differences in the gut microbiota between the different experiments, and the limited CRASF® flora in our mice does not drive the IFNγ response seen in the other experiments.

Trichuris muris is a well-established model of intestinal nematode infection, where expulsion of the parasite is dependent on the generation of a Th2 response. The complete IFNγR2 mutant was resistant to *T. muris* with all infected mice capable of expelling a low dose infection before the worms reached fecundity. In contrast, the control mice all harboured fecund worms in the intestine at day 35 post infection.

Infection of IFNγR2$^{fl/fl}$ mice drove a strong IgG1 and IgG2$_{a/c}$ response, however IFNγR2 deficient mice were unable to produce IgG2$_{a/c}$ antibodies. This is in keeping with previous reports describing IFNγ as a IgG2a switch factor (Finkelman *et al.*, 1988). Nevertheless, the mutant mice were capable of mounting a Th1 response evident through IFNγ production following lymph node re-stimulation. This needs to be further investigated to determine if there is a decreased polarisation of naïve T cells to a Th1 phenotype as observed in other IFNγ mutant mice (Lu *et al.*, 1998).

To further investigate the mechanism of action behind the resistant phenotype observed in complete IFNγR2 deficient mice, conditional mutant mice were infected with *T. muris*. Contrary to our hypotheses neither the T cell-specific mutant nor the macrophage/granulocyte-specific mutant duplicated the resistant phenotype observed in the complete knock-out mice, with both conditional knock-out mutants remaining susceptible to the parasitic infection. Analysis of double conditional, T cell- and macrophage/granulocyte- specific, IFNγR2 mutant mice produced inconsistent results with initial experiments suggesting that, in combination, these deficiencies are sufficient to duplicate the resistant phenotype observed in the complete mutant mice. However, subsequent experiments with the double conditional knockout mice found that they were susceptible to infection with fecund adults present at day 35 post infection. Therefore, whilst abrogation of IFNγ signalling in T cells and macrophages in combination can, under some circumstances, mimic the phenotype of the complete IFNγR2 deficient mice the lack of robustness suggests there must be other important IFNγ responsive cells. Further work will be performed to investigate the other potential candidates through crosses to new Cre lines including the hemapoietic cell specific Vav-Cre (Georgiades *et al.*, 2002), dendritic cell specific CD11c-Cre (Caton *et al.*, 2007), B cell specific CD19-Cre (Rickert *et al.*, 1997) and the intestinal epithelial cell specific Villin-Cre (el Marjou *et al.*, 2004).

The third *in vivo* model that we used to analyse IFNγR2 mutant mice was EAE. The mechanism of action and the involvement of IFNγ in EAE has, for a long time, been a matter of uncertainty. EAE was initially described as a Th1 driven disease and, as with many other putative Th1-diseases, upon the discovery of the Th17 subset was

reinvestigated and determined to be a Th17 driven disease. The current dogma is that the pathogenic cells in EAE can not be solely attributed to Th1 or Th17 cells but both subsets may play a role (for a review of the changing dogma see (Goverman, 2009)). Nevertheless, the role of IFNγ still remains uncertain with IFNγ deficient mice displaying more severe EAE (Willenborg *et al.*, 1996), suggesting a protective role of IFNγ; but other experiments demonstrating IFNγ expression in the CNS causes inflammation and tissue injury (Nikcevich *et al.*, 1997). The conditional IFNγR2 mouse mutant is an elegant method of dissecting the role of IFNγ signalling during EAE in different cell types. As this work was performed at the University of Zurich, through the collaboration with Prof. Burkhard Becher, I was only able to perform two experimental runs and members of his group will now continue this work.

Initial EAE induction was unsuccessful with very low disease penetrance and high levels of ulceration at the site of immunisation. It was hypothesised this could be due to differences in gut microbiota present at the University of Manchester and University of Zürch animal facilities. In an attempt to circumvent this discrepancy, prior to the initiation of the subsequent experiment, mice were left to acclimatise for a longer period and were exposed to the used bedding of mice normally housed at the University of Zürich animal facility. This subsequent experiment had successful EAE induction with good penetrance, although this cannot be conclusively attributed to an alteration in gut flora as no caecal analysis was performed. The complete IFNγR2 mutant mice demonstrated an atypical phenotype, with no signs of recovery. In contrast, the IFNγR2$^{fl/fl}$ control mice displayed classical EAE symptoms with almost complete recovery prior to the termination of the experiment. The severity of the atypical EAE symptoms correlated with the severity of inflammation in the cerebellum whereas the severity of the classical EAE symptoms correlated with the severity of the spinal cord inflammation. These results are consistent with the literature, and therefore further experiments analysing the existing conditional mutant mice, as well as new crosses to various brain-specific Cre lines will hopefully allow the elucidation of the actions of IFNγ to finally be achieved.

7.2 AREAS OF FURTHER INVESTIGATION

The work presented in this thesis demonstrates the successful targeting of the IFNγR2 allele, initiated by A. Fleige, and the generation of conditionally targeted T cell and macrophage/granulocyte mutant mice. The work has began to clearly dissect the mechanisms through which IFNγ acts but there are still unanswered questions that were beyond the scope of this thesis including the potential interaction of IFNγR2 and IFNγ signalling components with other signalling pathways, the importance of the *T. muris* derived IFNγ-homologue and it's mechanism of action and the role of IFNγ signalling in other models of parasitic infection. Our data has also demonstrated the importance of gut flora in multiple models of disease and this future work and the current literature surrounding these areas will be discussed in the remainder of this discussion.

7.2.1 The successful generation of a conditional IFNγR2 allele and further work using the complete IFNγR2 mutant mice

The first complete IFNγR deficient mouse was generated by Aguet and colleagues in 1993 and targeted IFNγR1 (Huang *et al.*, 1993) with the generation of a complete IFNγR2 deficient mouse subsequently performed by Rothman and colleagues (Lu *et al.*, 1998). The phenotypes observed in these mice include no overt abnormalities, normal development, impaired STAT1 phosphorylation to IFNγ stimulation and deficiencies in IgG2a class switching and were all duplicated in the IFNγR2$^{\Delta/\Delta}$ mice generated as part of this thesis. Furthermore, these deficiencies, observed in the IFNγR2$^{\Delta/\Delta}$ mice, were not seen in the IFNγR2$^{fl/fl}$ mice. Therefore, we conclude that the conditional allele has been successfully targeted and the complete mutant behaves as expected. Further analysis of the IFNγ complete mutant mouse resulted in the several key observations including an interaction with the IFNα signalling pathway, the importance of which is still not fully understood.

7.2.1.1. The importance of determining interactions in signalling pathways when using mutant mice.

The IFNγ signalling pathway has been widely investigated and initial research focused on the Jak-STAT pathway as the mediator of signal transduction, but recently it has become apparent that other pathways can act in parallel to the Jak-STAT pathway to regulate the effects of IFNγ signalling (for review of the different pathways and how the interact see (Gough *et al.*, 2008)). Despite this wealth of literature, on the multiple signalling pathways downstream of the IFNγ receptor, far less is known about the ability of IFNγ receptors to interact with other receptors. Takaoka and colleagues have demonstrated that the IFNγ and IFNα receptor chains cluster together in lipid rafts and there is cross talk between these pathways (Takaoka *et al.*, 2000). The results presented in this thesis support this observation, with a decreased response to IFNα signalling in cells lacking IFNγR2. The proposed mechanism of action for this crosstalk is that IFNαR1 facilitates the assembly of IFNγ-activated transcription factors, through an interaction between the two non ligand-binding components: IFNαR1 and IFNγR2 (Takaoka *et al.*, 2000). It is not known if a similar interaction between non-ligand binding chains also occurs with other members of the class II cytokine receptor family or other cytokine receptors. The class II cytokine receptor family contains the IFN type I (IFNαR1/2), IFN type II (IFNγR1/2) and IFN type III (the IFNλR1) receptors as well as the receptors for the IL-10 family and Factor VII/VIIa (Langer *et al.*, 2004). Further investigations will aim to investigate potential interactions between these signalling cascades. It will also be of interest to determine the functional impact of any associations under physiological conditions.

The cross-talk seen in the IFN pathways may also be important in other cytokine receptor families. It will be important to determine in other mice with cytokine receptor deficiencies if there is a deficiency in the expression or signalling of other receptors, due to an altered interaction of proteins at the membrane or other cellular locations.

7.2.1.2. Importance and mechanism of action of the negative regulator SOCS1 in IFNγ signalling

Negative regulators play an important role in the control of signalling cascades and are known to be capable of suppressing multiple signalling pathways. An important group of negative regulators are the Suppressor of cytokine signalling (SOCS) proteins: a family of 8 intracellular proteins which can be induced by cytokine signalling and act to regulate the magnitude and duration of responses through a classical negative feedback loop. As well as this feedback loop SOCS proteins are also capable of participating in 'cross-talk' and regulate the signalling downstream of other cytokines (for an overview of SOCS regulation of the Jak-STAT pathway see (Croker *et al.*, 2008)).

SOCS1 is the key SOCS molecule important in the IFNγ signalling pathway and acts through two key mechanisms (i) binding to the phosphorylation loop of Jak 2 to prevent the access of substrates to the catalytic pocket (Yasukawa *et al.*, 1999) and (ii) binding to tyrosine 441 on IFNγR1 blocking the access of STAT1 to the IFNγR1 chain (Qing *et al.*, 2005; Starr *et al.*, 2009). The importance of this negative feedback loop is highlighted through the analysis of SOCS-1 deficient mice, these mice die between 2 and 3 weeks of age due to a complex multi-organ disease that can be prevented by the administration of anti-IFNγ antibodies (Alexander *et al.*, 1999). Preliminary data in this thesis suggests that in unchallenged mice the level of SOCS1 present in the intestine of IFNγR2$^{\Delta/\Delta}$ mice is approximately seven fold the level in IFNγR2$^{fl/fl}$ mice. It will be interesting to determine if this effect is seen in all organs or if it is specific to the colon and if the data demonstrating changes in SOCS1 message are replicated when the protein levels are analysed. Moreover, the reason for this increase in SOCS1 message is unknown as, although IL-6 and GM-CSF are also capable of inducing SOCS1 proteins IL-6 does not appear to be up-regulated in the serum of IFNγR2$^{\Delta/\Delta}$ mice. Although we did not measure GM-CSF levels, previous reports have shown GM-CSF elevated in IFNγ deficient mice following infection but this not evident early in infection which suggests there is no elevation of GM-CSF in unchallenged mice (Allendoerfer & Deepe, 1997). As well as pro-inflammatory cytokines STAT proteins, primarily STAT1, can also induce SOCS1

expression, however, we see no evidence of STAT1 phosphorylation from un-stimulated cells of either IFNγR2$^{\Delta/\Delta}$ or IFNγR2$^{fl/fl}$ mice. Therefore, the mechanism for this elevation in SOCS1 needs to be further investigated and it will also be interesting to determine if there is an increase in other negative regulators of IFNγ signalling.

As SOCS proteins can act not only as negative regulators but can also participate in cross talk it will be important to determine if there are any implications of the high SOCS1 levels to other signalling pathways e.g. SOCS1 can also impact on the NFκB pathway by facilitating the degradation of p65 (Ryo *et al.*, 2003), and alter the JNK and p38 pathways through the degradation of ASK1 (He *et al.*, 2006).

SOCS1 also has an important role in colitis and can function as an anti-oncogene with SOCS1 methylation observed in colorectal cancer (Lin *et al.*, 2004). This observation has been duplicated in mice as both SOCS1/TCRα double deficient mice and SOCS1 deficient TG mice, where SOCS1 expression has been restored on T and B cells, develop colitis and colorectal cancer in an IFNγ dependant manner (Chinen *et al.*, 2006; Hanada *et al.*, 2006). Crossing the IFNγR2 mouse mutant with SOCS1 deficient mice will allow the key IFNγ responding cells that are important for the effects of SOCS1 deficiency to be determined, which may provide further insight into the anti-oncogenic functions of SOCS1.

7.2.2 The successful generation of a conditional IFNγR2 mutant mice and further work using the existing lines

We have demonstrated the successful generation of T cell- specific, granulocyte/macrophage- specific and a double T cell-, granulocyte/macrophage-specific conditional IFNγR2 deficient mouse mutants. Currently we have only tested the conditional mutant mice in *T. muris* infection, however there are multiple other models of infection, which these mice could provide further insight into. These include other models of parasitic infection e.g. *Toxoplasma gondii* to determine if IFNγ acts through a similar mechanism during other parasite infections.

7.2.2.1 The role of IFNγ during parasitic infection

Work presented within this thesis demonstrates that responsiveness to IFNγ is vital for the survival of the parasite, and complete deletion of IFNγR2 results in resistance to infection. Moreover, we have determined that is achieved, in part, through the actions of IFNγ on both T cells and macrophages/granulocytes. Further work on these conditional mouse mutants needs to be performed to better understand the magnitude and kinetics of the different T helper subset responses during infection. Although we have demonstrated no clear change in the Th1 or Th17 response at day 35 post infection, it will be interesting to look at earlier time points to determine in there is a skewing during the peak of the immune response away from Th1 phenotype and towards a Th17 or Th2 phenotype.

Another avenue of interest is the *T. muris* derived IFNγ homologue. This homologue has been demonstrated to share cross reactive epitopes to IFNγ and is capable of binding to the IFNγ receptor and inducing similar changes to those seen following IFNγ stimulation (Grencis & Entwistle, 1997). It has been proposed that the production of this IFNγ homologue by the parasite might be a mechanism through which the parasite is able to interfere with the host response and increase its own survival potential. Previous experiments have demonstrated the ability of the IFNγ homologue to bind to the IFNγR1 chain and upregulate Ly-6G (Grencis & Entwistle, 1997). It isn't known if this homologue signals through the same method as IFNγ with the need of the IFNγR2 chain, therefore future work will investigate the capacity of this IFNγ homologue to induce changes in IFNγR2$^{\Delta/\Delta}$ mice. It will also be interesting to determine if, in naïve and IFNγR2 deficient cells, this parasite derived molecule is capable of driving other IFNγ actions including skewing the macrophage phenotype towards a classically activated state and driving naïve T cells to preferentially differentiate into Th1 cells.

7.2.2.2. The role of IFNγ during *Toxoplasma gondii* infection

It will be interesting to examine the role of other IFNγ in other parasitic infections and future work will look at *Toxoplasma gondii (T. gondii)* infection. *T. gondii* is an

intracellular protozoan parasite which has proposed to be the 'most successful parasite' as it is found worldwide and is capable of infecting all warm-bloodied animals including humans (for an overview see (Innes, 2010)). *T. gondii* has a complex life cycle involving different developmental stages: the rapidly replicating tachyzoite, the slower growing bradyzoites and sporozoites within oocysts. The oocyst stage only occurs in the intestine of its definitive host – the feline and the oocysts are shed in the cat's feaces where they can sporulate and become infectious. Infection can also occur through the ingestion of bradyzoite tissue cysts. Infection is characterised by an acute phase when the rapidly dividing tachyzoite form of the parasite disseminates throughout the body. If the immune system is unable to control this stage of the infection extensive tissue damage can be done by the parasite. The later parasite stage, in contrast, is largely asymptomatic with the dormant bradyzoite form of the parasite residing in cysts in the host tissue particularly in the brain (for overview of the lifecycle see (Dubey, 1998)).

The importance of IFNγ during *T. gondii* infection is already well established as mice treated with anti-IFNγ antibodies and IFNγ deficient mice rapidly succumb even to avirulent strains of the parasite (Scharton-Kersten *et al.*, 1996; Suzuki *et al.*, 1988). As well as an important role in the acute phase of disease IFNγ has also been demonstrated to be important during the chronic phase of the disease and are involved in the maintenance of intact cysts and the prevention of toxoplasmic encephalitis (Suzuki *et al.*, 1989). Recent experiments using MIIG ("macrophages insensitive to IFNγ") mice have demonstrated that macrophages are one of the key responding cells during acute IFNγ infection as MIIG mice succumb to infection in a similar manner to IFNγ deficient mice. However, bone marrow chimera studies have demonstrated that IFNγ-responsive non-haemopoietic cells are also vital for protection again *T. gondii* mortality as reconstitution of IFNγR1 deficient mice with wild-type bone marrow is not sufficient to confer protection (Yap & Sher, 1999). The somatic cell(s) responsible for this phenotype are unknown but the conditional IFNγR2 mice present a good system for dissecting the importance of different somatic cells.

It will also be interesting to determine the key responding cells in chronic *T. gondii* infection given the importance of IFNγ in preventing *Toxoplasma* encephalitis (Suzuki *et al.*, 1989). Several brain resident cells have been demonstrated to respond to IFNγ to regulate toxoplasmosis, including astrocytes through the induction IGTP (Halonen *et al.*, 2001) and microglia through an action involving TNF (Chao *et al.*, 1993). Similarly to results from acute infections bone marrow chimera studies have demonstrated that IFNγR expression on non-haemopoietic as well as bone marrow-derived cells is essential for host survival in the chronic phase (Yap & Sher, 1999). One potential bone marrow derived candidate for driving host survival in both the chronic and the acute phases is the T cell. It has been demonstrated that IFNγ plays an important role in the apoptosis of activated T cells during infection and that the level of apoptosis in the acute stages of infection in mice correlates with a hosts genetic susceptibility to *T. gondii* infection (Begum-Haque *et al.*, 2009; Gavrilescu & Denkers, 2001). Indeed, some preliminary results, from our laboratory, suggests that IFNγR2$^{fl/fl}$CD4Cre^{+} display an increased sensitivity to the prugniaud strain of *T. gondii* compared to IFNγR2$^{fl/fl}$CD4Cre^{-} animals. This needs to be further investigated but, if confirmed, demonstrates that importance of both T cells and macrophages in controlling acute infection and that, unlike in *T. muris* infection, these cells have non-redundant roles.

T. gondii provides a well characterised, pathologically important model of parasitic infection in which IFNγ is known to play an important role. Recent work by Lykens and colleagues have demonstrated the importance of IFNγ responsive macrophages in controlling mortality in the acute stages of disease. However, little is known about the role of other cell types, especially somatic cells, which have been shown to be important through bone marrow chimera studies. Therefore, the conditional IFNγR2 mouse mutant provides a valuable tool to dissect the role of different cells during infection.

7.2.2.3. The importance of IL-10 in IFNγR2 deficient mice

As well as the generation of further IFNγR2 conditional mutant mice it will be interesting to cross these conditional mice onto an IL-10 deficient background. This

strategy has previously been used with the gp130 conditional mutant mice and has revealed important information on the role of gp130 signalling in regulating inflammatory processes (Fasnacht *et al.*, 2009). IL-10 is a cytokine with anti-inflammatory properties that arise primarily through it's ability to inhibit macrophage and dendritic cell function (for IL-10 overview see review by (Moore *et al.*, 2001)). IL-10 deficient mice have been well characterised and develop spontaneous colitis when house in conventional animal facilities (Kuhn *et al.*, 1993). If these mice are associated with a Charles River Altered Schaedler Flora, as found in our animal facility, IL-10 deficient mice remain free from colitis (Stehr *et al.*, 2009). Colitis can be induced in these mice through treatment with DSS and the IL-10 deficient mice develop a more severe colitis than wildtype control mice (Pils *et al.*, 2010a). Under these circumstances IL-10 deficient mice, but not wildtype mice, show an elevation in levels of serum IFNγ and the IFNγ-induced protein IP-10 (Pils *et al.*, 2010a). The generation of IFNγR2 conditional mutant mice on an IL-10 deficient background will allow the analysis of IFNγ during induced acute intestinal inflammation by removing the IL-10 that normally serves to counterbalance the inflammatory signals given from the gut flora. Furthermore, it has previously been shown that IFNγ is a key mediator of the spontaneous colitis observed conventionally housed IL-10 deficient mice, as treatment with anti-IFNγ monoclonal antibodies can prevent colitis development (Rennick *et al.*, 1997). It will be interesting to determine if IFNγ is also responsible for the increased colitis evident in the IL-10 deficient DSS-treated mice and, if so, which are the key responding cell types.

7.2.3 The importance of gut microflora in experimental design

The intestinal microflora plays an important role in host physiology and has been demonstrated to play important metabolic, trophic and protective functions (for review see (Guarner & Malagelada, 2003)). The major metabolic role of gut microflora is the fermentation of non-digestible dietary substances. However, as well as this metabolic role gut microflora has also been demonstrated, primarily through the use of germ-free mice, to be important in a wide range of other processes. Indeed, germ free mice have been documented to suffer from a wide range of abnormalities

including altered bile acid and bilirubin metabolism; low heart, lung and liver weights; low cardiac output; enlarged caecum and thin intestinal wall; decreased rate of enterocyte replacement and slow peristalsis; lowered body temperature and small lymph nodes compared to mice housed in a conventional environment (for overview see (Tannock, 2001)).

The data contained within this thesis has highlighted the importance of gut microflora in multiple mouse models, not just those confined to the analysis of intestinal inflammation. With increasing collaborations and importation of mice from other institutes it is vital that the role of gut flora in susceptibility to different disease models is not ignored. We now know that genetic background (Esworthy *et al.*, 2010) and genetic mutations e.g. peptidoglycan recognition protein deficiencies (Saha *et al.*, 2010) as well as differences between animal facilities can alter the gut microflora. These differences in gut microflora can in turn alter the phenotype of mice in various different diseases including models that do not focus on intestinal inflammation like EAE (Ochoa-Reparaz *et al.*, 2009; Yokote *et al.*, 2008). This all demonstrates the importance of gut flora and the need for this influence to be properly recognised, and taken into account, when designing and analysing experiments.

7.3 CONCLUSION

In conclusion, the work in this thesis has demonstrated the successful generation and characterisation of an IFNγR2 mouse mutant, work that was initiated by Anna Fleige during her PhD (Fleige, 2006). This mouse mutant has allowed the important IFNγ-responsive cells during *T. muris* infection to be dissected and has demonstrated that both T cells and macrophages/granulocytes are importance in mediating susceptibility to this parasite. Nevertheless, there are other important cell types also involved and the generation of further conditional mutant mice will allow further understanding of the mechanism of action of IFNγ. This thesis has also highlighted the importance of gut microflora in different experimental models with the poor EAE penetrance seen in the initial study and the lack of protection in DSS thought to be attributable to differences in gut flora. Finally the complete IFNγ deficient mouse

displays an atypical EAE phenotype and further work analysing different conditional mutant mice with our collaborators at the University of Zurich will allow a clearer understanding of the, currently controversial, role of IFNγ in EAE and MS. This mouse mutant is an extremely powerful tool that will allow a deeper understanding of the role of the pleiotropic cytokine IFNγ in many different models.

CHAPTER EIGHT

References

ABREMSKI, K. & HOESS, R. (1984). Bacteriophage P1 site-specific recombination. Purification and properties of the Cre recombinase protein. *J Biol Chem*, **259,** 1509-14.

ABREMSKI, K., HOESS, R. & STERNBERG, N. (1983). Studies on the properties of P1 site-specific recombination: evidence for topologically unlinked products following recombination. *Cell*, **32,** 1301-11.

ADAMS, R.B., PLANCHON, S.M. & ROCHE, J.K. (1993). IFN-gamma modulation of epithelial barrier function. Time course, reversibility, and site of cytokine binding. *J Immunol*, **150,** 2356-2363.

AHERN, P.P., SCHIERING, C., BUONOCORE, S., MCGEACHY, M.J., CUA, D.J., MALOY, K.J. & POWRIE, F. (2010). Interleukin-23 drives intestinal inflammation through direct activity on T cells. *Immunity*, **33,** 279-88.

ALEXANDER, W.S., STARR, R., FENNER, J.E., SCOTT, C.L., HANDMAN, E., SPRIGG, N.S., CORBIN, J.E., CORNISH, A.L., DARWICHE, R., OWCZAREK, C.M., KAY, T.W., NICOLA, N.A., HERTZOG, P.J., METCALF, D. & HILTON, D.J. (1999). SOCS1 is a critical inhibitor of interferon gamma signaling and prevents the potentially fatal neonatal actions of this cytokine. *Cell*, **98,** 597-608.

ALLENDOERFER, R. & DEEPE, G.S., JR. (1997). Intrapulmonary response to Histoplasma capsulatum in gamma interferon knockout mice. *Infect Immun*, **65,** 2564-9.

ANDERSON, C.F., OUKKA, M., KUCHROO, V.J. & SACKS, D. (2007). CD4(+)CD25(-)Foxp3(-) Th1 cells are the source of IL-10-mediated immune suppression in chronic cutaneous leishmaniasis. *J Exp Med*, **204,** 285-97.

ANNUNZIATO, F., COSMI, L., SANTARLASCI, V., MAGGI, L., LIOTTA, F., MAZZINGHI, B., PARENTE, E., FILI, L., FERRI, S., FROSALI, F., GIUDICI, F., ROMAGNANI, P., PARRONCHI, P., TONELLI, F., MAGGI, E. & ROMAGNANI, S. (2007). Phenotypic and functional features of human Th17 cells. *J Exp Med*, **204,** 1849-61.

ANTHONY, R.M., URBAN, J.F., JR., ALEM, F., HAMED, H.A., ROZO, C.T., BOUCHER, J.L., VAN ROOIJEN, N. & GAUSE, W.C. (2006). Memory T(H)2 cells induce alternatively activated macrophages to mediate protection against nematode parasites. *Nat Med*, **12,** 955-60.

ARIHIRO, S., OHTANI, H., SUZUKI, M., MURATA, M., EJIMA, C., OKI, M., KINOUCHI, Y., FUKUSHIMA, K., SASAKI, I., NAKAMURA, S., MATSUMOTO, T., TORII, A., TODA, G. & NAGURA, H. (2002). Differential expression of mucosal addressin cell adhesion molecule-1 (MAdCAM-1) in ulcerative colitis and Crohn's disease. *Pathol Int*, **52,** 367-74.

ARORA, S., HERNANDEZ, Y., ERB-DOWNWARD, J.R., MCDONALD, R.A., TOEWS, G.B. & HUFFNAGLE, G.B. (2005). Role of IFN-gamma in regulating T2 immunity and the development of alternatively activated macrophages during allergic bronchopulmonary mycosis. *J Immunol*, **174,** 6346-56.

ARTIS, D. & GRENCIS, R.K. (2008). The intestinal epithelium: sensors to effectors in nematode infection. *Mucosal Immunol*, **1,** 252-264.

ARTIS, D., POTTEN, C.S., ELSE, K.J., FINKELMAN, F.D. & GRENCIS, R.K. (1999). Trichuris muris: host intestinal epithelial cell hyperproliferation during chronic infection is regulated by interferon-gamma. *Exp Parasitol*, **92,** 144-53.

ARTIS, D., WANG, M.L., KEILBAUGH, S.A., HE, W., BRENES, M., SWAIN, G.P., KNIGHT, P.A., DONALDSON, D.D., LAZAR, M.A., MILLER, H.R., SCHAD, G.A., SCOTT, P. & WU, G.D. (2004). RELM β /FIZZ2 is a goblet cell-specific immune-effector molecule in the gastrointestinal tract. *Proc Natl Acad Sci U S A*, **101,** 13596-600.

AUSTIN, C.P., BATTEY, J.F., BRADLEY, A., BUCAN, M., CAPECCHI, M., COLLINS, F.S., DOVE, W.F., DUYK, G., DYMECKI, S., EPPIG, J.T., GRIEDER, F.B., HEINTZ, N., HICKS, G., INSEL, T.R., JOYNER, A., KOLLER, B.H., LLOYD, K.C., MAGNUSON, T., MOORE, M.W., NAGY, A., POLLOCK, J.D., ROSES, A.D., SANDS, A.T., SEED, B., SKARNES, W.C., SNODDY, J., SORIANO, P., STEWART, D.J., STEWART, F., STILLMAN, B., VARMUS, H., VARTICOVSKI, L., VERMA, I.M., VOGT, T.F., VON MELCHNER, H., WITKOWSKI, J., WOYCHIK, R.P., WURST, W., YANCOPOULOS, G.D., YOUNG, S.G. & ZAMBROWICZ, B. (2004). The knockout mouse project. *Nat Genet*, **36,** 921-4.

BAARS, J.E., LOOMAN, C.W., STEYERBERG, E.W., BEUKERS, R., TAN, A.C., WEUSTEN, B.L., KUIPERS, E.J. & VAN DER WOUDE, C.J. (2010). The Risk of Inflammatory Bowel Disease-Related Colorectal Carcinoma Is Limited: Results From a Nationwide Nested Case-Control Study. *Am J Gastroenterol*, **In press**.

BACH, E.A., AGUET, M. & SCHREIBER, R.D. (1997). THE IFN γ RECEPTOR:A Paradigm for Cytokine Receptor Signaling. *Annual Review of Immunology*, **15,** 563-591.

BANCROFT, A.J., ARTIS, D., DONALDSON, D.D., SYPEK, J.P. & GRENCIS, R.K. (2000). Gastrointestinal nematode expulsion in IL-4 knockout mice is IL-13 dependent. *Eur J Immunol*, **30,** 2083-91.

BANCROFT, A.J., ELSE, K.J., HUMPHREYS, N.E. & GRENCIS, R.K. (2001). The effect of challenge and trickle Trichuris muris infections on the polarisation of the immune response. *Int J Parasitol*, **31,** 1627-37.

BANCROFT, A.J., ELSE, K.J., SYPEK, J.P. & GRENCIS, R.K. (1997). Interleukin-12 promotes a chronic intestinal nematode infection. *Eur J Immunol*, **27,** 866-70.

BANCROFT, A.J., HUMPHREYS, N.E., WORTHINGTON, J.J., YOSHIDA, H. & GRENCIS, R.K. (2004). WSX-1: a key role in induction of chronic intestinal nematode infection. *J Immunol*, **172,** 7635-41.

BARTSCH, H., BARTSCH, C., MECKE, D. & LIPPERT, T.H. (1994). Seasonality of pineal melatonin production in the rat: possible synchronization by the geomagnetic field. *Chronobiol Int*, **11,** 21-6.

BAUER, J., SMINIA, T., WOUTERLOOD, F.G. & DIJKSTRA, C.D. (1994). Phagocytic activity of macrophages and microglial cells during the course of acute and chronic relapsing experimental autoimmune encephalomyelitis. *J Neurosci Res*, **38,** 365-75.

BAUMGART, D.C. & CARDING, S.R. (2007). Inflammatory bowel disease: cause and immunobiology. *Lancet*, **369,** 1627-40.

BAUMGART, D.C., OLIVIER, W.-A., REYA, T., PERITT, D., ROMBEAU, J.L. & CARDING, S.R. (1998). Mechanisms of Intestinal Epithelial Cell Injury and Colitis in Interleukin 2 (IL2)-Deficient Mice. *Cellular Immunology*, **187,** 52-66.

BECHER, B., DURELL, B.G. & NOELLE, R.J. (2002). Experimental autoimmune encephalitis and inflammation in the absence of interleukin-12. *J Clin Invest*, **110,** 493-7.

BEGUM-HAQUE, S., HAQUE, A. & KASPER, L.H. (2009). Apoptosis in Toxoplasma gondii activated T cells: the role of IFNgamma in enhanced alteration of Bcl-2 expression and mitochondrial membrane potential. *Microb Pathog*, **47,** 281-8.

BELLABY, T., ROBINSON, K., WAKELIN, D. & BEHNKE, J.M. (1995). Isolates of Trichuris muris vary in their ability to elicit protective immune responses to infection in mice. *Parasitology*, **111 (Pt 3),** 353-7.

BERG, D.J., DAVIDSON, N., KUHN, R., MULLER, W., MENON, S., HOLLAND, G., THOMPSON-SNIPES, L., LEACH, M.W. & RENNICK, D. (1996). Enterocolitis and Colon Cancer in Interleukin-10-deficient Mice Are Associated with Aberrant Cytokine Production and $CD4^+$ TH1-like Responses. *J. Clin. Invest.*, **98,** 1010-1020.

BERNABEI, P., COCCIA, E.M., RIGAMONTI, L., BOSTICARDO, M., FORNI, G., PESTKA, S., KRAUSE, C.D., BATTISTINI, A. & NOVELLI, F. (2001). Interferon-gamma receptor 2 expression as the deciding factor in human T, B, and myeloid cell proliferation or death. *J Leukoc Biol*, **70,** 950-60.

BETTS, C.J. & ELSE, K.J. (1999). Mast cells, eosinophils and antibody-mediated cellular cytotoxicity are not critical in resistance to Trichuris muris. *Parasite Immunol*, **21,** 45-52.

BETZ, U.A., BLOCH, W., VAN DEN BROEK, M., YOSHIDA, K., TAGA, T., KISHIMOTO, T., ADDICKS, K., RAJEWSKY, K. & MULLER, W. (1998). Postnatally induced inactivation of gp130 in mice results in neurological, cardiac, hematopoietic, immunological, hepatic, and pulmonary defects. *J Exp Med*, **188,** 1955-65.

BHATTI, M., CHAPMAN, P., PETERS, M., HASKARD, D. & HODGSON, H.J. (1998). Visualising E-selectin in the detection and evaluation of inflammatory bowel disease. *Gut*, **43,** 40-7.

BILLIAU, A., HEREMANS, H., VANDEKERCKHOVE, F., DIJKMANS, R., SOBIS, H., MEULEPAS, E. & CARTON, H. (1988). Enhancement of experimental allergic encephalomyelitis in mice by antibodies against IFN-gamma. *J Immunol*, **140,** 1506-10.

BINDER, V. (1998). Genetic epidemiology in inflammatory bowel disease. *Dig Dis*, **16,** 351-5.

BJARTMAR, C. & TRAPP, B.D. (2003). Axonal degeneration and progressive neurologic disability in multiple sclerosis. *Neurotox Res*, **5,** 157-64.

BLACKWELL, N.M. & ELSE, K.J. (2002). A comparison of local and peripheral parasite-specific antibody production in different strains of mice infected with Trichuris muris. *Parasite Immunol*, **24,** 203-11.

BLACKWELL, N.M. & ELSE, K.J. (2001). B cells and antibodies are required for resistance to the parasitic gastrointestinal nematode Trichuris muris. *Infect Immun*, **69,** 3860-8.

BLEICH, A., MAHLER, M., MOST, C., LEITER, E.H., LIEBLER-TENORIO, E., ELSON, C.O., HEDRICH, H.J., SCHLEGELBERGER, B. & SUNDBERG, J.P. (2004). Refined histopathologic scoring system improves power to detect colitis QTL in mice. *Mamm Genome*, **15,** 865-71.

BOHR, U.R., SELGRAD, M., OCHMANN, C., BACKERT, S., KONIG, W., FENSKE, A., WEX, T. & MALFERTHEINER, P. (2006). Prevalence and spread of enterohepatic Helicobacter species in mice reared in a specific-pathogen-free animal facility. *J Clin Microbiol*, **44,** 738-42.

BONILLA, F.A. & OETTGEN, H.C. (2010). Adaptive immunity. *J Allergy Clin Immunol*, **125,** S33-40.

BOUMA, G. & STROBER, W. (2003). The immunological and genetic basis of inflammatory bowel disease. *Nat Rev Immunol*, **3,** 521-33.

BRADLEY, A., EVANS, M., KAUFMAN, M.H. & ROBERTSON, E. (1984). Formation of germ-line chimaeras from embryo-derived teratocarcinoma cell lines. *Nature*, **309,** 255-6.

BRANDA, C.S. & DYMECKI, S.M. (2004). Talking about a revolution: The impact of site-specific recombinases on genetic analyses in mice. *Dev Cell*, **6,** 7-28.

BRINSTER, R.L. & PALMITER, R.D. (1984). Transgenic mice containing growth hormone fusion genes. *Philos Trans R Soc Lond B Biol Sci*, **307,** 309-12.

BRODERSON, J.R. (1989). A retrospective review of lesions associated with the use of Freund's adjuvant. *Lab Anim Sci*, **39,** 400-5.

BUISINE, M.P., DESREUMAUX, P., LETEURTRE, E., COPIN, M.C., COLOMBEL, J.F., PORCHET, N. & AUBERT, J.P. (2001). Mucin gene expression in intestinal epithelial cells in Crohn's disease. *Gut*, **49,** 544-51.

BUNDSCHUH, D.S., BARSIG, J., HARTUNG, T., RANDOW, F., DOCKE, W.D., VOLK, H.D. & WENDEL, A. (1997). Granulocyte-macrophage colony-stimulating factor and IFN-gamma restore the systemic TNF-alpha response to endotoxin in lipopolysaccharide-desensitized mice. *J Immunol*, **158,** 2862-71.

BUTCHER, J. (2007). Gastroenterology neglected in the UK. *Lancet*, **369,** 1591.

CALLENDER, J.E., GRANTHAM-MCGREGOR, S., WALKER, S. & COOPER, E.S. (1992). Trichuris infection and mental development in children. *Lancet*, **339,** 181.

CAMOGLIO, L., TE VELDE ANJE A., DE BOER, A., TEN KATE, F.J., KOPF, M. & VAN DEVENTER, S.J. (2000). Hapten-induced colitis associated with maintained Th1 and inflammatory responses in IFN-γ receptor-deficient mice. *European Journal of Immunology*, **30,** 1486-1495.

CARIO, E. (2007). Therapeutic impact of toll-like receptors on inflammatory bowel diseases: A multiple-edged sword. *Inflamm Bowel Dis*, **14,** 411-21.

CARIO, E. & PODOLSKY, D.K. (2000). Differential alteration in intestinal epithelial cell expression of toll-like receptor 3 (TLR3) and TLR4 in inflammatory bowel disease. *Infect Immun*, **68,** 7010-7.

CARTER, S.L., MULLER, M., MANDERS, P.M. & CAMPBELL, I.L. (2007). Induction of the genes for Cxcl9 and Cxcl10 is dependent on IFN-gamma but shows differential cellular expression in experimental autoimmune encephalomyelitis and by astrocytes and microglia in vitro. *Glia*, **55,** 1728-39.

CASTROP, H. (2010). Genetically modified mice-successes and failures of a widely used technology. *Pflugers Arch*, **459,** 557-67.

CASTROP, H., OPPERMANN, M., WEISS, Y., HUANG, Y., MIZEL, D., LU, H., GERMAIN, S., SCHWEDA, F., THEILIG, F., BACHMANN, S., BRIGGS, J., KURTZ, A. & SCHNERMANN, J. (2006). Reporter gene recombination in juxtaglomerular granular and collecting duct cells by human renin promoter-Cre recombinase transgene. *Physiol Genomics*, **25,** 277-85.

CATON, M.L., SMITH-RASKA, M.R. & REIZIS, B. (2007). Notch-RBP-J signaling controls the homeostasis of CD8- dendritic cells in the spleen. *J Exp Med*, **204,** 1653-64.

CHAO, C.C., HU, S., GEKKER, G., NOVICK, W.J., JR., REMINGTON, J.S. & PETERSON, P.K. (1993). Effects of cytokines on multiplication of Toxoplasma gondii in microglial cells. *J Immunol*, **150,** 3404-10.

CHAPAT, L., CHEMIN, K., DUBOIS, B., BOURDET-SICARD, R. & KAISERLIAN, D. (2004). Lactobacillus casei reduces CD8+ T cell-mediated skin inflammation. *Eur J Immunol*, **34,** 2520-8.

CHEAH, S.S. & BEHRINGER, R.R. (2000). Gene-targeting strategies. *Methods Mol Biol*, **136,** 455-63.

CHEN, L., ADAR, R., YANG, X., MONSONEGO, E.O., LI, C., HAUSCHKA, P.V., YAYON, A. & DENG, C.X. (1999). Gly369Cys mutation in mouse FGFR3 causes achondroplasia by affecting both chondrogenesis and osteogenesis. *J Clin Invest*, **104,** 1517-25.

CHINEN, T., KOBAYASHI, T., OGATA, H., TAKAESU, G., TAKAKI, H., HASHIMOTO, M., YAGITA, H., NAWATA, H. & YOSHIMURA, A. (2006). Suppressor of cytokine signaling-1 regulates inflammatory bowel disease in which both IFNgamma and IL-4 are involved. *Gastroenterology*, **130,** 373-88.

CHO, J.H. (2008). The genetics and immunopathogenesis of inflammatory bowel disease. *Nat Rev Immunol*, **8,** 458-466.

CHU, C.Q., WITTMER, S. & DALTON, D.K. (2000). Failure to suppress the expansion of the activated CD4 T cell population in interferon gamma-deficient mice leads to exacerbation of experimental autoimmune encephalomyelitis. *J Exp Med*, **192,** 123-8.

CLAUSEN, B.E., BURKHARDT, C., REITH, W., RENKAWITZ, R. & FORSTER, I. (1999). Conditional gene targeting in macrophages and granulocytes using LysMcre mice. *Transgenic Res*, **8,** 265-77.

CLIFFE, L.J., HUMPHREYS, N.E., LANE, T.E., POTTEN, C.S., BOOTH, C. & GRENCIS, R.K. (2005). Accelerated intestinal epithelial cell turnover: a new mechanism of parasite expulsion. *Science*, **308,** 1463-5.

CONSORTIUM, W.T.C.C. (2007). Genome-wide association study of 14,000 cases of seven common diseases and 3,000 shared controls. *Nature*, **447,** 661-678.

CORNISH, A.L., DAVEY, G.M., METCALF, D., PURTON, J.F., CORBIN, J.E., GREENHALGH, C.J., DARWICHE, R., WU, L., NICOLA, N.A., GODFREY, D.I., HEATH, W.R., HILTON, D.J., ALEXANDER, W.S. & STARR, R. (2003). Suppressor of cytokine signaling-1 has IFN-gamma-independent actions in T cell homeostasis. *J Immunol*, **170,** 878-86.

COSTELLOE, E.O., STACEY, K.J., ANTALIS, T.M. & HUME, D.A. (1999). Regulation of the plasminogen activator inhibitor-2 (PAI-2) gene in murine macrophages. Demonstration of a novel pattern of responsiveness to bacterial endotoxin. *J Leukoc Biol*, **66,** 172-82.

CROKER, B.A., KIU, H. & NICHOLSON, S.E. (2008). SOCS regulation of the JAK/STAT signalling pathway. *Semin Cell Dev Biol*, **19,** 414-22.

CROMPTON, D.W. (1999). How much human helminthiasis is there in the world? *J Parasitol*, **85,** 397-403.

CRUICKSHANK, S.M., DESCHOOLMEESTER, M.L., SVENSSON, M., HOWELL, G., BAZAKOU, A., LOGUNOVA, L., LITTLE, M.C., ENGLISH, N., MACK, M., GRENCIS, R.K., ELSE, K.J. & CARDING, S.R. (2009). Rapid dendritic cell mobilization to the large intestinal epithelium is associated with resistance to Trichuris muris infection. *J Immunol*, **182,** 3055-62.

CUA, D.J., SHERLOCK, J., CHEN, Y., MURPHY, C.A., JOYCE, B., SEYMOUR, B., LUCIAN, L., TO, W., KWAN, S., CHURAKOVA, T., ZURAWSKI, S., WIEKOWSKI, M., LIRA, S.A., GORMAN, D., KASTELEIN, R.A. & SEDGWICK, J.D. (2003). Interleukin-23 rather than interleukin-12 is the critical cytokine for autoimmune inflammation of the brain. *Nature*, **421,** 744-8.

D'ELIA, R., BEHNKE, J.M., BRADLEY, J.E. & ELSE, K.J. (2009). Regulatory T cells: a role in the control of helminth-driven intestinal pathology and worm survival. *J Immunol*, **182,** 2340-8.

D'ELIA, R. & ELSE, K.J. (2009). In vitro antigen presenting cell-derived IL-10 and IL-6 correlate with Trichuris muris isolate-specific survival. *Parasite Immunol*, **31,** 123-31.

DALTON, D.K., PITTS-MEEK, S., KESHAV, S., FIGARI, I.S., BRADLEY, A. & STEWART, T.A. (1993). Multiple defects of immune cell function in mice with disrupted interferon-gamma genes. *Science*, **259,** 1739-42.

DAVID, A.H., JACQUELINE, M.S., DAVID, E.A., KEVIN, C.O.C., PHILIP DE, J. & CLARE, B.-A. (2005). Multiple sclerosis. *Immunological Reviews*, **204,** 208-231.

DAVIDSON, N.J., FORT, M.M., MULLER, W., LEACH, M.W. & RENNICK, D.M. (2000). Chronic colitis in IL-10$^{-/-}$ mice: insufficient counter regulation of a Th1 response. *Int Rev Immunol*, **19,** 91-121.

DESCHOOLMEESTER, M.L. & ELSE, K.J. (2002). Cytokine and chemokine responses underlying acute and chronic Trichuris muris infection. *Int Rev Immunol*, **21,** 439-67.

DESCHOOLMEESTER, M.L., LITTLE, M.C., ROLLINS, B.J. & ELSE, K.J. (2003). Absence of CC chemokine ligand 2 results in an altered Th1/Th2 cytokine

balance and failure to expel Trichuris muris infection. *J Immunol*, **170,** 4693-700.

DESCHOOLMEESTER, M.L., MANKU, H. & ELSE, K.J. (2006). The innate immune responses of colonic epithelial cells to Trichuris muris are similar in mouse strains that develop a type 1 or type 2 adaptive immune response. *Infect Immun*, **74,** 6280-6.

DIELEMAN, L.A., PALMEN, M.J., AKOL, H., BLOEMENA, E., PENA, A.S., MEUWISSEN, S.G. & VAN REES, E.P. (1998). Chronic experimental colitis induced by dextran sulphate sodium (DSS) is characterized by Th1 and Th2 cytokines. *Clin Exp Immunol*, **114,** 385-91.

DIELEMAN, L.A., RIDWAN, B.U., TENNYSON, G.S., BEAGLEY, K.W., BUCY, R.P. & ELSON, C.O. (1994). Dextran sulfate sodium-induced colitis occurs in severe combined immunodeficient mice. *Gastroenterology*, **107,** 1643-52.

DIGHE, A.S., CAMPBELL, D., HSIEH, C.S., CLARKE, S., GREAVES, D.R., GORDON, S., MURPHY, K.M. & SCHREIBER, R.D. (1995). Tissue-specific targeting of cytokine unresponsiveness in transgenic mice. *Immunity*, **3,** 657-66.

DROGEMULLER, K., HELMUTH, U., BRUNN, A., SAKOWICZ-BURKIEWICZ, M., GUTMANN, D.H., MUELLER, W., DECKERT, M. & SCHLUTER, D. (2008). Astrocyte gp130 expression is critical for the control of Toxoplasma encephalitis. *J Immunol*, **181,** 2683-93.

DUBEY, J.P. (1998). Advances in the life cycle of Toxoplasma gondii. *Int J Parasitol*, **28,** 1019-24.

DUERR, R.H., TAYLOR, K.D., BRANT, S.R., RIOUX, J.D., SILVERBERG, M.S., DALY, M.J., STEINHART, A.H., ABRAHAM, C., REGUEIRO, M., GRIFFITHS, A., DASSOPOULOS, T., BITTON, A., YANG, H., TARGAN, S., DATTA, L.W., KISTNER, E.O., SCHUMM, L.P., LEE, A.T., GREGERSEN, P.K., BARMADA, M.M., ROTTER, J.I., NICOLAE, D.L. & CHO, J.H. (2006). A Genome-Wide Association Study Identifies IL23R as an Inflammatory Bowel Disease Gene. *Science*, **314,** 1461-1463.

DUONG, T.T., FINKELMAN, F.D., SINGH, B. & STREJAN, G.H. (1994). Effect of anti-interferon-gamma monoclonal antibody treatment on the development of experimental allergic encephalomyelitis in resistant mouse strains. *J Neuroimmunol*, **53,** 101-7.

DYMECKI, S.M. (1996). Flp recombinase promotes site-specific DNA recombination in embryonic stem cells and transgenic mice. *Proc Natl Acad Sci U S A*, **93,** 6191-6.

EGGER, B., BAJAJ-ELLIOTT, M., MACDONALD, T.T., INGLIN, R., EYSSELEIN, V.E. & BUCHLER, M.W. (2000). Characterisation of acute murine dextran sodium sulphate colitis: cytokine profile and dose dependency. *Digestion*, **62,** 240-8.

EHRT, S., SCHNAPPINGER, D., BEKIRANOV, S., DRENKOW, J., SHI, S., GINGERAS, T.R., GAASTERLAND, T., SCHOOLNIK, G. & NATHAN, C. (2001). Reprogramming of the macrophage transcriptome in response to interferon-gamma and Mycobacterium tuberculosis: signaling roles of nitric oxide synthase-2 and phagocyte oxidase. *J Exp Med*, **194,** 1123-40.

EL MARJOU, F., JANSSEN, K.P., CHANG, B.H., LI, M., HINDIE, V., CHAN, L., LOUVARD, D., CHAMBON, P., METZGER, D. & ROBINE, S. (2004). Tissue-specific and inducible Cre-mediated recombination in the gut epithelium. *Genesis*, **39,** 186-93.

ELSE, K.J. & DESCHOOLMEESTER, M.L. (2003). Immunity to Trichuris muris in the laboratory mouse. *J Helminthol*, **77,** 95-8.

ELSE, K.J., FINKELMAN, F.D., MALISZEWSKI, C.R. & GRENCIS, R.K. (1994). Cytokine-mediated regulation of chronic intestinal helminth infection. *J Exp Med*, **179,** 347-51.

ELSE, K.J. & GRENCIS, R.K. (1996). Antibody-independent effector mechanisms in resistance to the intestinal nematode parasite Trichuris muris. *Infect Immun*, **64,** 2950-4.

ELSON, C.O., CONG, Y., WEAVER, C.T., SCHOEB, T.R., MCCLANAHAN, T.K., FICK, R.B. & KASTELEIN, R.A. (2007). Monoclonal Anti-Interleukin 23 Reverses Active Colitis in a T Cell-Mediated Model in Mice. *Gastroenterology*, **132,** 2359-2370.

ESPEJO, C., PENKOWA, M., SAEZ-TORRES, I., XAUS, J., CELADA, A., MONTALBAN, X. & MARTINEZ-CACERES, E.M. (2001). Treatment with anti-interferon-gamma monoclonal antibodies modifies experimental autoimmune encephalomyelitis in interferon-gamma receptor knockout mice. *Exp Neurol*, **172,** 460-8.

ESWORTHY, R.S., SMITH, D.D. & CHU, F.F. (2010). A Strong Impact of Genetic Background on Gut Microflora in Mice. *Int J Inflam*, **2010,** 986046.

FANTINI, M.C., MONTELEONE, G. & MACDONALD, T.T. (2007). New players in the cytokine orchestra of inflammatory bowel disease. *Inflamm Bowel Dis*, **13,** 1419-23.

FARMER, M.A., SUNDBERG, J.P., BRISTOL, I.J., CHURCHILL, G.A., LI, R., ELSON, C.O. & LEITER, E.H. (2001). A major quantitative trait locus on chromosome 3 controls colitis severity in IL-10-deficient mice. *Proc Natl Acad Sci U S A*, **98,** 13820-5.

FASNACHT, N. (2008). Analysis of infection of mice with Trichuris muris. In *Department of Experimental Immunology*. Braunschweig: Helmholtz Cenrte for Infection Research.

FASNACHT, N., GREWELING, M.C., BOLLATI-FOGOLIN, M., SCHIPPERS, A. & MULLER, W. (2009). T-cell-specific deletion of gp130 renders the highly

susceptible IL-10-deficient mouse resistant to intestinal nematode infection. *Eur J Immunol*, **39,** 2173-83.

FASNACHT, N. & MULLER, W. (2008). Conditional gp130 deficient mouse mutants. *Semin Cell Dev Biol*, **19,** 379-84.

FEIL, R., BROCARD, J., MASCREZ, B., LEMEUR, M., METZGER, D. & CHAMBON, P. (1996). Ligand-activated site-specific recombination in mice. *Proc Natl Acad Sci U S A*, **93,** 10887-90.

FERBER, I.A., BROCKE, S., TAYLOR-EDWARDS, C., RIDGWAY, W., DINISCO, C., STEINMAN, L., DALTON, D. & FATHMAN, C.G. (1996). Mice with a disrupted IFN-gamma gene are susceptible to the induction of experimental autoimmune encephalomyelitis (EAE). *J Immunol*, **156,** 5-7.

FILIPE-SANTOS, O., BUSTAMANTE, J., CHAPGIER, A., VOGT, G., DE BEAUCOUDREY, L., FEINBERG, J., JOUANGUY, E., BOISSON-DUPUIS, S., FIESCHI, C., PICARD, C. & CASANOVA, J.L. (2006). Inborn errors of IL-12/23- and IFN-gamma-mediated immunity: molecular, cellular, and clinical features. *Semin Immunol*, **18,** 347-61.

FINKELMAN, F.D., KATONA, I.M., MOSMANN, T.R. & COFFMAN, R.L. (1988). IFN-gamma regulates the isotypes of Ig secreted during in vivo humoral immune responses. *J Immunol*, **140,** 1022-7.

FLEIGE, A. (2006). Konditionale Mutagenese in der Maus Generierung und Analyse konditionaler Mausmutanten. Braunschweig: Technischen Universität Carolo-Wilhelmina.

FREI, K., SIEPL, C., GROSCURTH, P., BODMER, S., SCHWERDEL, C. & FONTANA, A. (1987). Antigen presentation and tumor cytotoxicity by interferon-gamma-treated microglial cells. *Eur J Immunol*, **17,** 1271-8.

FRICK, J.S., FINK, K., KAHL, F., NIEMIEC, M.J., QUITADAMO, M., SCHENK, K. & AUTENRIETH, I.B. (2007). Identification of commensal bacterial strains that modulate Yersinia enterocolitica and dextran sodium sulfate-induced inflammatory responses: implications for the development of probiotics. *Infect Immun*, **75,** 3490-7.

FRIESE, M.A. & FUGGER, L. (2005). Autoreactive CD8+ T cells in multiple sclerosis: a new target for therapy? *Brain*, **128,** 1747-63.

FRISCHMANN, U. & MÜLLER, W. (2006). Nine fluorescence parameter analysis on a four-color fluorescence activated flow cytometer. *Cytometry*, **69A,** 124-126.

FROHMAN, E.M., RACKE, M.K. & RAINE, C.S. (2006). Multiple Sclerosis -- The Plaque and Its Pathogenesis. **354,** 942-955.

FRUCHT, D.M., FUKAO, T., BOGDAN, C., SCHINDLER, H., O'SHEA, J.J. & KOYASU, S. (2001). IFN-gamma production by antigen-presenting cells: mechanisms emerge. *Trends Immunol*, **22,** 556-60.

FUSS, I.J., NEURATH, M., BOIRIVANT, M., KLEIN, J.S., DE LA MOTTE, C., STRONG, S.A., FIOCCHI, C. & STROBER, W. (1996). Disparate CD4+ lamina propria (LP) lymphokine secretion profiles in inflammatory bowel disease. Crohn's disease LP cells manifest increased secretion of IFN-gamma, whereas ulcerative colitis LP cells manifest increased secretion of IL-5. *J Immunol*, **157,** 1261-70.

GAJEWSKI, T.F. & FITCH, F.W. (1988). Anti-proliferative effect of IFN-gamma in immune regulation. I. IFN-gamma inhibits the proliferation of Th2 but not Th1 murine helper T lymphocyte clones. *J Immunol*, **140,** 4245-52.

GANGADHARAN, B., HOEVE, M.A., ALLEN, J.E., EBRAHIMI, B., RHIND, S.M., DUTIA, B.M. & NASH, A.A. (2008). Murine gammaherpesvirus-induced fibrosis is associated with the development of alternatively activated macrophages. *J Leukoc Biol*, **84,** 50-8.

GAVRILESCU, L.C. & DENKERS, E.Y. (2001). IFN-gamma overproduction and high level apoptosis are associated with high but not low virulence Toxoplasma gondii infection. *J Immunol*, **167,** 902-9.

GEHRMANN, J., MATSUMOTO, Y. & KREUTZBERG, G.W. (1995). Microglia: intrinsic immuneffector cell of the brain. *Brain Res Brain Res Rev*, **20,** 269-87.

GEORGIADES, P., OGILVY, S., DUVAL, H., LICENCE, D.R., CHARNOCK-JONES, D.S., SMITH, S.K. & PRINT, C.G. (2002). VavCre transgenic mice: a tool for mutagenesis in hematopoietic and endothelial lineages. *Genesis*, **34,** 251-6.

GHOSH, S. & MITCHELL, R. (2007). Impact of inflammatory bowel disease on quality of life: Results of the European Federation of Crohn's and Ulcerative Colitis Associations (EFCCA) patient survey. *J Crohns and Colitis* **1,** 10-20.

GLOCKER, E.O., KOTLARZ, D., BOZTUG, K., GERTZ, E.M., SCHAFFER, A.A., NOYAN, F., PERRO, M., DIESTELHORST, J., ALLROTH, A., MURUGAN, D., HATSCHER, N., PFEIFER, D., SYKORA, K.W., SAUER, M., KREIPE, H., LACHER, M., NUSTEDE, R., WOELLNER, C., BAUMANN, U., SALZER, U., KOLETZKO, S., SHAH, N., SEGAL, A.W., SAUERBREY, A., BUDERUS, S., SNAPPER, S.B., GRIMBACHER, B. & KLEIN, C. (2009). Inflammatory bowel disease and mutations affecting the interleukin-10 receptor. *N Engl J Med*, **361,** 2033-45.

GOLD, R., LININGTON, C. & LASSMANN, H. (2006). Understanding pathogenesis and therapy of multiple sclerosis via animal models: 70 years of merits and culprits in experimental autoimmune encephalomyelitis research. *Brain*, **129,** 1953-71.

GORDON, J.W., SCANGOS, G.A., PLOTKIN, D.J., BARBOSA, J.A. & RUDDLE, F.H. (1980). Genetic transformation of mouse embryos by microinjection of purified DNA. *Proc Natl Acad Sci U S A*, **77,** 7380-4.

GORDON, S. (2003). Alternative activation of macrophages. *Nat Rev Immunol*, **3,** 23-35.

GOSSEN, M. & BUJARD, H. (1992). Tight control of gene expression in mammalian cells by tetracycline-responsive promoters. *Proc Natl Acad Sci U S A*, **89,** 5547-51.

GOUGH, D.J., LEVY, D.E., JOHNSTONE, R.W. & CLARKE, C.J. (2008). IFNgamma signaling-does it mean JAK-STAT? *Cytokine Growth Factor Rev*, **19,** 383-94.

GOUGH, D.J., SABAPATHY, K., KO, E.Y., ARTHUR, H.A., SCHREIBER, R.D., TRAPANI, J.A., CLARKE, C.J. & JOHNSTONE, R.W. (2007). A novel c-Jun-dependent signal transduction pathway necessary for the transcriptional activation of interferon gamma response genes. *J Biol Chem*, **282,** 938-46.

GOVERMAN, J. (2009). Autoimmune T cell responses in the central nervous system. *Nat Rev Immunol*, **9,** 393-407.

GREGORY, S.G., SEKHON, M., SCHEIN, J., ZHAO, S., OSOEGAWA, K., SCOTT, C.E., EVANS, R.S., BURRIDGE, P.W., COX, T.V., FOX, C.A., HUTTON, R.D., MULLENGER, I.R., PHILLIPS, K.J., SMITH, J., STALKER, J., THREADGOLD, G.J., BIRNEY, E., WYLIE, K., CHINWALLA, A., WALLIS, J., HILLIER, L., CARTER, J., GAIGE, T., JAEGER, S., KREMITZKI, C., LAYMAN, D., MAAS, J., MCGRANE, R., MEAD, K., WALKER, R., JONES, S., SMITH, M., ASANO, J., BOSDET, I., CHAN, S., CHITTARANJAN, S., CHIU, R., FJELL, C., FUHRMANN, D., GIRN, N., GRAY, C., GUIN, R., HSIAO, L., KRZYWINSKI, M., KUTSCHE, R., LEE, S.S., MATHEWSON, C., MCLEAVY, C., MESSERVIER, S., NESS, S., PANDOH, P., PRABHU, A.L., SAEEDI, P., SMAILUS, D., SPENCE, L., STOTT, J., TAYLOR, S., TERPSTRA, W., TSAI, M., VARDY, J., WYE, N., YANG, G., SHATSMAN, S., AYODEJI, B., GEER, K., TSEGAYE, G., SHVARTSBEYN, A., GEBREGEORGIS, E., KROL, M., RUSSELL, D., OVERTON, L., MALEK, J.A., HOLMES, M., HEANEY, M., SHETTY, J., FELDBLYUM, T., NIERMAN, W.C., CATANESE, J.J., HUBBARD, T., WATERSTON, R.H., ROGERS, J., DE JONG, P.J., FRASER, C.M., MARRA, M., MCPHERSON, J.D. & BENTLEY, D.R. (2002). A physical map of the mouse genome. *Nature*, **418,** 743-50.

GRENCIS, R.K. (2001). Cytokine regulation of resistance and susceptibility to intestinal nematode infection - from host to parasite. *Vet Parasitol*, **100,** 45-50.

GRENCIS, R.K. & ENTWISTLE, G.M. (1997). Production of an interferon-gamma homologue by an intestinal nematode: functionally significant or interesting artefact? *Parasitology*, **115 Suppl,** S101-6.

GU, H., MARTH, J.D., ORBAN, P.C., MOSSMANN, H. & RAJEWSKY, K. (1994). Deletion of a DNA polymerase beta gene segment in T cells using cell type-specific gene targeting. *Science*, **265,** 103-6.

GUARNER, F. & MALAGELADA, J.R. (2003). Gut flora in health and disease. *Lancet*, **361,** 512-9.

GULUBOVA, M.V., MANOLOVA, I.M., VLAYKOVA, T.I., PRODANOVA, M. & JOVCHEV, J.P. (2007). Adhesion molecules in chronic ulcerative colitis. *Int J Colorectal Dis*, **22,** 581-9.

GUTCHER, I. & BECHER, B. (2007). APC-derived cytokines and T cell polarization in autoimmune inflammation. *J Clin Invest*, **117,** 1119-27.

GUTCHER, I., URICH, E., WOLTER, K., PRINZ, M. & BECHER, B. (2006). Interleukin 18-independent engagement of interleukin 18 receptor-alpha is required for autoimmune inflammation. *Nat Immunol*, **7,** 946-53.

HAAK, S., CROXFORD, A.L., KREYMBORG, K., HEPPNER, F.L., POULY, S., BECHER, B. & WAISMAN, A. (2009). IL-17A and IL-17F do not contribute vitally to autoimmune neuro-inflammation in mice. *J Clin Invest*, **119,** 61-9.

HAFLER, D.A., SLAVIK, J.M., ANDERSON, D.E., O'CONNOR, K.C., DE JAGER, P. & BAECHER-ALLAN, C. (2005). Multiple sclerosis. *Immunol Rev*, **204,** 208-31.

HAFNER, M., WENK, J., NENCI, A., PASPARAKIS, M., SCHARFFETTER-KOCHANEK, K., SMYTH, N., PETERS, T., KESS, D., HOLTKOTTER, O., SHEPHARD, P., KUDLOW, J.E., SMOLA, H., HAASE, I., SCHIPPERS, A., KRIEG, T. & MULLER, W. (2004). Keratin 14 Cre transgenic mice authenticate keratin 14 as an oocyte-expressed protein. *Genesis*, **38,** 176-81.

HALONEN, S.K., TAYLOR, G.A. & WEISS, L.M. (2001). Gamma interferon-induced inhibition of Toxoplasma gondii in astrocytes is mediated by IGTP. *Infect Immun*, **69,** 5573-6.

HANADA, T., KOBAYASHI, T., CHINEN, T., SAEKI, K., TAKAKI, H., KOGA, K., MINODA, Y., SANADA, T., YOSHIOKA, T., MIMATA, H., KATO, S. & YOSHIMURA, A. (2006). IFNgamma-dependent, spontaneous development of colorectal carcinomas in SOCS1-deficient mice. *J Exp Med*, **203,** 1391-7.

HANAUER, S.B. (2006). Inflammatory bowel disease: epidemiology, pathogenesis, and therapeutic opportunities. *Inflamm Bowel Dis*, **12,** S3-9.

HARPAZ, N. & POLYDORIDES, A.D. (2010). Colorectal dysplasia in chronic inflammatory bowel disease: pathology, clinical implications, and pathogenesis. *Arch Pathol Lab Med*, **134,** 876-95.

HARRINGTON, L.E., HATTON, R.D., MANGAN, P.R., TURNER, H., MURPHY, T.L., MURPHY, K.M. & WEAVER, C.T. (2005). Interleukin 17-producing CD4+ effector T cells develop via a lineage distinct from the T helper type 1 and 2 lineages. *Nat Immunol*, **6,** 1123-32.

HASBOLD, J., HONG, J.S., KEHRY, M.R. & HODGKIN, P.D. (1999). Integrating signals from IFN-gamma and IL-4 by B cells: positive and negative effects on CD40 ligand-induced proliferation, survival, and division-linked isotype switching to IgG1, IgE, and IgG2a. *J Immunol*, **163,** 4175-81.

HASNAIN, S.Z., WANG, H., GHIA, J.E., HAQ, N., DENG, Y., VELCICH, A., GRENCIS, R.K., THORNTON, D.J. & KHAN, W.I. (2010). Mucin gene deficiency in mice impairs host resistance to an enteric parasitic infection. *Gastroenterology*, **138,** 1763-71.

HAYES, K.S., BANCROFT, A.J., GOLDRICK, M., PORTSMOUTH, C., ROBERTS, I.S. & GRENCIS, R.K. (2010). Exploitation of the intestinal microflora by the parasitic nematode Trichuris muris. *Science*, **328,** 1391-4.

HE, Y., ZHANG, W., ZHANG, R., ZHANG, H. & MIN, W. (2006). SOCS1 inhibits tumor necrosis factor-induced activation of ASK1-JNK inflammatory signaling by mediating ASK1 degradation. *J Biol Chem*, **281,** 5559-66.

HELMBY, H. & GRENCIS, R.K. (2003). Essential role for TLR4 and MyD88 in the development of chronic intestinal nematode infection. *Eur J Immunol*, **33,** 2974-9.

HELMBY, H., TAKEDA, K., AKIRA, S. & GRENCIS, R.K. (2001). Interleukin (IL)-18 promotes the development of chronic gastrointestinal helminth infection by downregulating IL-13. *J Exp Med*, **194,** 355-64.

HEMMER, B., NESSLER, S., ZHOU, D., KIESEIER, B. & HARTUNG, H.P. (2006). Immunopathogenesis and immunotherapy of multiple sclerosis. *Nat Clin Pract Neurol*, **2,** 201-11.

HEMMI, S., BOHNI, R., STARK, G., DI MARCO, F. & AGUET, M. (1994). A novel member of the interferon receptor family complements functionality of the murine interferon gamma receptor in human cells. *Cell*, **76,** 803-10.

HERRERO, C., HU, X., LI, W.P., SAMUELS, S., SHARIF, M.N., KOTENKO, S. & IVASHKIV, L.B. (2003). Reprogramming of IL-10 activity and signaling by IFN-gamma. *J Immunol*, **171,** 5034-41.

HIBI, T. & OGATA, H. (2006). Novel pathophysiological concepts of inflammatory bowel disease. *J Gastroenterol*, **41,** 10-6.

HILSDEN, R.J., MEDDINGS, J.B., HARDIN, J., GALL, D.G. & SUTHERLAND, L.R. (1999). Intestinal permeability and postheparin plasma diamine oxidase activity in the prediction of Crohn's disease relapse. *Inflamm Bowel Dis*, **5,** 85-91.

HIROTA, H., CHEN, J., BETZ, U.A., RAJEWSKY, K., GU, Y., ROSS, J., JR., MULLER, W. & CHIEN, K.R. (1999). Loss of a gp130 cardiac muscle cell survival pathway is a critical event in the onset of heart failure during biomechanical stress. *Cell*, **97,** 189-98.

HIROTSUNE, S., FLECK, M.W., GAMBELLO, M.J., BIX, G.J., CHEN, A., CLARK, G.D., LEDBETTER, D.H., MCBAIN, C.J. & WYNSHAW-BORIS, A. (1998). Graded reduction of Pafah1b1 (Lis1) activity results in neuronal migration defects and early embryonic lethality. *Nat Genet*, **19,** 333-9.

HO, H.H., ANTONIV, T.T., JI, J.D. & IVASHKIV, L.B. (2008). Lipopolysaccharide-induced expression of matrix metalloproteinases in human monocytes is suppressed by IFN-gamma via superinduction of ATF-3 and suppression of AP-1. *J Immunol*, **181,** 5089-97.

HOESS, R.H. & ABREMSKI, K. (1985). Mechanism of strand cleavage and exchange in the Cre-lox site-specific recombination system. *J Mol Biol*, **181,** 351-62.

HORIUCHI, M., ITOH, A., PLEASURE, D. & ITOH, T. (2006). MEK-ERK signaling is involved in interferon-gamma-induced death of oligodendroglial progenitor cells. *J Biol Chem*, **281,** 20095-106.

HORSNELL, W.G. & BROMBACHER, F. (2010). Genes associated with alternatively activated macrophages discretely regulate helminth infection and pathogenesis in experimental mouse models. *Immunobiology*, **215,** 704-8.

HORWITZ, M.S., EVANS, C.F., MCGAVERN, D.B., RODRIGUEZ, M. & OLDSTONE, M.B. (1997). Primary demyelination in transgenic mice expressing interferon-gamma. *Nat Med*, **3,** 1037-41.

HU, X., PAIK, P.K., CHEN, J., YARILINA, A., KOCKERITZ, L., LU, T.T., WOODGETT, J.R. & IVASHKIV, L.B. (2006). IFN-gamma suppresses IL-10 production and synergizes with TLR2 by regulating GSK3 and CREB/AP-1 proteins. *Immunity*, **24,** 563-74.

HU, X., PARK-MIN, K.H., HO, H.H. & IVASHKIV, L.B. (2005). IFN-gamma-primed macrophages exhibit increased CCR2-dependent migration and altered IFN-gamma responses mediated by Stat1. *J Immunol*, **175,** 3637-47.

HU, Y., HU, X., BOUMSELL, L. & IVASHKIV, L.B. (2008). IFN-gamma and STAT1 arrest monocyte migration and modulate RAC/CDC42 pathways. *J Immunol*, **180,** 8057-65.

HUANG, S., HENDRIKS, W., ALTHAGE, A., HEMMI, S., BLUETHMANN, H., KAMIJO, R., VILCEK, J., ZINKERNAGEL, R.M. & AGUET, M. (1993). Immune response in mice that lack the interferon-gamma receptor. *Science*, **259,** 1742-5.

HUE, S., AHERN, P., BUONOCORE, S., KULLBERG, M.C., CUA, D.J., MCKENZIE, B.S., POWRIE, F. & MALOY, K.J. (2006). Interleukin-23 drives innate and T cell-mediated intestinal inflammation. *J Exp Med*, **203,** 2473-2483.

HUGOT, J.P., LAURENT-PUIG, P., GOWER-ROUSSEAU, C., OLSON, J.M., LEE, J.C., BEAUGERIE, L., NAOM, I., DUPAS, J.L., VAN GOSSUM, A., ORHOLM, M., BONAITI-PELLIE, C., WEISSENBACH, J., MATHEW, C.G., LENNARD-JONES, J.E., CORTOT, A., COLOMBEL, J.F. & THOMAS, G. (1996). Mapping of a

susceptibility locus for Crohn's disease on chromosome 16. *Nature*, **379,** 821-3.

IMAI, Y., IBATA, I., ITO, D., OHSAWA, K. & KOHSAKA, S. (1996). A novel gene iba1 in the major histocompatibility complex class III region encoding an EF hand protein expressed in a monocytic lineage. *Biochem Biophys Res Commun*, **224,** 855-62.

INNES, E.A. (2010). A brief history and overview of Toxoplasma gondii. *Zoonoses Public Health*, **57,** 1-7.

IRVINE, E.J. & MARSHALL, J.K. (2000). Increased intestinal permeability precedes the onset of Crohn's disease in a subject with familial risk. *Gastroenterology*, **119,** 1740-4.

ISAACS, A. & LINDENMANN, J. (1957). Virus interference. I. The interferon. *Proc R Soc Lond B Biol Sci*, **147,** 258-67.

ITO, D., TANAKA, K., SUZUKI, S., DEMBO, T. & FUKUUCHI, Y. (2001). Enhanced expression of Iba1, ionized calcium-binding adapter molecule 1, after transient focal cerebral ischemia in rat brain. *Stroke*, **32,** 1208-15.

ITO, R., SHIN-YA, M., KISHIDA, T., URANO, A., TAKADA, R., SAKAGAMI, J., IMANISHI, J., KITA, M., UEDA, Y., IWAKURA, Y., KATAOKA, K., OKANOUE, T. & MAZDA, O. (2006). Interferon γ is causatively involved in experimental inflammatory bowel disease in mice. *Clinical & Experimental Immunology*, **146,** 330-338.

ITO, Y. (1991). The absence of resistance in congenitally athymic nude mice toward infection with the intestinal nematode, Trichuris muris: resistance restored by lymphoid cell transfer. *Int J Parasitol*, **21,** 65-9.

IZCUE, A., COOMBES, J.L. & POWRIE, F. (2009). Regulatory lymphocytes and intestinal inflammation. *Annu Rev Immunol*, **27,** 313-38.

IZCUE, A., HUE, S., BUONOCORE, S., ARANCIBIA-CÁRCAMO, C.V., AHERN, P.P., IWAKURA, Y., MALOY, K.J. & POWRIE, F. (2008). Interleukin-23 Restrains Regulatory T Cell Activity to Drive T Cell-Dependent Colitis. *Immunity*, **28,** 559-570.

JANKOVIC, D., KULLBERG, M.C., FENG, C.G., GOLDSZMID, R.S., COLLAZO, C.M., WILSON, M., WYNN, T.A., KAMANAKA, M., FLAVELL, R.A. & SHER, A. (2007). Conventional T-bet(+)Foxp3(-) Th1 cells are the major source of host-protective regulatory IL-10 during intracellular protozoan infection. *J Exp Med*, **204,** 273-83.

JENKINS, S.J. & ALLEN, J.E. (2010). Similarity and diversity in macrophage activation by nematodes, trematodes, and cestodes. *J Biomed Biotechnol*, **2010,** 262609.

JESS, T., LOFTUS, E.V., JR., HARMSEN, W.S., ZINSMEISTER, A.R., TREMAINE, W.J., MELTON, L.J., 3RD, MUNKHOLM, P. & SANDBORN, W.J. (2006). Survival and cause specific mortality in patients with inflammatory bowel disease: a long term outcome study in Olmsted County, Minnesota, 1940-2004. *Gut*, **55,** 1248-54.

JOHANSSON, M.E., GUSTAFSSON, J.K., SJOBERG, K.E., PETERSSON, J., HOLM, L., SJOVALL, H. & HANSSON, G.C. (2010). Bacteria penetrate the inner mucus layer before inflammation in the dextran sulfate colitis model. *PLoS One*, **5,** e12238.

JOHNSTON, C.E., BRADLEY, J.E., BEHNKE, J.M., MATTHEWS, K.R. & ELSE, K.J. (2005). Isolates of Trichuris muris elicit different adaptive immune responses in their murine host. *Parasite Immunol*, **27,** 69-78.

JUNG, S., RAJEWSKY, K. & RADBRUCH, A. (1993). Shutdown of class switch recombination by deletion of a switch region control element. *Science*, **259,** 984-7.

JURJUS, A.R., KHOURY, N.N. & REIMUND, J.-M. (2004). Animal models of inflammatory bowel disease. *J Pharmacol Toxicol*, **50,** 81-92.

KAGNOFF, M.F. & ECKMANN, L. (1997). Epithelial cells as sensors for microbial infection. *J Clin Invest*, **100,** 6-10.

KATAKURA, K., LEE, J., RACHMILEWITZ, D., LI, G., ECKMANN, L. & RAZ, E. (2005). Toll-like receptor 9-induced type I IFN protects mice from experimental colitis. *J Clin Invest*, **115,** 695-702.

KAWAGUCHI, S., ISHIGURO, Y., IMAIZUMI, T., MORI, F., MATSUMIYA, T., YOSHIDA, H., OTA, K., SAKURABA, H., YAMAGATA, K., SATO, Y., TANJI, K., HAGA, T., WAKABAYASHI, K., FUKUDA, S. & SATOH, K. (2009). Retinoic acid-inducible gene-I is constitutively expressed and involved in IFN-gamma-stimulated CXCL9-11 production in intestinal epithelial cells. *Immunol Lett*, **123,** 9-13.

KEBIR, H., IFERGAN, I., ALVAREZ, J.I., BERNARD, M., POIRIER, J., ARBOUR, N., DUQUETTE, P. & PRAT, A. (2009). Preferential recruitment of interferon-gamma-expressing T H 17 cells in multiple sclerosis. *Ann Neurol*, **66,** 390-402.

KEISER, J. & UTZINGER, J. (2008). Efficacy of current drugs against soil-transmitted helminth infections: systematic review and meta-analysis. *Jama*, **299,** 1937-48.

KELCHTERMANS, H., STRUYF, S., DE KLERCK, B., MITERA, T., ALEN, M., GEBOES, L., VAN BALEN, M., DILLEN, C., PUT, W., GYSEMANS, C., BILLIAU, A., VAN DAMME, J. & MATTHYS, P. (2007). Protective role of IFN-gamma in collagen-induced arthritis conferred by inhibition of mycobacteria-induced granulocyte chemotactic protein-2 production. *J Leukoc Biol*, **81,** 1044-53.

KERSTETTER, A.E., PADOVANI-CLAUDIO, D.A., BAI, L. & MILLER, R.H. (2009). Inhibition of CXCR2 signaling promotes recovery in models of Multiple Sclerosis. *Experimental Neurology*, **220,** 44-56.

KIKLY, K., LIU, L., NA, S. & SEDGWICK, J.D. (2006). The IL-23/Th17 axis: therapeutic targets for autoimmune inflammation. *Current Opinion in Immunology*, **18,** 670-675.

KIM, T.K. & MANIATIS, T. (1996). Regulation of interferon-gamma-activated STAT1 by the ubiquitin-proteasome pathway. *Science*, **273,** 1717-9.

KITAJIMA, S., TAKUMA, S. & MORIMOTO, M. (2000). Histological analysis of murine colitis induced by dextran sulfate sodium of different molecular weights. *Exp Anim*, **49,** 9-15.

KITAJIMA, S., TAKUMA, S. & MORIMOTO, M. (1999). Tissue distribution of dextran sulfate sodium (DSS) in the acute phase of murine DSS-induced colitis. *J Vet Med Sci*, **61,** 67-70.

KOBELT, G., LINDGREN, P., PARKIN, D., FRANCIS, D.A., JOHNSON, M., BATES, D. & JÖNSSON, B. (2000). Costs and Quality of Life in Multiple Sclerosis. A Cross-Sectional Observational Study in the UK. *Working Paper Series in Economics and Finance*, **398**.

KOFLER, J., BISSEL, S., STAUFFER, M., STARKEY, A. & WILEY, C. (2010). Classical and Alternative Activation States of Human Adult Microglia. *J Neuropathol Exp Neurol.*, **69,** 525-6.

KOFLER, J. & WILEY, C.A. (2010). Microglia: Key Innate Immune Cells of the Brain. *Toxicol Pathol*, **In press**.

KOTENKO, S.V., GALLAGHER, G., BAURIN, V.V., LEWIS-ANTES, A., SHEN, M., SHAH, N.K., LANGER, J.A., SHEIKH, F., DICKENSHEETS, H. & DONNELLY, R.P. (2003). IFN-lambdas mediate antiviral protection through a distinct class II cytokine receptor complex. *Nat Immunol*, **4,** 69-77.

KOYAMA, K. & ITO, Y. (1996). Comparative studies on immune responses to infection in susceptible B10.BR mice infected with different strains of the murine nematode parasite Trichuris muris. *Parasite Immunol*, **18,** 257-63.

KOYAMA, K., TAMAUCHI, H. & ITO, Y. (1995). The role of CD4+ and CD8+ T cells in protective immunity to the murine nematode parasite Trichuris muris. *Parasite Immunol*, **17,** 161-5.

KRAKOWSKI, M. & OWENS, T. (1996). Interferon-gamma confers resistance to experimental allergic encephalomyelitis. *Eur J Immunol*, **26,** 1641-6.

KRAMER, O.H., KNAUER, S.K., GREINER, G., JANDT, E., REICHARDT, S., GUHRS, K.H., STAUBER, R.H., BOHMER, F.D. & HEINZEL, T. (2009). A phosphorylation-acetylation switch regulates STAT1 signaling. *Genes Dev*, **23,** 223-35.

KRAUSE, C.D., LAVNIKOVA, N., XIE, J., MEI, E., MIROCHNITCHENKO, O.V., JIA, Y., HOCHSTRASSER, R.M. & PESTKA, S. (2006). Preassembly and ligand-induced restructuring of the chains of the IFN-γ receptor complex: the roles of Jak kinases, Stat1 and the receptor chains. *Cell Res*, **16,** 55-69.

KROENKE, M.A., CARLSON, T.J., ANDJELKOVIC, A.V. & SEGAL, B.M. (2008). IL-12- and IL-23-modulated T cells induce distinct types of EAE based on histology, CNS chemokine profile, and response to cytokine inhibition. *J Exp Med*, **205,** 1535-41.

KUHN, R., LOHLER, J., RENNICK, D., RAJEWSKY, K. & MULLER, W. (1993). Interleukin-10-deficient mice develop chronic enterocolitis. *Cell*, **75,** 263-274.

KUHN, R., SCHWENK, F., AGUET, M. & RAJEWSKY, K. (1995). Inducible gene targeting in mice. *Science*, **269,** 1427-9.

KULLBERG, M.C., JANKOVIC, D., FENG, C.G., HUE, S., GORELICK, P.L., MCKENZIE, B.S., CUA, D.J., POWRIE, F., CHEEVER, A.W., MALOY, K.J. & SHER, A. (2006). IL-23 plays a key role in Helicobacter hepaticus-induced T cell-dependent colitis. *J Exp Med*, **203,** 2485-94.

KULLBERG, M.C., WARD, J.M., GORELICK, P.L., CASPAR, P., HIENY, S., CHEEVER, A., JANKOVIC, D. & SHER, A. (1998). Helicobacter hepaticus triggers colitis in specific-pathogen-free interleukin-10 (IL-10)-deficient mice through an IL-12- and gamma interferon-dependent mechanism. *Infect Immun*, **66,** 5157-66.

KUTZELNIGG, A., LUCCHINETTI, C.F., STADELMANN, C., BRUCK, W., RAUSCHKA, H., BERGMANN, M., SCHMIDBAUER, M., PARISI, J.E. & LASSMANN, H. (2005). Cortical demyelination and diffuse white matter injury in multiple sclerosis. *Brain*, **128,** 2705-12.

KWAN, K.-M. (2002). Conditional alleles in mice: Practical considerations for tissue-specific knockouts. *Genesis*, **32,** 49-62.

LAGNA, G. & HEMMATI-BRIVANLOU, A. (1998). Use of dominant negative constructs to modulate gene expression. *Curr Top Dev Biol*, **36,** 75-98.

LAKSO, M., SAUER, B., MOSINGER, B., JR., LEE, E.J., MANNING, R.W., YU, S.H., MULDER, K.L. & WESTPHAL, H. (1992). Targeted oncogene activation by site-specific recombination in transgenic mice. *Proc Natl Acad Sci U S A*, **89,** 6232-6.

LANGER, J.A., CUTRONE, E.C. & KOTENKO, S. (2004). The Class II cytokine receptor (CRF2) family: overview and patterns of receptor-ligand interactions. *Cytokine Growth Factor Rev*, **15,** 33-48.

LANGRISH, C.L., CHEN, Y., BLUMENSCHEIN, W.M., MATTSON, J., BASHAM, B., SEDGWICK, J.D., MCCLANAHAN, T., KASTELEIN, R.A. & CUA, D.J. (2005). IL-23 drives a pathogenic T cell population that induces autoimmune inflammation. *J Exp Med*, **201,** 233-40.

LARNER, A.C., CHAUDHURI, A. & DARNELL, J.E., JR. (1986). Transcriptional induction by interferon. New protein(s) determine the extent and length of the induction. *J Biol Chem*, **261,** 453-9.

LEARY, S.M., PORTER, B. & THOMPSON, A.J. (2005). Multiple sclerosis: diagnosis and the management of acute relapses. *Postgrad Med J*, **81,** 302-8.

LEE, P.P., FITZPATRICK, D.R., BEARD, C., JESSUP, H.K., LEHAR, S., MAKAR, K.W., PEREZ-MELGOSA, M., SWEETSER, M.T., SCHLISSEL, M.S., NGUYEN, S., CHERRY, S.R., TSAI, J.H., TUCKER, S.M., WEAVER, W.M., KELSO, A., JAENISCH, R. & WILSON, C.B. (2001). A critical role for Dnmt1 and DNA methylation in T cell development, function, and survival. *Immunity*, **15,** 763-74.

LEE, T.D., WAKELIN, D. & GRENCIS, R.K. (1983). Cellular mechanisms of immunity to the nematode Trichuris muris. *Int J Parasitol*, **13,** 349-53.

LEE, Y.K., MUKASA, R., HATTON, R.D. & WEAVER, C.T. (2009). Developmental plasticity of Th17 and Treg cells. *Curr Opin Immunol*, **21,** 274-80.

LEENAARS, P.P., HENDRIKSEN, C.F., KOEDAM, M.A., CLAASSEN, I. & CLAASSEN, E. (1995). Comparison of adjuvants for immune potentiating properties and side effects in mice. *Vet Immunol Immunopathol*, **48,** 123-38.

LEENAARS, P.P., KOEDAM, M.A., WESTER, P.W., BAUMANS, V., CLAASSEN, E. & HENDRIKSEN, C.F. (1998). Assessment of side effects induced by injection of different adjuvant/antigen combinations in rabbits and mice. *Lab Anim*, **32,** 387-406.

LEES, J.R., GOLUMBEK, P.T., SIM, J., DORSEY, D. & RUSSELL, J.H. (2008). Regional CNS responses to IFN-gamma determine lesion localization patterns during EAE pathogenesis. *J Exp Med*, **205,** 2633-42.

LEON, C., NANDAN, D., LOPEZ, M., MOEENREZAKHANLOU, A. & REINER, N.E. (2006). Annexin V associates with the IFN-γ receptor and regulates IFN-γ signalling. *J Immunol*, **176,** 5934-42.

LEVINE, S. & WENK, E.J. (1961). Studies on the mechanism of altered susceptibility to experimental allergic encephalomyelitis. *Am J Pathol*, **39,** 419-41.

LIMBERGEN, J., RUSSELL, R., NIMMO, E. & SATSANGI, J. (2007). The Genetics of Inflammatory Bowel Disease. *Am J Gastroenterol* **102,** 2820-2831.

LIN, S.Y., YEH, K.T., CHEN, W.T., CHEN, H.C., CHEN, S.T., CHIOU, H.Y. & CHANG, J.G. (2004). Promoter CpG methylation of tumor suppressor genes in

colorectal cancer and its relationship to clinical features. *Oncol Rep*, **11,** 341-8.

LITTLE, M.C., BELL, L.V., CLIFFE, L.J. & ELSE, K.J. (2005). The characterization of intraepithelial lymphocytes, lamina propria leukocytes, and isolated lymphoid follicles in the large intestine of mice infected with the intestinal nematode parasite Trichuris muris. *J Immunol*, **175,** 6713-22.

LIU, Q., LIU, Z., WHITMIRE, J., ALEM, F., HAMED, H., PESCE, J., URBAN, J.F., JR. & GAUSE, W.C. (2006). IL-18 stimulates IL-13-mediated IFN- γ -sensitive host resistance in vivo. *Eur J Immunol*, **36,** 1187-98.

LOCK, C., HERMANS, G., PEDOTTI, R., BRENDOLAN, A., SCHADT, E., GARREN, H., LANGER-GOULD, A., STROBER, S., CANNELLA, B., ALLARD, J., KLONOWSKI, P., AUSTIN, A., LAD, N., KAMINSKI, N., GALLI, S.J., OKSENBERG, J.R., RAINE, C.S., HELLER, R. & STEINMAN, L. (2002). Gene-microarray analysis of multiple sclerosis lesions yields new targets validated in autoimmune encephalomyelitis. *Nat Med*, **8,** 500-8.

LOFTUS, E.V., JR. (2004). Clinical epidemiology of inflammatory bowel disease: Incidence, prevalence, and environmental influences. *Gastroenterology*, **126,** 1504-17.

LOFTUS, E.V., JR., SILVERSTEIN, M.D., SANDBORN, W.J., TREMAINE, W.J., HARMSEN, W.S. & ZINSMEISTER, A.R. (1998). Crohn's disease in Olmsted County, Minnesota, 1940-1993: incidence, prevalence, and survival. *Gastroenterology*, **114,** 1161-8.

LOPEZ-SERRANO, P., PEREZ-CALLE, J.L., PEREZ-FERNANDEZ, M.T., FERNANDEZ-FONT, J.M., BOIXEDA DE MIGUEL, D. & FERNANDEZ-RODRIGUEZ, C.M. (2010). Environmental risk factors in inflammatory bowel diseases. Investigating the hygiene hypothesis: a Spanish case-control study. *Scand J Gastroenterol*, **45,** 1464-71.

LOSCHER, W. & FIEDLER, M. (1996). The role of technical, biological and pharmacological factors in the laboratory evaluation of anticonvulsant drugs. VI. Seasonal influences on maximal electroshock and pentylenetetrazol seizure thresholds. *Epilepsy Res*, **25,** 3-10.

LOUKAS, A., BETHONY, J., BROOKER, S. & HOTEZ, P. (2006). Hookworm vaccines: past, present, and future. *Lancet Infect Dis*, **6,** 733-41.

LU, B., EBENSPERGER, C., DEMBIC, Z., WANG, Y., KVATYUK, M., LU, T., COFFMAN, R.L., PESTKA, S. & ROTHMAN, P.B. (1998). Targeted disruption of the interferon-gamma receptor 2 gene results in severe immune defects in mice. *Proc Natl Acad Sci U S A*, **95,** 8233-8.

LUBLIN, F.D. & REINGOLD, S.C. (1996). Defining the clinical course of multiple sclerosis: results of an international survey. National Multiple Sclerosis Society (USA) Advisory Committee on Clinical Trials of New Agents in Multiple Sclerosis. *Neurology*, **46,** 907-11.

LYKENS, J.E., TERRELL, C.E., ZOLLER, E.E., DIVANOVIC, S., TROMPETTE, A., KARP, C.L., ALIBERTI, J., FLICK, M.J. & JORDAN, M.B. (2010). Mice with a selective impairment of IFN-gamma signaling in macrophage lineage cells demonstrate the critical role of IFN-gamma-activated macrophages for the control of protozoan parasitic infections in vivo. *J Immunol*, **184,** 877-85.

MAHLER, M., BRISTOL, I.J., LEITER, E.H., WORKMAN, A.E., BIRKENMEIER, E.H., ELSON, C.O. & SUNDBERG, J.P. (1998). Differential susceptibility of inbred mouse strains to dextran sulfate sodium-induced colitis. *Am J Physiol*, **274,** G544-51.

MAHLER, M. & LEITER, E.H. (2002). Genetic and environmental context determines the course of colitis developing in IL-10-deficient mice. *Inflamm Bowel Dis*, **8,** 347-55.

MALOY, K.J. (2008). The Interleukin-23 / Interleukin-17 axis in intestinal inflammation. *Journal of Internal Medicine*, **263,** 584-590.

MANTOVANI, A., SICA, A., SOZZANI, S., ALLAVENA, P., VECCHI, A. & LOCATI, M. (2004). The chemokine system in diverse forms of macrophage activation and polarization. *Trends Immunol*, **25,** 677-86.

MARKS, D. & SEGAL, A. (2008). Innate immunity in inflammatory bowel disease: a disease hypothesis. *J Pathol*, **214,** 260-6.

MARTIN, R., MCFARLAND, H.F. & MCFARLIN, D.E. (1992). Immunological aspects of demyelinating diseases. *Annu Rev Immunol*, **10,** 153-87.

MARTINEZ, F.O., SICA, A., MANTOVANI, A. & LOCATI, M. (2008). Macrophage activation and polarization. *Front Biosci*, **13,** 453-61.

MATTHYS, P., VERMEIRE, K., MITERA, T., HEREMANS, H., HUANG, S., SCHOLS, D., DE WOLF-PEETERS, C. & BILLIAU, A. (1999). Enhanced autoimmune arthritis in IFN-gamma receptor-deficient mice is conditioned by mycobacteria in Freund's adjuvant and by increased expansion of Mac-1+ myeloid cells. *J Immunol*, **163,** 3503-10.

MELGAR, S., KARLSSON, A. & MICHAELSSON, E. (2005). Acute colitis induced by dextran sulfate sodium progresses to chronicity in C57BL/6 but not in BALB/c mice: correlation between symptoms and inflammation. *Am J Physiol Gastrointest Liver Physiol*, **288,** G1328-38.

MELGAR, S., KARLSSON, L., REHNSTRÖM, E., KARLSSON, A., UTKOVIC, H., JANSSON, L. & MICHAËLSSON, E. (2008). Validation of murine dextran sulfate sodium-

induced colitis using four therapeutic agents for human inflammatory bowel disease. *International Immunopharmacology*, **8,** 836-844.

MERRILL, J.E., IGNARRO, L.J., SHERMAN, M.P., MELINEK, J. & LANE, T.E. (1993). Microglial cell cytotoxicity of oligodendrocytes is mediated through nitric oxide. *J Immunol*, **151,** 2132-41.

METZGER, D., CLIFFORD, J., CHIBA, H. & CHAMBON, P. (1995). Conditional site-specific recombination in mammalian cells using a ligand-dependent chimeric Cre recombinase. *Proc Natl Acad Sci U S A*, **92,** 6991-5.

MEYERS, E.N., LEWANDOSKI, M. & MARTIN, G.R. (1998). An Fgf8 mutant allelic series generated by Cre- and Flp-mediated recombination. *Nat Genet*, **18,** 136-41.

MIKI, K., MOORE, D.J., BUTLER, R.N., SOUTHCOTT, E., COUPER, R.T. & DAVIDSON, G.P. (1998). The sugar permeability test reflects disease activity in children and adolescents with inflammatory bowel disease. *J Pediatr Gastroenterol Nutr*, **133,** 750-4.

MINER, L.L. (1997). Cocaine reward and locomotor activity in C57BL/6J and 129/SvJ inbred mice and their F1 cross. *Pharmacol Biochem Behav*, **58,** 25-30.

MOLDOVAN, I.R., RUDICK, R.A., COTLEUR, A.C., BORN, S.E., LEE, J.C., KARAFA, M.T. & PELFREY, C.M. (2003). Interferon gamma responses to myelin peptides in multiple sclerosis correlate with a new clinical measure of disease progression. *J Neuroimmunol*, **141,** 132-40.

MONTELEONE, G., FINA, D., CARUSO, R. & PALLONE, F. (2006). New mediators of immunity and inflammation in inflammatory bowel disease. *Curr Opin Gastroenterol*, **22,** 361-4.

MONTRESOR A, C.D., GYORKOS TW, SAVIOLI L (2002). *Helminth control in school-age children*. Geneva: World Health Organisation.

MOOLENBEEK, C. & RUITENBERG, E.J. (1981). The "Swiss roll": a simple technique for histological studies of the rodent intestine. *Lab Anim*, **15,** 57-9.

MOORE, K.W., DE WAAL MALEFYT, R., COFFMAN, R.L. & O'GARRA, A. (2001). Interleukin-10 and the interleukin-10 receptor. *Annu Rev Immunol*, **19,** 683-765.

MORRISSEY, P.J., CHARRIER, K., BRADDY, S., LIGGITT, D. & WATSON, J.D. (1993). CD4+ T cells that express high levels of CD45RB induce wasting disease when transferred into congenic severe combined immunodeficient mice. Disease development is prevented by cotransfer of purified CD4+ T cells. *J Exp Med*, **178,** 237-44.

MOSER, M. & MURPHY, K.M. (2000). Dendritic cell regulation of TH1-TH2 development. *Nat Immunol*, **1,** 199-205.

MULLER, M., CARTER, S.L., HOFER, M.J., MANDERS, P., GETTS, D.R., GETTS, M.T., DREYKLUFT, A., LU, B., GERARD, C., KING, N.J. & CAMPBELL, I.L. (2007). CXCR3 signaling reduces the severity of experimental autoimmune encephalomyelitis by controlling the parenchymal distribution of effector and regulatory T cells in the central nervous system. *J Immunol*, **179,** 2774-86.

MURRAY, P.J., YOUNG, R.A. & DALEY, G.Q. (1998). Hematopoietic remodeling in interferon-gamma-deficient mice infected with mycobacteria. *Blood*, **91,** 2914-24.

NAGY, A., MAR, L. & WATTS, G. (2009). Creation and use of a cre recombinase transgenic database. *Methods Mol Biol*, **530,** 365-78.

NANDA KUMAR, N.S., BALAMURUGAN, R., JAYAKANTHAN, K., PULIMOOD, A., PUGAZHENDHI, S. & RAMAKRISHNA, B.S. (2008). Probiotic administration alters the gut flora and attenuates colitis in mice administered dextran sodium sulfate. *J Gastroenterol Hepatol*, **23,** 1834-9.

NANDI, D., TAHILIANI, P., KUMAR, A. & CHANDU, D. (2006). The ubiquitin-proteasome system. *J Biosci*, **31,** 137-55.

NAPOLI, I. & NEUMANN, H. (2010). Protective effects of microglia in multiple sclerosis. *Exp Neurol*, **225,** 24-8.

NAVA, P., KOCH, S., LAUKOETTER, M.G., LEE, W.Y., KOLEGRAFF, K., CAPALDO, C.T., BEEMAN, N., ADDIS, C., GERNER-SMIDT, K., NEUMAIER, I., SKERRA, A., LI, L., PARKOS, C.A. & NUSRAT, A. (2010). Interferon-gamma regulates intestinal epithelial homeostasis through converging beta-catenin signaling pathways. *Immunity*, **32,** 392-402.

NEDERGAARD, M., RANSOM, B. & GOLDMAN, S.A. (2003). New roles for astrocytes: redefining the functional architecture of the brain. *Trends Neurosci*, **26,** 523-30.

NEUMAN, M.G. (2007). Immune dysfunction in inflammatory bowel disease. *Transl Res*, **149,** 173-86.

NI, J., CHEN, S.F. & HOLLANDER, D. (1996). Effects of dextran sulphate sodium on intestinal epithelial cells and intestinal lymphocytes. *Gut*, **39,** 234-41.

NIEUWENHUIS, E.E. & BLUMBERG, R.S. (2006). The role of the epithelial barrier in inflammatory bowel disease. *Adv Exp Med Biol*, **579,** 108-16.

NIGHTINGALE, A. (2007). Diagnosis and management of inflammatory bowel disease. *Nurse Prescribing* **5,** 289-296.

NIKCEVICH, K.M., GORDON, K.B., TAN, L., HURST, S.D., KROEPFL, J.F., GARDINIER, M., BARRETT, T.A. & MILLER, S.D. (1997). IFN-gamma-activated primary murine astrocytes express B7 costimulatory molecules and prime naive antigen-specific T cells. *J Immunol*, **158,** 614-21.

NIMMERJAHN, A., KIRCHHOFF, F. & HELMCHEN, F. (2005). Resting microglial cells are highly dynamic surveillants of brain parenchyma in vivo. *Science*, **308,** 1314-8.

NOKES, C. & BUNDY, D.A. (1992). Trichuris trichiura infection and mental development in children. *Lancet*, **339,** 500.

NYMAN, T.A., MATIKAINEN, S., SARENEVA, T., JULKUNEN, I. & KALKKINEN, N. (2000). Proteome analysis reveals ubiquitin-conjugating enzymes to be a new family of interferon-alpha-regulated genes. *Eur J Biochem*, **267,** 4011-9.

O'CONNOR, R.A., PRENDERGAST, C.T., SABATOS, C.A., LAU, C.W., LEECH, M.D., WRAITH, D.C. & ANDERTON, S.M. (2008). Cutting edge: Th1 cells facilitate the entry of Th17 cells to the central nervous system during experimental autoimmune encephalomyelitis. *J Immunol*, **181,** 3750-4.

OBERMEIER, F., KOJOUHAROFF, G., HAN, S.W., SCHOLMERICH, J., GROSS, V. & FALK, W. (1999). Interferon γ and tumour necrosis factor (TNF)-induced nitric oxide as toxic effector molecule in chronic dextran sulphate sodium (DSS)-induced colitis in mice. *Clinical & Experimental Immunology*, **116,** 238-245.

OCHOA-REPARAZ, J., MIELCARZ, D.W., DITRIO, L.E., BURROUGHS, A.R., FOUREAU, D.M., HAQUE-BEGUM, S. & KASPER, L.H. (2009). Role of gut commensal microflora in the development of experimental autoimmune encephalomyelitis. *J Immunol*, **183,** 6041-50.

OKAMURA, H., TSUTSI, H., KOMATSU, T., YUTSUDO, M., HAKURA, A., TANIMOTO, T., TORIGOE, K., OKURA, T., NUKADA, Y., HATTORI, K. & ET AL. (1995). Cloning of a new cytokine that induces IFN-gamma production by T cells. *Nature*, **378,** 88-91.

OKAYASU, I., HATAKEYAMA, S., YAMADA, M., OHKUSA, T., INAGAKI, Y. & NAKAYA, R. (1990). A novel method in the induction of reliable experimental acute and chronic ulcerative colitis in mice. *Gastroenterology*, **98,** 694-702.

OLERUP, O. & HILLERT, J. (1991). HLA class II-associated genetic susceptibility in multiple sclerosis: a critical evaluation. *Tissue Antigens*, **38,** 1-15.

ORHOLM, M., BINDER, V., SORENSEN, T.I., RASMUSSEN, L.P. & KYVIK, K.O. (2000). Concordance of inflammatory bowel disease among Danish twins. Results of a nationwide study. *Scand J Gastroenterol*, **35,** 1075-81.

PACE, J.L., RUSSELL, S.W., TORRES, B.A., JOHNSON, H.M. & GRAY, P.W. (1983). Recombinant mouse gamma interferon induces the priming step in macrophage activation for tumor cell killing. *J Immunol*, **130,** 2011-3.

PAN, J., ZHANG, M., WANG, J., WANG, Q., XIA, D., SUN, W., ZHANG, L., YU, H., LIU, Y. & CAO, X. (2004). Interferon-gamma is an autocrine mediator for dendritic cell maturation. *Immunol Lett*, **94,** 141-51.

PANESAR, T. (1989). The moulting pattern in *Trichuris muris* (Nematoda: Trichuroidea). *Can J Zool*, **67,** 2340-2343.

PANITCH, H.S., HIRSCH, R.L., HALEY, A.S. & JOHNSON, K.P. (1987). Exacerbations of multiple sclerosis in patients treated with gamma interferon. *Lancet*, **1,** 893-5.

PARRONCHI, P., ROMAGNANI, P., ANNUNZIATO, F., SAMPOGNARO, S., BECCHIO, A., GIANNARINI, L., MAGGI, E., PUPILLI, C., TONELLI, F. & ROMAGNANI, S. (1997). Type 1 T-helper cell predominance and interleukin-12 expression in the gut of patients with Crohn's disease. *Am J Pathol*, **150,** 823-32.

PEIRIS, M., MONTEITH, G.R., ROBERTS-THOMSON, S.J. & CABOT, P.J. (2007). A model of experimental autoimmune encephalomyelitis (EAE) in C57BL/6 mice for the characterisation of intervention therapies. *J Neurosci Methods*, **163,** 245-54.

PELUSO, I., PALLONE, F. & MONTELEONE, G. (2006). Interleukin-12 and Th1 immune response in Crohn's disease: pathogenetic relevance and therapeutic implication. *World J Gastroenterol*, **12,** 5606-10.

PETTINELLI, C.B. & MCFARLIN, D.E. (1981). Adoptive transfer of experimental allergic encephalomyelitis in SJL/J mice after in vitro activation of lymph node cells by myelin basic protein: requirement for Lyt 1+ 2- T lymphocytes. *J Immunol*, **127,** 1420-3.

PHAM, C.T., MACIVOR, D.M., HUG, B.A., HEUSEL, J.W. & LEY, T.J. (1996). Long-range disruption of gene expression by a selectable marker cassette. *Proc Natl Acad Sci U S A*, **93,** 13090-5.

PHAM, H., RAMP, A.A., KLONIS, N., NG, S.W., KLOPSTEIN, A., AYERS, M.M. & ORIAN, J.M. (2009). The astrocytic response in early experimental autoimmune encephalomyelitis occurs across both the grey and white matter compartments. *J Neuroimmunol*, **208,** 30-9.

PICARELLA, D., HURLBUT, P., ROTTMAN, J., SHI, X., BUTCHER, E. & RINGLER, D.J. (1997). Monoclonal antibodies specific for beta 7 integrin and mucosal addressin cell adhesion molecule-1 (MAdCAM-1) reduce inflammation in the colon of SCID mice reconstituted with $CD45RB^{high}$ $CD4^{+}$ T cells. *J Immunol*, **158,** 2099-106.

PILS, M.C., BLEICH, A., PRINZ, I., FASNACHT, N., BOLLATI-FOGOLIN, M., SCHIPPERS, A., ROZELL, B. & MULLER, W. (2010a). Commensal gut flora reduces susceptibility to experimentally induced colitis via T-cell-derived interleukin-10. *Inflamm Bowel Dis*, **In press**.

PILS, M.C., PISANO, F., FASNACHT, N., HEINRICH, J.M., GROEBE, L., SCHIPPERS, A., ROZELL, B., JACK, R.S. & MULLER, W. (2010b). Monocytes/macrophages and/or neutrophils are the target of IL-10 in the LPS endotoxemia model. *Eur J Immunol*, **40,** 443-8.

PLATANIAS, L.C. (2005). Mechanisms of type-I- and type-II-interferon-mediated signalling. *Nat Rev Immunol*, **5,** 375-86.

PODOLSKY, D.K. (2002). Inflammatory Bowel Disease. *NEJM*, **347,** 417-429.

POTTEN, C.S. (1998). Stem cells in gastrointestinal epithelium: numbers, characteristics and death. *Philos Trans R Soc Lond B Biol Sci*, **353,** 821-30.

PUGLIATTI, M., ROSATI, G., CARTON, H., RIISE, T., DRULOVIC, J., VECSEI, L. & MILANOV, I. (2006). The epidemiology of multiple sclerosis in Europe. *Eur J Neurol*, **13,** 700-22.

QING, Y., COSTA-PEREIRA, A.P., WATLING, D. & STARK, G.R. (2005). Role of tyrosine 441 of interferon-gamma receptor subunit 1 in SOCS-1-mediated attenuation of STAT1 activation. *J Biol Chem*, **280,** 1849-53.

QING, Y. & STARK, G.R. (2004). Alternative activation of STAT1 and STAT3 in response to interferon-gamma. *J Biol Chem*, **279,** 41679-85.

RAJEWSKY, K., GU, H., KUHN, R., BETZ, U.A., MULLER, W., ROES, J. & SCHWENK, F. (1996). Conditional gene targeting. *J Clin Invest*, **98,** 600-3.

RASMUSSEN, S., WANG, Y., KIVISAKK, P., BRONSON, R.T., MEYER, M., IMITOLA, J. & KHOURY, S.J. (2007). Persistent activation of microglia is associated with neuronal dysfunction of callosal projecting pathways and multiple sclerosis-like lesions in relapsing--remitting experimental autoimmune encephalomyelitis. *Brain*, **130,** 2816-29.

RATH, H.C., HERFARTH, H.H., IKEDA, J.S., GRENTHER, W.B., HAMM, T.E., JR., BALISH, E., TAUROG, J.D., HAMMER, R.E., WILSON, K.H. & SARTOR, R.B. (1996). Normal luminal bacteria, especially Bacteroides species, mediate chronic colitis, gastritis, and arthritis in HLA-B27/human beta2 microglobulin transgenic rats. *J Clin Invest*, **98,** 945-53.

RATH, H.C., SCHULTZ, M., FREITAG, R., DIELEMAN, L.A., LI, F., LINDE, H.J., SCHOLMERICH, J. & SARTOR, R.B. (2001). Different subsets of enteric bacteria induce and perpetuate experimental colitis in rats and mice. *Infect Immun*, **69,** 2277-85.

REGIS, G., CONTI, L., BOSELLI, D. & NOVELLI, F. (2006). IFN γ R2 trafficking tunes IFN γ -STAT1 signaling in T lymphocytes. *Trends Immunol*, **27,** 96-101.

RENNICK, D., FORT, M. & DAVIDSON, N. (1997). Studies with IL-10-/- mice: an overview. *J Leukoc Biol*, **61,** 389-396.

RENNO, T., KRAKOWSKI, M., PICCIRILLO, C., LIN, J.Y. & OWENS, T. (1995). TNF-alpha expression by resident microglia and infiltrating leukocytes in the central nervous system of mice with experimental allergic encephalomyelitis. Regulation by Th1 cytokines. *J Immunol*, **154,** 944-53.

RICKERT, R.C., ROES, J. & RAJEWSKY, K. (1997). B lymphocyte-specific, Cre-mediated mutagenesis in mice. *Nucleic Acids Res*, **25,** 1317-8.

ROACH, T.I., ELSE, K.J., WAKELIN, D., MCLAREN, D.J. & GRENCIS, R.K. (1991). Trichuris muris: antigen recognition and transfer of immunity in mice by IgA monoclonal antibodies. *Parasite Immunol*, **13,** 1-12.

ROSE, R.W., VOROBYEVA, A.G., SKIPWORTH, J.D., NICOLAS, E. & RALL, G.F. (2007). Altered levels of STAT1 and STAT3 influence the neuronal response to interferon gamma. *J Neuroimmunol* **192,** 145-156.

RYO, A., SUIZU, F., YOSHIDA, Y., PERREM, K., LIOU, Y.C., WULF, G., ROTTAPEL, R., YAMAOKA, S. & LU, K.P. (2003). Regulation of NF-kappaB signaling by Pin1-dependent prolyl isomerization and ubiquitin-mediated proteolysis of p65/RelA. *Mol Cell*, **12,** 1413-26.

SADOVNICK, A.D., EBERS, G.C., DYMENT, D.A. & RISCH, N.J. (1996). Evidence for genetic basis of multiple sclerosis. The Canadian Collaborative Study Group. *Lancet*, **347,** 1728-30.

SAHA, S., JING, X., PARK, S.Y., WANG, S., LI, X., GUPTA, D. & DZIARSKI, R. (2010). Peptidoglycan recognition proteins protect mice from experimental colitis by promoting normal gut flora and preventing induction of interferon-gamma. *Cell Host Microbe*, **8,** 147-62.

SANCHEZ-GUAJARDO, V., FEBBRARO, F., KIRIK, D. & ROMERO-RAMOS, M. (2010). Microglia acquire distinct activation profiles depending on the degree of alpha-synuclein neuropathology in a rAAV based model of Parkinson's disease. *PLoS One*, **5,** e8784.

SANSONETTI, P.J. (2004). War and peace at mucosal surfaces. *Nat Rev Immunol*, **4,** 953-64.

SCHARTON-KERSTEN, T.M., WYNN, T.A., DENKERS, E.Y., BALA, S., GRUNVALD, E., HIENY, S., GAZZINELLI, R.T. & SHER, A. (1996). In the absence of endogenous IFN-gamma, mice develop unimpaired IL-12 responses to Toxoplasma gondii while failing to control acute infection. *J Immunol*, **157,** 4045-54.

SCHMIDT-SUPPRIAN, M. & RAJEWSKY, K. (2007). Vagaries of conditional gene targeting. *Nat Immunol*, **8,** 665-8.

SCHOPF, L.R., HOFFMANN, K.F., CHEEVER, A.W., URBAN, J.F., JR. & WYNN, T.A. (2002). IL-10 is critical for host resistance and survival during gastrointestinal helminth infection. *J Immunol*, **168,** 2383-92.

SCHRODER, K., HERTZOG, P.J., RAVASI, T. & HUME, D.A. (2004). Interferon γ : an overview of signals, mechanisms and functions. *J Leukoc Biol*, **75,** 163-189.

SCHRODER, K., SWEET, M.J. & HUME, D.A. (2006). Signal integration between IFNgamma and TLR signalling pathways in macrophages. *Immunobiology*, **211,** 511-24.

SCHURMANN, G.M., BISHOP, A.E., FACER, P., VECCHIO, M., LEE, J.C., RAMPTON, D.S. & POLAK, J.M. (1995). Increased expression of cell adhesion molecule P-selectin in active inflammatory bowel disease. *Gut*, **36,** 411-8.

SCOTT, P. (1991). IFN-gamma modulates the early development of Th1 and Th2 responses in a murine model of cutaneous leishmaniasis. *J Immunol*, **147,** 3149-55.

SELBY, G.R. & WAKELIN, D. (1973). Transfer of immunity against Trichuris muris in the mouse by serum and cells. *Int J Parasitol*, **3,** 717-22.

SELLON, R.K., TONKONOGY, S., SCHULTZ, M., DIELEMAN, L.A., GRENTHER, W., BALISH, E., RENNICK, D.M. & SARTOR, R.B. (1998). Resident enteric bacteria are necessary for development of spontaneous colitis and immune system activation in interleukin-10-deficient mice. *Infect Immun*, **66,** 5224-31.

SERAFINI, B., MAGLIOZZI, R., ROSICARELLI, B., REYNOLDS, R., ZHENG, T.S. & ALOISI, F. (2008). Expression of TWEAK and its receptor Fn14 in the multiple sclerosis brain: implications for inflammatory tissue injury. *J Neuropathol Exp Neurol*, **67,** 1137-48.

SETHNA, M.P. & LAMPSON, L.A. (1991). Immune modulation within the brain: recruitment of inflammatory cells and increased major histocompatibility antigen expression following intracerebral injection of interferon-gamma. *J Neuroimmunol*, **34,** 121-32.

SHUAI, K. & LIU, B. (2003). Regulation of JAK-STAT signalling in the immune system. *Nat Rev Immunol*, **3,** 900-11.

SIMMONS, R.D. & WILLENBORG, D.O. (1990). Direct injection of cytokines into the spinal cord causes autoimmune encephalomyelitis-like inflammation. *J Neurol Sci*, **100,** 37-42.

SINGH, U.P., SINGH, S., SINGH, R., CONG, Y., TAUB, D.D. & LILLARD, J.W., JR. (2008). CXCL10-producing mucosal CD4+ T cells, NK cells, and NKT cells are associated with chronic colitis in IL-10(-/-) mice, which can be abrogated by anti-CXCL10 antibody inhibition. *J Interferon Cytokine Res*, **28,** 31-43.

SIZEMORE, N., AGARWAL, A., DAS, K., LERNER, N., SULAK, M., RANI, S., RANSOHOFF, R., SHULTZ, D. & STARK, G.R. (2004). Inhibitor of kappaB

kinase is required to activate a subset of interferon gamma-stimulated genes. *Proc Natl Acad Sci U S A*, **101,** 7994-8.

SMITHSON, J.E., CAMPBELL, A., ANDREWS, J.M., MILTON, J.D., PIGOTT, R. & JEWELL, D.P. (1997). Altered expression of mucins throughout the colon in ulcerative colitis. *Gut*, **40,** 234-40.

SODERHOLM, J.D., OLAISON, G., PETERSON, K.H., FRANZEN, L.E., LINDMARK, T., WIREN, M., TAGESSON, C. & SJODAHL, R. (2002). Augmented increase in tight junction permeability by luminal stimuli in the non-inflamed ileum of Crohn's disease. *Gut*, **50,** 307-13.

STARR, R., FUCHSBERGER, M., LAU, L.S., ULDRICH, A.P., GORADIA, A., WILLSON, T.A., VERHAGEN, A.M., ALEXANDER, W.S. & SMYTH, M.J. (2009). SOCS-1 binding to tyrosine 441 of IFN-gamma receptor subunit 1 contributes to the attenuation of IFN-gamma signaling in vivo. *J Immunol*, **183,** 4537-44.

STEHR, M., GREWELING, M.C., TISCHER, S., SINGH, M., BLOCKER, H., MONNER, D.A. & MULLER, W. (2009). Charles River altered Schaedler flora (CRASF) remained stable for four years in a mouse colony housed in individually ventilated cages. *Lab Anim*, **43,** 362-70.

STEIMLE, V., SIEGRIST, C.A., MOTTET, A., LISOWSKA-GROSPIERRE, B. & MACH, B. (1994). Regulation of MHC class II expression by interferon-gamma mediated by the transactivator gene CIITA. *Science*, **265,** 106-9.

STEINMAN, L., MARTIN, R., BERNARD, C., CONLON, P. & OKSENBERG, J.R. (2002). Multiple sclerosis: deeper understanding of its pathogenesis reveals new targets for therapy. *Annu Rev Neurosci*, **25,** 491-505.

STEINMAN, L. & ZAMVIL, S.S. (2006). How to successfully apply animal studies in experimental allergic encephalomyelitis to research on multiple sclerosis. *Ann Neurol*, **60,** 12-21.

STEPHENSON, L.S., HOLLAND, C.V. & COOPER, E.S. (2000). The public health significance of Trichuris trichiura. *Parasitology*, **121,** S73-95.

STRAUCH, U. & SCHOLMERICH, J. (2010). Emerging drugs to treat Crohn's disease. *Expert Opin Emerg Drugs*, **15,** 309-22.

STREETZ, K.L., WUSTEFELD, T., KLEIN, C., KALLEN, K.J., TRONCHE, F., BETZ, U.A., SCHUTZ, G., MANNS, M.P., MULLER, W. & TRAUTWEIN, C. (2003). Lack of gp130 expression in hepatocytes promotes liver injury. *Gastroenterology*, **125,** 532-43.

STROMNES, I.M., CERRETTI, L.M., LIGGITT, D., HARRIS, R.A. & GOVERMAN, J.M. (2008). Differential regulation of central nervous system autoimmunity by T(H)1 and T(H)17 cells. *Nat Med*, **14,** 337-42.

SUNDBERG, J.P., ELSON, C.O., BEDIGIAN, H. & BIRKENMEIER, E.H. (1994). Spontaneous, heritable colitis in a new substrain of C3H/HeJ mice. *Gastroenterology*, **107,** 1726-35.

SUZUKI, Y., CONLEY, F.K. & REMINGTON, J.S. (1989). Importance of endogenous IFN-gamma for prevention of toxoplasmic encephalitis in mice. *J Immunol*, **143,** 2045-50.

SUZUKI, Y., ORELLANA, M.A., SCHREIBER, R.D. & REMINGTON, J.S. (1988). Interferon-gamma: the major mediator of resistance against Toxoplasma gondii. *Science*, **240,** 516-8.

SWAMY, M., JAMORA, C., HAVRAN, W. & HAYDAY, A. (2010). Epithelial decision makers: in search of the 'epimmunome'. *Nat Immunol*, **11,** 656-65.

SWANBORG, R.H. (1995). Experimental autoimmune encephalomyelitis in rodents as a model for human demyelinating disease. *Clin Immunol Immunopathol*, **77,** 4-13.

SWEET, M.J., STACEY, K.J., KAKUDA, D.K., MARKOVICH, D. & HUME, D.A. (1998). IFN-gamma primes macrophage responses to bacterial DNA. *J Interferon Cytokine Res*, **18,** 263-71.

SWIHART, K., FRUTH, U., MESSMER, N., HUG, K., BEHIN, R., HUANG, S., DEL GIUDICE, G., AGUET, M. & LOUIS, J. (1995). Mice from a genetically resistant background lacking the interferon gamma receptor are susceptible to infection with Leishmania major but mount a polarized T helper cell 1-type $CD4^+$ T cell response. *J. Exp. Med.*, **181,** 961-971.

SYDORA, B.C., WAGNER, N., LÖHLER, J., YAKOUB, G., KRONENBERG, M., MÜLLER, W. & ARANDA, R. (2002). β7 Integrin expression is not required for the localization of T cells to the intestine and colitis pathogenesis. *Clin Exp Immunol*, **129,** 35-42.

TAKAOKA, A., MITANI, Y., SUEMORI, H., SATO, M., YOKOCHI, T., NOGUCHI, S., TANAKA, N. & TANIGUCHI, T. (2000). Cross talk between interferon-gamma and -alpha/beta signaling components in caveolar membrane domains. *Science*, **288,** 2357-60.

TANNOCK, G.W. (2001). Molecular assessment of intestinal microflora. *Am J Clin Nutr*, **73,** 410S-414S.

THOMAS, K.R. & CAPECCHI, M.R. (1987). Site-directed mutagenesis by gene targeting in mouse embryo-derived stem cells. *Cell*, **51,** 503-12.

THOMPSON, A.J., POLMAN, C.H., MILLER, D.H., MCDONALD, W.I., BROCHET, B., FILIPPI, M.M.X. & DE SA, J. (1997). Primary progressive multiple sclerosis. *Brain*, **120 (Pt 6),** 1085-96.

THOMPSON, N.P., DRISCOLL, R., POUNDER, R.E. & WAKEFIELD, A.J. (1996). Genetics versus environment in inflammatory bowel disease: results of a British twin study. *Bmj*, **312,** 95-6.

TOZAWA, K., HANAI, H., SUGIMOTO, K., BABA, S., SUGIMURA, H., AOSHI, T., UCHIJIMA, M., NAGATA, T. & KOIDE, Y. (2003). Evidence for the critical role of interleukin-12 but not interferon γ ; in the pathogenesis of experimental colitis in mice. *J Gastroen and Hepatol*, **18,** 578-587.

TRAN, E.H., HARDIN-POUZET, H., VERGE, G. & OWENS, T. (1997). Astrocytes and microglia express inducible nitric oxide synthase in mice with experimental allergic encephalomyelitis. *J Neuroimmunol*, **74,** 121-9.

TRINDER, M.W. & LAWRANCE, I.C. (2009). Efficacy of adalimumab for the management of inflammatory bowel disease in the clinical setting. *J Gastroenterol Hepatol*, **24,** 1252-7.

TRONCHE, F., KELLENDONK, C., KRETZ, O., GASS, P., ANLAG, K., ORBAN, P.C., BOCK, R., KLEIN, R. & SCHUTZ, G. (1999). Disruption of the glucocorticoid receptor gene in the nervous system results in reduced anxiety. *Nat Genet*, **23,** 99-103.

TSUNODA, I., KUANG, L.Q., THEIL, D.J. & FUJINAMI, R.S. (2000). Antibody association with a novel model for primary progressive multiple sclerosis: induction of relapsing-remitting and progressive forms of EAE in H2s mouse strains. *Brain Pathol*, **10,** 402-18.

TYAS, D., KERRIGAN, J., RUSSELL, N. & NIXON, R. (2007). The distribution of the cost of multiple sclerosis in the UK: how do costs vary by illness severity? *Value Health*, **10,** 386-9.

UHLIG, H.H., MCKENZIE, B.S., HUE, S., THOMPSON, C., JOYCE-SHAIKH, B., STEPANKOVA, R., ROBINSON, N., BUONOCORE, S., TLASKALOVA-HOGENOVA, H., CUA, D.J. & POWRIE, F. (2006). Differential Activity of IL-12 and IL-23 in Mucosal and Systemic Innate Immune Pathology. *Immunity*, **25,** 309-318.

UHLIG, H.H. & POWRIE, F. (2009). Mouse models of intestinal inflammation as tools to understand the pathogenesis of inflammatory bowel disease. *Eur J Immunol*, **39,** 2021-6.

ULLOA, L., DOODY, J. & MASSAGUE, J. (1999). Inhibition of transforming growth factor-beta/SMAD signalling by the interferon-gamma/STAT pathway. *Nature*, **397,** 710-3.

UNGUREANU, D., SAHARINEN, P., JUNTTILA, I., HILTON, D.J. & SILVENNOINEN, O. (2002). Regulation of Jak2 through the ubiquitin-proteasome pathway involves phosphorylation of Jak2 on Y1007 and interaction with SOCS-1. *Mol Cell Biol*, **22,** 3316-26.

UNNO, N., MENCONI, M.J., SMITH, M. & FINK, M.P. (1995). Nitric oxide mediates interferon-gamma-induced hyperpermeability in cultured human intestinal epithelial monolayers. *Crit Care Med*, **23,** 1170-6.

VARTANIAN, T., LI, Y., ZHAO, M. & STEFANSSON, K. (1995). Interferon-gamma-induced oligodendrocyte cell death: implications for the pathogenesis of multiple sclerosis. *Mol Med*, **1,** 732-43.

VERES, G., SZEBENI, B., MRAZ, M., DEZSOFI, A., VANNAY, A., VASARHELYI, B., MAJOROVA, E. & ARATO, A. (2007). Expression of Toll-like receptors 2, 3 and 4 in children with inflammatory bowel disease. *J Crohns and Colitis* **1,** 12.

VICTORIO, S.C., HAVTON, L.A. & OLIVEIRA, A.L. (2010). Absence of IFNgamma expression induces neuronal degeneration in the spinal cord of adult mice. *J Neuroinflammation*, **7,** 77.

VOOIJS, M., JONKERS, J. & BERNS, A. (2001). A highly efficient ligand-regulated Cre recombinase mouse line shows that LoxP recombination is position dependent. *EMBO Rep*, **2,** 292-7.

VOORTHUIS, J.A., UITDEHAAG, B.M., DE GROOT, C.J., GOEDE, P.H., VAN DER MEIDE, P.H. & DIJKSTRA, C.D. (1990). Suppression of experimental allergic encephalomyelitis by intraventricular administration of interferon-gamma in Lewis rats. *Clin Exp Immunol*, **81,** 183-8.

VOWINKEL, T., KALOGERIS, T.J., MORI, M., KRIEGLSTEIN, C.F. & GRANGER, D.N. (2004). Impact of dextran sulfate sodium load on the severity of inflammation in experimental colitis. *Dig Dis Sci*, **49,** 556-64.

WAKELIN, D. (1967). Acquired immunity to *Trichuris muris* in the albino laboratory mouse. *Parasitology*, **57,** 515-524.

WAKELIN, D. (1969). The development of the early larval stages of Trichuris muris in the albino laboratory mouse. *J Helminthol*, **43,** 427-36.

WAKELIN, D. (1973). The stimulation of immunity to Trichuris muris in mice exposed to low-level infections. *Parasitology*, **66,** 181-9.

WANG, Z.E., REINER, S.L., ZHENG, S., DALTON, D.K. & LOCKSLEY, R.M. (1994). CD4+ effector cells default to the Th2 pathway in interferon gamma-deficient mice infected with Leishmania major. *J Exp Med*, **179,** 1367-71.

WENNER, C.A., GULER, M.L., MACATONIA, S.E., O'GARRA, A. & MURPHY, K.M. (1996). Roles of IFN-gamma and IFN-alpha in IL-12-induced T helper cell-1 development. *J Immunol*, **156,** 1442-7.

WENSKY, A.K., FURTADO, G.C., MARCONDES, M.C., CHEN, S., MANFRA, D., LIRA, S.A., ZAGZAG, D. & LAFAILLE, J.J. (2005). IFN-gamma determines distinct clinical outcomes in autoimmune encephalomyelitis. *J Immunol*, **174,** 1416-23.

WHO (1999). *The World Health Report 1999*. Geneva: World Health Organisation.

WILLENBORG, D.O., FORDHAM, S., BERNARD, C.C., COWDEN, W.B. & RAMSHAW, I.A. (1996). IFN-gamma plays a critical down-regulatory role in the induction and effector phase of myelin oligodendrocyte glycoprotein-induced autoimmune encephalomyelitis. *J Immunol*, **157,** 3223-7.

WILLENBORG, D.O., FORDHAM, S.A., STAYKOVA, M.A., RAMSHAW, I.A. & COWDEN, W.B. (1999). IFN-gamma is critical to the control of murine autoimmune encephalomyelitis and regulates both in the periphery and in the target tissue: a possible role for nitric oxide. *J Immunol*, **163,** 5278-86.

WILLIAMS, A., PIATON, G. & LUBETZKI, C. (2007). Astrocytes--friends or foes in multiple sclerosis? *Glia*, **55,** 1300-12.

WINDHAGEN, A., NEWCOMBE, J., DANGOND, F., STRAND, C., WOODROOFE, M.N., CUZNER, M.L. & HAFLER, D.A. (1995). Expression of costimulatory molecules B7-1 (CD80), B7-2 (CD86), and interleukin 12 cytokine in multiple sclerosis lesions. *J Exp Med*, **182,** 1985-96.

WINSLET, M.C., ALLAN, A., POXON, V., YOUNGS, D. & KEIGHLEY, M.R. (1994). Faecal diversion for Crohn's colitis: a model to study the role of the faecal stream in the inflammatory process. *British Medical Journal* **35,** 236-242.

WIRTZ, S. & NEURATH, M.F. (2007). Mouse models of inflammatory bowel disease. *Adv Drug Deliv Rev*, **59,** 1073-83.

WORLD BANK (1993). *World development report 1993*. New York: Oxford University Press.

XU, Y., HUNT, N.H. & BAO, S. (2008). The effect of restraint stress on experimental colitis is IFN-gamma independent. *J Neuroimmunol*, **200,** 53-61.

YAP, G.S. & SHER, A. (1999). Effector cells of both nonhemopoietic and hemopoietic origin are required for interferon (IFN)-gamma- and tumor necrosis factor (TNF)-alpha-dependent host resistance to the intracellular pathogen, Toxoplasma gondii. *J Exp Med*, **189,** 1083-92.

YASUKAWA, H., MISAWA, H., SAKAMOTO, H., MASUHARA, M., SASAKI, A., WAKIOKA, T., OHTSUKA, S., IMAIZUMI, T., MATSUDA, T., IHLE, J.N. & YOSHIMURA, A. (1999). The JAK-binding protein JAB inhibits Janus tyrosine kinase activity through binding in the activation loop. *Embo J*, **18,** 1309-20.

YEN, D., CHEUNG, J., SCHEERENS, H., POULET, F., MCCLANAHAN, T., MCKENZIE, B., KLEINSCHEK, M.A., OWYANG, A., MATTSON, J., BLUMENSCHEIN, W., MURPHY, E., SATHE, M., CUA, D.J., KASTELEIN, R.A. & RENNICK, D. (2006). IL-23 is essential for T cell-mediated colitis and promotes inflammation via IL-17 and IL-6. *J Clin Invest.* , **116,** 1310-6.

YOKOTE, H., MIYAKE, S., CROXFORD, J.L., OKI, S., MIZUSAWA, H. & YAMAMURA, T. (2008). NKT cell-dependent amelioration of a mouse model of multiple sclerosis by altering gut flora. *Am J Pathol*, **173,** 1714-23.

YONG, V.W., MOUMDJIAN, R., YONG, F.P., RUIJS, T.C., FREEDMAN, M.S., CASHMAN, N. & ANTEL, J.P. (1991). Gamma-interferon promotes proliferation of adult human astrocytes in vitro and reactive gliosis in the adult mouse brain in vivo. *Proc Natl Acad Sci U S A*, **88,** 7016-20.

YOSHIDA, K., TAGA, T., SAITO, M., SUEMATSU, S., KUMANOGOH, A., TANAKA, T., FUJIWARA, H., HIRATA, M., YAMAGAMI, T., NAKAHATA, T., HIRABAYASHI, T., YONEDA, Y., TANAKA, K., WANG, W.Z., MORI, C., SHIOTA, K., YOSHIDA, N. & KISHIMOTO, T. (1996). Targeted disruption of gp130, a common signal transducer for the interleukin 6 family of cytokines, leads to myocardial and hematological disorders. *Proc Natl Acad Sci U S A*, **93,** 407-11.

ZAPH, C., TROY, A.E., TAYLOR, B.C., BERMAN-BOOTY, L.D., GUILD, K.J., DU, Y., YOST, E.A., GRUBER, A.D., MAY, M.J., GRETEN, F.R., ECKMANN, L., KARIN, M. & ARTIS, D. (2007). Epithelial-cell-intrinsic IKK-beta expression regulates intestinal immune homeostasis. *Nature*, **446,** 552-6.

ZHANG, L., DANON, S.J., GREHAN, M., CHAN, V., LEE, A. & MITCHELL, H. (2005). Natural colonization with Helicobacter species and the development of inflammatory bowel disease in interleukin-10-deficient mice. *Helicobacter*, **10,** 223-30.

ZHAO, A., URBAN, J.F., JR., ANTHONY, R.M., SUN, R., STILTZ, J., VAN ROOIJEN, N., WYNN, T.A., GAUSE, W.C. & SHEA-DONOHUE, T. (2008). Th2 cytokine-induced alterations in intestinal smooth muscle function depend on alternatively activated macrophages. *Gastroenterology*, **135,** 217-225 e1.

ZIVADINOV, R., IONA, L., MONTI-BRAGADIN, L., BOSCO, A., JURJEVIC, A., TAUS, C., CAZZATO, G. & ZORZON, M. (2003). The use of standardized incidence and prevalence rates in epidemiological studies on multiple sclerosis. A meta-analysis study. *Neuroepidemiology*, **22,** 65-74.

ZOZULYA, A.L. & WIENDL, H. (2008). The role of regulatory T cells in multiple sclerosis. *Nat Clin Pract Neuro*, **4,** 384-398.

APPENDIX A

Tail Lysis Buffer: 50mM KCl, 10mM Tris, 2.5mM $MgCl_2$, 0.1mg/ml gelatine, 0.4% w/v NP40, 0.4% w/v Tween 20 (all Sigma-Aldrich)

Western Blot Running buffer: 25mM Tris (Sigma-Aldrich), 0.192M glycine (BDH), 0.1% w/v SDS (BDH)

TBS: 25mM Tris, 0.125M NaCl pH 8.0 (all Sigma-Aldrich)

TBS-Tween: TBS, 1% v/v Tween-20 (Sigma-Aldrich)

Ponceau-S stain: 0.1% Ponceau S, 5% v/v acetic acid (all Sigma-Aldrich)

Western blot gels:

	Resolving Gel (10%)	Stacking Gel
1M Tris (Sigma-Aldrich) pH8.8	4.5ml	-
1M Tris (Sigma-Aldirch) pH6.8	-	0.5ml
Protogel (30% acrylamide; National Diagnostics)	4ml	680µl
10% SDS (BDH)	120µl	40µl
TEMED (Sigma-Aldrich)	12µl	4µl
Water	3.34ml	2.74ml
10% ammonium persulfate (Sigma-Adrich)*	160µl	80µl

Strip Buffer: 60mM Tris (Sigma-Aldrich), 2% w/v SDS (BDH) pH 6.8. 0.7% β-mercaptoethanol (Sigma-Aldrich) added prior to use

API buffer: 300mM Tris (Sigma-Aldrich), 20% v/v Methanol (BDH)

APII buffer: 25mM Tris (Sigma-Aldrich), 20% v/v Methanol (BDH)

CP buffer: 40mM β-aminocaproic acid (Sigma-Aldrich), 0.01% w/v SDS (BDH), 20% v/v Methanol (BDH)

Laemelli buffer 5x: 32mM Tris (Sigma-Aldrich), 5% SDS (BDH), 25% Glycerol (Sigma-Aldrich), 0.5% β-mercaptoethanol (Sigma-Aldrich), 0.2mg/ml bromophenol blue (Sigma-Aldrich)

Western blot blocking buffer: 4% low-fat milk (Marvel) in TBS-Tween

Complete DMEM: Dulbecco's modified Eagle's medium (DMEM; PAA) containing 10% v/v fetal calf serum (PAA) , 2 mM L-glutamine (PAA), 100 units/ml penicillin and 100 µg/ml streptomycin (PAA)

Complete RPMI: RPMI-1640 media (PAA) containing 10% v/v fetal calf serum (PAA), 2 mM L-glutamine (PAA), 100 units/ml penicillin and 100 µg/ml streptomycin (PAA)

FACS buffer: PBS, 2% FCS (PAA), 0.05% sodium azite (Sigma-Aldrich)

FACS staining buffer: PBS, 2% FCS (PAA), 1% rat serum (eBioscience), 0.05% sodium azite (Sigma-Aldrich)

Carbonate bicarbonate buffer: 15mM Na_2CO_3 (Sigma-Aldrich), 35mM $NaHCO_3$ (Sigma-Aldrich), pH 9.6

ELISA blocking buffer: 3% w/v BSA (Sigma-Aldrich) in 100ml PBS

PBS: 3.2mM Na_2HPO_4, 0.5mM KH_2PO_4, 1.3mM KCl, 135mM NaCl, pH7.4 (all Sigma-Aldrich)

PBS-T: PBS, 0.05% v/v Tween 20 (Sigma-Aldrich)

MACS buffer: PBS, pH 7.2, 0.5% BSA (Sigma-Aldrich), 2 mM EDTA (Sigma-Aldrich)

Citrate buffer: 10mM sodium citrate (Sigma-Aldrich), 0.05% Tween 20 (Sigma-Aldrich) pH 6.0

Adapted NBF fixative: 4% v/v formaldehyde (BDH), 0.154M NaCl (Sigma-Aldrich), 2% v/v glacial acetic acid (BDH), 1.37μM hexadecyl trimethyl-ammonium bromide (Sigma-Aldrich).